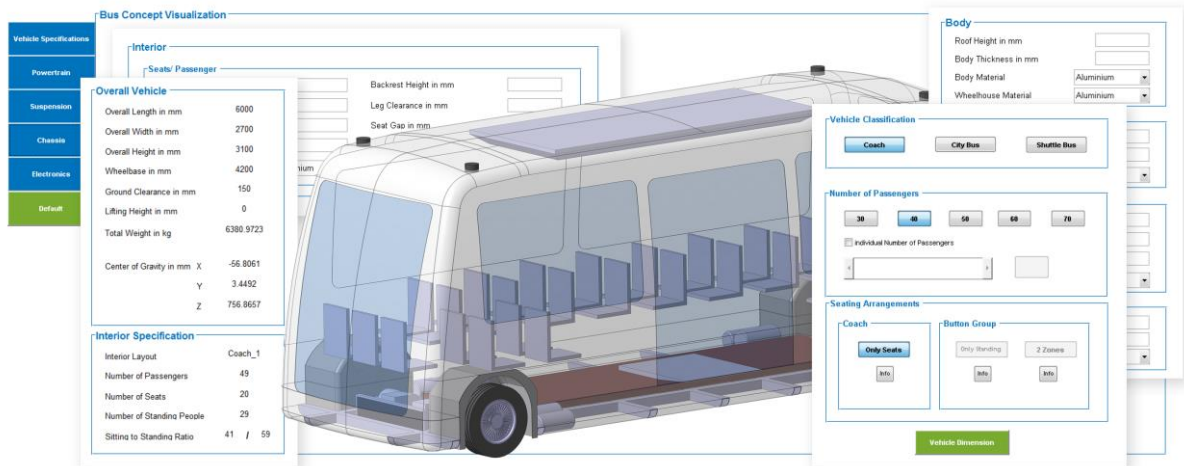Doctoral Dissertation

Vehicle Component Configuration Design and Packaging in Virtual Environment for Autonomous Electric Buses

Thesis submitted in partial fulfilment of the requirements for the degree of

Doctor of Engineering

Department of Mechanical Systems Engineering

Tokyo University of Agriculture and Technology

Ganesh Sethuraman, M.Sc.

07/08/2020

Acknowledgement

a lot from his composed behaviour and his mature working attitude. Sincere thanks to Dr Matthias Felgenhauer for playing the role of a mentor and helping me to kick start my topic and Dr Christian Angerer for offering great help and support during the early research and my stay in Munich.

I wish to acknowledge very important people, Mr Manferd Schwarz, Mr Stefan Maxl, Mr Phi Tran and Mr Sebastian Krapf who contributed greatly towards this work with their Master Thesis. I would not have reached this far without their contribution. Apart from working on the topic, they brought very good insights that further helped to improve the research outputs. Besides, I wish to thank everyone from IMVS and DAM teams of TUMCREATE for being the best colleagues and better friends.

I have been tremendously supported by my family and friends, to whom I am very grateful. My wife Ms Akshaya Sivaramakrishnan always stood by me during the toughest of the times. Her perseverance and immense support that helped me to finish my dissertation. I sincerely thank her for everything she has offered. I am grateful to my parents Mr Sethuraman and Ms Padma and my sister Ms Vandana Arvind for their endless love and care, encouragement, sincere prayers and constant support in all the aspects through the years. Thanks for believing and supporting my career and personal decisions.

Finally, tons of thanks to my best friends in Singapore and India for me making me who I am today. I would like to express my gratitude to all the individuals and organizations, whom I have failed to cover in this short acknowledgement.

Singapore, August 2020
Ganesh Sethuraman

Table of Contents

List of Abbreviation

3D	Three Dimensional
AEV	Autonomous Electric Vehicle
ASHRAE	American Society of Heating, Refrigerating and Air Conditioning Engineers
ASM	Asynchronous Motor
AV	Autonomous Vehicle
BRT	Bus Rapid Transit
CAV	Connected and Autonomous Vehicles
CETRAN	Centre of Excellence for Testing and Research of Autonomous Vehicles
CFD	Computational Fluid Dynamics
CNG	Compressed Natural Gas
CO_2	Carbon dioxide
COG	Centre of Gravity
DOE	Design of Experiments
DSM	Design Structure Matrix
GHG	Greenhouse Gas
GUI	Graphical User Interface
GUIDE	Graphical User Interface Development Environment
HVAC	Heating, Ventilation and Air Conditioning
HX	Heat exchanger
ICEV	Internal Combustion Engine Vehicle
IGBT	Insulated-Gate Bipolar Transistor
JPG	(JPEG) Joint Photographic Experts Group, digital image
LCA	Life Cycle Assessment
LIDAR	Light detection and ranging
LTA	Land Transport Authority
MaaS	Mobility as a service
MBS	Multibody Simulation
MOSFET	Metal-Oxide-Semiconductor Field-Effect Transistor
MOSFET	Metal-Oxide-Semiconductor Field-Effect Transistor
NaN	Not a number
NTU	Nanyang Technological University
OEM	Original Equipment Manufacturers
PDF	Portable Document Format
PHEV	Plug-In Hybrid Electric Vehicle
PID	Proportional Integral Derivative
PM	Particulate Matter
PNG	Portable network graphics
PSM	Permanent Magnet Synchronous Motor
SAE	Society of Automotive Engineers
SOP	Start of Production
TCO	Total Cost of Ownership
UL1	Urban Layout 1
UL2	Urban Layout 2
VB	Visual Basic
VBA	Visual Basic for Applications
VCC	Vapour compression cycle
VLSI	Very large scale integration

List of Symbols

Symbol	Unit	Description
$a_{area,i}$	mm²	Area of the defined zone
$a_{standing}$	mm²	Standing area for passenger
a_{bus}	mm²	Total floor area of vehicle
a_{dead_zone}	mm²	Dead zone area of vehicle floor
$a_{effective}$	in²	Effective suspension area
$a_{passenger}$	mm²	Area of a passenger
a_{rest}	mm²	Seat gap area
a_{seat}	mm²	Area of seat
$a_{wheelhouse}$	mm²	Area of wheelhouse from top view
bd_{body_depth}	mm	Body depth of passenger
d_{gap}	mm	Gap between the seats
d_{spring}	mm	Air spring diameter
d_{tire}	mm	Tire diameter
l_{cabin}	mm	Cabin length
l_{door}	mm	Length available for seats on both sides of the door
$l_{clearance}$	mm	Legroom clearance length
$l_{overall}$	mm	Overall vehicle length
l_{rear}	mm	Available length for seats in vehicle front and rear
l_{seat}	mm	Length of the seat
$l_{wheelbase}$	mm	Length of wheelbase
l_{window}	mm	Available length to place seats along the window
m_{curb}	kg	Curb weight
n_{door}	-	Number of seats along the door
$n_{passenger,area_i}$	-	Number of passengers in the defined area
$n_{passenger}$	-	Total number of passengers fitting in the bus
n_{rear}	-	Number of seats along the front and rear
n_{seats}	-	Total number of seats
$n_{standing}$	-	Number of standing passengers
n_{window}	-	Number of seats along the window
$ratio_{standing/sitting}$	%	Ratio of standing to sitting passengers
t_{body}	mm	Body Thickness
t_{seat}	mm	Seat thickness
w_{cabin}	mm	Width of the cabin
w_{door}	mm	Width of the door
w_{door}	mm	Door width
$w_{overall}$	mm	Overall vehicle width
$w_{passenger\_shoulder}$	mm	Shoulder width of passenger
$w_{rest\_gap\_door}$	mm	Width of the rest gap after placing seats at the door
$w_{rest\_gap\_rear}$	mm	Width of the rest gap after placing seats at the front and rear
$w_{rest\_gap\_window}$	mm	Width of the rest gap after placing seats at the window
w_{seat}	mm	Width of the seat
w_{seat}	mm	Seat width
w_{seat_gap}	mm	Seat gap width
w_{tire}	mm	Tire width
$FAWL$	kg	Laden axle weight
PL	kg	Pay load

SM	kg	Sprung mass per wheel
USM	kg	Unsprung mass per wheel
j	-	Overload factor
wb	mm	Wheelbase
$load_{max}$	lbs	Maximum load at the default pressure
$p_{default}$	lbs/in^2	Default pressure at the design height
$p_{required}$	lbs/in^2	Required pressure at a certain load
K	lbs/inch	Vertical Spring Rate
A_c	in^2	Effective Area at ½ inch below the design height
A_e	in^2	Effective Area at ½ inch above the design height
V_1	in^3	Internal volume at the design height
V_c	in^3	Internal volume at ½ inch below the design height
V_e	in^3	Internal volume at ½ inch above the design height
f_n	cpm	Natural frequency
$F_{B,axle,ideal}$	N	Ideal brake force per axle
$F_{G,axle,static}$	N	Weight force per axle
$\ddot{x}_B$	m/s^2	Minimum brake deceleration
g	m/s^2	Acceleration of gravity
$m_{vehicle}$	kg	Overall mass of the vehicle concept
h_{cg}	m	Height of center of gravity
l	m	Wheelbase of the vehicle concept
$M_{B,axle,ideal}$	Nm	Ideal brake torque per axle
r_{tire}	m	Static tire radius
F_{cl}	N	Calliper Force
η	-	Efficiency of the brake system
A_{pad}	mm^2	Brake pad area
$p_{hydraulic}$	N/mm^2	Hydraulic pressure of the brake system
F_{circ}	N	Circumferential force
μ	-	Coefficient of friction between the brake pads and the brake disc
r_{eff}	m	Effective radius of the brake disc
$r_{disc,outer}$	m	Outer diameter of the brake disc
$M_{B,est}$	Nm	Estimated brake torque
S_{Slalom}	-	Steering input
t	s	Simulation time
$M_{bending,max}$	Nm	Maximum bending moment
$l_{wishbone}$	m	Length of the lower wishbone
$F_{z,max}$	N	Maximum wheel force in z-direction
W_{pipe}	mm^3	Moment of resistance of a pipe
D	mm	Outer diameter of a pipe
d	mm	Inner diameter of a pipe
$\sigma_{bending}$	N/mm^2	Bending stress of a suspension link
i_{TM}	-	Transmission gear ratio
$i_{thirdAxle}$	-	Boolean to indicate the existence of a third drive axle
$k_{c,bat}$	-	Factor for the cost estimation of the battery
$k_{m,bat}$	-	Factor for the mass estimation of the battery
$n_{parallel}$	-	Number of parallel battery cells
$n_{passenger}$	-	Number of passengers
n_{serial}	-	Number of serial battery cells
C_{bat}	EUR	Cost of battery
C_{inv}	EUR	Cost of inverter
C_{PSM}	EUR	Cost of PSM
C_{ASM}	EUR	Cost of ASM
C_{TM}	EUR	Cost of transmission
$C_{material}$	EUR	Cost of transmission material
$C_{production}$	EUR	Cost of transmission production
$C_{add.parts}$	EUR	Cost of transmission additional parts

Symbol	Units	Description
$C_{initial}$	EUR	Initial Powertrain Cost
C_{mot}	EUR	Cost of motor
m_{cell}	kg	Mass of one battery cell
m_{inv}	kg	Mass of ASM
m_{PSM}	kg	Mass of PSM
m_{tire}	kg	Mass of tire
m_{TM}	kg	Mass of transmission
m_{body}	kg	Mass of body
$m_{passenger}$	kg	Mass of passenger
m_{PWT}	kg	Mass of powertrain
m_{veh}	kg	Gross mass of vehicle
$m_{housing}$	kg	Mass of transmission housing
m_{gears}	kg	Mass of gears
r_{dyn}	m	Dynamic tire radius
P_n	kW	Nominal power
P_{max}	kW	Maximum Power
E_{bat}	kWh	Battery energy content
T_n	Nm	Nominal torque
D	m	Characteristic length
$depth_{HX}$	m	Heat exchanger depth
h_1	J/kg	Enthalpy at suction line
h_2	J/kg	Enthalpy at discharge line
h_3	J/kg	Enthalpy at condenser outlet
h_4	J/kg	Enthalpy at evaporator inlet
$\Delta h_{air,evap}$	J/K	Enthalpy difference between evaporator air inlet and outlet
$\Delta h_{ref,compr}$	J/kg	Enthalpy difference between compressor inlet and outlet
$\Delta h_{ref,evap}$	J/kg	Enthalpy difference over the evaporator refrigerant side
$height_{HX}$	m	Heat exchanger height
htc	W/m^2 K	Heat transfer coefficient
$htc_{ext,conv}$	W/m^2 K	External convective heat transfer coefficient of bus cabin
k	W/m K	Thermal conductivity
$\dot{m}$	kg/s	Mass flow rate
$\dot{m}_{air,evap}$	kg/s	Mass flow rate of air through evaporator
$\dot{m}_{ref,compr}$	kg/s	Refrigerant mass flow rate over the compressor
$\dot{m}_{ref,evap}$	kg/s	Refrigerant mass flow rate over evaporator
Ntu	-	Number of transfer units of heat exchanger
Nu_l	-	Single phase liquid Nusselt number
p	Pa	Pressure
P_{compr}	W	Compressor power
P_{rd}	-	Reduced pressure
Pr	-	Prandtl number
p_{pol}	Pa	Polynomial expression of pressure drop
Q	W	Heat load
Q_{dem}	W	Heat transfer rate demand
Q_{pol}	W	Polynomial expression of heat transfer rate
Re	-	Reynolds number
v_{cabin}	m/s	Vehicle cabin velocity
v	km/h	Vehicle speed
$width_{HX}$	m	Heat exchanger width
x	-	Quality of refrigerant

1   Introduction

The rapid urbanization has led to a swift increase in the urban population. It is expected that around 70 % of the global population will be living in urban cities by 2050 [1]. The growth in the number of inhabitants has resulted in an increased demand for transportation. By the year 2050, the global fleet of vehicles will reach 2 billion and this surge in vehicles lead to several problems such as congestion and predominantly emissions [2]. Transportation is a major contributor of greenhouse gases (GHG) emissions and accounts for nearly 23 % of the worldwide emissions [3] of which 72 % is contributed by road transportation [4]. This has direct implications on urban mobility and therefore, major cities have started to emphasize on public transportation.

Providing a safe, efficient, and clean transportation to the population commuting in cities are the key objectives of urban mobility[5]. The automotive industry has a major part in contributing in terms of mobility solutions to the arising needs due to urbanization. The transportation of the future is expected to be electrified, autonomous, shared and connected [6]. Although the road-based public transportation in the major cities is dominated by the internal combustion engine vehicles, electrification and automation of vehicles are emerging swiftly due to several advantages such as higher powertrain efficiencies, reduced maintenance needs and zero tailpipe emissions, resulting in reduced urban emissions [7–9]. With the emergence in technologies automation of vehicles is also gaining further importance with the possibility of improved safety, efficiency, accessibility and cost reduction [10–14]. Besides, studies have also shown that the deployment of autonomous vehicles in urban cities may reduce the number of private cars by around 80% [15].

Numerous projects are testing various autonomous shuttles and buses as shared and public transportation. A study by AINSALU ET. AL. summarised 36 different pilot tests that have been performed with autonomous electric buses with passengers in open public roads of different cities around the world [16]. The tests also showed that different vehicles were used in different cities. The vehicle size plays an important role in determining the efficiency of the public transportation and automation of buses would bring change in the operation to improve the service quality [16, 17]. Therefore, the autonomous vehicle makers have been exploring into different vehicle types such as vans, minibus, and the mid-size bus with varying passenger capacities. To cater to these changes, vehicle manufacturers are expected to develop new vehicle concepts and bring them to the market.

1.1 Research Motivation

The automotive development process takes several years from the project launch until a vehicle is manufactured [18]. This is due to the complex steps involved in designing, integrating and packaging all the components [19]. The vehicle package includes the definition and design of several subsystems such as the powertrain, chassis, body and structure,

exterior trim and interior trim. All the subsystems and the components have interdependencies and hence are designed and packaged concurrently. The component subsystems decisions are made in the early concept development phase. Therefore, in the early phase of the vehicle development, the concept has to be carefully planned and defined, as changes in the subsequent phases might prove to be costly. Hence, the time-to-market of the vehicle completely depend on the early phase concept [18, 20].

Several software programs and tools support the engineers in the early phase vehicle concept development. Figure 1-1 illustrates some of the widely used tools in the development of new vehicle concepts. Computer Aided Design (CAD) software such as CATIA are used in the design of components and helps to package and visualise the entire vehicle concept. Therefore CAD programs are used throughout the vehicle development process [21]. Some software programs such as the Tesis Dynaware, Simpack helps in design and simulation of specific systems such as the chassis and powertrain [22, 23]. Similarly, software programs such as ANSYS are used for finite element simulations to verify the strength of the structure and crash safety of the vehicle [24]. Tools like MATLAB are used extensively for performing simulations and to develop custom mathematical models [25].
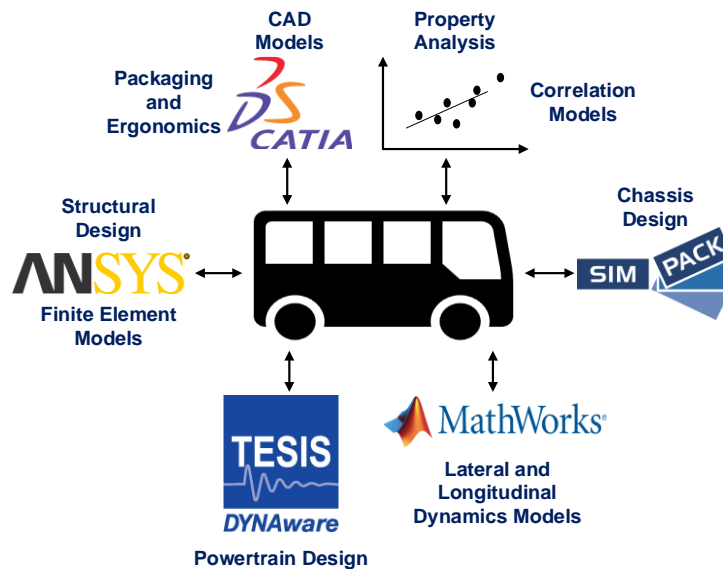
Figure 1-1   Tools in Early Concept Phase

These tools aid in the shortening of the concept development process by supporting the engineers. However, the programs and tools work independently and are not connected or interfaced with each other. Therefore, for every change made in the vehicle package, the engineers are required to update the programs making the process more tedious and time-consuming.

The problems can be solved by parameterisation of the entire vehicle concept and its components. The objective of parametric modelling is to base the entire system on mathematical models and functions that connects all individual components. This allows improvement in flexibility in the development process. Parametric modelling techniques have proved to significantly reduce the design process time up to 55% [26, 27] and hence the overall design costs by up to 30% [28]. Therefore, parameterisation allows manufacturers to react to the market changes quickly. Although the parametric modelling technology would help manufacturers reduce their product development cycle, only limited research is available for complete vehicle package development. Majority of existing studies focus on passenger cars

2

with a capacity of 5-7 passengers. Therefore, the variation on the domain of the component is minimal and there has been no consideration of parametric packaging development for vehicle types of buses/minibuses.

1.2 Research Objective

It can be seen that the vehicle development process is time consuming due to the complexities in the early phase of the concept development and iterations involved in the selection of components and packaging them in the vehicle. In addition, a holistic parametric process to develop vehicle concepts in the early concept phase are not considered. The objective of this thesis is the development of the Autonomous Electric Vehicle Tool (AEV Tool), a holistic application that sizes and packages the components for autonomous electric vehicles for vehicle sizes between 4 m – 14 m. The tool helps to create and visualise the vehicle concepts in the early concept phase and allows for comparison of the initial costs, energy consumption, and environmental impacts of different concepts.

With a few steps, the person using the tool will be able to variate a parametric vehicle model with the most important components of the powertrain, the chassis and the air conditioning system. All the relevant parameters required to develop new bus concepts are included in the tool. For example, the interior layout of the vehicle, such as the seating arrangements, doors and standing places is taken into consideration.

The tool also enables the user to select the vehicles of different classifications such as a city bus, coach or a shuttle. To enhance the usability, tool is developed with two working modes namely the manual and automated mode. The manual mode is meant for the expert users where every component can be sized individually. The automated mode is meant for users with a low level of vehicle knowledge, where pre simulated component databases are used to automatically size the components based on basic user inputs.

In addition to the design of the vehicle and the components, the tool calculates the energy consumption using detailed longitudinal dynamics model and the total cost of the configured vehicle concept. A spider chart summarizes all characteristics and offers an overview in order to compare different concepts. A scalable Life-cycle assessment (LCA) model is developed from the outputs of the tool and is used to summarise the greenhouse gas emissions of the generated concept. In summary, the AEV tool enables the user to configure, visualise and calculate the energy consumption, costs, and life cycle emissions of a bus in a very short period.

1.3 Thesis Structure

The thesis is structured into nine chapters as shown in Figure 1-2. Chapter 1 introduces the growing trend in autonomous and electric public transportation and discusses the motivation and the problem. Consequently, the need for parametric concept development tool and objectives of the thesis are explained. Chapter 2 provides the state of the art of electric and autonomous electric buses. The current approach in the vehicle development process and vehicle packaging strategies are discussed. The chapter also details the benefits of parametric concept development, present the existing vehicle concept development tools that use a parametric approach, and highlights the research gap. The Chapter explains the methodology for the development of the AEV Tool. A general overview of the tool is discussed and target

requirements are defined. Further, the framework of the method is explained. The chapter also discusses the definition of vehicle concept and decision on all package relevant components and subsystems. Chapter 4 explains algorithm development for the selection of all the components based on subsystems. The chapter includes a selection of powertrain, chassis and HVAC (Heating Ventilation and Air Conditioning) subsystem. Chapter 5 explains the designing of the parametric CAD model of the vehicle concept and the components. All the required parameter of the tool is defined and the CAD model is developed with the same parameters. Chapter 6 explains the architecture design of the tool. The chapter explains the implementation of different modes of operation and explains the GUI design of the tool. Chapter 7 describes various vehicle concept evaluation methods considered in tool development. The methods include energy consumption simulation, cost estimation and a detailed life cycle emissions assessment. Vehicle concept generation results are discussed in Chapter 8. Further, the results are validated with benchmark vehicles and by comparing with the results of existing studies. The chapter also presents a case study to show the overall applicability of the AEV tool. Chapter 9 provides a detailed discussion of the results and its implications and further points out the limitations in the method. Finally, the entire thesis is summarised and the accomplishments of the work are discussed and concluded. The chapter also provides insights for future work.

Chapter 1	**Introduction**
	Motivation · Objective · Structure

Chapter 2	**State of the Art**
	Electrified and Autonomous Buses
	Vehicle Concept Development Process
	Parametric Vehicle Concept Development

Chapter 3	**Methodology**
	Overview of the Tool and Requirements
	Framework of the Method
	Definition of Vehicle and Componens

Chapter 4	**Development of Components Selection Algorithm**
	Powertrain Sizing and Selection
	Chassis Sizing and Selection
	HVAC Sizing and Selection

Chapter 5	**Development of the Parametric CAD Model**
	Definition and Nomenclature of Parameters
	Design of Boundaries and Constraints
	Design of the Parametric CAD Model

Chapter 6	**Implementation of the AEV Tool**
	Architecture of the Tool
	Manual Mode Development
	Automated Mode Developent
	Design of the GUI

Chapter 7	**Vehicle Concept Evaluation Methods**
	Energy Consumption Simulation
	Vehicle Concept Cost Estimation
	Life Cycle Assessment

Chapter 8	**Results**
	Vehicle Concept Generation
	Evaluation of the Results
	Comparison of Concepts : Case Study

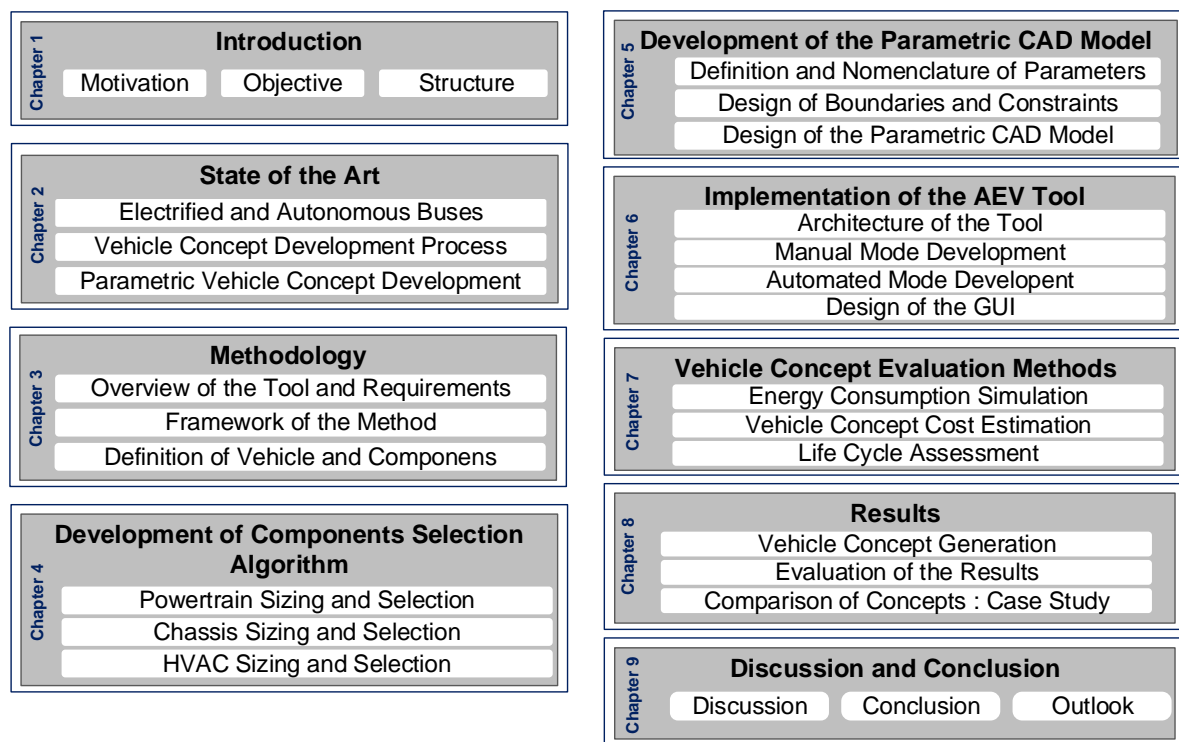| Chapter 9	**Discussion and Conclusion**
	Discussion · Conclusion · Outlook

Figure 1-2   Thesis Structure

2   State of the Art

The state of the art chapter first gives an overview of the electric buses and autonomous buses currently under development. Afterwards, the following section discusses in detail about the steps in the vehicle concept development and the processes. The definition phase in the vehicle development process gets the primary focus since vehicle packaging decisions are carried out in this phase. Subsequently, the parametric modelling approach in vehicle packaging is discussed and existing vehicle concept development approaches and the tools are analysed. The research gaps are identified and discussed at the end of this chapter.

2.1 Electrified and Autonomous Buses

2.1.1 Electric Bus Systems

Transportation being a major contributor to GHG emissions and accounts for around 23 % of the worldwide GHG emissions [3]. Of this around 72 % of the GHG emissions are from road transportation [4]. Currently, the diesel buses in Singapore makeup only 2 % of the total vehicle fleet [29] but account for 15 % of GHG emissions arising from road transport [30]. Consequently, major cities promote public transport to significantly reduce the vehicles on the road. Hence, alternative powertrain technologies are widely explored of which electrification of buses is gaining popularity. In the last decade, electric bus technology has developed and progressed. In Europe, the market share of battery-electric buses will surpass other propulsion technologies by 2030 [31]. Electric buses have several advantages such as higher powertrain efficiencies, lesser maintenance and zero tailpipe emissions, hence less urban emissions compared to conventional diesel buses [8].

There have been numerous studies on electrification of buses. KUNITH presented an extensive literature review of the comparing buses with different powertrain technologies and summarized the studies into three different and interconnected categories namely, energy consumption, environment and costs [32]. The vehicle/technology costs were given more importance compared to the other two categories. Based on the technological evaluation, it was concluded by the author that, the electric city buses have the potential to reduce the cost and would be more economical compared to diesel buses after 2020 [32].

LAJUNEN has widely contributed to the research in the field of electric buses by publishing several studies on electric bus concepts, powertrain architecture, battery requirements, powertrain optimisation and lifecycle costs and emissions [33–41]. The author analysed different powertrain configuration in electric city buses. The configuration variations included the batteries, motors and transmission. Simulations were performed for different driving cycles and showed that the electric powertrain was efficient in general and the energy consumption greatly relied on the auxiliary load [34, 36]. LAJUNEN compared hybrid and electric powertrain configuration for city bus and showed that the electric city bus has the best potential to reduce

energy consumption and emissions [37]. In another study by LAJUNEN AND LIPMAN, electric buses were compared with other technologies such as the diesel buses, hybrid buses, fuel cell and natural gas. The results showed that electric buses had the potential to reduce GHG emissions by 75 % and are energy-efficient [39]. However, the overall cost is high because of the batteries [33, 39]

PATHAK ET. AL. conducted a study on the optimisation of the powertrain for electric city buses based on a design exploration method [42]. The authors used realistic passenger load profiles and speed profiles derived from a selected bus route in Singapore. Six different powertrain configurations with single speed and multi-speed gearboxes and more than 10,000 unique solutions were evaluated. These results showed that multiple motor configurations resulted in better vehicle characteristic and lower total costs and energy costs compared to the conventional single motor configurations. The concepts with multiple motors were able to distribute power between the motors and shift the load points to higher operating efficiencies.

Several studies have examined the impacts of electric buses on energy consumption and environmental emissions in order to examine real-time feasibility [43–49]. COONEY ET. AL. [43] conducted a complete vehicle life cycle assessment comparing the environmental impacts of a diesel bus and an electric bus. The acquisition cost of the electric bus was around twice as much as the diesel bus and the study concluded that the electric buses have less GHG emissions only in eight states of the USA considering the electricity mix.

ZHOU ET. AL.[46] evaluated the real-world performance of two 12 m and an 8 m battery electric buses and their life cycle benefits concerning energy consumption and GHG emissions. The authors compared the diesel and electric buses under different scenarios in Macao by varying the different air-conditioning loads and passenger occupancy loads. The results showed that under empty condition, the electric bus is around 11 % more cost efficient than the diesel bus. Under full load condition, the cost reduction is increased to around 26 % in comparison. The results showed that the electric bus has a reduction of up to 35 % in terms of CO_2 emissions. The authors concluded that electric buses are beneficial in cities with high load and low-speed operation.

XU ET. AL. compared buses with different powertrain such as internal combustion, hybrid electric and fully electric [47]. The study emphasizes on the daily transit scenarios evaluating complete daily operations of the buses. The results showed that if the electric buses are used in the local transit services in San Francisco, the GHG emission can reduce by around 70 %. CHOI ET. AL. presented a study on commercial operation of electric buses in Seoul city [49]. The study was conducted for a period of 17 months with more than 674000 passengers in total. The results showed that the GHG emissions from electric buses were around 54 % lower than the compressed natural gas (CNG) buses and the cost of operation of electric buses are only 21.6 % of the CNG buses. Therefore, the authors concluded based on their validation that the electric buses are economically beneficial and environmentally sustainable.

The literature review shows that electric buses are advantageous and have great potential, especially in public transport systems. The automation of electric buses may further reduce energy consumption and emissions during the lifetime of the vehicle [16, 50]. However, no studies have been conducted to evaluate the environmental impacts of autonomous buses in public transport.

2.1.2 **Autonomous Vehicles**

Autonomous Vehicles (AVs) are gaining popularity because of their potential toward improved safety and accessibility [10–13]. AVs can independently drive the vehicle to a predefined destination in real road conditions. In general, AVs function without active human interference and function based on the visual data sources available [51]. There are six levels of automation for road traffic defined by SAE International standards as shown in Figure 2-1 [52]. The levels are: no automation (0), driver assistance (1), partial automation (2), conditional automation (3), high automation (4) and the last stage of full automation (5).

Level	Name	Narrative definition	Execution of steering and acceleration/ deceleration	Monitoring of driving environment	Fallback performance of *dynamic driving task*	System capability (*driving modes*)
Human driver monitors the driving environment						
0	No Automation	the full-time performance by the *human driver* of all aspects of the *dynamic driving task*, even when enhanced by warning or intervention systems	Human driver	Human driver	Human driver	n/a
1	Driver Assistance	the *driving mode*-specific execution by a driver assistance system of either steering or acceleration/deceleration using information about the driving environment and with the expectation that the *human driver* perform all remaining aspects of the *dynamic driving task*	Human driver and system	Human driver	Human driver	Some driving modes
2	Partial Automation	the *driving mode*-specific execution by one or more driver assistance systems of both steering and acceleration/deceleration using information about the driving environment and with the expectation that the *human driver* perform all remaining aspects of the *dynamic driving task*	**System**	Human driver	Human driver	Some driving modes
Automated driving system ("system") monitors the driving environment						
3	Conditional Automation	the *driving mode*-specific performance by an *automated driving system* of all aspects of the *dynamic driving task* with the expectation that the *human driver* will respond appropriately to a *request to intervene*	System	**System**	Human driver	Some driving modes
4	High Automation	the *driving mode*-specific performance by an *automated driving system* of all aspects of the *dynamic driving task*, even if a *human driver* does not respond appropriately to a *request to intervene*	System	System	**System**	Some driving modes
5	Full Automation	the full-time performance by an *automated driving system* of all aspects of the *dynamic driving task* under all roadway and environmental conditions that can be managed by a *human driver*	System	System	System	**All driving modes**

Figure 2-1   SAE Levels of Vehicle Automation [52]

Studies by FANGNANT ET.AL. and BROWN ET.AL. points out that AVs are more energy-efficient than human driven vehicles [53, 54]. This reduction in energy consumption may lower the environmental impacts of the vehicles [55]. In addition, AVs are expected to reduce congestion and improve traffic safety [56]. The report on planning for autonomous vehicles by ANTONIO LORO CONSULTING [57] points out that the AVs have precise control over the vehicles compared to the human drivers. The report also points out that the 75 %to 95 % of the accidents are caused by the human errors and AVs with even lower levels of automation reduces the accidents by 27 % with the help of automatic emergency braking. The report also estimates that with AVs the lane capacity can be increased by 50 % - 100 %. This is because of the shorter reaction time and precise control enables the AVs to platoon with small inter-vehicle distance. However, high automation is required for AVs to platoon closely but platooning can help in further energy savings. BULLIS estimated that with an inter-vehicle spacing of four metres, trucks can reduce fuel consumption by 10-15 % [58]. This scenario of trucks can be implemented to buses.

STOCKER and SHAHEEN published research on shared vehicles to understand the requirements of the passengers commuting in major cities. The authors pointed out that a combination of AVs and shared mobility might help to reduce the gap between public and private transportation. At the same time, the adoption of AVs in the shared user mobility such

as taxis, courier network services, fractional ownership and public transport will significantly have greater environmental potential benefits than privately owned AVs [59].

SETHURAMAN ET.AL. published a work on the impact assessment of the Autonomous Electric Vehicles (AEVs) in public transportation [60]. The impacts were evaluated and quantified based on the service quality attributes such as comfort, travel time, energy, environment and infrastructure. The study included platooning of AEVs with up to 10 vehicles and included the energy consumption by the CAV (Connected and Autonomous Vehicles) components in the simulation. The study concluded that the AEVs significantly contributed to the service quality The AEVs can optimize their driving profiles to improve comfort and as well increase the energy saving by up to 8 % compared to the human driven vehicles and platooning of the AEVs increases the energy savings further by around 6 %. [60]

Based on the literature review presented, it can be seen that the autonomous electric vehicles have higher potential. However, unlike the electric buses, there are no studies conducted on real time investigation of autonomous electric buses. Therefore, the next section discusses benchmarking of existing autonomous electric buses to understand the technology and applications.

2.1.3 Benchmarking of Autonomous Buses

This section provides an overview of the existing autonomous electric buses and some future concepts. Table 2-1 shows the list of vehicles that are benchmarked. The list consists of buses from different manufacturers and important information such as the vehicle dimensions, passenger capacity, and some key specifications are shown to provide an easy comparison. Each AEV concept shown are briefly described in the following paragraphs to give an outlook and detailed information can be found in the manufacturer`s webpages [61–67].

Table 2-1   Benchmarking of Autonomous Buses

Vehicle	Name/ Manufacturer	Passenger Capacity	Dimensions Length x Width x Height in mm	Kerb Weight kg
	EZ10 Easymile [61]	12 6 sitting, 6 standing	3928 x 1986 x 2750	2750
	Autonom Shuttle Navya [62]	15 11 sitting, 4 standing	4750 x 2110 x 2650	3450
	Olli Local Motors [63]	9-12	3920 x 2050 x 2500	2640

	Rivium GRT 2getthere [64]	24 8 sitting, 16 standing	6000 x 2100 x 2800	5418
	NEXT Future Transportation [65]	10 6 sitting, 4 standing	2700mm length	2500
	M2B8 Matreshka [66]	8 - 12	4500 x 1700 x 2600	2800
	Future Bus Mercedes Benz [67]	31	12100 x 2600 x 3100	n/a

Easymile - EZ10: The Easymile EZ10 is one of the most popular AEVs that is functioning in several countries. The Easymile EZ10 has been deployed in more than 25 countries over four continents. The EZ 10 has been deployed in the public and private roads and has been tested for over more than 600000 km. The AEV is being tested in some closed campus areas in many cities like Singapore. Easymile offers mobility-as-a-service (MaaS) in three different modes. The *metro-mode*, which functions as a shuttle and stops at stations along the route. The *bus-mode,* where the AEV stops at designated bus-stops on request. The *on-demand-mode* functions more like a taxi to fill the gap between the first and last mile [61].

Navya - Autonom Shuttle: The Navya Autonom shuttle is currently the most popular autonomous shuttle and are operating in several cities around the word. The shuttle has been developed for urban and suburban transport needs [62]. Around 87 Navya Autonom shuttles are being operated in 16 countries as of now [68]. In Singapore, the shuttle is being tested in the Nanyang Technological University (NTU) as a Campus shuttle bus. In addition, the Autonom shuttle is a playing a part in Singapore's future mobility project and is being tested at the facility of Centre of Excellence for Testing and Research of Autonomous Vehicles (CETRAN) [69].

Local Motors – Olli: Olli from the Local Motors is another autonomous shuttle similar to the Easymile EZ10. The Olli shuttle has been deployed in four countries and is being tested in public and private places similar to the EZ10. Although similar to the other vehicle, Local motors offers solutions that manages and optimizes the operations of the autonomous shuttle and provide an end to end seamless experience to the passengers. Another innovation with Olli is that, major parts of the vehicle are manufactured using the 3D printing technology

making the process faster and efficient. The entire assembly of vehicle is carried out within 10 hours [63].

Rivium GRT 2getthere: 2getthere started the world`s first autonomous park shuttle operation with the Rivium GRT autonomous shuttles. The first shuttle was put into operation in 1999 with a vehicle capacity of 10 passengers. The second generation of the Rivium GRT with a maximum capacity of 24 passengers was deployed in 2005. The vehicles were tested in private facility with limited vehicle interaction. In 2019, the third generation Rivium GRT shuttle were deployed and in the mid 2020 the autonomous shuttle will be tested in the mixed traffic conditions in Rotterdam, Netherlands with operations such as platooning [64].

NEXT Future Transportation: Next Transportation is an advanced system based on multiple modular autonomous electric vehicles. The idea is to have multiple capsule like modules than can attach or detach dynamically. When attached, the modules facilitate inter module passenger exchange and performs like a bus. The modules can detach and re-route themselves. The transfer within the bus to different modules would decrease the travelling time, as the passengers are not required to alight and transfer. Next transportation also has a vision to offer services in motion, which might include receiving couriers or coffee during the ride. In 2018 the Next prototypes we tested in Dubai, however they have not been launched for service yet [65].

Matreshka - Volgabus: The Volgabus is the manufacturers of the Matreshka autonomous shuttle. The Matreshka is built on a modular platform called as the "m2". For example, the "m2c6" is a chassis built on the platform to carry cargo up to 1300 kg. "m2b8" is the autonomous passenger shuttle that can take between 8 – 12 passengers. Due to the modularity the autonomous shuttle can automatically decouple to perform different operations such as carrying passengers during the day and delivering cargo or cleaning the roads during the night. The modularity also allows to quickly swap the batteries that enables the vehicles to run throughout the day. The m2b8 is planned to be used both as a scheduled shuttle and as an on-demand shuttle [66].

Future Bus Mercedes-Benz: The Future bus from Mercedes is the first futuristic autonomous bus by a well-established Original Equipment Manufacturer (OEM). Unlike the other autonomous shuttles, the Future bus is similar to the conventional 12 m city buses. The other shuttles are smaller in the range between 4 m - 6 m. The Future bus operated semi autonomously with the supervision of a driver in a project called City Pilot. The passenger cabin of the future bus as three zones based on different length of stay by the passengers. The front zone is focused on the services during the ride. Currently a driver compartment is positioned in the front zone since the vehicle is in the test phase. The middle zone is designed for the short distance passenger and facilitates a fast boarding and alighting with standing area. The rear zone has a lounge type seating for the long distance passengers [67].

The benchmarking analysis has shown multiple approaches to the autonomous and electrified transportation. The vehicles range from small capsule sizes to a large conventional bus sized vehicle illustrating the need for different vehicle concepts.

2.2 Vehicle Development Process

Lienkamp [20] defines the automotive vehicle development process in general irrespective of the type of vehicle concept. The vehicle development process can be divided into four major phases: initialisation phase, definition phase, implementation phase and production phase, as shown in Figure 2-2. The vehicle development process typically takes three to six years from the start of the product idea to the Start of Production (SOP) as seen in Figure 2-2. The product ideation starts at the initial phase where the aim is to develop a product plan and to define the preliminary vehicle concept. The product planning comprises of an initial estimation of the product cost and the timeline of the project. The project is then reviewed and the vehicle development process proceeds further based on positive feedback.

The aim of the definition phase is a detailed vehicle concept with overall specifications. The definition phase includes the major design decisions related to vehicle packaging. This includes decisions such as vehicle geometry and vehicle topology and as well as the decisions regarding the choice of subsystems, components, materials, etc. Therefore, it can be seen that the first two phases of the vehicle development process together with make up the vehicle concept development as shown in Figure 2-2. The implementation phase includes processes like detailed CAD modelling, the vehicle concept and components validation and prototyping, testing and production of a pilot vehicle lot. Design freeze is a milestone in the implementation phase that ceases any further design changes to the vehicle concept. The SOP occurs in the manufacturing phase after successful testing and validation of the vehicle concept [18, 20].

It can be observed from Figure 2-2 that the vehicle concept development phase is the most time consuming phase. This is because the initial and definition phase is challenging and multifaceted as it involves numerous vehicle subsystems for packaging thereby requiring cooperation from various engineering teams. Therefore, the first two phases have a significant impact on the duration of the vehicle development process. The vehicle concept development tool developed in this thesis addresses the early vehicle development phase and looks closely into the vehicle definition phase and describes the need for parametric vehicle development models in the following sections.
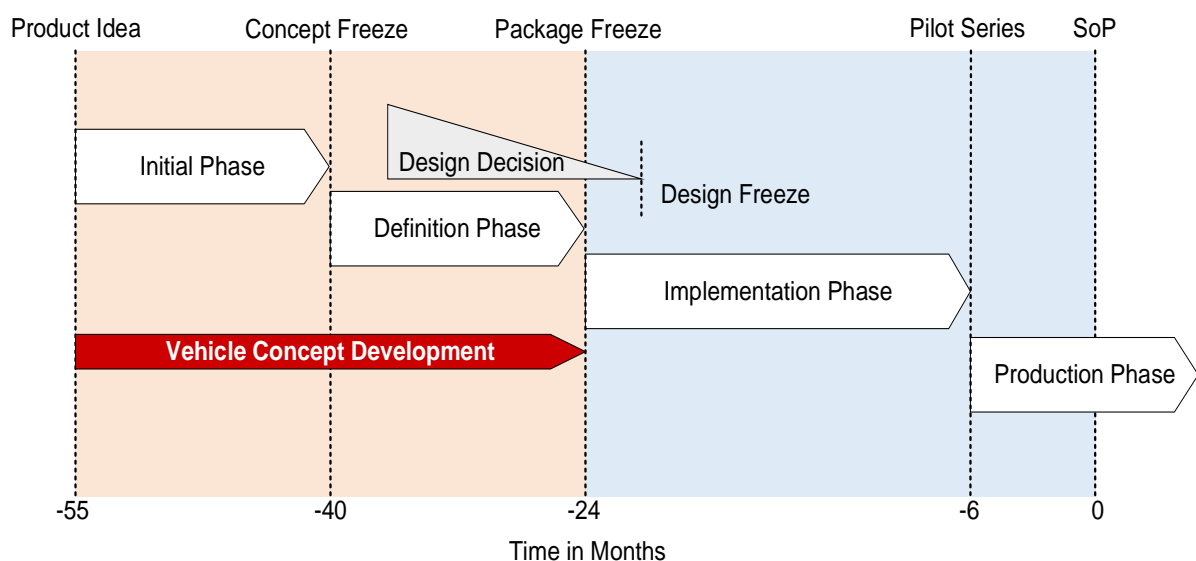

Figure 2-2   Vehicle Development Process, based on [20, p. 19]

2.2.1 **Early Phase Vehicle Concept Development**

The vehicle concept is an output of the definition phase as seen in the previous section. According to LIENKAMP [20, p. 229], the vehicle concept includes interior and exterior design, component selection, concept definition and vehicle package used in the subsequent phases. Figure 2-3 shows the steps in the vehicle definition phase. As seen, the vehicle development process is an iterative loop as explained by LIENKAMP [20, p. 229]. Based on the output of the initial phase, the definition phase begins with ergonomics layout. This includes the interior layout of the vehicle. The following step is the interior and exterior design which is determined by the virtual sketches and mock-up prototypes. Consequently, the required component subsystems are selected. The major subsystems include chassis, powertrain, heating and cooling system, etc. As seen in Figure 2-3, since the process is iterative, the vehicle concept is required to be updated based on the changes or updates in the component decisions.

Following the selection of component subsystems, the vehicle structure and the body is designed. At this point in the definition phase, the target vehicle concept has been generated. Furthermore, the vehicle concept is checked for legal regulations and homologation standards in the target markets. Finally, all vehicle properties can be determined and compared to other vehicle concepts as shown in Figure 2-3 [20, pp. 226-228].
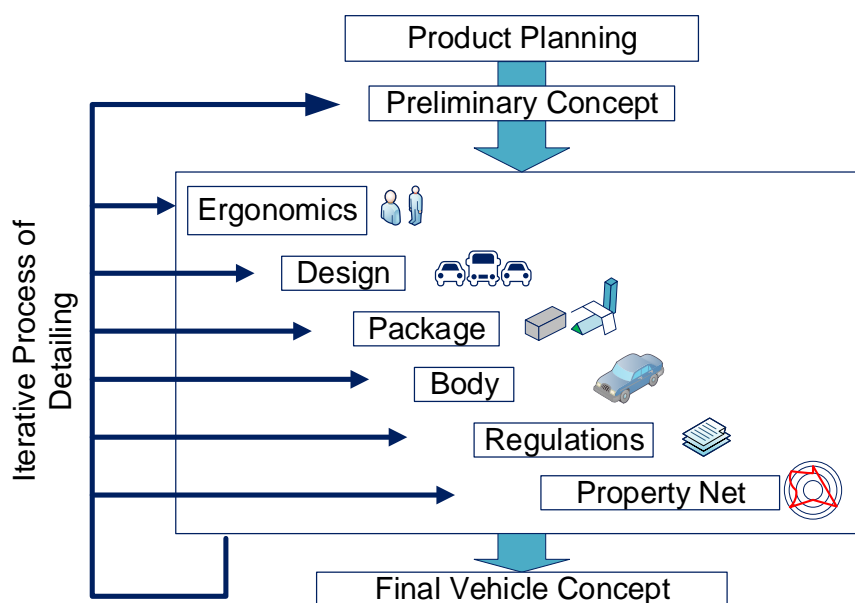
Figure 2-3   Concept Defining Process [51, 1.2 - 8]

We can see that the vehicle definition is an elaborate process and hence economic feasibility plays an important role in the development process. ASIEDU ET.AL. points out that around 70 % of the total lifecycle costs attributed to the early development phase [70].

2.2.2 **Vehicle Packaging in Early Concept Phase**

The vehicle packaging, in general, is the integration of all the components in the vehicle. The main challenge in the vehicle package design is the limited available space for the installation of the components. Certain components such as brakes or steering system have predefined constraints in terms of packaging. Thus, apart from geometric positioning and integration, vehicle packaging is influenced by several factors like functional interdependencies.

Therefore, an efficient concept package tool should consider a wide range of requirements and constraints before the design freeze [71, p. 604].

FRICK ET. AL. points out the vehicle package influencing factors and categorises them into five groups [71, p. 604]. Figure 2-4 shows the characteristics of vehicle packaging and influencing factors. The categories as shown are the design features, functional features, system specific features, costs, and external requirements.

The design features of vehicle includes the dimensional concept and the dimensions of the components as shown in Figure 2-4. The size of the components and the positioning of the components influences the dimensional concept and hence the overall vehicle concept. Functional features as shown are associated with the functions of the whole concept. This includes ergonomics, passive safety features and driving characteristics. Ergonomic being an important factor includes features like suspension kneeling for easy access, ramp for wheelchair access, etc. Therefore, the component sizing, position in the design stage should take these functions into account. Passive safety includes features such as seat belts, airbags and vehicle structure itself. The driving characteristics which are another functional feature comprise of features like vehicle acceleration and deceleration that are associated with comfort and performance of the vehicle and hence influences the packaging.

The system specific features as shown include the constructive integration and functional integration. For example, conventional vehicles and electric vehicles have different subsystems and functions that must be evaluated for both geometric and functional integration before finalizing the package. The costs definitely have a significant influence on the vehicle package. These are divided into vehicle costs, system costs and external costs. Furthermore, a vehicle package concept does not accomplish its objective, if it is not feasible to produce or run on the roads. To guarantee feasibility, close cooperation with the production department is mandatory [71]. A similar approach in vehicle packaging is used in the tool developed in this thesis.
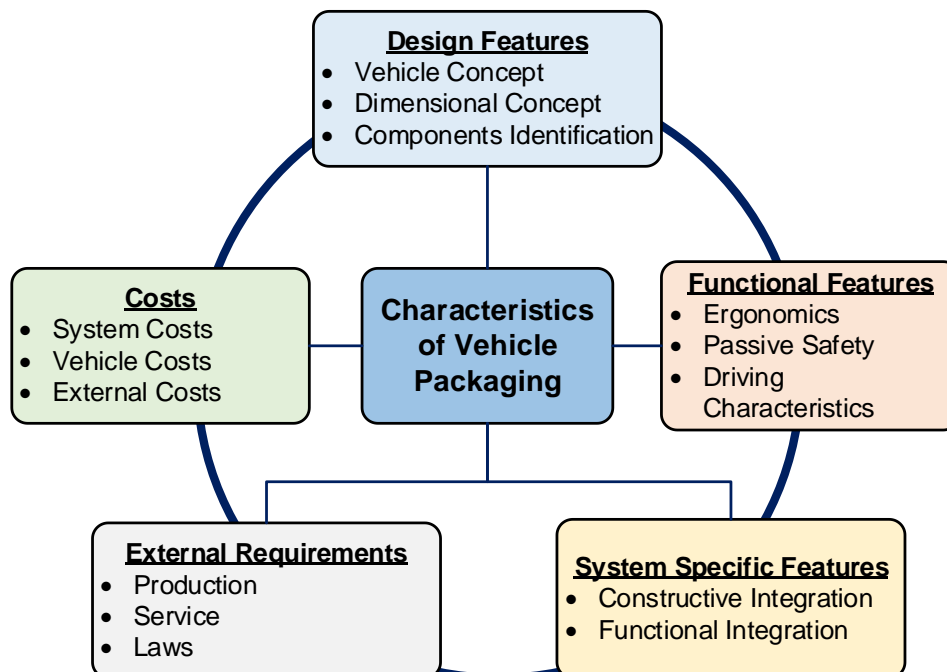

Figure 2-4   Characteristics of Vehicle Packaging, based on [71, p. 608]

As seen in the previous paragraphs, the packaging of components is a complex process in the vehicle concept development. This is because the components in the vehicle must fulfil all the functions but also should be installed in the available space within the package. As seen in Section 2.2, the vehicle packaging process consumes a lot of time in the development cycle. Standardization and improvement in packaging have a potential to reduce the time and most importantly the cost and most important a time reduction. The following paragraphs explain different packaging strategies.

Packaging Strategies

KUCHENBUCH published a book on the methodology for identification and design of package of electric vehicles. The author points out that the packaging of components can influence the properties of the vehicle and driving characteristics. For instance, during the 3D (three dimensional) design, the components such as the motor, battery, the suspension system are packaged in Methodology for identification and design of package optimized electric vehicles an efficient space-saving way but might not meet all requirements [72, 91 pp]. This is known as the 3D packaging problem and has been addressed in several works of literature [73–76]. In the following section, different packaging strategies are introduced and the pros and cons are discussed.

Absolute Packaging Strategies

CAGAN ET. AL. in their study describes that the components in a package cannot overlap with one another. Some components have predefined boundary conditions within which the other components cannot be defined. The package solutions with overlaps are considered invalid.

Centre of Gravity (COG) method is a vector based absolute packaging strategy that uses the position and directional vectors. Each component is assigned a vector based on the COG and the position and the direction are determined. In order to avoid the overlap between the components, all the objects are identified first as defined by MIAO [74]. The following Equations (2.1) and (2.2) show the calculations. The points SP_i are the centre of the area of the objects based on their coordinates in space. R_i is the distance between the centre of gravity and the boundary of the object in the corresponding direction in space. The objects overlap if both the equations are true [74] However, the COG method is only valid for objects with simple rectangular geometry. Polygon representation is appropriate for complex geometries [73].

$$| SP_{1X} - SP_{2X} | < R_{1X} - R_{2X} \tag{2.1}$$

$$| SP_{1Y} - SP_{2Y} | < R_{1Y} - R_{2Y} \tag{2.2}$$

The alternative method in the absolute packaging strategy is segmenting the available space for packaging into several discrete sections. The objects are arranged based on the position vector and the direction vector as seen above. In this method, if any defined section is occupied by two different objects, it results in an overlap. This method is also called a voxel method in several studies [74, 77–79]. A voxel is a term defined by combining volume and pixel. This method can be applied to complex geometries [80].

Figure 2-5 illustrates the overlap or collision detection infinite segmentation method with an example [72, p. 75]. As shown, each section is associated with coordinates. The sections occupied by individual components are assigned with value '1' and empty sections are

assigned with '0'. If there is an overlap or collision, the section is assigned with value '2'. These values used in the representation are used in packaging optimisation.
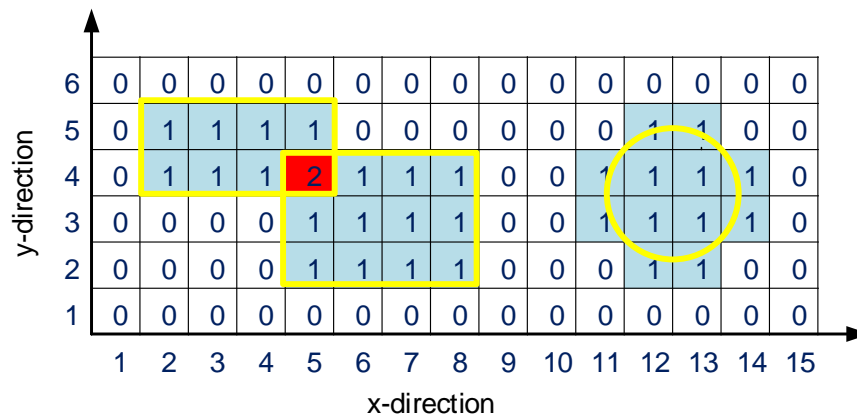

Figure 2-5   Collision-detection using finite segmentation method [72, p. 75]

However, the precision of mapping depends on the resolution of the segments. For a vehicle package with large volume, if the resolution is small, it would result in millions of segments. Each segment is evaluated for finding an overlap or collision and hence the computing time in this method increases. Several studies in the optimization of the packaging processes focus on reducing computing time for the absolute packaging strategies as seen above. However, avoiding the collisions from the start is possible with relative packaging strategies, which are described in the following section.

Relative Packaging Strategies

In the book by KUCHENBUCH, the author described different relative packaging strategies and are discussed briefly in this section [72, 76 pp.]. As discussed above, the disadvantage of absolute packaging is high computing time while evaluating all the possibilities of packaging. In order to overcome this, only the valid packaging configurations have to be considered. Relative packaging strategies eliminate the collision or overlap of objects and the packaging process is executed based on mutual location relations [72]. JACQUENOT recommends the usage of geometrical relations which is based on the heuristic method instead of error values [81].

Several publications using the relative packaging in different fields were listed by [72]. YAO, CHEN ET AL. [82] and CHEN, CHANG [83] applied the method to solve floorplan and VLSI (very large scale integration) packaging problem with the focus to package all objects and minimise the packaging area. The disadvantage with the relative packaging is that the method does not display all the solutions. Figure 2-6 illustrates different approaches in the floor plan packaging problem: (a) slicing floorplan, (b) mosaic floorplan and (c) general floorplan.

As shown in Figure 2-6 (a), the slicing floorplan method cuts the available area into vertical and horizontal sections [84]. Mosaic structures, as seen in Figure 2-6 (b) is characterised by T-junctions, also known as corner blocks. For the problem published by YAO, 745 million solutions were found with slicing floor plan [82], whereas 2 billion solutions were found with mosaic floor plan [85]. Another efficient evaluation of the whole solution area is possible through the general floorplan where the order of the positions of the objects are determined in the horizontal and vertical direction to finally reach the arrangement. [82, 86, 87].
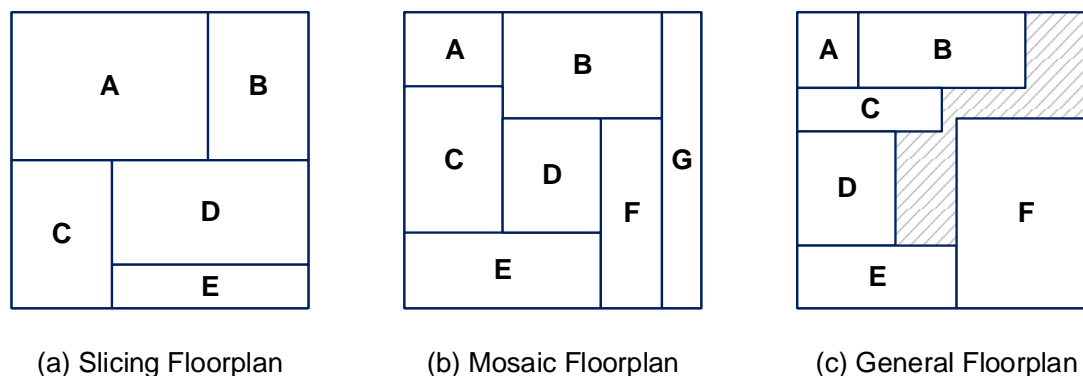
| (a) Slicing Floorplan | (b) Mosaic Floorplan | (c) General Floorplan |

Figure 2-6   Floorplan Representations for a 2-D packaging problem [82]

2.3 Parametric Modelling in Vehicle Concept Development

The previous section explained the influencing factors in vehicle packaging and the state of the art approaches or techniques used in the efficient packaging of the components. However, it can be seen that the packaging strategies only work independently and components do not influence each other based on the requirement of the vehicle package. The primary focus of the proposed vehicle packaging tool is not the creation of new vehicle package for AEVs but improving the speed and flexibility of the vehicle development process. Thereby the resulting vehicle package is adaptable and scalable for different user requirements.

This goal can be achieved by parameterization of the overall vehicle model and all its components. The objective of parametric modelling is to define the complete vehicle package by several mathematical models that interconnect the individual elements within the vehicle concept [88]. The parametric modelling is a technique controlled by numerous parameters. Parameters can either be dimensional parameters or other parameters, such as logical or decision parameters, selection parameters and material parameters. The parametric models allow the definition of dependencies between the components and their geometric models. Thus the geometry can be defined among themselves as well as control the parameters and geometry of other components [89].

Compared to the conventional design, the parametric design requires a higher degree of information and deeper knowledge in the early development phase of the project and hence required higher initial expenditure. Figure 2-7.illustrate the design expenditure comparison. However, it can be seen that the overall expenditure reduces with a balanced cost distribution over time [28]. Another study by KUKEC clearly explains the reduction in time in the vehicle development process [26]. In the comparative analysis between the parametric and conventional modelling, the author demonstrates a significant time reduction with a maximum time savings of 78 % and a minimum time saving of 55 % for the parametric model. The author used a custom-built GUI to minimize the errors during the development process [26]

As discussed above, it is evident that the parametric modelling would help the manufacturers in reducing the time taken for vehicle development. However, only limited research is available for the complete development of the vehicle package. This thesis presents a holistic vehicle concept development tool which is completely parametric. The tool includes parametric

models to size various subsystems and components and a parametric CAD model to visualise the vehicle concepts. The following sections explain some existing studies related to parametric tools for developing vehicle concept and parametric CAD modelling. Furthermore, the advantages, disadvantages and the research gaps are addressed.
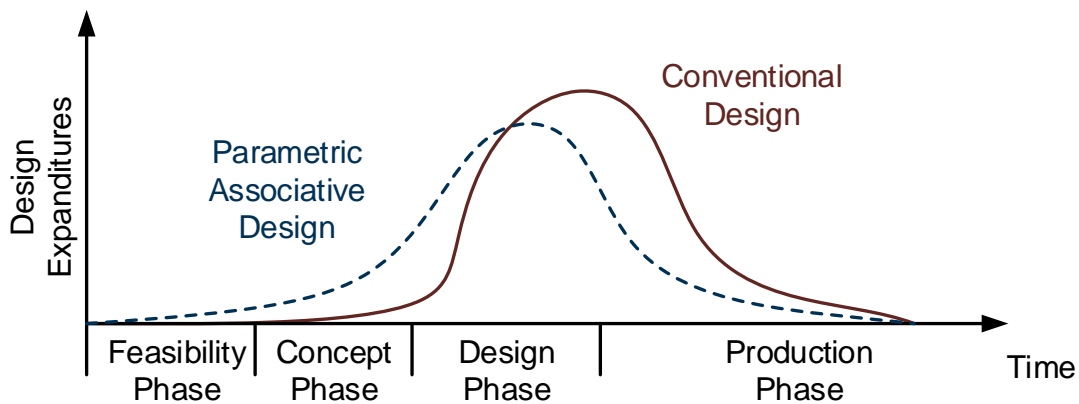

Figure 2-7   Design Expenditures Comparison [28]

2.3.1 Existing Methods in Parametric Vehicle Concept Development

This section discusses the existing tools in vehicle concepts development using the parametric modelling approach. [72, 90, 91] developed and executed different methods for parametric vehicle concept development for vehicle types of passenger cars and trucks. The scope of the methods developed by each study is however different. Some methods analyse the solution space within one vehicle concept. Some methods generate and compare multiple vehicle concepts. The parametric vehicle modelling requires several component models for the development of the package. Such models can be either database, regression models or empiric and physical models in order to select and scale the components.

Table 2-2 lists all the studies compared and provides an overview of the studies for parametric vehicle concept development. Table 2-2 clearly shows the type of vehicle concept developed, the component systems considered, and the solution areas the study addresses. Based on the focus of the investigation of each study, the methods compared are categorised into these six solution areas, namely,

- Component Size (1)
- Component Type (2)
- Control Strategy (3)
- Vehicle Concept (4)
- Topology (5)
- Transportation Type (6)

For the development of a holistic vehicle model, (1) and (2) are mandatory since all the components have to be sized and selected. Besides, Table 2-2 shows the studies using component databases for selection. The criteria used for the component selection with and without the database are explained in the following section since the tools with and without databases are investigated.

.

Table 2-2   Overview of the Existing Literature

Work	Vehicle Concept Type	Considered Components	Solution Area	Component Database	Component Selection Criteria
FRIES ET AL. [90]	Passenger Cars	Hybrid Powertrain	(1) (2) (4) (5)	No	-
KUCHENBUCH [72]	Passenger Cars	Overall Vehicle Design	(1) (4) (5)	No	-
FUCHS [91]	Passenger Cars	Overall Vehicle Design	(1) (2)	No	-
WIEDEMANN [92]	Passenger Cars	Electric Powertrain	(1) (2) (4) (5)	No	-
MATZ [93]	Passenger Cars	Electric Powertrain; Suspension Components	(1) (2) (4) (5) (6)	Yes	Not specified
RIED ET AL. [94]	Passenger Cars	Hybrid Powertrain	(1) (2)	Yes	Not specified
FÖRG ET AL.[95]	Trucks	Overall Vehicle Design	(1), (2) (4)	Yes	Not specified

2.3.2 **Tools without the Component Database**

This section discusses the vehicle concept development tools that do not use databases for the components modelled as described in Table 2-2.

The tool developed by FRIES ET AL. [90] is a tool for optimizing the operational strategy of electric hybrid commercial vehicles. The primary focus is on the total cost of ownership (TCO) which is mainly influenced by the fuel costs. The fuel costs can be minimized by combining the route information and predictive cruise control system. The model uses a genetic algorithm based in Matlab/Simulink to optimize the variables. In the vehicle concept optimisation, the simulations used three different hybrid configurations with different energy storage systems, motors and engines. The results showed total power savings ranging between 8 % and 11 % based on the powertrain configuration. Apart from the drivetrain components, the model did not include influence and selection of other subsystems such as chassis, heating or cooling, etc.

KUCHENBUCH [72] developed a holistic vehicle concept tool to generate electric passenger cars. The tool considers vehicle properties, geometric packaging, ergonomics etc. The 3D CAD model of the tool enables a simple visualisation of the drivetrain, battery systems, suspension system and the passenger compartment. The absolute and relative packing strategies used by the author for packaging the CAD model were explained clearly in Section 2.2.2 in detail. Figure 2-8 shows the vehicle package visualised with the tool. As shown, the simple CAD model can also display the suspension of a developed vehicle concept. No further information concerning the suspension or brakes development, sizing and selection were provided.
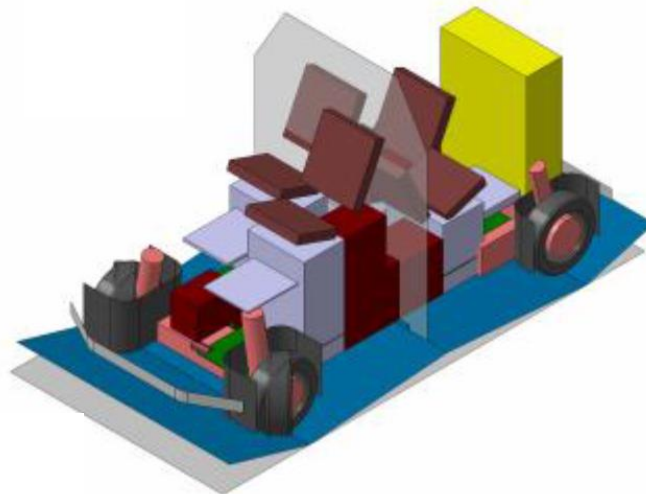

Figure 2-8   Visualisation of the Concept [72]

FUCHS [91] developed a vehicle packaging tool for the development of electric passenger cars and to estimate the mass of the concept. The estimation of the mass is parametric and is influenced by numerous vehicle parameters such as the exterior dimensions of the vehicle, size of components, components architecture, type of vehicle structure, vehicle characteristics such as intended range, passenger space, boot space and longitudinal dynamics characteristics such as maximum speed, acceleration, etc. In his work, the author describes that the selection of components significantly influences the mass of the vehicle concept. Based on the mass of the concept, the tool can choose different chassis components such as

the McPherson struts and axles or multi-link suspension and axles and sub-frames [91, p. 42]. However, the author did not provide an explanation of the selection process of the chassis systems. Since the tool was focussed on detailed mass estimation model, the tool did not provide any visualisations of the developed concept.

WIEDEMANN [92] developed a tool to generate electric vehicle concepts for different passenger car types with the aim of optimizing customer-specific properties. The tool considers both the customer requirements and technical specifications during the process of concept development and analyses them using complex correlations. This is achieved through the implementation of property-based concept development. Figure 2-9 shows an illustration of the method used by the tool. At the beginning of the development process, the user specifies target vehicle properties with 28 customer-relevant parameters. By correlating technical specifications with a property value scale, the developed concept can be automatically compared with the target specifications. All property values are combined in a holistic evaluation function. The genetic optimisation algorithm is used in the search for the global optimum. The tool does not include a three-dimensional visualisation of the vehicle concept. The tool uses two-dimensional vehicle plots, and vehicle property comparisons are displayed with the help of spider plots. The author does not provide information on the selection and sizing of the component systems such as chassis, body, etc.
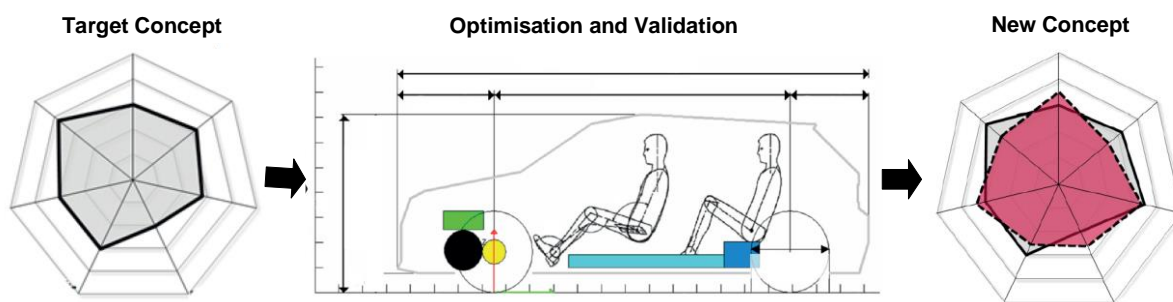

Figure 2-9   Property Based Vehicle Concept Development Tool [92]

2.3.3 **Tools with a Component Database**

The vehicle concept development tools introduced in the previous section did not include a database to size and select the components of the vehicle package. They rather used some regression models. This section discusses about the tools using component databases and attempts to analyse the component selection criteria of each of the tools discussed.

Matz [93] developed a tool to develop optimised battery electric passenger car concepts. In order to develop the overall vehicle concept, the author defines three parts namely, dimensional concept, the topology and the component sizing and selection. To accomplish this, the tool comprises of a complete parametric model that includes vehicle longitudinal dynamics, a package model and 28 customer-relevant vehicle properties based on [92]. For the packaging of the components into the vehicle concept and avoid geometric collisions or overlap, the tool uses a Java library called as the jReality developed by Technical University of Berlin as shown in Figure 2-10 [96]. Similar to the other approaches, the tool uses a multi-objective optimisation algorithm, to identify the best architectures based on the vehicle requirements. The component-specific information is stored in databases of the tool. The vehicle assembly module in the tool accesses the database and selects the required components. Besides electric powertrain components, the assembly module also selects tires and suspension components. The author did not provide information regarding the selection

of chassis components from the database. The tool includes a basic three-dimensional visualisation of the vehicle concept.
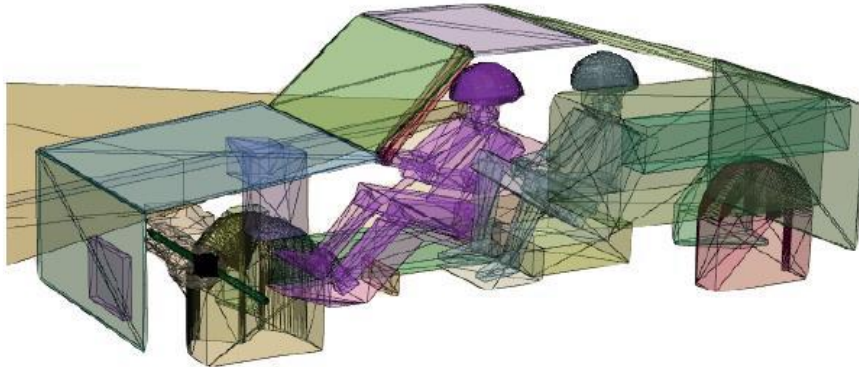

Figure 2-10   Visualisation of the Concept within the Tool[93]

RIED ET AL. [94] developed a parametric tool for development for plug-in hybrid electric vehicle (PHEV) concepts. Figure 2-11 provides an overview of the tool. As shown, the tool comprises of three modules namely the overall vehicle concept, the topologies and the component models. The overall vehicle concept includes input parameters such as the exterior and interior dimensions. The parametric component models include the primary powertrain components such as the electric motors, batteries, internal combustion engines, transmission etc. The vehicle topologies include the possible powertrain architectures. The objective of the tool is to analyse the solution space of the PHEV based on the battery volume. The battery is restricted to the underbody of the vehicle and hence only powertrain architectures are possible. The vehicle concept generated can be visualised in 3D with a parametric CAD model developed using the software CATIA [21]. The tool has a GUI to process user inputs. The parameter is communicated to CATIA through Visual Basic for Applications (VBA) macros. The 3D model is basic visualisation showing the interior exterior and components. Since the tool focuses on the powertrain, the chassis, suspension is not discussed in the component selection process and the authors did not provide the selection criteria of these components.
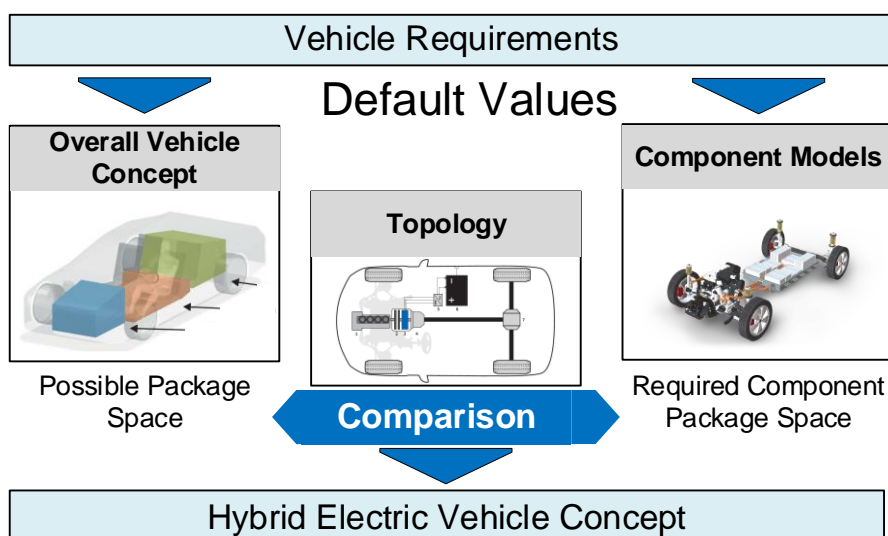

Figure 2-11   Overview of the tool, based on [94, p. 24]

Förg et al.[95] developed a method and tool to generate multiple commercial vehicle concepts and to standardise them. The tool allows one to manually define the architecture of the vehicle concept by selecting components from a database. The tool database is limited to internal combustion engine vehicle components. The tool proposes component types and installation positions based on the standards of predefined vehicle architectures. The tool rates the generated vehicle concept on the overall degree of standardisation. The tool supports the manual generation of concepts and the identification of architectural standards. However, the tool does not include any automation to identify the best solution. The resulting design vehicle concepts are presented as CAD models as shown in Figure 2-12.
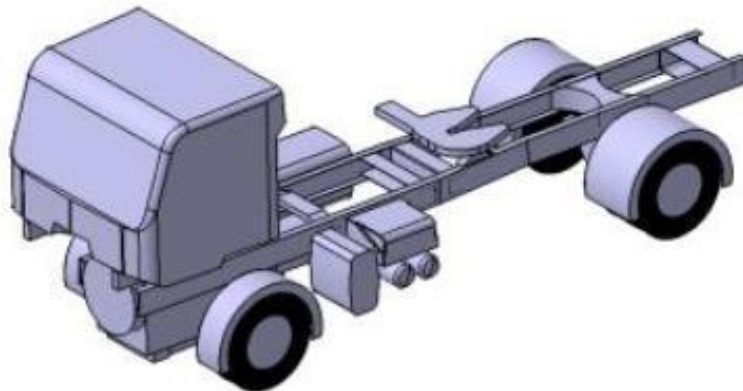
Figure 2-12   Visualisation of the Concept within the Tool [95]

2.4   Research Gap

Section 2.1 explained the increasing demand for autonomous and electrified bus systems and summarised the areas of research. The analysis clearly showed the advantages of the electric powertrain due to its design flexibility, efficiency and potential for environmental sustainability. The studies also showed the real time feasibility of the autonomous and electrified buses for public transportation. However, the AEVs currently in use are functioning as shuttles with a maximum length of only around 6 m. In order to be operated in public transits, the AEVs have to be developed in different passenger capacities based on the requirement of the target city.

Therefore, development of new AEVs plays an important role. Section 2.2 explained that the vehicle development process can take up to 6 years and the processes should speed up in individual phases. In addition, it was seen that the early concept phase is the most time consuming and expensive phase because the most important decisions regarding the vehicle specifications and package are taken here as discussed in Section 2.2.1. Section 2.2.2 discussed various steps and strategies suggested and used by the manufacturers in the vehicle packaging. However, in order to cater the iterative process of vehicle concept development, an approach of parametric sizing and packaging of the overall vehicle concept can improve the development process in the early phase as discussed in section 2.3.

The literature review in Table 2-2 of Section 2.3.1 showed different existing approaches for vehicle packaging and parametric modelling. However, most of the studies were restricted to vehicle type of passenger cars with a maximum of 5 seaters. It can be seen that majority of researcher only focussed on the optimisation of the powertrain and the powertrain architecture in the early vehicle concept phase. The tools with and without the component databases did

not provide any specific selection criteria to select and size the chassis components such as suspension system, braking system, tires, wheel and vehicle structure. The tool on concept development of commercial vehicles was based on standardisation of the components and parts and focussed mainly on the frame-mounted components. Therefore, they had a lack of models for scaling continuously. Also, the outcomes of the tools are basic 3D CAD models of the package with simple geometries. Additionally, none of the literature reviews showed that the studies have included the sizing and selection of the air conditioning system and its influence in the powertrain sizing.

Consequently, there has been no consideration of parametric packaging development for autonomous and electric vehicle types of buses/minibuses for vehicle sizes between 4 m – 14 m. Such a tool would reduce the development time for generating bus concepts and hence would result in the possibility of having several bus sizes to enhance the service quality of public transport.

3 Methodology

The tool development process requires a well-structured method and defined processes to generate the expected results and meet the desired requirements. This chapter provides an overview of the AEV Tool in the first section followed by the definition of the requirements. Section 3.2 explains in detail the framework of the method applied in the tool development. Furthermore, the initial vehicle specifications are discussed in Section 3.3. Section 3.4 explains the definition of the vehicle that include exterior and interior layout planning and the decision of components and subsystem are explained in the final Section 3.5.

3.1 Overview of the AEV Tool

Figure 3-1 illustrates the basic overview of the proposed tool. The resulting holistic tool facilitates the users to generate autonomous electric vehicle concepts in the early phase of the development. The steps involved in the vehicle concept development as shown in Figure 3-1 are

- Vehicle specifications- (Passengers, Vehicle dimensions, Interior and Weight)
- Powertrain selection and sizing (Motor, Transmission, Battery and Inverter)
- Chassis system selection and sizing (Axle, Suspension, Brake and Wheel)
- Cooling system selection and sizing (Condenser, Evaporator, Cooler)
- Energy consumption analysis (Consumption through a driving cycle and Energy loses)
- Cost estimation of vehicle package (Powertrain, Chassis and Vehicle Cost)
- Life Cycle Assessment (LCA) of the generated vehicle concept

The first step is the vehicle specifications, which includes the dimensions, glider weight (vehicle weight excluding powertrain) of the vehicle based on basic user inputs and basic parameters such as the number of passengers, preferred interior seating layout (Coach bus layout, City bus Layout). Next step is the selection of the powertrain subsystem based on the weight and dimensions and of the vehicle concept. The selection offers multiple variants in terms of powertrain architecture and the desired range of the vehicle. Subsequently, the chassis components and Heating Ventilation and Air-Conditioning (HVAC) components are sized and selected from the available components database. The program also calculates different elements of energy consumption and estimates the cost of the vehicle concept generated. One output is a spider chart that gives the users an overview of the characteristic of the generated vehicle concept. The tool is able to provide a precise estimation of the life cycle emissions of the generated concepts. It is possible to create multiple concepts and to compare them simultaneously. Finally, in the last step, the designed vehicle concepts are visualised as 3-Dimensional Computer Aided Design (3D CAD) models.

The tool uses a parametric 3D CAD model developed by the author with CATIA for the visualisation of the vehicle concepts [97] and parametric functions developed using MATLAB for the generation of new concepts. Through a graphical user interface (GUI) in MATLAB, all parameters of components and measurements required to define the model can be changed or adjusted. The parameter changes in the GUI have a direct impact on the CATIA 3D visualisation of the vehicle concept.
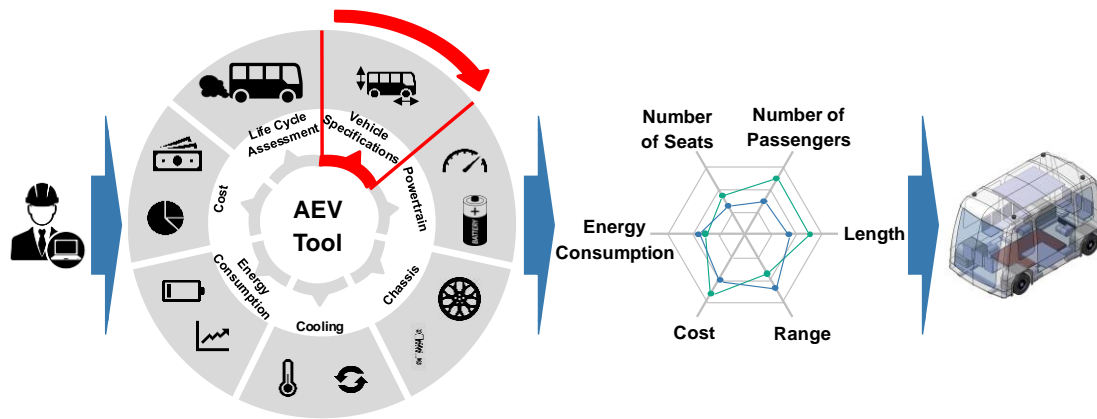

Figure 3-1   Overview of the AEV Tool

To ensure a clear and structured workflow of this work, the target requirements of the tool are discussed in detail.

Modes of Operation

Users have different levels of knowledge. For instance, in an automotive OEM, there are people with different specializations and hence different expertise and knowledge in regard to the design of a bus [98–100]. Hence, the tool development should address this difference in the levels of knowledge and two work modes are defined in this work. One mode, in which the concept development is automated by limiting the scope of the user selection. All the calculations required to create a vehicle package happens in the background automatically. Another mode, in which each component required to define the vehicle can be sized individually and thus requires greater expertise.

Scope of Components

The vehicle concept is defined by all the components that are important for packaging. Moreover, each component is associated with a 3D CAD model along with the material properties in CATIA. To ensure the best combination of all the components for the AEV and to provide a cost and energy-efficient vehicle, all the major sub-systems have to be taken into account as explained in section 3.1. Different layouts of seating configurations are developed and compared with each other.

Joint Interface

Several models and algorithms are developed and used in the AEV Tool to size and select various components. Consequently, it must be ensured that all the parameters of the individual models interact with each other in the AEV Tool. A joint interface ensures communication between the models, convert the parameters and adapt them to the system.

Expandability of the tool

The AEV Tool should be modular and flexible to integrate new models and functions. The tool structure should enable users to implement new parameters and configurations. Furthermore, the structure of the CAD model has to be expandable, so that a user can add more assemblies, parts and parameters to the parametric bus model.

Usability of the tool

The AEV Tool is operated by a graphical user interface (GUI) which is based on MATLAB. The user interface provides the foreground for the inputs and outputs while the calculations are processed in the background. Therefore, the usability of the tool is an important requirement. The goal of the tool is to create vehicle concepts in a short time, so the GUI should be easy for the user to achieve its objective.

Performance of the Tool

The stability of the program should be ensured when used. The tool interacts with different software programs and different databases for component sizing and visualization. Incorrect user inputs are the main cause of program instability. To avoid incorrect or missing user inputs, the algorithm of the tool has to be implemented with error and warning messages. The performance of the tool can be optimised for speed by improving the code in MATLAB.

3.2 The Framework of the Method

Figure 3-2 illustrates the framework of the approach used in the development of the AEV tool. The implementation of each module, components and the development of a common interface, as well as the user interface, is explained in the following sections.

The structure of the method is divided into four phases: Input, Definition, Design and Results Evaluation as shown in Figure 3-2. The input phase comprises of all the vehicle specifications required for the vehicle concept development. The specifications are derived from the general vehicle policy and legal requirements and explained in Section 3.3. In addition, the benchmarking of existing vehicles and vehicle technologies provides insights into the evolving technologies. Benchmarking helps to understand packaging strategies of different companies as seen in Section 2.1. The benchmarked vehicles are used to validate the concept generated by the AEV Tool in addition.

The main constituents of the definition phase are the vehicle and the components definition and definition of all parameters required for the vehicle concept development. The vehicle definition includes the classification of vehicles/buses. In this work, the tool can develop three vehicle concepts classes namely, the city bus, the coach bus and the shuttle. Each vehicle classification is distinguished mainly by the vehicle layout. The vehicle layout definition includes several factors like the permissible vehicle dimensions, maximum and minimum number of passengers and the interior design, such as the seating arrangement and the standing area. Section 3.4 explains the definition of a vehicle. The vehicle concept development includes the packaging of several components and subsystems. Therefore, all the package relevant components have to be identified and classified into respective subsystems based on their interactions and interdependencies. Furthermore, algorithms for sizing all the component systems are defined and is explained in Chapter 4 in detail. The

vehicle definition and component definition in combination lead to the definition of all the parameters used in the parametric model.

The main elements of the design phase are the design of the parametric CAD vehicle model, the architecture of the AEV Tool and a joint interface. The joint interface provides the interface between the parametric CAD model and functions of the tool and helps to translate the user inputs into the tool parameters to generate and visualise new concepts. CATIA software is used to design the 3D parametric CAD model of the vehicle concept [21]. The structure of the design is important for the parametric CAD model. Therefore, the model is designed with different coordinate systems, boundaries and constraints. Each subsystem and components are designed using the defined parameters and the CAD model is automated to function coherently with the other mathematical models and respond to vehicle concepts of different sizes. The design of the CAD model is explained in Chapter 5 and CAD automation is explained in Section 6.2.6. The architecture design of the tool includes the implementation of different modes of operation as explained in the previous section. Chapter 6 discusses the implementation of different operation modes in detail. The subsystems and their components are selected from multiple database models and the selection processes are controlled by backend functions.
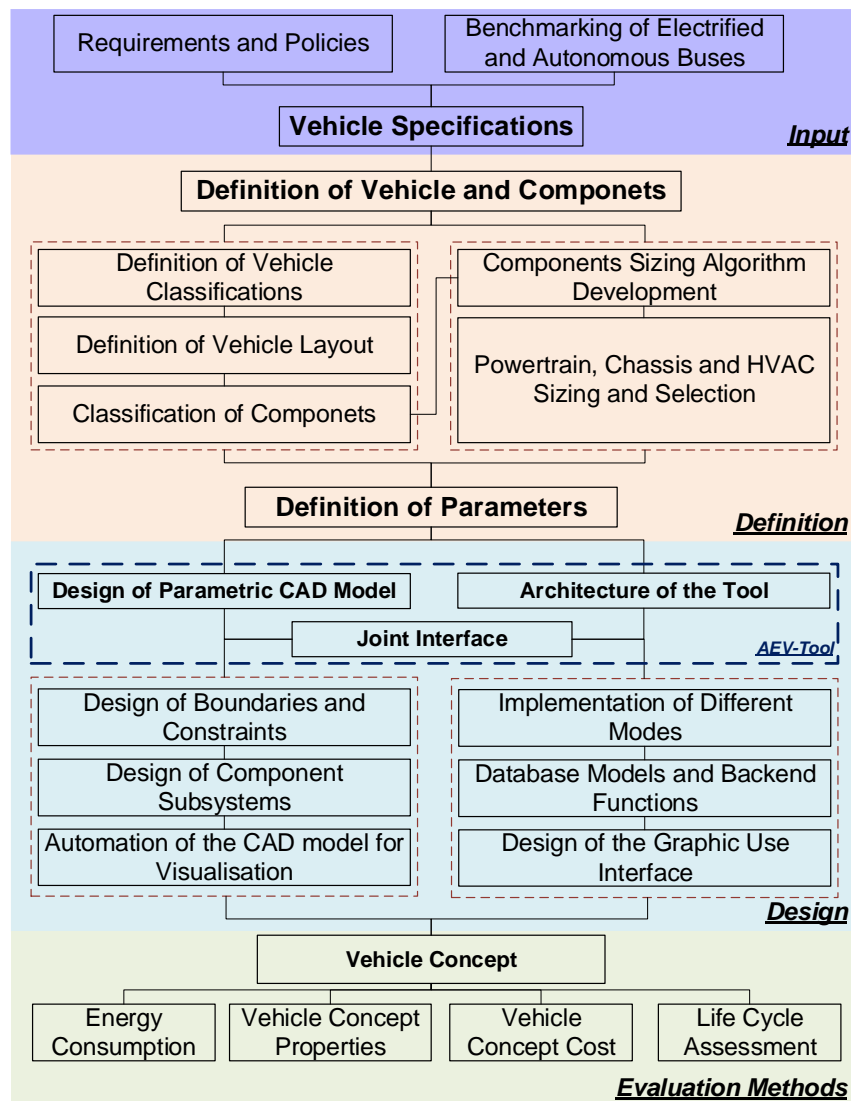

Figure 3-2   Framework of the Method.

Chapter 6 provides an extensive overview of the database approach and functions. A well designed is GUI is required to provide ease of use to the user and MATLAB software is used for GUI design and is explained in Section 6.4.

The primary result of the AEV Tool is the vehicle concept. However, it is important to evaluate the generated concepts. Chapter 7 explains all the evaluation methods. The energy consumption of the concept is evaluated using a longitudinal dynamics model. The initial costs of the concept are calculated using several cost models and a detailed LCA model is developed to evaluate the emissions from the concept. The other vehicle properties such as the dimensions, passenger capacity, number of seats, etc. are evaluated and are visualised in combination with a spider chart.

3.3 Vehicle Specifications

As described in the previous section, the first step to identify the required vehicle specifications is to analyse the legal vehicle requirements and the policies. In addition, benchmarking of existing vehicles provide all the necessary information to define the vehicle systems as explained in Section 2.1. Vehicle benchmarking analysis provides the list of the necessary subsystems of the vehicle while providing insights to upcoming technologies to be implemented in future vehicles.

The road vehicle requirements are distinct and unique for each country and primarily depends on the regulations and existing infrastructure. The vehicle requirements in this thesis are based on the regulations of Singapore. Complete set of requirements required for a road transit vehicle in Singapore are explained in standards called, (i) The Road Traffic Rules of Singapore [101, Sec. 2,4,6,8,44,99]. (ii) Existing reports of the Land Transport Authority of Singapore namely, the "Bus Bay Dimensions" that discusses the infrastructure requirements and the "Street Hump Design Guidelines" that helped to define parameters such as ground clearance are taken into consideration [102, 103].

Table 3-1 provides a list of the vehicle specifications required, subsystems and the component requirement derived from vehicle benchmarking, regulations and policies of Singapore. The specifications of the vehicle concept are defined on the basis of the list of requirements and parameters.

Vehicle type and size includes the vehicle classification i.e. the coach, city bus and the shuttle, and the specifications defining external vehicle dimensions, ground clearance and the passenger capacity. Vehicle body and structure describes the type of vehicle structure such as space frame or monocoque, the exterior layout, doors and its parameters. The interior layout of the vehicle includes the seats, seating layout, accessibility features such as step-free floor and the defined space for wheelchairs, emergency exits, etc. Powertrain subsystem includes the battery, motors, inverters, transmissions and other power electronics components. There are several possible powertrain topologies and this influences both the vehicle packaging and the performance of the concept. A detailed explanation regarding the influence is powertrain configuration is provided in the next section. The chassis subsystem primarily consists of the suspension, brakes, steering, wheel and tire. The position of the chassis components is defined in the vehicle layout and hence have a fixed position in the vehicle package. However, additional functions can be incorporated to improve the performance or function of vehicle concepts such as kneeling system integrated into the air

suspension system to improve accessibility. Similarly, the requirement of the HVAC and CAV systems are defined as shown in Table 3-1.

Table 3-1   Required Vehicle Specifications Parameters

Requirement	Description
Vehicle Type and Size	• Vehicle classification • Length • Width • Height • Ground clearance • Passenger capacity
Vehicle Body and Structure	• Type of structure • Exterior layout • Number of doors • Door width
Interior Layout	• Different seating configurations • Accessibility and Wheelchair space • Emergency Exits
Powertrain	• Battery • Motor and Transmission • Power electronics
Chassis	• Suspension System and Kneeling system • Braking System • Air compressor capacity • Steering system • Wheel and Tire • Axles
HVAC	• Air conditioning • Heat Exchangers • Compressor
CAV Components	• LIDAR • Cameras • Ultrasonic Sensors • Computers

3.4 Definition of Vehicle

As explained in Section 3.2, the definition of the vehicle follows the input vehicle specifications in order to plan the vehicle boundaries and packaging of components. The layout of the vehicle is required to be changed based on vehicle classification and passenger capacity. The following sections discusses the influence of the exterior and the interior layout on the vehicle concepts and further discusses the influence of components on the layout definition.

Generally, the exterior and the interior layout of a bus is composed of components such as the vehicle body, windows, doors, seats, standing area, grab poles and handles, emergency exits, etc. Hence, the passengers are the major stakeholders in the vehicle exterior and interior layout and to define them, the ergonomic measures of the passengers are important. The anthropometric body size dimensions are summarised in Figure A-1 and Table A-1 in Appendix A based on [104, 105] The anthropometric data provides the space requirement of the passengers and section describes the important parameters for the design of exterior and interior.

3.4.1 Exterior Layout

Vehicle Body and Windows

The vehicle body, windows and the doors are the main constituents of the vehicle`s exterior. The design of the vehicle body depends on the aesthetics and form of the vehicle. However, ergonomic and anthropometric considerations have to be accounted for the design of windows and doors. Figure 3-3 illustrates the field of view of the passengers. Both sitting and the standing passengers are taken into account. It should be noted that 5th percentile female and the 95th percentile male are taken into account as proposed by OPENSHAW, TAYLOR; [106]. As shown, the lower body section (940 mm) provides the necessary impact structure for passenger crash safety and on the other hand, the window area provides the visibility for free sight to the surroundings outside of the bus. The gangway height regulation of 1800 mm [101] for vehicle seating capacity more than fourteen passengers has been considered. The door height is fixed to 2225 mm for better comfort and accessibility.
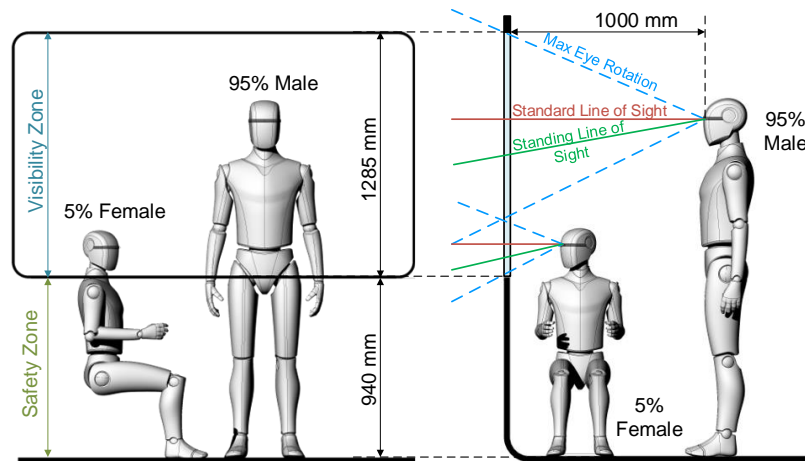

Figure 3-3   Anthropometric Field of View [107]

Vehicle Entry Height

The entrance height of the vehicle and the platform gap (the gap between the vehicle and the curb) influences the accessibility of passengers especially the wheelchair users during boarding and alighting. The standard curb height of 150 mm has been defined by Singapore`s Land Transport Authority (LTA) [108]. In order to improve the accessibility, the vehicles are implemented with suspension kneeling, 4 wheel steering and a ramp. Figure 3-4 provides an illustration of the kneeling system and the ramp considered in the vehicle definition of the AEV

Tool. As shown, the suspension kneeling function of the suspension system helps to lower the height of the floor by lowering the vehicle cabin and a ramp helps to close the platform gap. It should be noted that the vehicle kneeling affects the ground clearance of the vehicle as shown and is taken into account in the package definition.
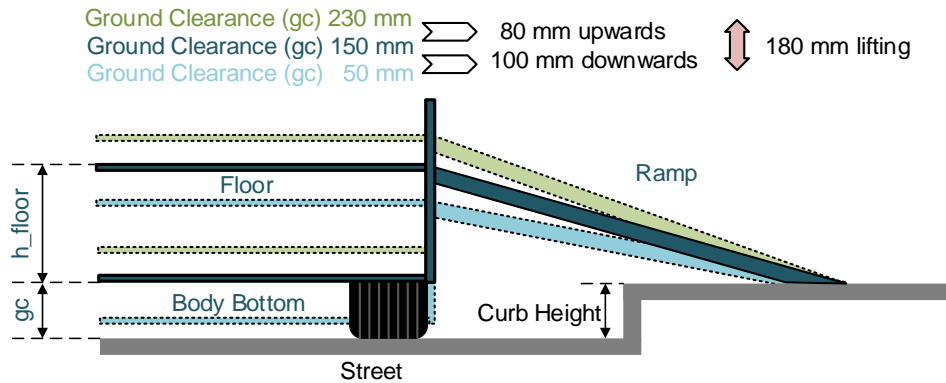

Figure 3-4   Illustration of Suspension Kneeling and Ramp

3.4.2 Interior Layout

To facilitate a block free access within the vehicle, specifically for the wheelchair users, the floor of the vehicle in passenger cabin is targeted to be step free or flat.

Passenger Seats

The seat dimensions and the space around the seats are derived from the UNECE R080 seat dimensioning release [109]. Based on the regulations of Singapore, the passenger seats might be placed towards the forward or backward direction, and might also be placed sideward facing the gangway [101, Sec. 86]. Around 300 mm of leg clearance should be provided by the seats based on the UNECE regulation No. R036 [110, Ch. 5.7.8.5.2]. Apart from the minimum passenger seat dimensions, no other directions or boundaries are provided regarding the minimum area for seating passengers [101, Sec. 86, 111].

Sitting and Standing Passengers:

According to UNECE regulation R036 [110], the number of fixed seating spots should be at least the area available for passengers in m^2 (or 90% of this area) [110, ch. 5.3.1]. Otherwise, there are no seating-to-standing ratio regulations mentioned for the passengers. An area of at least around 0.125 m^2 (0.150 m^2) for standing passengers is recommended [110, ch. 5.3.2.2]. Another recommendation based on LEVIS suggests around four - six passengers per square meter, which results in an area of 0.167 m^2 to 0.250 m^2 per passenger [111].

3.4.3 Influence of Components

The component systems have a significant impact on vehicle packaging. For instance, chassis systems such as suspension, brakes, wheel, the tire have fixed positioning or placement within the package. However, powertrain or HVAC have more freedom and hence influences the

package development process. This section describes the impact of powertrain components and configurations.

Figure 3-5 shows the different powertrain configurations for electric buses. The figure shows the motor, battery, inverter, gearbox, differential and auxiliaries. As shown, several configurations include multiple motors, inverters and transmissions. These configurations thus influence the overall bus concept in terms of the vehicle's package, performance, and cost and weight distribution. The author in an earlier study examined several powertrain configurations for electric city buses and compared different powertrain layouts with each other [42]. The study evaluated eight different powertrain configurations and showed a significant change in the performance and energy consumption between them. Therefore, this work includes multiple configurations for evaluation and the visualization of the concept.
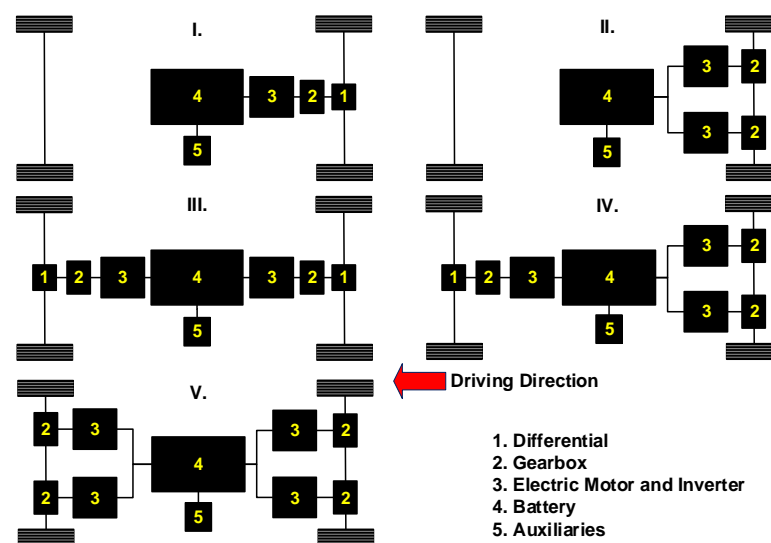
Figure 3-5   Different Powertrain Configurations for Electric Buses

The battery is one of the heaviest components of an electric vehicle. Positioning the batteries is important because of its impacts on vehicle dynamics, packaging and safety. Current buses position the batteries on the roof, floor or on the sides. Since it is associated with safety, the study published by German In-Depth Accident Study (GIDAS) is used in our approach [112]. The study evaluated deformations of 2293 types of accidents and deformations of more than 20000 passenger vehicles. The evaluation results of the deformation frequencies provided a recommendation of safe zones for battery placement. [112, 113, p. 82]. The space in-between the front and rear axles with sufficient safety distance from the lateral sides of the vehicle is suitable for the safe battery placement. This space competes with interior space in general and thus, requires a trade-off between them. Therefore, in this work, the battery compartment is designed and located under the floor between the axles and is limited by the space between the wheelhouses.

3.5 Definition of Components

For the design of vehicle concept and definition of all the necessary parameters, the definition of components is essential. Components in vehicle concepts are defined majorly based on their specific functions, interdependency and size for packaging. The following paragraph explains the decision of components considered in the tool to develop a complete vehicle concept.

The components considered in the parametric vehicle concept are selected from the data available in the existing literature. MAN's "Fundamentals of Commercial Vehicles" provides a general overview of truck and bus components [114]. More detailed information on the technology of commercial vehicles can be found in HOEPKE, BREUER [68]. Similarly [115–117] provides information on components for electro vehicles, passenger vehicles and autonomous vehicles. The list of the components is derived from these books and is displayed in Appendix B in Table B-1.

Four general interactions exist between components [118, p. 4]

- Spatial: This interaction describes a geometric or spatial dependency. An example of this dependency is the connection between the electric motor and the transmission.

- Energy: An energy interaction exists between two components when energy is transferred between them. The battery transfers energy to the electric motor and thus indicates an energy interaction.

- Material: When a material interaction is existent, the material is transferred between two components. This could be solids, liquids or gases.

- Information: An information interaction indicates the information or a signal exchange between two components. An example is a communication between LIDAR-sensor to the board computer of the autonomous vehicle.

In our approach, the energy, material and information interactions are merged into the term "functional" interaction.

To visualize the interactions of the defined components, a matrix-based visualization is selected. [119] describes several options for matrix-based visualization. For the visualization of the vehicle components, a DSM (Design Structure Matrix) is used. A DSM is an intra-domain matrix and maps all interactions of the within a domain. A subsystem, an assembly or a whole product, which consists of parts, can define the domain. Figure 3-6 displays the DSM of the vehicle, where all main components are mapped. The form of a DSM is always quadratic; all components are ordered in an identical order within the row and column. A green mark within the matrix, also marked with the number 1, indicates that an interaction between the component in the row and the component in the column exists. The diagonal fields do not contain any information and thus, they are coloured black.

Besides the information on the interactions, the DSM provides a rating on the active and passive sum. The active sum is the sum of interactions per row and indicates how much a component influences the other. The passive sum is calculated by adding up all interaction values in each column and represents the influence of other components on it [120]. The dependency matrix in Figure 3-6 helps to identify the components with the highest interaction rate. According to those interactions, the components are further grouped into assemblies. The list shown in Table 3-2 defines the components that are considered for both the tool and

3D CAD model for the concept development and visualization. The components are defined under their respective subsystems, such as chassis, powertrain, suspension, interior, Connected and Autonomous Vehicle (CAV) components, HVAC (Heating Ventilation and Cooling). The components from the list in Appendix B in Table B-1 that have a design priority of 1 are classified and grouped into assemblies.

Matrix of Dependencies	Frame	Floor	Wheelhouse	Body	Doors	Windows	Range Sensing	Seats	Handles/ Poles	Computer	Air Conditioning	Motor	Transmission	Inverter	Battery	Axles	Cooling System Motor	Heat Exchanger Battery	Wheels	Wheel Carrier	Spring/ Air Suspension	Steering System	Air Compressor	Air Tanks	Braking System	Active Sum
1 Frame	■	1	0	1	0	0	0	0	0	0	0	1	1	0	0	1	0	0	0	0	1	1	0	1	0	8
2 Floor	0	■	0	1	1	0	0	1	1	0	0	1	0	0	0	0	0	0	0	0	0	0	0	0	0	5
3 Wheelhouse	1	1	■	1	0	0	0	1	1	0	0	1	1	0	1	1	1	0	0	0	0	1	1	1	0	13
4 Body	1	0	0	■	1	1	1	0	1	0	1	0	0	0	0	0	0	0	0	0	0	0	0	0	0	6
5 Doors	1	1	0	1	■	1	0	1	1	0	1	0	0	0	0	0	0	0	0	0	0	0	0	0	0	7
6 Windows	0	0	0	1	1	■	0	0	0	0	0	0	0	0	0	0	0	0	0	0	0	0	0	0	0	2
7 Range Sensing	0	0	0	1	0	0	■	0	0	1	0	0	0	0	0	0	0	0	0	0	0	0	0	0	0	2
8 Seats	0	1	0	1	0	0	0	■	0	0	0	0	0	0	0	0	0	0	0	0	0	0	0	0	0	2
9 Handles/ Poles	0	1	0	1	0	0	0	0	■	0	0	0	0	0	0	0	0	0	0	0	0	0	0	0	0	2
10 Computer	0	0	0	0	0	0	1	0	0	■	0	0	1	1	0	1	1	0	0	0	1	1	1	0	1	9
11 Air Conditioning	0	0	0	1	0	0	0	0	0	0	■	0	0	0	0	0	0	0	0	0	0	0	0	0	0	1
13 Motor	1	1	0	0	0	0	0	1	0	0	0	■	1	0	0	1	1	0	0	0	1	0	0	0	0	7
14 Transmission	1	0	0	0	0	0	0	0	0	0	0	1	■	0	0	1	0	0	0	0	0	0	0	0	0	3
15 Inverter	0	0	0	0	0	0	0	0	0	0	0	1	0	■	1	0	0	0	0	0	0	0	0	0	0	2
16 Battery	1	1	0	0	0	0	0	0	0	0	0	0	0	1	■	1	0	0	0	0	0	0	0	0	0	4
17 Axles	1	0	0	0	0	0	0	0	0	0	0	0	0	0	0	■	0	0	0	0	0	0	0	0	0	1
18 Cooling System Motor	1	0	0	0	0	0	0	0	0	1	0	1	0	0	0	0	■	0	0	0	0	0	0	0	0	3
19 Heat Exchanger Battery	1	0	0	0	0	0	0	0	0	0	0	0	0	0	1	0	0	■	0	0	0	0	0	0	0	2
20 Wheels	1	1	1	1	0	0	0	0	0	0	0	0	0	0	0	1	0	0	■	1	1	1	0	0	1	9
21 Wheel Carrier	0	0	1	0	0	0	0	0	0	0	0	0	0	0	0	1	0	0	1	■	1	1	0	0	1	6
22 Spring/ Air Suspension	1	0	1	1	0	0	0	0	0	0	0	0	0	0	0	0	0	0	0	0	■	0	1	1	0	5
23 Steering System	1	0	0	0	0	0	0	0	0	1	0	0	0	0	0	0	0	0	0	1	0	■	0	0	0	3
24 Air Compressor	0	0	0	0	0	0	0	0	0	0	0	0	0	0	0	0	0	0	0	0	1	0	■	1	0	2
25 Air Tanks	1	0	0	0	0	0	0	0	0	0	0	0	0	0	0	0	0	0	0	0	1	0	1	■	0	3
26 Braking System	0	0	0	0	0	0	0	0	0	1	0	0	0	0	0	0	0	0	1	1	0	0	0	0	■	3
Passiv Sum	13	8	3	11	3	2	2	4	4	4	2	6	3	2	4	7	3	1	2	3	6	6	4	4	3	

Figure 3-6   Design Structure Matrix (DSM)

Table 3-2   List of Subsystems and Components

Vehicle Body and Structure	Powertrain	Chassis	HVAC	CAV Components
Body	Motor	Tires	Evaporator	LiDAR
Windows	Transmission	Rims	Condenser	Camera
Floor	Inverter	Axles	Compressor	Sensors
Frame	Battery	Brake Discs	Radiator	
Door	Battery Box	Brake Pads		
Ramp	Cooler	Brake Callipers		
Wheelhouses		Air Spring		
		Air Compressor		
		Air Tank		
		Wheel Carrier		
		Wishbones (A-Arms)		
		Dampers		

4 Components Sizing Algorithm Development

The previous chapter explained the framework of the tool, the definition of required vehicle specifications followed by the definition of vehicle layout and the decision of the component subsystems. However, as described in Section 3.1, the AEV Tool can size and select the components for a targeted vehicle concept. This section precisely describes the models and simulations involved in the sizing and selection of the subsystem and its components. Section 4.1 describes the selection of the powertrain subsystem, followed by the selection of the chassis and the HVAC subsystem in Section 4.2 and Section 4.3 respectively. The algorithms and functions required for sizing and selection of components are implemented in Matlab.

4.1 Powertrain Sizing and Selection

The powertrain subsystem significantly influences energy consumption, the cost, and the vehicle range. The powertrain system in the tool consists of the battery, electric motor, inverter and transmission. The implementation of the powertrain component sizing within the tool is based on the simulation model from the master thesis of SEBASTIAN KRAPF [121] and a previous work of the author [42].

4.1.1 Powertrain Components Design

Figure 4-1 gives an overview of the powertrain sizing process. The input parameters and vehicle requirements affect the powertrain design of the vehicle. The vehicle input parameters comprise of the external dimensions of the vehicle such as the frontal area, the vehicle length, rolling radius of the tire and other specifications such as passenger capacity and vehicle weight. In addition, further inputs include a different system such as the HVAC demand, Auxiliary load and Autonomous components demand are required. The vehicle requirements for powertrain comprises of operational requirements specified by vehicle top speed, gradeability, maximum acceleration and vehicle range. These characteristics must be satisfied to create a feasible powertrain design concept.

Based on the vehicle input and requirements, the powertrain component models are designed. An equivalent circuit model is used for the implementation of the battery design. Efficiency maps are used in the design of motors, inverters and transmissions due to the advantages of the computational effort and the level-of-detail. As seen in Figure 4-1, the simulation necessitates control strategies for shifting operation of the transmissions, distribution of power for multi-motors configurations, and the driver model. Comparable to the efficiency maps, look-

up tables are used in the approach. The control strategies are initialized in every step before the simulation and are stored as characteristic maps.

Furthermore, the mass of the powertrain is calculated, which along with the vehicle parameters and is used in a longitudinal dynamics simulation to calculate the energy consumption. The initial costs of the powertrain are also calculated based on the powertrain components design.
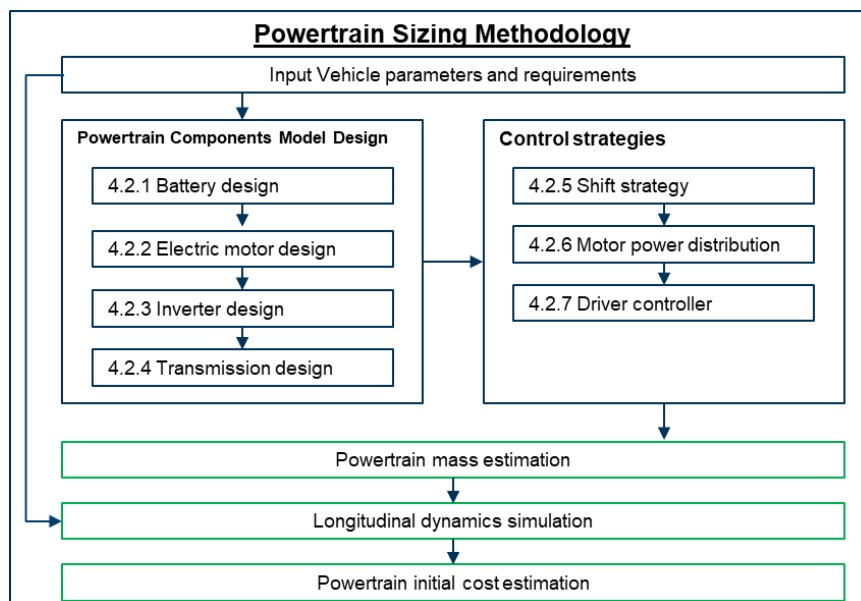

Figure 4-1   Vehicle Powertrain Design Process [42, 121]

Battery design

As discussed above, the equivalent circuit model of a "18650 2.05 Ah Sanyo UR18650E NMC cell" is used for the battery design and is based on the model from MUELLER ET AL [122]. The behaviour of a single cell is used to represent the equivalent circuit model. The battery pack architecture is made up of several cells in series and parallel. The maximum voltage is used to define the number of cells in series and required energy capacity is thus used to define the total sum of cells. Therefore, the total battery capacity is divided into single cell based on the architecture and is evaluated for the losses. Subsequently, the losses are added to simulate the whole battery pack. This approach is flexible and can be applied to a wide variety of designs. The model is developed in Simulink and the impacts of the state of charge of the cell and the temperature on the battery losses are included. The thermal and ageing effects are neglected in the scope of this thesis.

Electric motor design

The generic way to model the electric motors are by using the efficiency maps especially when multi-motor configurations are considered. A motor design tool developed by HORLBECK [123] is used in our approach. The tool automatically generates efficiency maps based on the performance specifications of the motors, especially, the automotive traction motors.

Figure 4-2 illustrates an overview of the approach used in the generation of efficiency maps. First, the motor input parameters such as nominal power and speed, maximum speed, nominal voltage etc. are specified. Two different motors, Asynchronous Motors (ASM) and Permanent Magnet Synchronous machines (PSM) are considered in the simulation. HORLBECK [123] provides a detailed explanation of the efficiency maps generation for different motors types.

Following the generation of the efficiency maps, the data-points have to be treated in order to standardize them into a uniform grid size. This increases the usability in the subsequent process. Also, the data-points from the simulation includes some "NaN"-values at the limits of the motors' operation range. The values are interpolated and the data is saved to the memory.
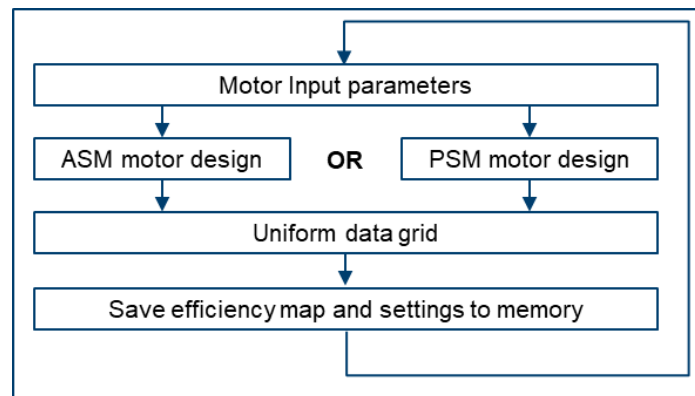

Figure 4-2   Overview of Efficiency Maps Generation [121]

Inverter design

The design of inverters is similar to motor design since the efficiency map generation method is applied. The models developed by CHANG for a six-pack IGBT inverter and a MOSFET inverter in a cascaded H-Bridge topology is used in our approach [124]. Based on the inputs from the design of battery and the motor, the switching and the conduction losses are evaluated for each valid operational data point of the inverter. Based on the calculation, the losses are extrapolated linearly in accordance with the maximum motor torque and the nominal battery voltage. The data points and the NaN values are adjusted similarly as explained in the motor design.

Transmission design

In general, electric vehicles use single speed transmission due to the wide operational range of electric motors. On the other hand, a multi-speed transmission for electric powertrain could improve vehicle acceleration and grade performance and efficiency [125–129]. Hence, the multi-speed transmission is considered for evaluation in this work by incorporating two design stages namely the transmission ratio and the generation of the efficiency. The primary input is the required maximum torque at the vehicle wheels and is calculated based on the preliminary vehicle mass estimation by the author [97, 130]. Consequently, a gearbox design is initialised depending on the defined number of gears. NAUNHEIMER ET AL. in their study, provide design recommendations to define the maximum gear step for the transmission [131]. In this approach, a geometrical gear step with the largest step of 1.7 is used in the design based on the recommendations.

A transmission efficiency map generation method similar to the motors and inverters based on the works of PESCE and SEEGER is used. PESCE [132, p. 57] presented an initial qualitative method to assess the efficiency of a two-speed transmission depending on the input load. Later SEEGER used this approach to expand it for multi-speed transmissions [133, pp. 53-58].

4.1.2 **Control Strategies**

As described in the previous section, the powertrain components design includes several control strategies for performing gear shifting in transmission unit, in order to distribute power between motors, driver model to control the vehicle in the longitudinal dynamics. The section explains the development of control strategies.

Transmission Shift strategy

The shift strategy of the gearbox for a heuristic energy optimal shift logic is based on the combined approaches of NGO [134] and LEE ET AL. [125]. For every load point, the algorithm checks whether a gear shift results in higher efficiency of the powertrain. In this way, the three areas downshift (I), no shift (II), and upshift (III) are identified, as shown in Figure 4-3. Figure 4-3 shows the three areas with respect to motor speed and torque. The downshift area is expanded for a low motor speed or high required torques, whereas the upshift area is enlarged at high motor speeds to avoid an operation outside of the feasible operation area.
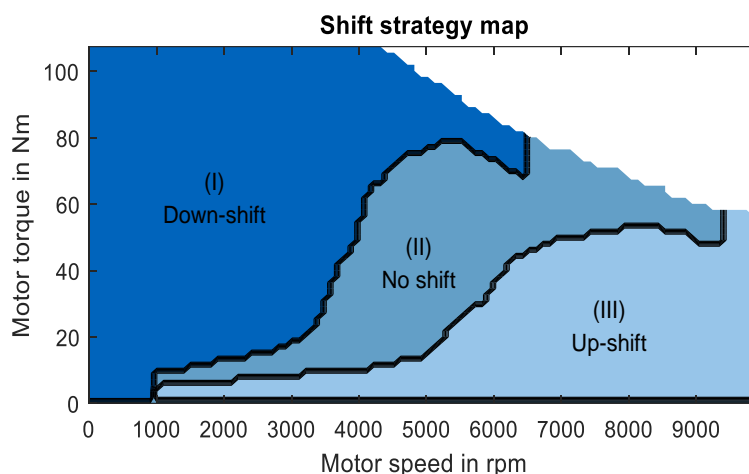
Shift strategy map

Figure 4-3   Shift strategy map [42]

Motor power distribution

The framework allows the simulation of multiple powertrain architectures with multi-motor configurations. Therefore, there is a requirement for power distribution and hence the torque distribution between the motors based on the request arising from vehicle load. This work considers only the torque distribution between the front axle and rear axle, while torque distribution in the same axle is not considered. In this work, the motor power distribution is calculated using the approach by PESCE [132, pp. 64-66]. The approach tries to minimize the losses of powertrain components (inverter, motor, transmission) by taking into consideration all the efficiency maps of the powertrain components. However, the transmission has a higher impact due to its influence on vehicle power characteristics.

For example, different speed-torque characteristics arise for every gear combination of the transmission at different axles and have to be determined at every point. Therefore, the maximum torque characteristics for each gear combination is calculated. Further, the maximum speed at the axle is fixed comparing the speed of two axles. The axle with lower maximum speed is used and the torque provided is added up. At each speed point, all possible torque combinations of the two axles are derived. All the generated power distribution point is

stored in a 3D-look-up table. Finally, the data is processed for the usage in Simulink. The power demand of the virtual motor for a two-motor axle is split equally.

Driver controller

A forward simulation model is used and it requires control of the feedback signal. The driver controller is implemented as a PID controller to minimize the difference between the vehicle target velocity and the actual velocity. Therefore, the pedal position of the throttle is converted into a torque request for the vehicle and subsequently as the target current from the battery. Owing to numerous possible powertrain configurations and the variations to simulate different sized buses with the same model, the installed power and the vehicle mass can vary significantly and affect the sensitivity. Hence, an inverse approach based on [93, p. 37] is implemented to ensure that for different vehicle concepts simulated, identical velocity difference leads to identical acceleration request by the driver.

$4.1.3$ **Mass and Cost Estimation**

The weight and inertia are required inputs for the energy consumption simulation and are therefore calculated within the initialization of the powertrain design. The initial costs of the powertrain are required to calculate the vehicle concept cost.

Estimation of the weight and inertia

The mass of the battery, inverter, motor, motor inertia, tire, and tire inertia are calculated using the regression functions developed by [132]. Each component is represented by regression functions shown in equations (4.1) to (4.6) in Table 4-1. The weight of the vehicle body excluding the powertrain is modelled by a regression function (see (4.7)) derived by a parametric CAD model from [130]. The overall vehicle mass consists of the sum of all powertrain components, the weight of the body and the passenger weight as in equations (4.7) to (4.10). Refer List of Symbols for the following equations.

<div align="center">Table 4-1   Mass Estimation Functions</div>

Battery

PESCE [132, p. 56]
$$m_{bat} = n_{serial} n_{parallel} m_{cell} k_{m,bat} \tag{4.1}$$

Inverter

PESCE [132, p. 53]
$$m_{inv} = 0.0886\, P_n + 3.357 \tag{4.2}$$

Motor

PESCE [132, p. 48]
$$m_{PSM} = \frac{13.847 \ln(P_n) - 13.003 + 10.979\ \ln(T_n) - 17.908}{2} \tag{4.3}$$

PESCE [132, p. 48]
$$m_{ASM} = \frac{16.152\ \ln(P_n) - 3.4576 + 24.184\ \ln(T_n) - 49.245}{2} \tag{4.4}$$

Tire

PESCE [132, p. 61]
$$m_{tire} = 106.67\, r_{dyn} - 13.179 \tag{4.5}$$

Transmission

SEEGER [133, p. 64]
$$m_{TM} = \sum_{i=1}^{n_{DU}} (m_{housing,i} + m_{gears,i}) \tag{4.6}$$

Vehicle Mass

SCHWARZ [130]

$$m_{body} = 6.431\,l^2 + 243\,l + 2123 + 283\,i_{thirdAxle} \tag{4.7}$$

$$m_{passenger} = 70\,kg * n_{passenger} \tag{4.8}$$

$$m_{PWT} = m_{bat} + \sum_{i=1}^{n_{inv}} m_{inv,i} + \sum_{i=1}^{n_{mot}} m_{mot,i} + \sum_{i=1}^{n_{TM}} m_{TM,i} \tag{4.9}$$

$$m_{veh} = m_{body} + m_{passenger} + m_{PWT} \tag{4.10}$$

Estimation of the powertrain costs

Similar to the mas estimation of the powertrain components, the initial costs are determined with regression functions, except for the transmission, which was included with a more detailed cost model by EROGLU [135]. The implemented functions are shown in (4.11) to (4.15) in Table 4-2. The initial costs are the sum of all installed powertrain components.

Table 4-2   Initial Cost Estimation Functions

Battery

FRIES ET AL. [136, p. 12]

$$C_{bat} = k_{c,bat}\,110\,E_{bat} + 200 \tag{4.11}$$

Inverter

EROGLU [135, p. 82] (from DOMINGUES et al. [137])

$$C_{inv} = 7.5\,P_{max} + 145 \tag{4.12}$$

Motor

EROGLU [135, p. 63]

$$C_{PSM} = 9.2\,P_{max} + 250 \tag{4.13}$$

EROGLU [135, p. 63]

$$C_{ASM} = 8.5\,P_{max} + 220$$

Transmission

EROGLU [135, p. 75]

$$C_{TM} = \sum_{i=1}^{n_{DU}} C_{material,i} + C_{production,i} + C_{add.parts,i} \tag{4.14}$$

Initial costs

$$C_{initial} = C_{bat} + \sum_{i=1}^{n_{DU}} (C_{inv} + C_{mot} + C_{TM}) \tag{4.15}$$

4.1.4 Longitudinal Dynamics Simulation

The model computes the energy consumption of the electric vehicle powertrain concept in Simulink with a forward simulation approach. The motor operation strategy demands the power of each motor as specified in the static control maps. The shift control evaluates if a shift process leads to lower energy consumption. A heuristic restricts the shifting to avoid shift oscillation. Auxiliary and HVAC power is constant. Energy regeneration is possible up to the maximum power of the components and it is reduced by the components power losses. The additional deceleration can be covered by the braking system at all times and wheel slip is neglected. The Simulink model allows simulating all feasible powertrain structures. In theory, two inverters, motors, and transmissions can be installed at each axle. Hence, the model incorporates four subsystems of each component which can be switched on and off depending on the selected powertrain design. Figure 4-4 illustrates the eight options of the flexible powertrain architecture, which are implemented in MATLAB Simulink.
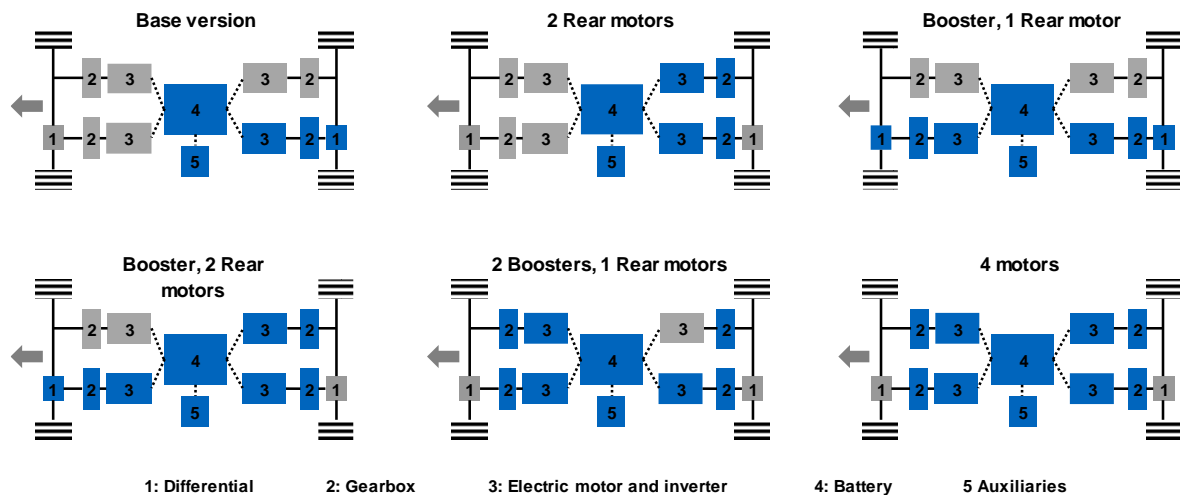
| 1: Differential | 2: Gearbox | 3: Electric motor and inverter | 4: Battery | 5 Auxiliaries |

Figure 4-4   Powertrain Architectures

4.2 Chassis Sizing and Selection

The chassis system consists of the suspension system, the brake system, wheel, and tire. The implementation of the chassis component algorithm within the tool is based on the model from the master thesis of STEFAN MAXL [138] The selection of these components is facilitated by the chassis database, which is based on the DB Browser for SQLite. SQLite databases does not require any external applications and can be connected to Matlab [139]. The database contains off-the-shelf standard components of suspension, axles, brake, wheel and tire components. To get and use data from the database, SQL queries in Matlab are implemented. To add, delete and manipulate component data, the software application DB Browser for SQLite is used. DB Browser for SQLite is a visual, open-source application to create, design, and edit database files [140].

4.2.1 Tire Sizing and Selection Model

The road vehicle wheels include two elements: the rim and the tire. PACEJKA [141, pp. 1-2] points out that amongst other factors, tires influence the steering system, the driving behaviour and the suspension system. The two main functions of the vehicle wheel and tire are supporting the vehicle load, withstand the longitudinal and lateral forces from the road surface, move the vehicle, and control its path. Tires and rims are standardized parts and share common parameters [142, p. 53].

To size and select tires from the database, the load per wheel is required. A function is used to calculate the load per wheel based on the user input. For the calculation, the vehicle mass, the mass of the passengers, the luggage of the passengers as well as the unsprung mass of the suspension system are considered. Secondly, the function compares the maximum load of all tires in the database to the required load and selects all suitable tires. Afterwards, the function selects the tires with the smallest possible rim size. Finally, the function selects the tire with the smallest possible tire width, which can handle the load. The flowchart is shown in Figure D-1 of Appendix D.

The calculation steps are as follows. First, the load per axle is calculated as shown in equation (4.16) [143]:

$$FAWL = \frac{m_{vehicle} + n_{passenger} * (m_{person} + m_{luggage})}{2} \qquad (4.16)$$

where $FAWL$ is the laden axle weight in kg, $m_{vehicle}$ the unladen mass of the vehicle concept in kg, $n_{passenger}$ is the number of passengers, m_{person} *is* the mass of a single passenger in kg and $m_{luggage}$ is the mass of a passenger's luggage in kg. Equation (4.17) shows the calculation of the payload using the unladen and laden weight [143]:

$$PL = \frac{m_{vehicle}}{2} + j * (WL - \frac{m_{vehicle}}{2}) \qquad (4.17)$$

where PL is the payload in kg and j an overload factor. The maximum overload factor was set to 25%. To select a suitable tire, the sprung mass of each wheel is required. Equation (4.18) shows how to calculate the sprung mass for each wheel [143]:

$$SM = PL - \frac{USM}{2} \qquad (4.18)$$

where SM is the sprung mass per wheel in kg and USM is the unsprung mass per wheel in kg. The sprung mass is the effective load, which each tire has to handle. Based on the sprung mass, the tire selection function can choose a suitable tire from the database. Further calculations are not needed. Equations (4.16) to (4.18) are also used for the air spring selection and sizing process in Section 4.2.2.

4.2.2 Air Suspension Sizing and Selection Model

Rigid beam axle systems have been replaced by independent axle suspensions, which offer better ride quality and driving behaviour of the bus for passengers. The development of low floor buses offer ease of access to wheelchair users without affecting the ride and driving comfort of the bus [144, pp. 1-4]. The state of the art suspension systems for buses/minibuses are the air springs [145, p.6]. Some advantages of air springs over other systems include implementation of vehicle kneeling and constant natural frequency of the vehicle. The constant natural frequency delivers higher passenger comfort.

The air springs sizing and selection is based on the engineering manual and design guide from Firestone Tire and Rubber Company [146]. This design guide provides information on the calculation of air springs size as well as technical specifications for different air spring sizes that are added to the database. From the database, three smallest springs are initially selected based on the maximum load rating and the sprung mass of the concept and a minimum of 180 mm of spring travel to facilitate kneeling. The average isolation effectiveness is calculated for each of the springs. Isolation effectiveness is the capability of an air spring to isolate the vehicle from road vibrations. Furthermore, only the two air springs with the smallest average isolation effectiveness values are considered. The pressure level of the air springs influences their natural frequency. Therefore, a preselection of the lowest pressure level is done. As the

last step, the natural frequencies of the two air springs are calculated. The air spring, which has the closest natural frequency to 1 Hz, is selected for the vehicle concept as identified by MITSCHKE ET AL. [147, pp. 408-409]. A natural frequency close to 1 Hz ensures a comfortable driving experience for the passengers. Figure D-2 schematically shows the selection process of the air spring in Appendix D.

This section presents the detailed calculations for the air spring sizing and selection process. As described in Section 4.2.1, Equations (4.16) to (4.18) are also used to calculate the load per spring. After determining the isolation effectiveness and the design height of every spring, which can handle the required load, the vertical spring rate needs to be found for the selected springs. To calculate the vertical spring rate, the effective area and the required pressure are needed. Equation (4.19) shows the calculation of the effective area [146, pp. 21-22]:

$$a_{effective} = \frac{load_{max}}{p_{default}} \tag{4.19}$$

where $a_{effective}$ is the effective area in in^2, $load_{max}$ is the maximum load at the default pressure in lbs and $p_{default}$ is the pressure at the design height in lbs/in^2. With the effective area of the spring, the required pressure can be determined with Equation (4.20) [146, pp. 21-22]:

$$p_{required} = \frac{SM}{a_{effective}} \tag{4.20}$$

where $p_{required}$ is the required pressure at a certain load in lbs/in^2. With these pieces of information, the vertical spring rate can be determined. Equation (4.21) shows the calculation of the vertical spring rate for a certain load [146, pp. 21-22]:

$$K = \left[\left[P_{required} + 14.7 \right] \left[A_c \left(\frac{V_1}{V_c} \right)^{1.38} - A_e \left(\frac{V_1}{V_e} \right)^{1.38} \right] - 14.7(A_c - A_e) \right] \tag{4.21}$$

where, K is the vertical spring rate in lbs/inch, A_c is the effective area at ½ inch below the design height in in^2, A_e is the effective area at ½ inch above the design height in in^2, V_1 is the internal volume at the design height in in^3, V_c is the internal volume at ½ inch below the design height in in^3 and V_e is the internal volume at ½ inch above the design height in in^3. Lastly, the natural frequency of the two remaining springs can be determined with Equation (4.22) [146, pp. 21-22]:

$$f_n = 188 \sqrt{\frac{K}{SM}} \tag{4.22}$$

where f_n is the natural frequency in Hz. As described, the function selects the spring with the natural frequency, which is closest to 1 Hz. A natural frequency close to 1 Hz ensures a comfortable driving experience.

4.2.3 Brake Sizing and Selection Model

The brakes are responsible for slowing and stopping the vehicle. Brake systems have significant importance in a vehicle concept development process since it is highly related to safety. Friction brakes are widely in automotive applications. BREUER ET AL. [148, P. 150] identified four important requirements that ought to be optimized in the brake system design

phase: Maximum brake torque, Durability of the brake system, Maximum continuous braking output, Minimum package space.

BREUER ET AL. [148, p. 147] points out that the disc brakes are used for modern heavy vehicle design. The Disc brakes have become the state of the art and are used in trucks and buses as well as passenger cars and hence considered in this approach. The advantages of disc brakes include low fading, high thermal resistance and low maintenance costs.

DEGENSTEIN [149] introduced brake dimension calculations, which are used to develop the brake sizing and selection function. The wheel and tire size parameters are required for the calculation and are acquired from the outputs of Section 4.2.1. The brake force and the required braking torque is calculated based on the tire size parameters. The available brakes that could handle the required torque are selected from the database. For brakes without information about the maximum torque, can be calculated with effective brake pad area based on [149, p. 10]. Following the determination of the maximum brake torque, the brake systems will be checked against the minimum required brake torque and the maximum tire size. If both criteria are fulfilled, the largest possible brake system is selected because of safety reasons. Figure D-3 schematically shows the selection process of the brake system in Appendix D.

This section presents the detailed calculations for the brake sizing and selection process. Equation (4.23) shows the calculation of the ideal brake force for the rear or front axle [150, p. 94]:

$$F_{B,axle,ideal} = F_{G,axle,static} \frac{\ddot{x}_B}{g} + m_{vehicle} \ddot{x}_B \frac{h_{cg}}{l} \frac{\ddot{x}_B}{g} \tag{4.23}$$

where $F_{B,axle,ideal}$ is the ideal brake force per axle in N, $F_{G,axle,static}$ is the weight force per axle in N, $\ddot{x}_B$ is the minimum deceleration in m/s^2, g is the acceleration of gravity in m/s^2, $m_{vehicle}$ is the overall mass of the vehicle in kg, l is the wheelbase of the vehicle and h_{cg} is the height of the centre of gravity in m. The minimum deceleration was set to 5 m/s^2 according to legal regulations [151, p. 1]. Pre-tests with the parametric CAD model showed a maximum centre of gravity height of 1 m. Hence, the height of the centre of gravity was set to 1 m. With the ideal brake force per axle, the ideal brake torque can be calculated with Equation (4.24) [149, p. 10]:

$$M_{B,axle,ideal} = F_{B,axle,ideal} \, r_{tire} \tag{4.24}$$

where $M_{B,axle,ideal}$ is the ideal brake torque in N/m and r_{tire} is the static tire radius. To keep the calculations as simple as possible, the dynamic tire radius was neglected. As described in Figure D-2 in Appendix D, if no brake torque values are available, the brake calliper force and respectively the brake torque can be estimated with Equation (4.25) [149, p. 10]:

$$F_{cl} = \eta \, A_{pad} \, p_{hydraulic} \tag{4.25}$$

where F_{cl} is the brake calliper force in N, η is the efficiency of the brake system, A_{pad} is the brake pad area in mm^2 and $p_{hydraulic}$ is the hydraulic pressure of the brake system in N/mm^2. The efficiency of the hydraulic brake system was set to 0.95 [149, p. 13]. Because of package reasons, there were no further investigations performed on pneumatic brake systems. Equation (4.26) shows how to calculate the circumferential force based on the calliper force [149, p. 10]:

$$F_{circ} = 2 \, \mu \, F_{cl} \tag{4.26}$$

where F_{circ} is the circumferential force in N and μ the coefficient of friction between the brake pads and the brake disc. The coefficient of friction was set to 0.4 [149, p. 13]. To estimate the required brake torque, the radius from the centre of the brake disc to the centre of gravity of the brake pad is needed. Since there is hardly any information available about the centre of gravity of brake pads, DEGENSTEIN [149, p. 47] introduced an approximation for the effective radius in Equation (4.27):

$$r_{eff} = \frac{2}{3} \frac{r_{disc,outer}^3 - r_{disc,inner}^3}{r_{disc,outer}^2 - r_{disc,inner}^2} \qquad (4.27)$$

where r_{eff} is the effective radius in m, $r_{disc,outer}$ is the outer diameter of the brake disc in m and $r_{disc,inner}$ is the inner diameter of the brake disc in m. With this simple approximation of the effective radius, the required brake torque can be estimated. Equation (4.28) shows the calculation of the estimated brake torque [149, p. 10]:

$$M_{B,est} = F_{cl} r_{eff} \qquad (4.28)$$

where $M_{B,est}$ is the estimated brake torque in Nm.

4.2.4 **Axle Sizing and Selection**

The axle connects the wheel directly or indirectly to the vehicle body through the suspension system of the vehicle. According to [142, p. 133], axles should allow distribution of forces, exchanged by the wheels with the ground, complying with design specifications in every load condition. Based on the axle database from ZF Friedrichshafen AG, independent suspensions axle can be used for a maximum of up to 9000 kg per axle [152].

The axle sizing and selection function in this thesis determine the minimum diameter of the suspension links in the parametric model for independent suspension systems. This function uses calculations and a Multi-Body Simulation (MBS) model in Simscape. MATHWORKS [153] provides a simple MBS model for vehicle suspension design. The model offers a visualization of the vehicle with a focus on suspension system response. The model comprises of six component subsystems, one road subsystem and an input subsystem as shown in Figure 4-5. The component subsystems are connected with suitable multibody joints to each other. MILLER [154] provides further information about the Simscape multibody contact force library. The driving parameters include the longitudinal data as well as the driving path of the vehicle. To get the maximum bending force, for standard driving manoeuvres, the longitudinal data contains the maximum acceleration and deceleration for buses. The driving path is a slalom track with alternating radii. The path equation of the template was adapted and can be seen in Equation (4.29)

$$S_{Slalom} = 15 \frac{\pi}{180} \sin(0.4 \frac{\pi}{10} t + \frac{\pi}{2} + 0.03) \qquad (4.29)$$

where S_{Slalom} is the steering input and t the simulation time in seconds. The frequency of the sin wave was changed to $0.4 \frac{\pi}{10} t$. This change results in sufficiently large turns for the driving manoeuvre of the MBS model.
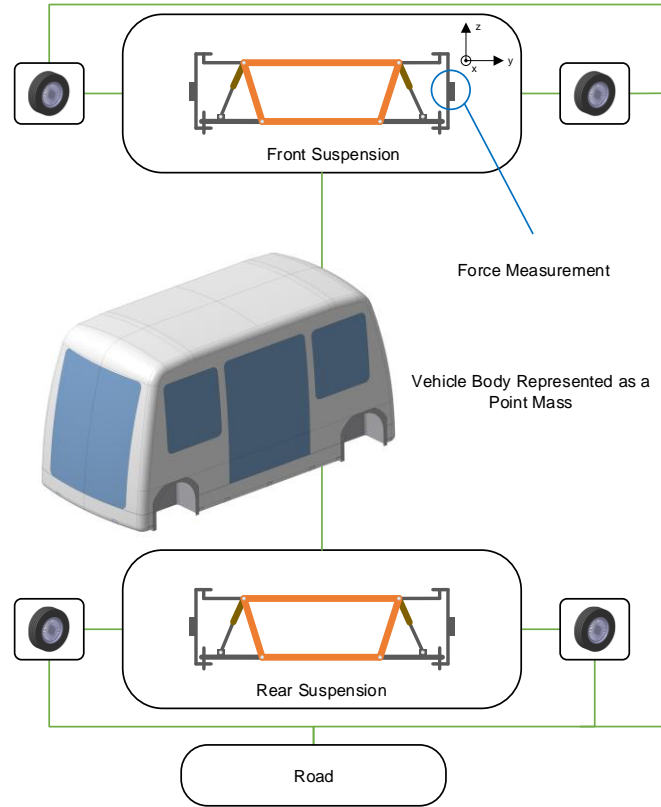
Figure 4-5   Structure of the MBS model

The bending moment of each suspension link ca be calculated bases in the lateral forces acting on them. Further, the bending stress on the links can be determined. The axle sizing model iteratively compares the calculated bending stress to the permissible bending stress of the material by increasing the diameter of the link by 1 mm at every step. For all calculations, the maximum lateral force is used Equation (4.30) shows the calculation of the maximum bending moment

$$M_{bending,max} = l_{wishbone} \, F_{z,max} \tag{4.30}$$

where $M_{bending,max}$ is the maximum bending moment in Nm, $l_{wishbone}$ the length of the lower wishbone in m and $F_{z,max}$ the maximum bending force in N. The moment of resistance of pipe can be calculated with Equation (4.31):

$$W_{pipe} = \frac{\pi}{32} \frac{D^4 - d^4}{D} \tag{4.31}$$

where W_{pipe} is the moment of resistance in mm³, D the outer diameter of the pipe in mm and d the inner diameter of the pipe in mm. Based on the maximum bending moment and the minimum moment of resistance, the actual bending stress can be calculated with Equation (4.32):

$$\sigma_{bending} = \frac{M_{bending,max}}{W_{pipe}} \tag{4.32}$$

where $\sigma_{bending}$ is the actual bending stress in the suspension links in N/mm².

4.3 HVAC Sizing and Selection

The HVAC selection algorithm is based on the parametric HVAC sizing model developed by BINDER [155] and PATHAK [156] for electric buses. The HVAC system is responsible for the thermal comfort and acceptable indoor air quality which are pursued as the goal in designing the system [157]. In addition, the HVAC system influenced energy consumption and hence the powertrain design significantly. Thus, a parametric approach in HVAC system sizing aids to find the power demand requirements of an electric vehicle concept and vehicle packaging.

The HVAC system consists of different elements. The evaporator and the condenser are the heat exchangers that facilitates heat transfer between the coolant and the environment. The compressor helps to pressurise the coolant and the blower creates the flow of air [158]. This section covers the parametric methodology developed to size the component by providing an overview of the workflow employed. It involves the calculation of the cooling load demand and determination of cabin air inlet conditions and examines the design of heat exchangers.

The approach used for sizing the heat exchangers is based on the study by SHAH ET AL. [159, P. 80] . Figure 4-6 shows the method employed in this work.
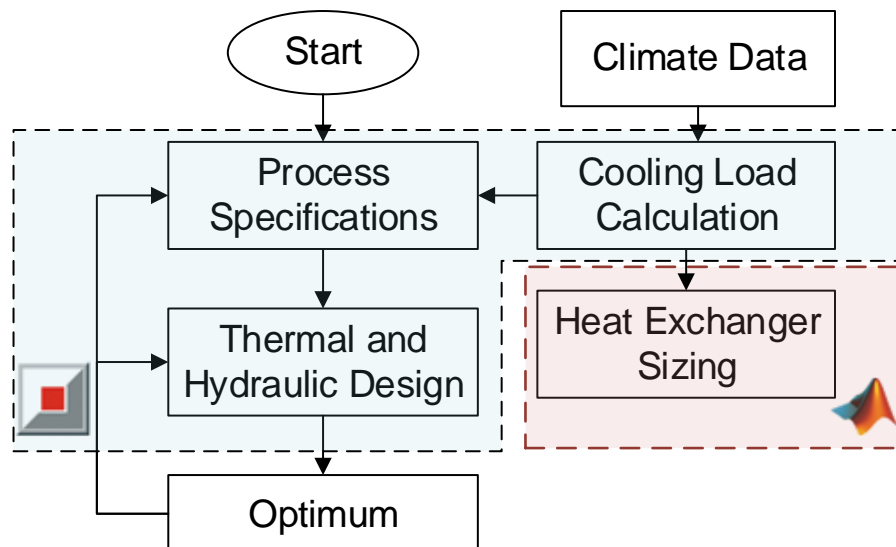
Figure 4-6   HVAC Sizing Methodology [155]

Firstly, the boundary conditions of the operation and the process are required for sizing the heat exchangers. The required heat transfer rate, the cooling demand determination plays a significant part in the process. The type of heat exchanger and the required dimension of the same to fulfil the defined process is determined in the thermal and hydraulic design. The heat exchangers are designed with two software programs. GT SUITE is used for Computational Fluid Dynamics (CFD) and the numerical processes are carried out in MATLAB [25, 160]. The following sections explain the estimation of cooling load and the design steps involved in sizing the heat exchangers and the compressor.

4.3.1 Cooling Load Calculation

Cooling power is a significant input parameter for the design of HVAC in order to attain the anticipated cabin conditions. Based on the previous studies on prediction of thermal comfort [161] and the standards of fresh-air supply and the occupants thermal comfort by ASHRAE [162, 163], the target cabin temperature fixed to 24 ºC, the relative humidity is less than 60 %

with the fresh air supply of 3.5 l/s per passenger. The outside ambient conditions are assumed to be 32 °C and relative humidity of 70 % based on Singapore`s climate conditions. The metabolic load input and sweat input of each passenger is assumed as 73.3 W of sensible heat and 116 g/s of water vapour respectively [162]. For evaluating the maximum cooling power, the vehicle concept is assumed with a 100 % passenger occupancy.

A vehicle cabin model is developed using the specifications of the vehicle concept as parametric input. Figure 4-7 shows the illustration of a vehicle cabin model. The model is comprised of a lumped mass of air in the interior of the vehicle cabin, the solar radiation from outside, the internal and external convective heat loads, the long-range radiation between the vehicle and sky, and the metabolic loads of the occupants

The solar load is absorbed by the covering parts such as the roof and door, and as well transmitted partially into the cabin by the glazing. The vehicle body and interior transmit the heat into the cabin by internal convection. The internal convective heat transfer coefficient is a constant and assumed to be 15 W/m^{2}K while the external convective heat transfer coefficient ($htc_{ext,conv}$) is calculated based on the vehicle velocity v in km/h based on a driving cycle for transit buses defined by [160] and [164] as shown in Equation (4.33).

$$htc_{ext,conv} = 1.163 \left(4 + 12 \sqrt{\frac{v}{3.6}} \right)$$

(4.33)
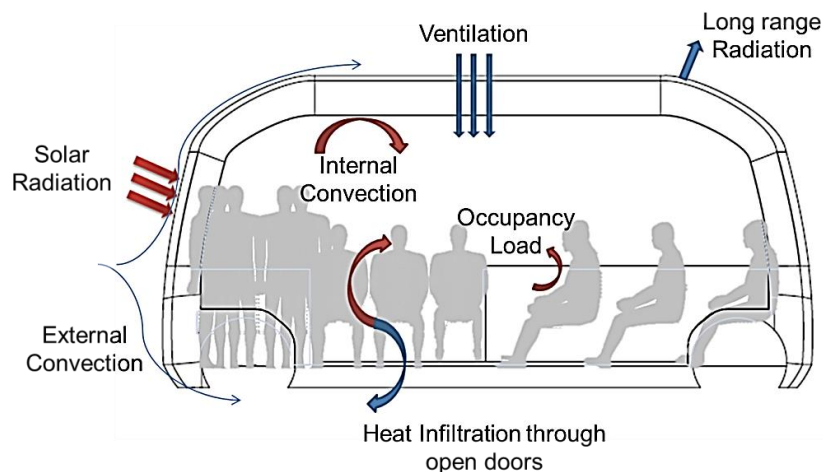
Figure 4-7   Illustration of the Cabin Model

The cooling power of the HVAC, Q is equal to the difference in enthalpy, $\Delta h_{air,evap}$ of the air entering and leaving the evaporator times the air mass flow rate $\dot{m}_{air,evap}$.

$$Q = \Delta h_{air,evap} \, \dot{m}_{air,evap}$$

(4.34)

For a given cooling load demand, the enthalpy difference can be decreased by increasing the mass flow rate. When the enthalpy difference decreases, the air temperatures at the evaporator outlet increases, thus resulting in a lower dehumidification rate. The cool air through the evaporator condenses on the surface of the coil when the temperature is below the dew point temperature of the air entering the heat exchanger. This leads to the requirement of dehumidification. The HVAC model in this work uses a PID controller that aims to retain a constant cabin temperature of 24 °C by controlling the air from the evaporator.

Design of Heat Exchangers

The heat exchangers design process is an iterative process to achieve the desired rate of heat transfer while maintaining the pressure and the temperature demand [165] and [159]. In this method, the dimensions of the heat exchanger are calculated by computer-aided methodology. It is based on a high-efficiency vapour compression cycle (VCC), followed by the scaling of the predefined heat exchanger to match its performance to the operational points of the VCC.

A heat exchanger is a microchannel tube-fin and is defined by its geometry, the core layout and the heat transfer correlations. In this method, the height, width, and the depth and the number of cores of the heat exchanger are established as variables and hence, are directly used in the vehicle concept packaging. The scaling leads to a change in the heat transfer coefficients. Hence for the correlation heat transfer coefficients with test data of the base exchangers, mathematical formulations used are provided by GT-SUITE [160].

Single phase and two phase evaporation and condensation occur due to the convective heat transfer process on the refrigerant side of the exchangers. Therefore, different correlations are employed. The Dittus-Boelter correlation is used in the determination of the heat transfer rates in the heat exchanger sections where single-phase vapour (condenser entry and evaporator exit) and single-phase liquid (condenser exit) is existent. The heat transfer coefficient, htc is defined as a function of the Reynolds number Re, the Prandtl number Pr, the fluid thermal conductivity k and the reference length D as shown in Equation (4.35).

$$htc = 0.023 \, Re^{0.8} \, Pr^{0.3} \, \frac{k}{D} \qquad (4.35)$$

The heat transfer coefficients in the two-phase condensation region are calculated as shown in Equation (4.36) with the single-phase liquid Nusselt number Nu_l and the quality x. The reduced pressure P_{rd} is the ratio of the actual pressure to the critical pressure.

$$htc = Nu_l \left((1-x)^{0.8} + \frac{3.8 \, x^{0.76}(1-x)^{0.04}}{P_{rd}^{0.38}} \right) \frac{k}{D} \qquad (4.36)$$

Compressor Sizing

The compressor has the highest power consumption in the HVAC system. Therefore, a high-efficiency VCC is required to reduce the compressor power. This can be achieved by maintaining a lower pressure rise in the compressor. Figure 4-8 shows the p-h diagram of the VCC comparing different pressure ratios (High and Low). Equation (4.37) shows that the cooling load, Q is equal to the enthalpy change of the air, multiplied by the air mass flow rate through the evaporator. Following the first law of thermodynamics and the heat out of the airflow equals the heat flow into the refrigerant where, $\dot{m}_{\mathrm{ref,evap}}$ is the refrigerant mass flow rate over evaporator and h_i is enthalpy as shown in Figure 4-8.

$$Q = \Delta h_{\mathrm{ref,evap}} \, \dot{m}_{\mathrm{ref,evap}} = (h_1 - h_4) \, \dot{m}_{\mathrm{ref,evap}} \cdot \qquad (4.37)$$

The compressor power P_{compr} equals the refrigerant's enthalpy difference h_2-h_1, multiplied with its mass flow rate as shown in Equation (4.38) [160, p. 63]

$$P_{\mathrm{compr}} = \Delta h_{\mathrm{ref,compr}} \, \dot{m}_{\mathrm{ref,compr}} = (h_2 - h_1) \, \dot{m}_{\mathrm{ref,comp}} \cdot \qquad (4.38)$$

In order to minimize the overall power consumption, based on the Equations (4.37) and (4.38), a low pressure-ratio VCC has to be chosen.
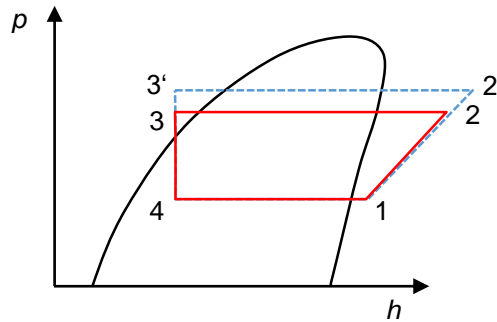
Figure 4-8   p-h diagram of a VCC for Different Pressure Ratios

Heat Exchangers Scaling

With the definition of Heat Exchangers (HX) and compressor, the dimensions of the heat exchanger can be parameterised and scaled. This is accomplished by scaling the base heat exchanger from the previous section in order to achieve the heat transfer requirements of VCC of the compressor. Therefore, the pressure drop is minimized in the heat exchanger in order to reduce the compression ratio and the load of the compressor. A design of experiments (DOE) tool provided by the GT SUITE allows the users to select different parameters from the model that are intended to be used as independent variables for a particular set of simulations [166, DOE Setup].

The approach depends on finding the heat transfer rate, Q_{pol} and the pressure drop, p_{pol} as polynomial functions of the heat exchanger height, width and depth as shown in the Equations (4.39) and (4.40).

$$Q_{pol} = f(height_{HX}, width_{HX}, depth_{HX}) \tag{4.39}$$

$$P_{pol} = f(height_{HX}, width_{HX}, depth_{HX}) \tag{4.40}$$

In order to find the optimum dimensions of the heat exchangers, a minimization problem of the P_{pol} is evaluated by constraining the heat transfer requirements as shown in Equation (4.41). The P_{pol} is constrained by the polynomial expression of the heat transfer rate Q_{pol} being equated to the heat transfer demand rate, Q_{dem}. The results of the optimization are the dimensions of the heat exchangers where the pressure drop is minimal while attaining the required heat transfer rate.

$$[height_{HX}, width_{HX}, depth_{HX}] = \min_{hwd}(p_{pol}) \quad for \ (Q_{pol} - Q_{dem}) = 0 \tag{4.41}$$

5 Design of the Parametric CAD Model

The visualization of the developed vehicle concept is a prime objective of the AEV-tool and is implemented as a parametric CAD model. As described in Section 3.3, the parametric model is the second element of the AEV-tool after the vehicle concept is generated in the GUI. A 3D CAD software is required to translate the geometric description of a part or component to the form of a surface or volume. Furthermore, it should provide all non-geometric characteristics that are important for manufacturing, such as material, mass or tolerance information. CATIA V5 is the widest spread design software in the automotive sector. CATIA allows parameterisation the geometry to associate different components and to build hierarchical assemblies of parts. The possibility to derive all parameters and automated modelling processes executed by macros ensures an efficient interface to MATLAB. Moreover, the software provides a large selection of features which allows integrating design knowledge into a digital mock-up [167]. The implementation of the design of the parametric model within the tool is based on the master thesis of MANFRED SCHWARZ [130]

5.1 Definition of Parameters

At the beginning of the parametric vehicle design, it is important to identify the correct parameters. The parameters define the 3D model and the complexity of the overall model and computation time increases with new parameters. In addition, parameters of different components are interdependent as seen in DSM (Section 3.6).

All the defined parameters are enlisted in Appendix C. This list comprises of 150 parameters that define all designed components. Every component is completely constrained by parameters defining the simple geometry of the part.

The parameters are distinguished and identified in three logical groups:

Dimensional Parameters: The dimensional parameters govern the definition of the components geometry and the overall dimensions of the vehicle concept. The dimensional parameters define the volume of the components for packaging.

Material Parameters: The material parameters define the material associated with each component of the vehicle. All the material parameters are comprised of common materials such as steel, aluminium, copper, rubber, etc. Material parameters and the material properties are associated and hence contribute to mass properties of the components.

Layout and Configuration parameters: These parameters are responsible for the definition of topology or architecture or layout of the subsystems. These are logical parameters and are defined as either as a true/false statement.

The tool has several component sizing and selection functions that determine the parameters. The functions are defined in MATLAB and the concept visualisation id performed by CATIA. Hence, a nomenclature and rules to assign certain names to the components parameters are required to unify the communication between different platforms. The standardisation also helps in the future expansion of the tool in terms of defining new components and functions in CATIA and MATLAB. The nomenclature used in the development of the tool is displayed in the following Table 5-1. The table contains parameters from three groups.

Table 5-1   Standardised nomenclature for parameter names

Symbol	Description	Example
l	Length of a component	$l_{overall}$
w	Width of a component	w_{seat}
h	Height of a component	$h_{headrest}°$
t	The thickness of a component	t_{body}
d	The diameter of a component	d_{motor}
n	Number of component copies	$n_{seat\_window\_UL1}$
a	Angle within components	$a_{steering\_front}$
wb	Wheelbase	wb
gc	Ground clearance	gc
mat	Material of component	mat_{floor}
lay	The layout of component configuration	lay_{Urban_1}
pat	Pattern of component arrangement	$pat_{seat\_door\_CL1}$

5.2 Boundaries, Constraints and Interfaces

It is important to define the boundaries and constraints of the vehicle CAD model. In addition, the parametric model should have a defined interface between interdependent components to facilitate efficient packaging. Figure 5-1 specifies the outer boundaries and the inner sections of the CAD model. On the right side of Figure 5-1, the inner sections that divide the vehicle model are limited by the component that has a direct impact on vehicle package as shown. These sections divide the bus into several functional sections or just limit certain components that have an impact on packaging, such as the wheelhouses. The components that have a direct impact on the packaging are considered through their either specific function, size or dependencies among each other as seen in Section 3.5. These boundaries, interfaces and constraints are used to design the CAD model in the following section.
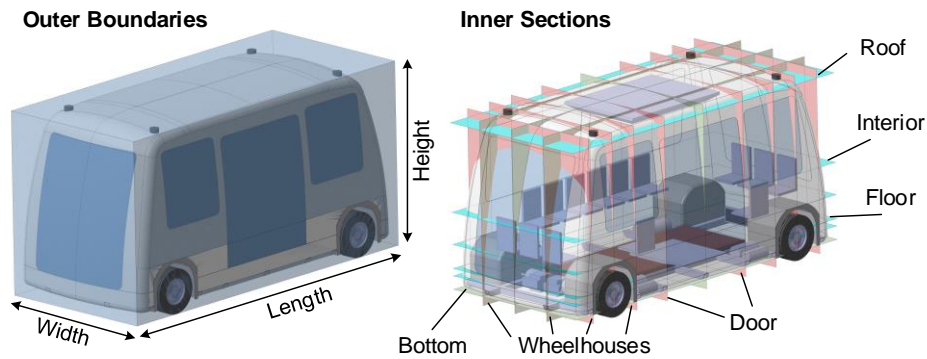
Figure 5-1   Boundaries and sections of the CAD model

5.3 Hierarchical CAD Model

The parametric CAD model is required to be organised hierarchically, with respective components are designated to their respective subsystems. For example, the powertrain subsystem assembly comprises components such as motor, transmission, inverter, etc. Figure 5-2 states the hierarchy of the CAD model and illustrates the hierarchical levels of the structure. The interface to MATLAB is directly linked to the overall CAD product.

However, in order to share parameters among different assemblies and parts/components, the parameter is required to be published globally as shown. The design specification of each component consists of derived published parameters (external parameters) and internal parameters that are specific for the components. The thickness of the parts/components, thickness or volume offset of the surface are predefined. Based on designed volume, density can be assigned and mass is calculated. The preliminary mass of the vehicle model is used in simulations to size and select the components suspension, brake and powertrain.
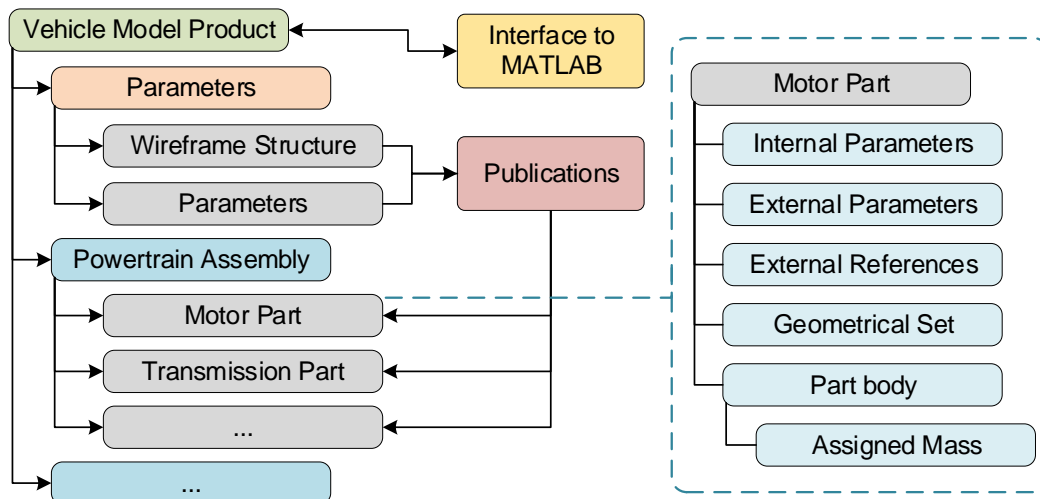
Figure 5-2   Hierarchy of the CAD model

Figure 5-3 shows the wireframe structure for the parametric vehicle model that comprises of several planes splitting the vehicle into numerous sections. The wireframe and the vehicle parameters are published as 'CATIA Publications' as explained in the earlier section. Each plane has its function of defining the limits of components or assemblies. The front and rear boundary planes limit the overall length of the bus. If the length of the model is modified, all the other planes and hence the associated parameters change and thus, the model gets

updated automatically. The planes in the wireframe are linked through formulas using the main input parameters. With this approach, everything adjusts when new parameters are written to the CATIA-MATLAB-interface.
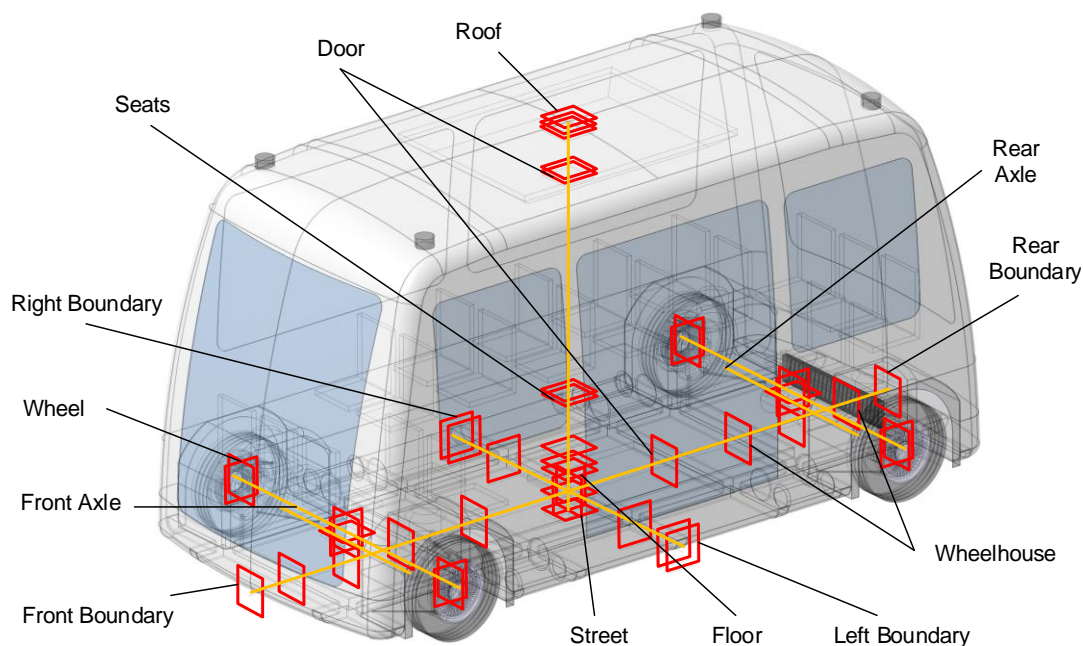
Figure 5-3   Wireframe of CAD Model

5.4 Design of Subsystems

The following sections discuss the design of the main subsystems in the parametric CAD model and describe the components in the assemblies.

5.4.1 Body and Structure Assembly

The body and structure assembly of the bus represents the carrying structure to provide an equal load distribution from all acting loads on the vehicle's structure. Figure 5-4 shows the complete chassis assembly consisting of several parts such as frame, vehicle body, wheelhouse, ramp, floor, door, and windows. The frame is the load-carrying structure of the bus model. It is directly connected to the body and varies in length with all the stringers. Two of the stringers mark the beginning and the end of the wheelhouses. The wheelhouses are designed in relation to the wheels. The tire and rim size determine the length, the height, and the width of the wheelhouses. These dependencies are integrated as formulas in the two dimensional sketches. A ramp is included to provide easy access to passengers using a wheelchair.

The floor divides the interior of the vehicle package from the functional space for assemblies in the package. The functional space of the bus contains powertrain assembly and chassis components assembly. The door, windows and the body form the exterior of the vehicle. Thus, the design of the doors and windows, and the vehicle body are interdependent of each other.
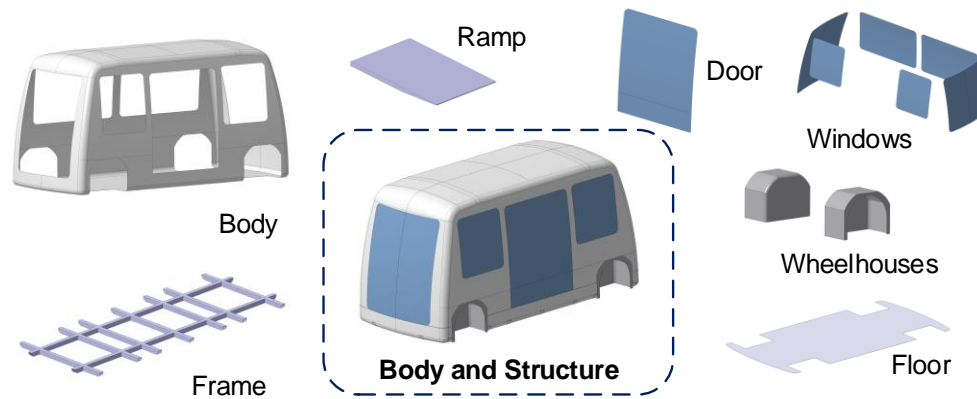
Figure 5-4   Body and Structure Assembly of the CAD Model

5.4.2 Powertrain Assembly

The powertrain assembly includes three subassemblies, which represent the three different powertrain configurations including a central rear motor, a dual rear motor, and an all-wheel drive configuration. Each configuration has a motor, differential, inverter, cooler and transmission. The powertrain assembly also consists of the battery cells and the battery box. Figure 5-5 illustrates the powertrain assembly with all its components.
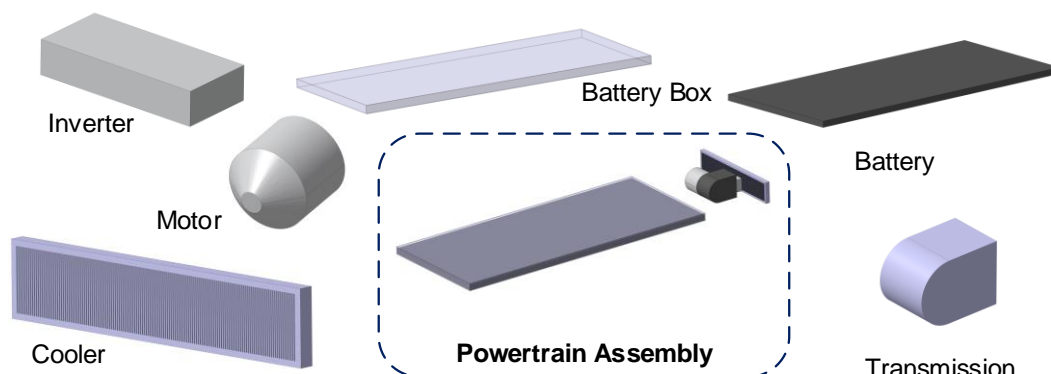
Figure 5-5   Powertrain Components

5.4.3 Interior Assembly

The interior assembly has only one part integrated, the seat. But the seat appears in three different seating layouts. For each new pattern used in the layout, the seat has to be designed new to avoid any interference or connections between the different layout configurations. For each seating layout, an own wireframe is designed where the seats are aligned. The following Figure 5-6 illustrates the three different seating layouts for a 6 m bus; the Urban 1, the Urban 2 and the Coach layout.

Urban 1 is designed that seats are placed along the walls and in between the wheelhouses. Layout Urban 2 is filling the left and right side of the vehicle, while the Coach layout leans on a normal passenger bus layout with a 2-2 configuration. A 2-2 configuration indicates that 2 seats are in a row on the left and on the right side.
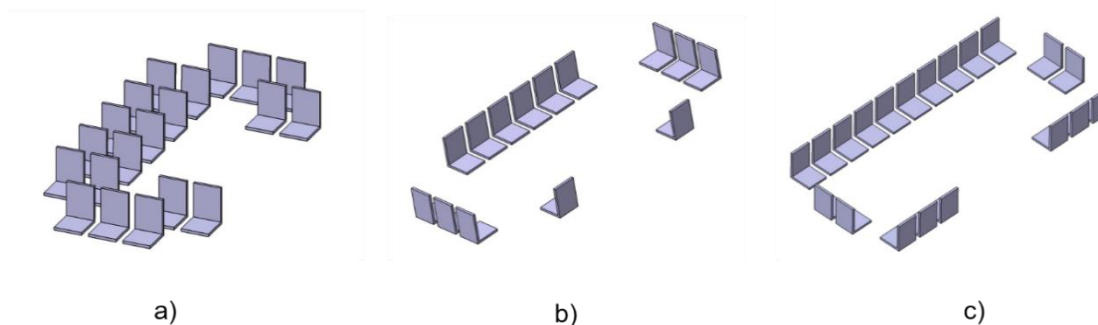
Figure 5-6   Interior Seating Layouts

5.4.4 **Chassis Assembly**

The chassis assembly has the most parts in the parametric CAD model. Chassis components include the suspension air springs, brake discs, the brake calliper, the brake pads, the rim and the tire. To connect the wheel to the chassis, a-arms (Control Arms), a damper and wheel carrier are designed. Figure 5-7 shows all components in the chassis components assembly. The air suspension consists of the air spring, air compressor, and air tanks. The air spring is designed to perform the variable lifting height of 180 mm.
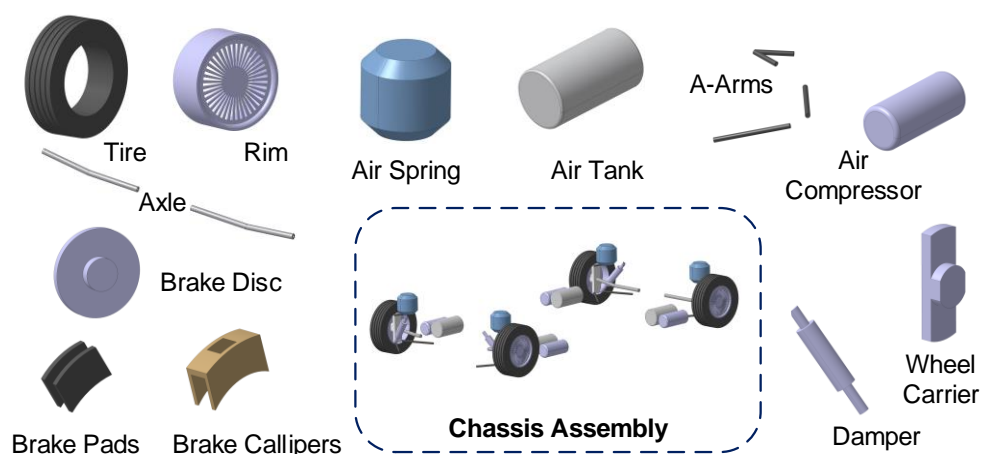
Figure 5-7   Chassis Components

5.4.5 **CAV Assembly**

The CAV components assembly in the tool consists of LIDARs (Light Detection and Ranging), cameras, and ultrasonic sensor system. The LIDAR system plays an important role in autonomous vehicles for obstacle detection. LIDAR enables a 3D environment to scan with accurate distance readings to obstacles. This works very efficiently in a medium range of few meters until around 120 m [15]. It is recommended to have four LIDAR sensors, one at every corner of the vehicle in order to have good 360-degree sensing with a small blind spot. Hence, for packaging, it is positioned on the top of the vehicle due to the impact of sensor visibility. For providing additional redundancy in the system as well as for localisation and traffic sign recognition, two stereo cameras are placed at the front and the back of the vehicle [25].

6   Implementation of the AEV Tool

The previous chapters explained in detail the development methodology of the tool, components selection and sizing and the design and development of the parametric CAD model for visualization. This chapter explains the integration of all the developed modules into the AEV Tool. It discusses the architecture and different modes of the tool thereby explaining the sequence of creating vehicle concepts based on the user input/requirements and the GUI design of the tool.

6.1   AEV Tool - Architecture

This section describes the design of software architecture. Figure 6-1 illustrates an overview of the AEV Tool. There are two modes in the main selection, the Manual Mode and Automated Mode.

The Manual Mode is intended for users with expert knowledge and provides a step-by-step development of the vehicle concept. The user can define all the component dimensions and choose between different configuration and topologies. The concept developed in the manual mode follows logical sequence to select and size the subsystems groups: Vehicle specifications, body and structure powertrain, suspension, chassis and HVAC components. Following the component definition, the developed concept can be visualised and stored.

The Automated Mode of the tool enables automatic concept development with basic inputs user inputs. The algorithm behind this mode is explained in the following sections. For the packaging, the selection options for the user is identical to the manual mode with subsystems groups: Vehicle specifications, powertrain, chassis and HVAC. Based on the selection, the tool shows the vehicle properties, energy consumption simulation, cost estimation of the concept, mass estimation, lifecycle emissions and visualisation.
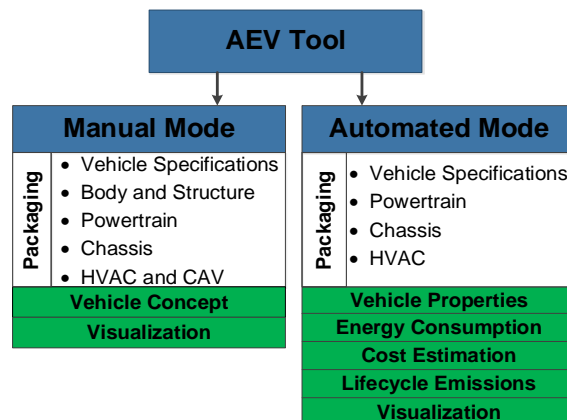
Figure 6-1   AEV Tool software architecture design.

6.2 Manual Mode

The manual mode provides a step-by-step development of the autonomous bus vehicle. As discussed above, the user can define all component dimensions and choose between various vehicle configurations or topologies.

Figure 6-2 shows the flowchart of the process steps of the manual mode. The figure is divided into six zones A1 to A6 based on the subsystems. A1 illustrates the vehicle specifications where the user can input the vehicle dimensions and select the preferred interior layout. A1 results in the number of passengers, seats and vehicle parameters. A2 is the selection of vehicle body and structure. A3 is the selection of powertrain that includes motors, inverter and battery. Subsequently, A4 and A5 describe the selection of chassis, and HVAC and CAV components, respectively. Where is A6??

Figure 6-2 clearly distinguishes between input parameters or dimensional parameters, configuration parameters and calculations. In total, the user can define seventy-eight fields to input or change the parameter values. In addition, the tool provides the user twenty-eight popup-menu fields to input predefined materials. Furthermore, the user can choose between eight-vehicle configurations that split up into three interior seating layouts, three powertrain topologies and two ramp configurations. MATLAB functions are used to process data from the user input, process them through the calculation codes and store the final result inside a struct array. MATLAB uses struct arrays to store data. The struct data is then used to write the parameters into the interface connected to the tool via update functions. The update function writes the calculated parameters to the interface after each calculation function is completed. This avoids transferring workspace data within the back end.
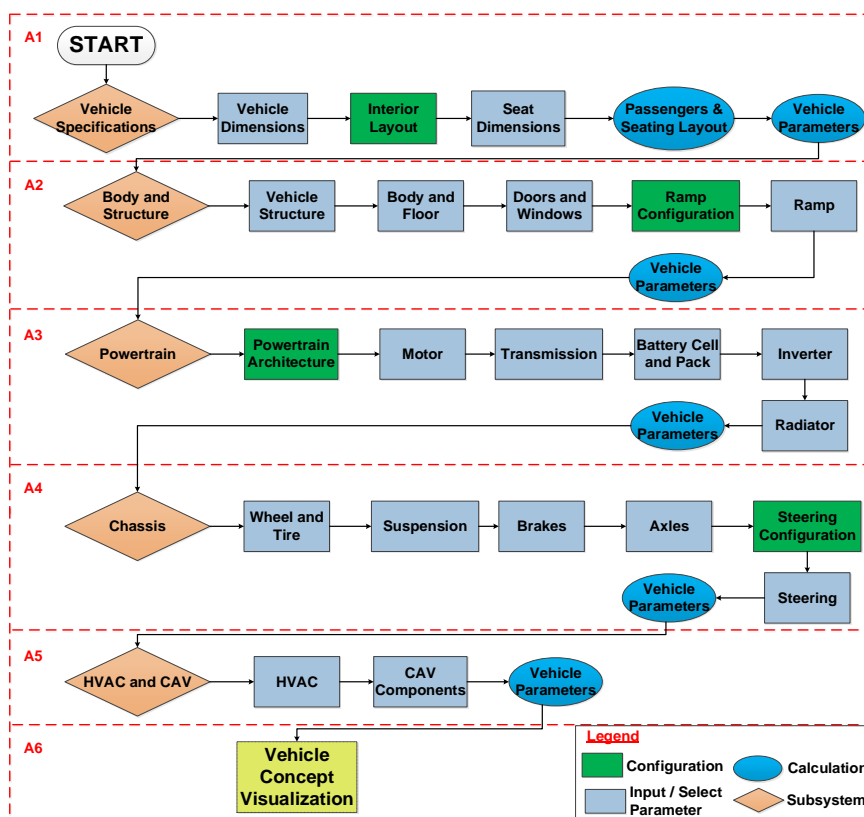
Figure 6-2   Flow Chart of the Manual Mode

6.2.1 **Vehicle Specifications**

Figure 6-3 shows the flowchart of the vehicle specifications (from Figure 6-2). The vehicle specifications comprise vehicle dimensions such as length, width, height, wheelbase, etc. The model is able to adjust to all major vehicle and components dimensions to the new parameters without performing any calculations.

The input parameters have pre-defined maximum and minimum values. This limits the user from choosing the wrong parameters. A warning has been implemented that includes a pop-up window with a valid range for a particular parameter. For example, the overall length of the vehicle is limited to the range from a minimum value of 4000 mm and a maximum value of 17000 mm. For other fields such as wheelbase, the limits are set based on prior calculation. This dimensional chain helps to predetermine the packaging space and thus avoids collision between components while packaging. This feature has been implemented through all the subsystems of the tool.
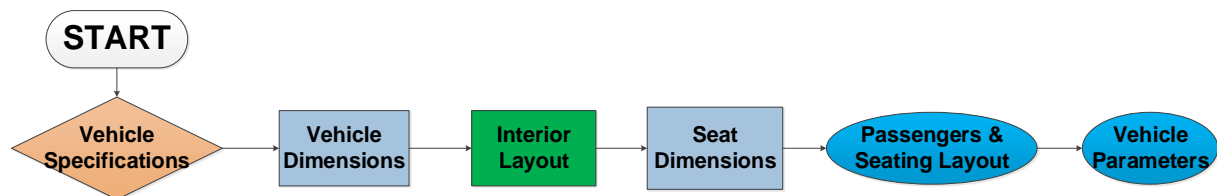
Figure 6-3　　　Flowchart of Vehicle Specifications

Based on the vehicle dimensions, seat dimensions and a selected interior layout the maximum passenger capacity, the number of seats and placement of seats are calculated and the parameters have to be updated to change the parametric CAD model. A code for the interior calculation is implemented as functions in MATLAB. Each function calculates the interior layout parameter and based on the preferred layout selection. Figure E-1 in Appendix E illustrates the bus design with an example explaining the different areas needed for calculation and shows the equation required for this evaluation within the bus area. In the end, when all calculations are completed, the parameters are written to the TXT file as illustrated as the end of the flow chart.

6.2.2 **A2 Body and Structure**

Figure 6-4 illustrates the flowchart of the vehicle body and structure selection. This subsystem follows the vehicle specifications. The user input parameters define the vehicle structure, vehicle body and floor, doors and windows, and the ramp for wheelchair access. The inputs are dimensional such as thickness, length, height as well as material parameters based on the component. The ramp configuration can be activated or deactivated and is exclusively meant for visualisation.
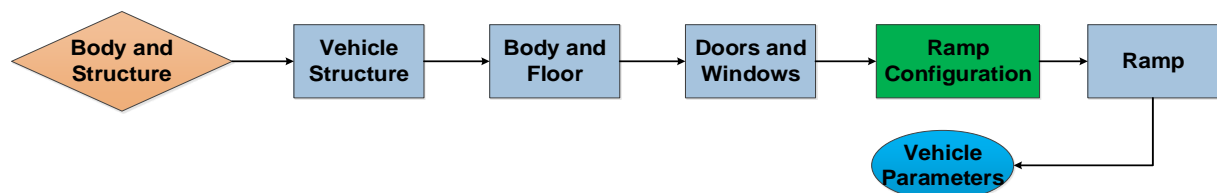
Figure 6-4　　　Flowchart of Body and Structure

6.2.3 **A3 Powertrain**

Figure 6-5 illustrates the flowchart of powertrain selection. The powertrain has three possible architectures that can be chosen. The topologies include a single motor, two motors and four motor configurations. The selected topology affects the packaging and mass of the vehicle concept. Furthermore, similar to the previous section, the user can input dimensional and material parameter to size the motor, transmission, inverters, battery cell, battery pack and the radiator or the cooler. The vehicle parameters are calculated and updated accordingly.
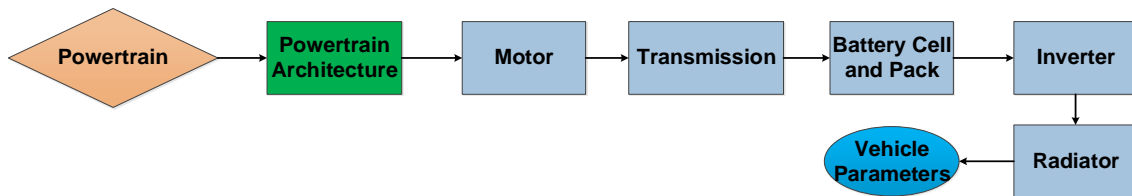
Figure 6-5   Flowchart of Powertrain Selection

6.2.4 **A4 Chassis**

Figure 6-6 shows the chassis selection flowchart. The chassis subsystem comprises of wheel and tire, suspension, brakes, axles and steering. The subsystem selection is identical to the previous sections with dimensional and material parameters. The chassis system includes steering system configuration which accounts for 4-wheel independent steering. The maximum steering angle of each wheel can be defined which affects the parameters of the wheelhouse, suspension arms, axles and interior layout. The vehicle parameters are calculated and updated accordingly.
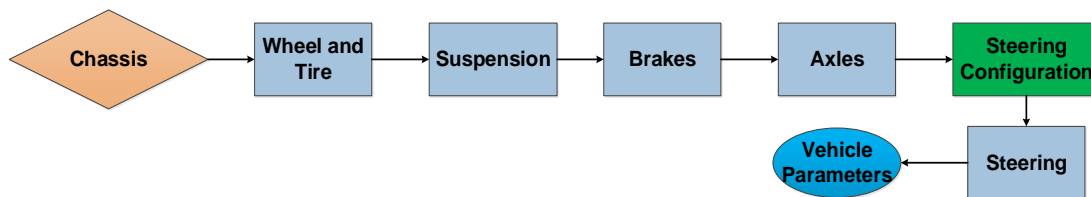
Figure 6-6   Flowchart for Chassis Selection

6.2.5 **A5 HVAC and CAV components**

The HVAC and CAV components systems are simple input parameters. These parameters have less influence on packaging since the layout has been defined to the roof of the vehicle concepts. The impact on the overall weight of the vehicle concept is also less significant.

6.2.6 **A6 Vehicle Concept Visualisation**

For the visualisation of the vehicle concept, all the parameters calculated parameters and the component and the packaging information should be transferred to update the parametric CAD model for visualisation. The software used for visualisation, CATIA supports parameter exchange through an external application such as a TXT or MS Excel (ref) in the form of a spreadsheet. The spreadsheet can later be accessed from external tools and parameter changes can be updated.

The AEV- Tool is implemented with two main software programs, MATLAB handles all the functions and CATIA supports visualisation. All the parameters have to be exchanged between MATLAB and CATIA. Furthermore, apart from the 3D model, the concept visualization

provides pictures of the developed concept on the GUI to make the tool more intuitive. Hence, this requires the function to create screenshots of the CAD to illustrate the final concept vehicle to the user. The interface of the AEV-tool offers an effective workflow between the programs. Different data files are created and stored for the programs to access, read data or write data in those files.

The following listed data files are used for the MATLAB-CATIA interface and are explained in the next paragraphs:

- TXT file for parameters
- VB Script - CATScript macro for executing function
- PNG or JPG files for visualisation
- PDF file for documentation

TXT file:

TXT is used in the development of the interface since it provides simple data storage and is a stable file extension. This makes the computation faster. The AEV Tool uses three different TXT files

- CAD_Model_Parameter_Table
- CATIA_Inertia_COG
- CATIA_Trigger

The *CAD_Model_Parameter_Table* consists of all the parameters required to modify and package the parametric CAD model. The parameter list has to be defined in the beginning and updated when new components are added to the model. The parameters are structurally organised within the TXT file. The dimensional parameters followed by all the component materials, all the activation states and patterns of different configurations are added to the end. Based on the user inputs, MATLAB modifies and updated the previous values in the TXT.

The *CATIA_Inertia_COG* contains information on the mass properties of the developed vehicle concept in CATIA. CATIA calculates the weight of all components automatically for each part and product based on the input parameters.

The *CATIA_Trigger* file is used as an activation document while execution of each VB Script (Macros). The file contains the text "trigger" during the execution of macro and a tab (" ") when the process is finished.

VBScript:

The VB scripts are used in the automation of CATIA models in the form of macros. The programming of the CATScripts macros for the AEV-tool is based on books from HANSEN and ZIETHEN [168, 169]. A macro can either be stored in a *CAT Document* file (part or product) as integrated macro or as independent *CATScript* file. In this work, only independent CATScripts are used since MATLAB can access the files externally.

The macros are executed to translate parameter inputs to 3D visualisation. Multiple macros are used for executing different functions. AEV Tool uses macros to carry out the following functions:

- Opening CATIA,
- Loading the vehicle model,
- Updating the model,
- Saving the model,

- Screenshots of ISO, side and front view of the CAD,
- Loading certain assemblies (interior layout and suspension),
- Creating assembly screenshots,
- Measuring weight and position of the centre of gravity, Closing CATIA.

PNG or JPG files:

PNG and JPG are the most used files for graphical images. The file type to be generated can be controlled by macros. The CATScript macro generates the images and is stored in the exchange folder to be accessed by MATLAB. The image files are later used in the concept visualization GUI.

PDF file:

The *MATLAB Report Generator* is a toolkit provide for report generation. This toolkit is used to generate a final report of the vehicle concept that includes the vehicle specifications, the component information and the concept pictures. The report can be saved by the user in PDF (Portable Document Format) to later compare different vehicle concepts.

6.3 Automated Mode

The automated mode is meant for developing an autonomous electric bus concept with basic user inputs such as the required vehicle type, passenger capacity and interior layout. The complete parameterisation and interlinking of developed component modules explained in Section 4 and Section 5, facilitates the process of vehicle concept development based on the user inputs. Figure 6-7 illustrates the flow chart of the automated mode. Similar to Section 6.2, for better understanding, the flowchart is divided into eight areas, A1 to A8. A1 illustrates the process of the vehicle classification or the selection of vehicle type, which results in the mass estimation and dimensioning of the concept. Two vehicle concepts can be developed and the results can be compared simultaneously within the tool as shown. A2 is the selection of the powertrain, which offers four variants for each configuration concept. A3 shows the selection of chassis and its components. A4 is the selection of the HVAC system. The selection of the four main subsystems results in a developed vehicle concept.

The inputs and outputs of subsystem parameters are managed by databases as illustrated in this figure. The databases are required to store the standard components and aids transfer for data between interdependent subsystems. In addition, the databases can be expanded as required. The functions of each database are explained in the following sections. This work outlines three different variations of databases:

- **SQLite**: SQLite database is used to store the standard chassis components as seen in Section 4.2. SQLite is connected to MATLAB through the JDBC or ODBC driver [139]. To create or edit database files, DB Browser is used [140].

- **Microsoft Excel**: Microsoft Excel is used as a database. An integrated interface for communicating with Excel in Matlab is available.

- **Matlab Array**: To store Matlab files as an array in a folder structure is another database model which is used in this work. Arrays are the fundamental representation of information and data in MATLAB.

Zones A5 to A8 illustrate the results and analysis of the vehicle concept. A5 shows the calculation of different elements of energy consumption. A6 shows the cost estimation of the concept. A7 shows the vehicle properties with the help of a spider chart. A8 shows the lifecycle emissions of the developed vehicle concept.
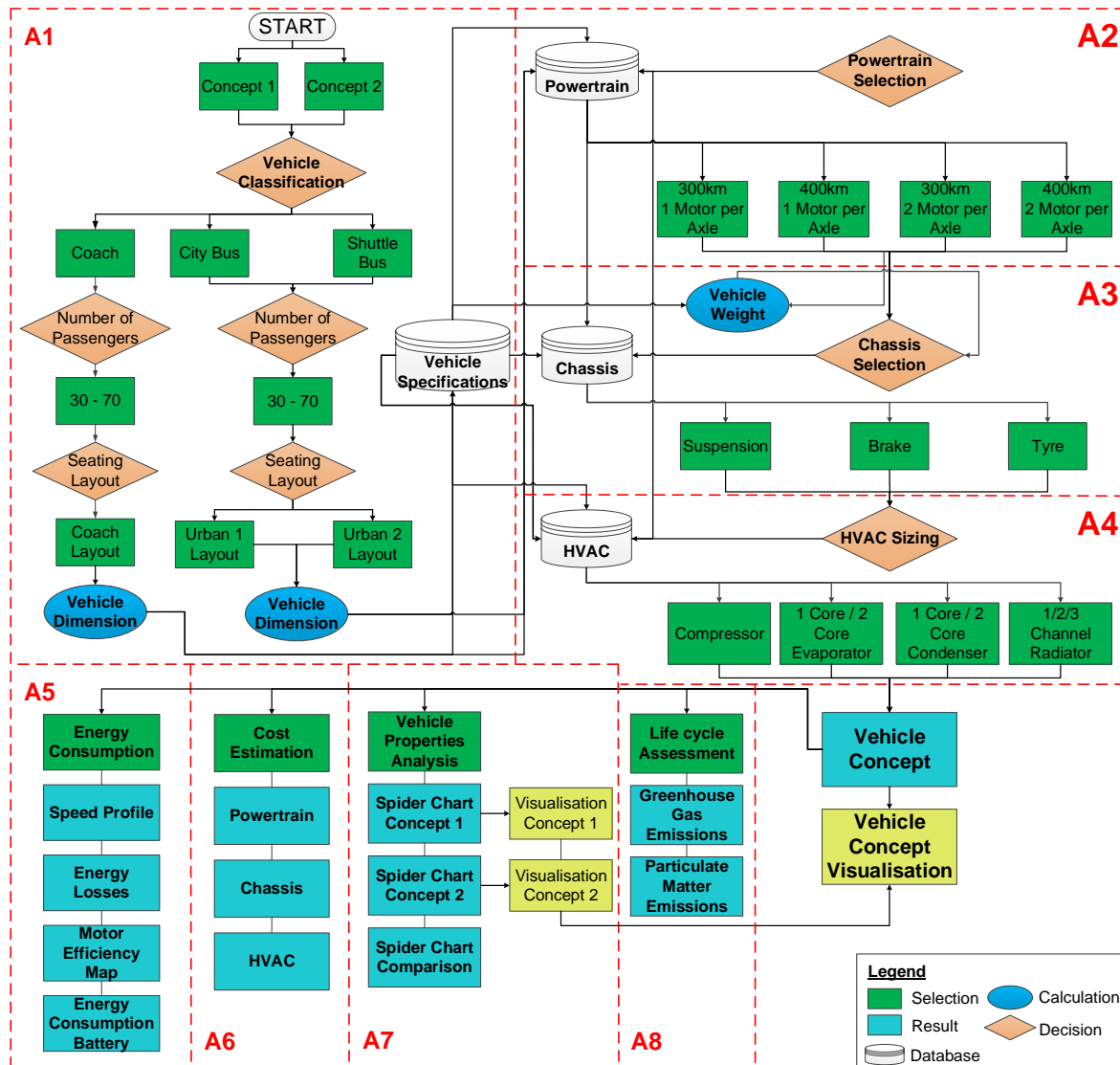

Figure 6-7   Flow Chart of the Automated Mode.

6.3.1 **A1 Vehicle Specifications**

The user requirements define the dimensional specifications of the vehicle. The tool provides a selection between three different bus classifications at the beginning, namely, the coach, the city bus and shuttle configuration. The coach is an intercity bus operated for long-distance trips. The city bus can be compared to public transport buses and shuttles can be used for regular round-trip transport or within specific infrastructures such as airports and parks. The occupancy can be selected between 30 passengers – 70 passengers. The next step is to choose between the three pre-defined seating layouts as explained in the interior assembly of Section 3.4.2. Based on the selected seating layout, the number of seats and the position of seats is calculated similarly to section 6.3.1.

The selection of the vehicle classification, number of passengers and the seating layout make up together the main inputs for sizing the bus as seen in Figure 6-7. The outputs of the vehicle specifications are the glider weight and vehicle dimensions. The interior and exterior of the vehicle define the boundary condition for the other subsystems and Figure 6-7 shows that the vehicle specification database has an impact on the powertrain, chassis and HVAC. Therefore, the Automated Mode in the AEV Tool starts with the sizing of the vehicle's body.

The calculation steps involved in the overall sizing of the bus concept based on the number of passengers and the layout. The calculation steps are derived from the calculations in Section 6.2.1 and are explained in Appendix E. The seating arrangement of the Urban Layout 2 is used as an example in the explanation. The code for the interior calculation is implemented as functions in MATLAB.

Another output of the vehicle specifications, the glider weight of the concept is modelled by a regression function derived from the parametric CAD model [97]. Figure 6-8 shows the weight of the glider over the vehicle length for different vehicle lengths. The database for the vehicle specification with vehicle classification, number of passengers and seat arrangement is created in Matlab. This serves as an input for the remaining databases. With the determination of the vehicle dimensions and weight, the appropriate powertrain is selected in the next step.
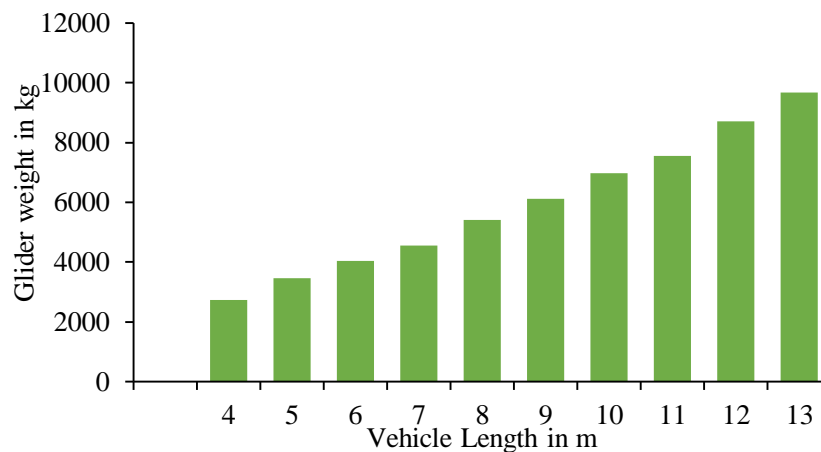
Figure 6-8   Glider Weight Over Vehicle Length [95]

6.3.2 A2 Powertrain

Figure 6-9 illustrates the implementation of powertrain selection in the AEV Tool with a flow chart. The powertrain component selection in the automated mode is the output of the longitudinal dynamics model explained in section 4.1. The components include the battery, motor, inverter and transmission. The results of the model in section 4.1 are used to create the powertrain database shown in the figure. As explained in the previous section, the results of A1 are stored in the vehicle specification database. The HVAC consumes has significant energy consumption and hence has a direct influence on the battery. The cabin volume and number of passengers required for the cooling are obtained from the vehicle specification database. It should be noted that the autonomous technology components are added as auxiliary load in the simulation.

The tool allows a selection from four different powertrain variants for each vehicle concept as shown in Figure 6-9. The author conducted a holistic design exploration to find the optimal powertrain configuration for electric city buses [42, 170]. The results of showed that the overall efficiency of the powertrain is significantly improved multiple motor configurations and is found

to have lower energy consumption and improved vehicle characteristics. Based on the results, the tool allows a selection between two motor configurations: one or two motors per axle and two-vehicle range options: 300km or 400km.

As shown in Figure 6-9, the powertrain model is controlled with a Matlab script and the results are stored in the powertrain database as arrays. The script defines the motor type and its power, as well as the topology of the drivetrain. The script executes the simulation twice, the first time to determine the energy consumption under consideration of the vehicle specification. The second run is to define the capacity of the battery for the specified range using the derived energy consumption. The total mass of the vehicle is an input for chassis components selection and the mass of the powertrain components are calculated from the mass estimation model in section 4.1.
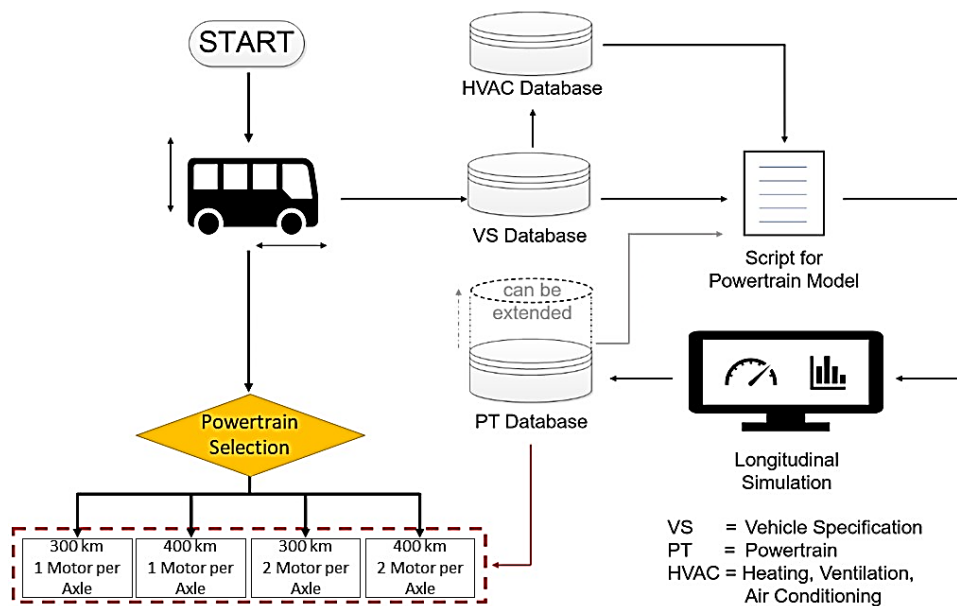
Figure 6-9   Flow Chart of Powertrain Selection

6.3.3 **A3 Chassis**

Figure 6-10 illustrates the process of the chassis components selection. The chassis system in the tool comprises of the suspension system, brake system, wheel, and tire. The inputs for the chassis component model are the overall length, width, height, the number of passengers, vehicle mass and the wheelbase. All parameters except the wheelbase are out of section 6.3.1 and section 6.3.2. The wheelbase limits depend on the length and are defined by ISO 612 / DIN 70000 [171]. The components are stored in the chassis database, the DB Browser for SQLite. The chassis component selection in the automated mode is implemented from the models explained in section 4.2. The selection of components from the database is by exclusion mechanism to systematically sort out the unsuitable components to narrow down the list. The selection process is same as explained in section 4.2. First, the wheel and tires are sized and selected. The suspension system and brake system are selected consequently.
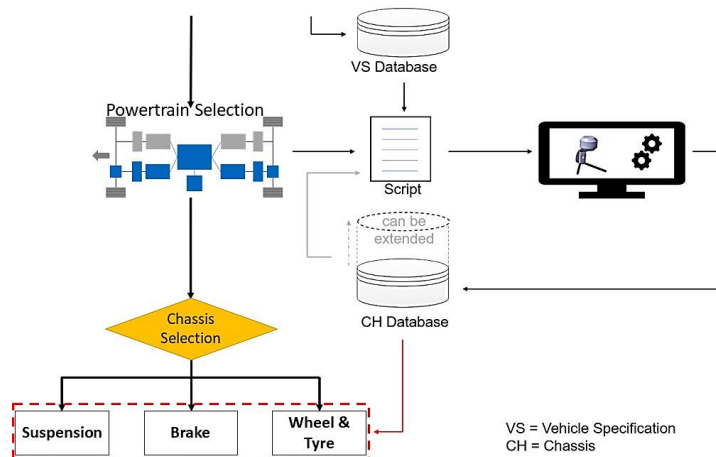
Figure 6-10   Flow chart of Chassis Selection

6.3.4 **A4 HVAC**

Figure 6-11 illustrates the flow chart of the HVAC selection. The inputs for the HVAC sizing are cabin volume and the number of passengers. The simulation is based on the design of HVAC components in section 4.3. The required inputs for the HVAC simulation are geometric dimensions of the vehicle, glazing ratio and the maximum occupancy to calculate the cabin volume for the evaluation of the cooling demand. This is provided by the vehicle specification database. The outputs of the HVAC simulation are the sizing of the compressor, evaporator, condenser and the radiator, as shown in Figure 6-11. Standard catalogue products of the HVAC components are stored in the HVAC database. Based on the sizing calculations, the tool allows for the selection of the standard components from the database. The tool allows the user to choose between different types of possible components, such as a 1-core or 2-core evaporator or condenser. The tool provides the change in the dimensions of the selected components and, hence, helps with the HVAC packaging. For the compressor, the simulation also determines the efficiency and power. All this information is stored in the HVAC database in addition. Furthermore, the cabin temperature and the cooling demand is calculated and presented by the tool. The cooling demand is an input for the powertrain design. The required cooling power is stored in the database as the energy consumption of the HVAC system. With the selection of the HVAC components, the configuration of the vehicle concept is complete.
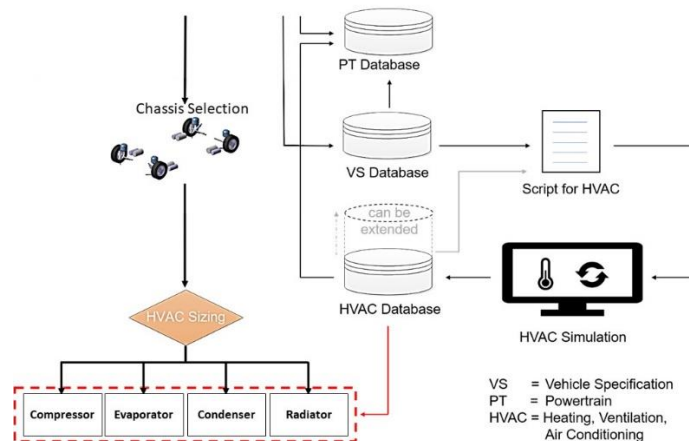
Figure 6-11   Flowchart for HVAC Sizing

6.4 GUI Design

An intuitive GUI is a main requirement of the tool as discussed in section 3.2. The GUI is designed in MATLAB. MATLAB R2017b is used in this work. MATLAB is a well-known and widespread software in the industries and the universities [25]. A MATLAB toolbox called as GUIDE is used for the development of graphical user interfaces In the AEV Tool [172]. Table F- 1 in Appendix F, illustrates the list of objects used in the creation of the GUI.

The GUI is developed with several main systems controlled by sub-systems. The definition of system boundaries is essential. The system boundaries are selected based on the functions and objectives. Figure 6-12 illustrates the software architecture design of the GUI.

As shown in the figure, the main systems are connected to each other through a joint interface and different sub-systems can interact with each other. This enables the characteristic model of a parametric model. All main systems and sub-systems are connected to a joint interface which converts the individual parameters to a global parameter in the main workspace. The joint interface provides a clear definition for the systems, which has to be followed. The parameter database is a dynamic storage location for all the inputs and outputs. It is connected to all main systems and enables an exchange of variables. Each system can access the database for storing or selecting data variables.
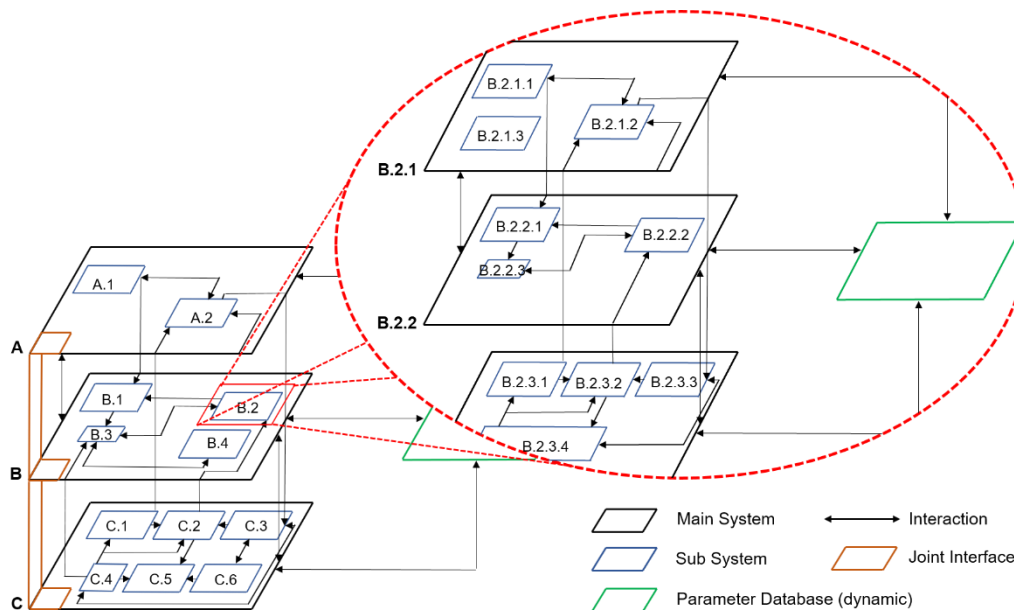
Figure 6-12   Software Architecture Design

In order to improve the AEV Tool script, it is divided into sections. This enables the developers of the script a better overview and ease of use. The script is divided into the following seven sections:

1 – Header: It gives an introduction to the structure and content of the script. It also provides an overview of the label of the individual main systems and the colour scheme used in the tool. Furthermore, the header defines the path on which the tool is working.

2 – Object Configuration: This section runs the first loading session of all objects as well as their design in the tool. Several databases will be loaded as well as the images. Additionally, the priority of the main systems is set to start the tool. The reason for summarizing all possible loading sessions at the beginning of the tool is the associated optimization of the

performance of the tool. Thus, no loading operations occur during the tool. It is just loaded at the beginning, when it is done, there is no unnecessary latency time while working with the AEV Tool anymore.

3 – Screen Setting: The setting for full screen is set in this section.

4 – Main Page: This section describes the start page of the tool. The user can select the different modes from this point. Depending on the selection, the script jumps to section 5 for Automated Mode or Section 6 for Manual Mode.

5 – Automated Mode: The Automated Mode is the most complex in term of its structure. This section contains all implementations of the individual components. Calculations must consider all parameters that have an influence on it. Before the evaluation and visualization part, there is a second slightly smaller loading session. All input is converted and calculated accordingly for evaluation and visualization.

6 – Manual Mode: Manual Mode lists 87 possible input options for the parametric model of an electric autonomous bus.

7 – Additional Features: Several additional features of the tool are defined in this section like Home Button, Delete Button, Currency Change or Interface for Presentation.

7 Concept Evaluation Methods

The previous sections dealt with the automatic selection of all the systems required for the vehicle concept development. The step following the selection of components is the evaluation of vehicle properties such as energy consumption and the cost. Energy Consumption Simulation

7.1 Energy Consumption Simulation

The powertrain components define the vehicle in terms of performance, driving dynamics, energy consumption and cost. Therefore, it is important to examine and compare the performance of the selected powertrain configuration. The entire calculation of energy consumption is based on a specific drive cycle. The Bus Rapid Transit (BRT) Beijing driving cycle developed by [164] has been considered for this evaluation since the vehicles in BRT system could be used to replicate the AEVs in public transport [170]. Figure 7-1 shows the velocity profile versus the time of the BRT driving cycle. The important indicators of the BRT cycle, such as average speed, maximum speed, cycle duration and cycle distance, are presented in Table 7-1 below [164].
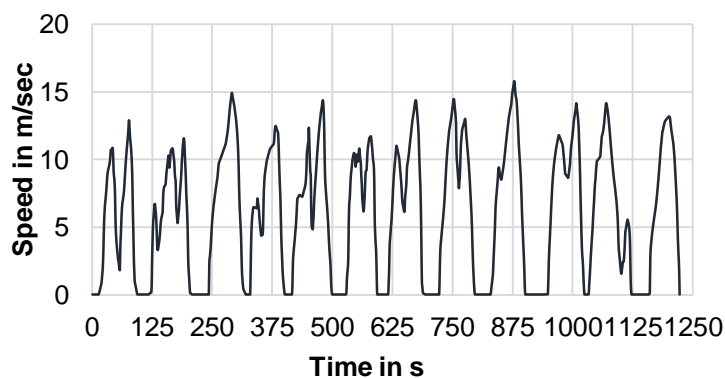
Figure 7-1   Speed profile - Beijing BRT Cycle

Table 7-1   Indicators of BRT Beijing driving cycle

Characteristics	Value
Speed range	15-25 km/h
Average speed	21.7 km/h
Maximum speed	54.8 km/h
Cycle duration	1,220 s
Cycle distance	7,356m

The energy consumption of the battery is calculated using the driving cycle. The tool illustrates battery power over time and shows the consumption, as well as the recuperation at any time of the driving cycle. The evaluation includes the energy consumption by the HVAC system and consumption by the CAV sensors or autonomous technology components and auxiliaries.

The CAV sensors included in the tool are LIDARs, sensors, cameras, and the processing unit. The energy consumption is considered to be between 1.01 - 1.5 kWh/100 km based on the size of the vehicle concept [173].

Further evaluation of the energy consumption is based on the consideration of the losses in energy conversion. The energy losses summarised in this work are the powertrain losses (loss of the motor, inverter, transmission and the battery) and the losses due to roll resistance, air resistance and slope resistance. Another aspect of the energy calculation of the vehicle concept is the visualisation of the motor efficiency map. For each selected motor, an efficiency map is generated with the motor torque over the motor speed and the associated loading points [174]. This illustration helps to identify whether the motor is operating in the high-efficiency area during its operation through the driving cycle.

7.2 Cost Estimation Model

The tool estimates the initial costs of the generated vehicle concepts. Due to the lack of the exact data of the costs, the cost estimation for this work is based on scientific publications and reports. Therefore, the cost values generated by the tool give the user an impression of the cost of the early phase vehicle concept. The total cost (C_{Total}) is the sum of the individual cost of the vehicle body (C_{Body}), powertrain ($C_{Powertrain}$), chassis components ($C_{Chassis}$), autonomous technology components ($C_{Autonomous}$) and the HVAC components (C_{HVAC}), as shown in Equation (7.1).

$$C_{Total} = C_{Body} + C_{Powertrain} + C_{Chassis} + C_{Autonomous} + C_{HVAC} \qquad (7.1)$$

The cost of the powertrain is significant since the battery is the most expensive component of an electric vehicle. The cost calculation of the powertrain and its components have been explained in Section 4.1.3. The cost of autonomous technology components is also significant and impacts the total vehicle cost. The autonomous technology hardware cost includes the LIDARs, sensors, cameras, and processing unit prices. The autonomous technology costs are calculated as described in [14]. The vehicle body includes the structure, interior and exterior. The vehicle body costs are calculated based on the weight and materials of the generated concept. The cost model to calculate the cost of the vehicle body and chassis components is derived from [175] [136] and [176].

7.3 Vehicle Properties Analysis

After the inputs are defined and the energy consumption is simulated, as well as the estimation of the total cost, this part will create a spider chart for the analysis on the top level. As already mentioned in section x the early development process comes out with a property chart in the end, in order to illustrate the desired bus concept. A spider chart is used in this tool, which represents graphically values of several equivalent categories. This is used as a comparison chart, which is particularly suitable for evaluations based on previously defined criteria. The top-level analysis in the part of the AEV Tool intents to round off the design of a concept with a spider chart. All relevant parameters, which define the key data of the bus, will be illustrated. Table 7-2 shows an overview of the key data and their range.

Table 7-2   Overview of the Spider Chart Parameters

Key Data	Range
Overall Length	5m-15m
Number of Passengers	30 – 70
Seats	20 – 40
Range	0 -400km
Energy Consumption	$60\frac{kWh}{100km}$ - $180\frac{kWh}{100km}$
Manufacturing Cost	80000SGD – 200000SGD

The lower values are determined based on the smallest, cheapest and most economical bus. Similarly, the upper limit comes from the largest, most expensive and highest consumption concept. In Automated Mode, two concepts can be compared together. It is possible to return to the configuration page at any time to change or adapt the concept. Furthermore, the different concepts can be visualized in CATIA. Therefore, the user gets the first idea of how the concept looks like. The chart provides a quick overview of the evaluation criteria and correlations. It is easy to understand, and the advantage is the limited interpretation effort. In addition, it is possible to get a quick and clear recognition of deviations. The spider chart is also used as the main tool for validating the AEV Tool in this thesis.

7.4 Life Cycle Assessment

The Life cycle assessment (LCA) is a tool used in the evaluation of the environmental impacts of any product through its lifecycle i.e. from the cradle to grave. The LCA follows a standardised process by the International Organization for Standardization (ISO) [177]. The LCA methodology is applied to the vehicle concepts developed with the tool. The stages of the LCA are explained below.

7.4.1 Goal, Scope and General Considerations

The goal of this LCA is to assess the environmental impacts different autonomous and electrified vehicle concepts of size between 4 m – 14 m in Singapore based on the results generated by the AEV tool. The life cycle emissions are compared with the conventional 12 m Internal Combustion Engine Bus (ICEV) in addition. The emissions are analysed based on two impact categories, greenhouse gas (GHG) emissions and particulate matter (PM).

The LCA study in this work includes emissions from all the major phases namely the production, distribution, use phase and end of life. Table 7-3 summarises the scope definition. The assumptions are based on the life cycle cost assessment study conducted by the author [14]. The functional unit for the comparison is set as $passenger\ kilometer$ (pkm). The travelled distance per day is 213 km and it is assumed that the buses are used 329 days per year for a period of 17 years [178]. The average passenger capacity of the buses in Singapore is 17 % [178]. The LCA is modelled in Umberto-LCA [179] software with the lifecycle inventory databases from Ecoinvent version 3.5 [180].

Table 7-3   LCA Scope Definition

Parameters	Value
Functional Unit	pkm
Service life in years	17
Average occupancy in %	17
Average distance per day in km	213
Annual use in days	329
Average occupancy in %	17
Bus length in m	4-14

7.4.2 Life Cycle Inventory

The life cycle inventory comprises of the compilation and quantification of emissions from the inputs and the outputs throughout the lifecycle of the product. Figure 7-2 depicts the process flow and the phases of the life cycle inventory process. As shown, all the major phases are considered in the inventory process in sequence.

In the production phase, the Autonomous Electric Bus (AEV) concept comprise of three major parts: the glider (chassis, body and structure), the powertrain (motor, inverter and electronics) and the battery, while the ICEV is comprised of the glider and the powertrain (internal combustion engine and the gearbox). The manufactured vehicle components are assumed to be assembled in Eastern Europe and subsequently transported by a train and a transoceanic ship to Singapore. The use phase of the buses is divided into the Well-To-Tank (WTT) phase and the Tank-To-Wheel (TTW) phase. The WTT phase is comprised of the upstream emissions such as the production of electricity and diesel fuel as shown. In addition, the emissions arising from vehicle maintenance is added in the WTT phase in this work. The TTW phase includes the emissions from the ICEV exhaust and the non-exhaust emissions from tire, brakes and road. The End-of-Life (EOL) phase comprises recycling of the battery pack and other materials. The inventory data for each process is discussed in detail in the next sections. All the processes are modelled using *Umberto LCA+* [179] and the *Ecoinvent* database [180].
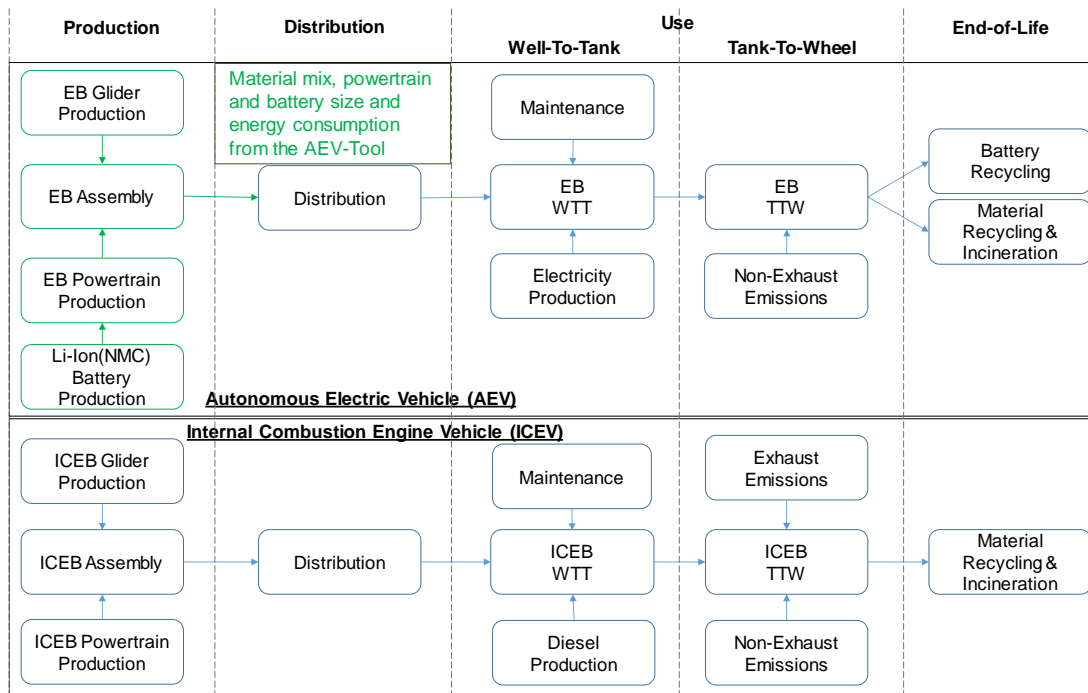
Figure 7-2   Lifecycle Inventory Process Flow

7.4.2.1 Bus Production Inventory

Since the ICEV is a standard vehicle, the material composition is based on the data from "GREET Model" [181] developed by Argonne Lab. It is an analytical tool with databases for the material mix of different components such as the body/chassis, the engine and the gearbox.

For the case of AEV, the material composition of the concept is calculated using the AEV Tool [97]. As discussed above, the concept developed by tool includes all the systems namely, the body and structure, chassis, powertrain, HVAC and autonomous components The upstream production emissions of all of the materials are based on the Ecoinvent database [180].

The electric powertrain of the AEV has the highest contribution in the production emissions. This is because the lithium-ion battery production is the most energy-intensive process and has a higher impact on the results [182]. Various studies compiled the energy demand for battery production and the results have a high deviation ranging from 34 – 744 kWh energy demand per kWh of battery capacity produced [182, 183]. In this work we assume, an energy demand of 313 $kWh/kWh_{\text{[battery capacity]}}$ from the most recent report published by the Swedish Environmental Research Institute (IVL) [184]. The transparent report provides data on the energy and emissions in different steps of battery production.

The energy demand for the production of the glider, material wastes and emissions during vehicle glider production based on the data from MAN Truck & Bus report [185].

7.4.2.2 Distribution Inventory

As discussed, the vehicles are assumed to be manufactured in Ankara, Turkey, based on [14]. The buses are transported by train from Ankara to Rotterdam, Netherlands and later shipped to Singapore with a transoceanic ship. All the required data for distribution are derived from the Ecoinvent database [180].

7.4.2.3 Use Phase

The use phase or the Well-to-Wheel (WTW) phase, comprises of two independent stages: Well-to-Tank (WTT) and Tank-to-Wheel (TTW).

Well-to-Tank (WTT) Phase

The WTT phase is comprised of the upstream emissions of electricity and diesel production in Singapore. In addition, maintenance of the vehicle throughout the lifetime is included in the WTT phase. The electricity mix is the key factor for analysing electricity production emissions. In Singapore, natural gas contributes to 95 % of the total electricity production. The remaining 5 % is shared between petroleum products, coal, municipal waste, biomass and solar [186]. The total electrical energy demand is calculated by considering the energy consumption of the electric and autonomous electric bus, the mileage, and the efficiencies of the supply chain. The energy consumption of the AEV is calculated with a longitudinal dynamics model explained in section 4.1.

The supply chain for diesel in Singapore is the main component to analyse the emissions arising from diesel production. Singapore imports around 32 % crude oil and 68 % refined petroleum products [186]. The efficiency of the different processes in the production and supply chain for the LCA model is derived from the Ecoinvent database [180].

Tank-to-Wheel (TTW) Phase

The TTW phase includes driving emissions or exhaust emissions and non-exhaust emissions. The average consumption of the ICEV is 51 l/100 km in Singapore [187]. The tailpipe CO_2 emissions of diesel buses are calculated based on [188] and the other exhaust emissions are based on the emission's standard Euro VI for heavy-duty vehicles and the investigations of Gemis and COPERT for ICEV [189–191]. The 6 m EB and AEV have zero TTW emissions.

7.4.3 End of Life

The EOL phase includes battery recycling and material recycling. The EOL treatment and recycling of the battery is based on the LithoRec project, developed for the recycling of traction batteries [192]. For the treatment of the glider and powertrain, different recycling rates are assumed based on the component`s material mix [193–196].

8 Results

The preceding chapters described the methodology to develop individual modules required for the tool and explained the implementation of the AEV Tool by the integration of the developed work packages. In this chapter, the results of the AEV tool are discussed extensively. The results of different modes of the tools are discussed and the advantages of using different modes of the tool are clearly explained. Subsequently, the vehicle concept results are evaluated and validated based on benchmark values and existing studies. Furthermore, the lifecycle impacts of developed vehicle concepts are assessed. Finally, the multiple vehicle concepts developed by the tool are compared by considering a case study from Singapore. The concepts are compared based on cost and emissions.

8.1 Vehicle Concepts Generation

As explained in the architecture of the AEV tool in section 6.1, the tool has 2 different modes to generate vehicles concepts. Figure G-1 in Appendix G illustrates the main screen GUI of the AEV tool. The manual mode, intended for the users with expert vehicle knowledge is designed as a step by step process to size the subsystem, thereby creating the vehicle concept. In the case of the automated mode, the tool is designed to automatically select all the subsystems and create a vehicle concept based on basic inputs such as the desired vehicle type, passenger capacity and layout. The following sections discuss the vehicle concept generation results of each mode in detail.

8.1.1 Manual Mode

Figure 8-1 shows the GUI of the manual mode of the AEV tool. As described earlier, the tool allows the user to define the dimensions of all the components and choose between different configurations and topologies of components.

There are 78 fields to input or change the values of the parameters and 18 vehicle configurations that comprise of three interior seating layouts, three powertrain topologies, and two ramp configurations. Only one vehicle concept can be generated for each configuration. For instance, a vehicle concept generated could either have a central motor at the rear axle configuration or dual motor configuration, but having the two topologies together is not possible at the same time. Apart from the dimensional and configuration parameters, the material of the components can be defined. Therefore, in addition, there are 28 drop-down fields to select the materials from a predefined list. Only one material can be chosen for a component at any point in time.

As shown in Figure 8-1, the GUI of the manual mode is divided into subsystem groups as explained in section 3.5:

- Vehicle Specifications
- Powertrain
- Chassis
- Body and Structure

- Electronics
- Default

It should be noted that the structure of the parametric 3D CAD model is identical to the selection process. This allows for better modularity and expandability of the tool.

The parameter input fields of the tool have been implemented with several warning features to help the users. The limits of each input parameters have been predefined. For instance, the length of the vehicle concept is within 4 m - 14 m. Hence, if the input is out of the range, the tool displays a pop-up window suggesting the appropriate values. Similarly, there is a 'check' button feature as shown in Figure 8-1 that aids the users to ensure if all the input parameters have been entered. The check button highlights the empty fields with red to warn the user. Furthermore, the 'Default' button feature is a list of the predefined parameter for a 6 m autonomous electric concept. The default values help the user to get an insight into all the parameters required to define such a concept. Only error-free acceptance of the parameters, the tool allows proceeding for visualization of the developed vehicle concept.
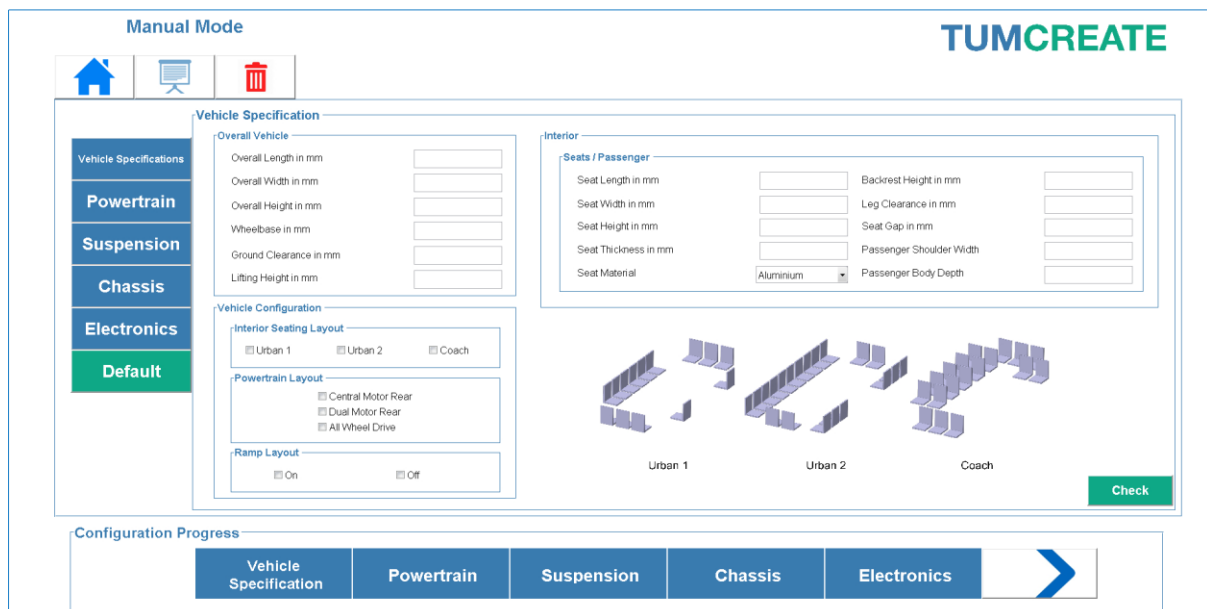
Figure 8-1   GUI of Manual Mode

Figure G-6 shows the visualisation of the concept developed with manual mode. Visualisation of the concept is the last step in this mode. On execution of the 'visualization' button, all the vehicle parameters are converted and saved into the txt file as explained in section 6.2.6. Thereby, the 3D-CAD model, through CATIA macros, gets updated to the recent parameters. Thus, CATIA automatically makes geometric changes and creates the final vehicle concept. Figure 8-2 shows two 3D vehicle concepts generated by the tool with different lengths and different interior and ramp configuration.

As explained in section 6.2.6, the visualisation process generates screenshots of 3D models in the background. The visualisation shows the important external dimensions such as the overall vehicle length, the vehicle width, the height, the wheelbase, and the ground clearance. Furthermore, the calculated mass of vehicle concept and the centre of gravity values are displayed as shown in Figure G-6. The tool illustrates the seating layout and provides occupants information such as the number of passengers and the number of seats.

As seen in Figure G-6, the 'CAD Model' button facilitated the users to view the 3D model of the vehicle concept in CATIA. This enables to provide a detailed overview of the vehicle and component package to the users. The users can also save the vehicle concept as a PDF file containing all information and pictures presented within the concept visualization.

(a)   (b)
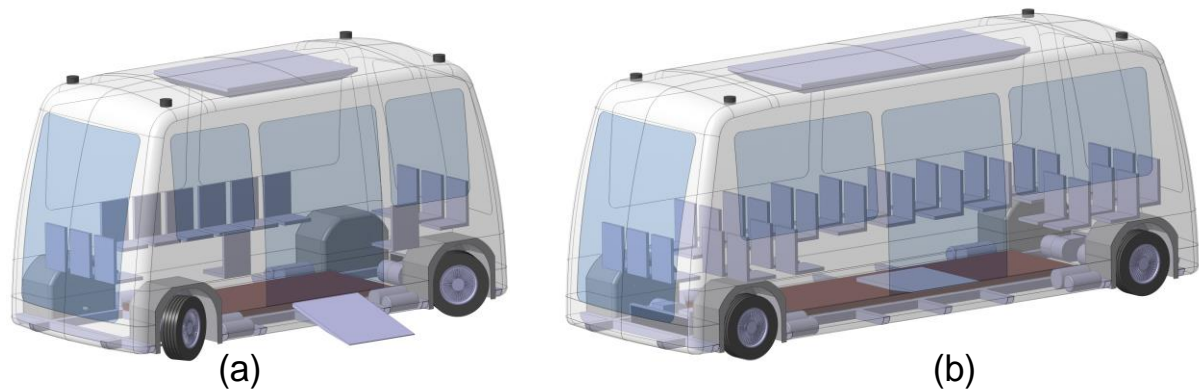
Figure 8-2 Parametric CAD model (a) 6 m AEV (b) 8 m AEV

8.1.2 Automated Mode

Figure 8-3 shows the GUI of the automated mode. Figure G-3 - Figure G-5 in Appendix G illustrates the GUI of the selection of other subsystems i.e. the powertrain, the chassis and the HVAC. As explained in section 6.3, the automated selects the components automatically based on user inputs. Two vehicle concepts can be created simultaneously and compared. Apart from the generation of vehicle concept and visualisation, the automated mode provides numerous results intermediate such as the size and weight of component subsystems, cost of components, energy consumption and performance parameters. Therefore, in order to improve the clarity of the concept development process, a results overview is integrated into the GUI that gives an indication of the results at the end of every step.

In this mode, the tool allows the generation of a large number of plausible vehicle concepts. Figure 8-3 shows the first stage where the user inputs are vehicle specification parameters. The user can choose between three vehicle classes, namely, the coach, city and shuttle bus. The selection of the number of passengers is the following input and the range to choose is between 30 and 70 passengers. Subsequently, the user can select between 3 different seating layouts based on the selected vehicle type. Based on the input, the tool instantly generates the vehicle dimensions and the gilder mass which is displayed in the results overview as seen in Figure 8-3.
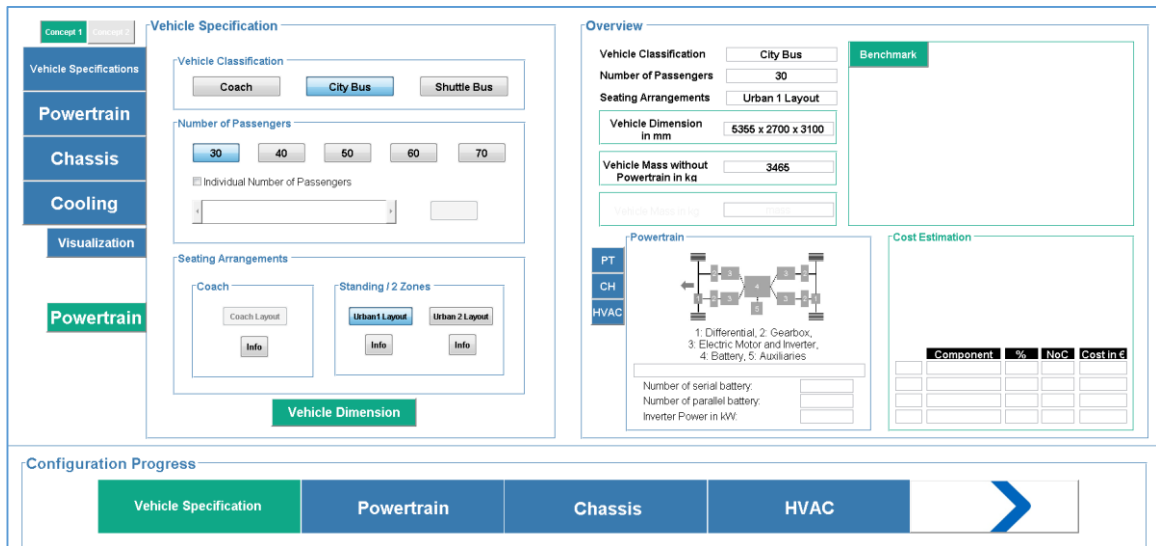
Figure 8-3   GUI of the Automated mode

Figure 8-4 illustrates the selection possibilities at each level to show the maximum number of vehicle concepts that could be generated. As shown, for each vehicle concept, there are four options in the powertrain concepts with two possible architectures and vehicle ranges (refer to Appendix G Figure G-3). Following the powertrain selection, the overview displays the vehicle mass, the architecture of the selected powertrain and the cost of each powertrain component. Further, the chassis components are sized based on the vehicle specification (refer to Appendix G - Figure G-4). The tool shows the selected chassis components and the specifications in the overview as seen in Figure G-4. As the last step, there are twelve possible HVAC architectures for each vehicle concept (refer to Appendix G, Figure G-5). In the overview, the tool displays specifications of each component and calculates the energy consumption and cabin temperature. Thus, in total, over 9600 unique vehicle concepts can be generated in the automated mode. As discussed in Section 6.3, the tool also supports the development of two-vehicle concepts simultaneously for comparison.

S = Stage, PT = Powertrain, C = possible Combinations, SL = Seating Layout, AC = Air Conditioning
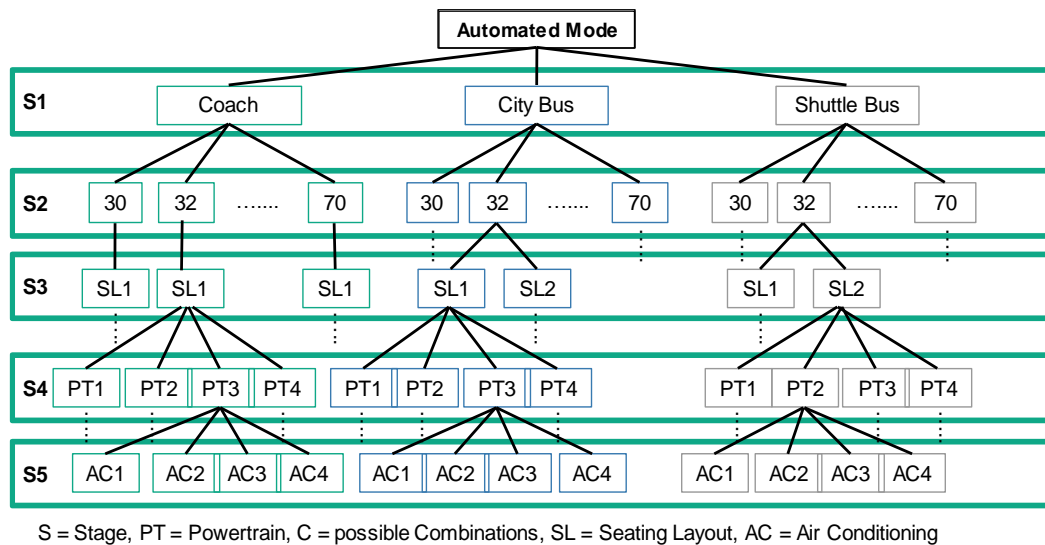
Figure 8-4   Vehicle Concept Combinations

The results of the vehicle concept generated with the automated mode are the cost estimation, energy consumption simulation, and 3D-visualisation of the generated vehicle concepts. Figure G-8 - Figure G-9 in Appendix H shows the interface of the results. However, the results are further analysed based upon the vehicle properties. A spider chart/radar chart displays the relevant parameters, namely, the vehicle length, number of passengers, seats, vehicle range, energy consumption and initial costs of the vehicle concept. Table 8-1 shows the values of all the individual parameters from the spider chart for the two-vehicle concepts that are compared. In addition, Table 8-1 shows the minimum and maximum range of each parameter illustrated within the spider chart. The spider charts are later used for comparison of simultaneously developed concepts. Figure 8-5 illustrates the spider chart by comparing two different vehicle concepts. As seen in Figure 8-5, the lower limit and upper limit of the model are used in this comparison. A total capacity of 30-passengers with ten seats is selected as *'Concept 1' (dark blue),* and a concept with 70-passengers with 56 seats is selected as *'Concept 2' (light blue).* The properties of the two-vehicle concepts can be overlapped as displayed. This is to facilitate easy comparison and enables the users to understand the influence of a property over the other. In addition, Figure 8-5 shows the generated 3D CAD model of the two concepts for better illustration.

Table 8-1   Vehicle Parameters on the Spider Chart

Criteria	30-Passenger	70-Passenger	Range
Vehicle Dimension in mm	5355 x 2700 x 3100	13235 x 2700 x 3100	5000 – 15000
Number of Passengers	30	70	30 – 70
Number of Seats	10	56	10 – 60
Energy Consumption in kWh/100 km	83	179	60 – 185
Range in km	300	300	0 – 400
Cost in Euro	126223	210297	80000 – 240000
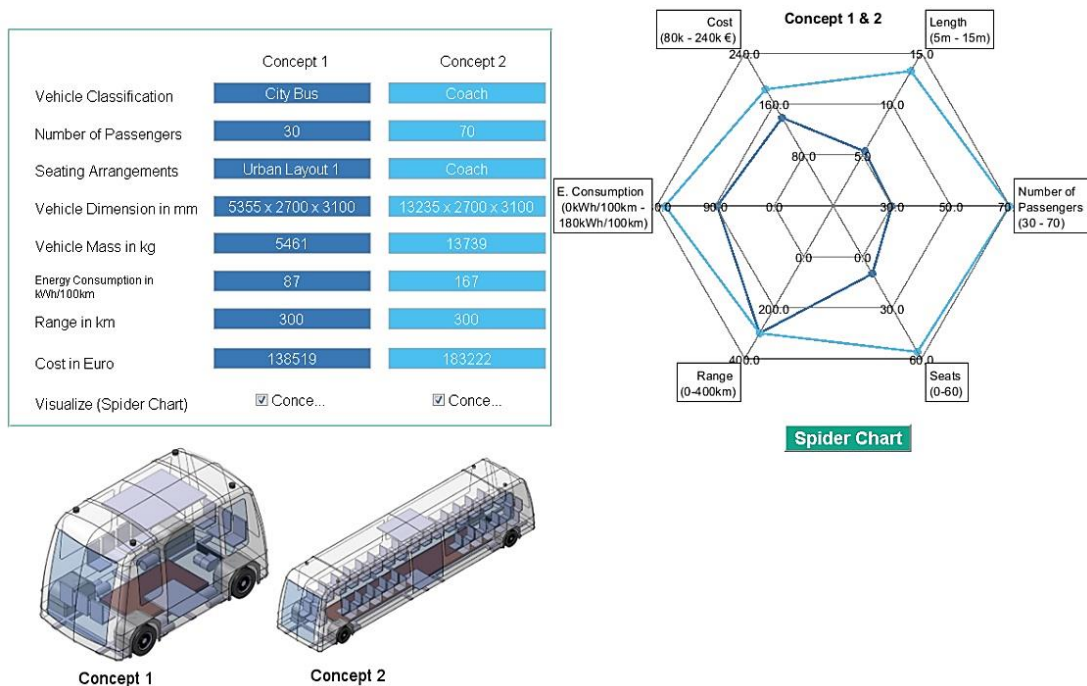
Figure 8-5   Vehicle Properties Comparison

This helps the users to optimise the parameters of the vehicle concepts based on their target specifications before visualisation of the package. For instance, if the user has a target passenger capacity and the vehicle cost as the main limiting factor, the tool helps in a quick decision making allowing the user to vary the selection parameters. Figure 8-6 shows the spider plot of an example scenario with a capacity of 40 passengers and maximum range 300 km as the target. For illustration and the ease of understanding, the properties of all the selected vehicle concepts have been plotted in a single spider plot.

We know that the tool can generate several vehicle concepts for the targeted capacity by varying the vehicle classification, the layout, the powertrain or the HVAC architecture. However, the properties of each vehicle concept would be different. Table 8-2 shows six different vehicle concepts generated by varying the powertrain configuration and the seating layout. We can see that, out of the six concepts, three concepts have repeating seating layouts and three powertrain configuration.

From the vehicle properties comparison shown in Figure 8-6, it can be observed that all the selected concepts have the same range and passenger capacity. All the other properties are varying based on the selected configurations. The number of seats changes based on the seating layout. The City-1 and City-2 vehicle concepts with 18 seats have the least number of seats compared to the others. The seating layout affects the number of seats and vehicle length. Thus the City-1 and City-2 concepts are the smallest concepts with a length of 6.6 m. On the other hand, Coach-1 & 2 have 28 seats which are 70 % more than the City-1 & 2. This increases the vehicle concept length by around 15 % to 7.6 m. City-3 & 4 are the intermediate concepts with 25 seats and 7.1 m in length.

The mass of the vehicle concept contributes to energy consumption. However, the powertrain configuration has significant impacts on energy consumption and also on the vehicle cost. As it can be seen in Table 8-2, all the concepts with 2-Motors at each axle configuration has less energy consumption compared to the 1-Motor at each axle configuration. Although the Coach-2 concept is longer and weighs more than the City-1 concept, the energy consumption is 92 kWh/100 km which is slightly less than the City-1. In a similar way, the City-4 consumes less than the City-1. However, City-2 concept has the least energy consumption with 84 kWh/100 km. The most interesting result as seen in Figure 8-6 is the cost. The cost of vehicle concepts with 2-Motors per axle is lesser in comparison. Although the initial costs of the drivetrain components are high, because of the reduced energy the concepts require a smaller battery capacity to meet the 300 km range requirement. Therefore, the battery cost and hence the vehicle costs are lower.

Therefore to summarise from the spider plot (Figure 8-6), City-4 concept appears to be the ideal solution based on the vehicle properties. The vehicle concept has 25 seats that improve passenger comfort, with 90 kWh/ 100 km consumption and an initial cost of 135335 Euros. However, the least expensive concept is the City-2 concept at 133210 Euros. Thus the user can easily choose a vehicle concept by comparing different properties with the help of the spider plots.
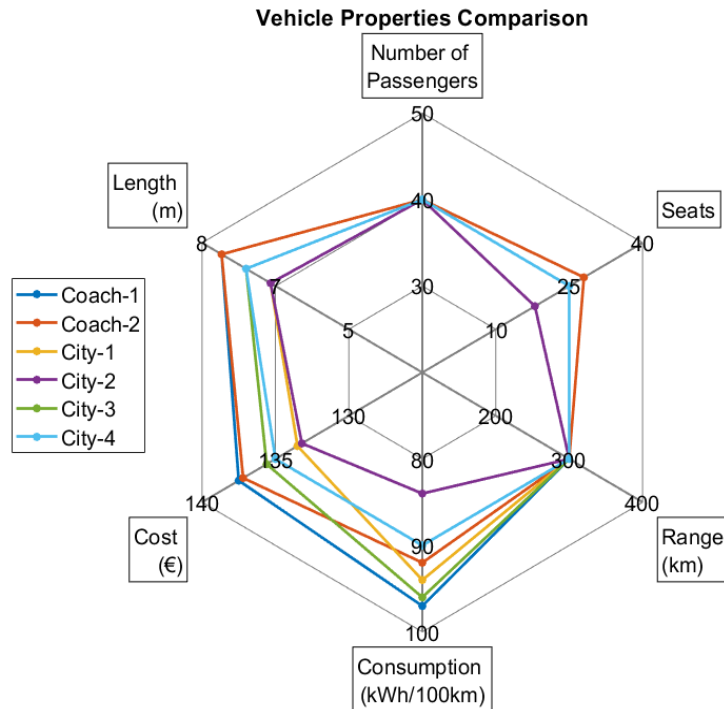
Figure 8-6   Vehicle Concepts Comparison

Table 8-2   Vehicle Properties Comparison for 400 Passenger Concepts

Vehicle Concept	Powertrain Concept	Seating Layout	Number of Seats	Vehicle Length (m)	Vehicle Mass (kg)	Cost (Eur)	Consumption (kWh/100 km)
Coach-1	1 Motor at each axle	Coach	30	7.6	7565	137492	97
Coach-2	2 Motors at each axle	Coach	30	7.6	7696	137207	92
City-1	1 Motor at each axle	Urban Layout 1	18	6.6	6590	133527	94
City-2	2 Motors at each axle	Urban Layout 1	18	6.6	6702	133210	84
City-3	1 Motor at each axle	Urban Layout 2	25	7.1	7061	135637	96
City-4	2 Motors at each axle	Urban Layout 2	25	7.1	7210	135335	90

From the description above, we can see that the spider plots provide top-level results of the vehicle concept such as overall cost, energy consumption, etc. for facilitating a fast decision-making process. However, the user would require detailed results for further analysis. Therefore, as explained in section 7 and section 7.2, the AEV-tool is implemented with energy consumption simulation and component level cost assessment.

Figure G-8 in Appendix H shows the GUI of the energy consumption simulation. A shown in Figure G-8, the tool provides numerous details such as the simulated driving cycle, the losses incurred during the driving, the powertrain losses, the energy consumption from the battery and energy recuperation, the overall powertrain and drivetrain efficiency and the efficiency maps of each motor. As discussed in 4.1.1, the multiple motor architectures enable the distribution of the load in order to optimise their operation. Figure 8-7 (a) and (b) shows the load points on the motors in the front axle and rear axle respectively. Figure 8-7 (a) shows that

the front axle motor is able to meet the requested torque often and is assisted by the rear axle motor whenever the requested load exceeds the front motor`s capacity as seen in Figure 8-7 (b). Furthermore, this leads to the accumulation of load points in higher efficiency regions of the motors. Thus the overall powertrain efficiency improves and reduces energy consumption.

(a)   (b)
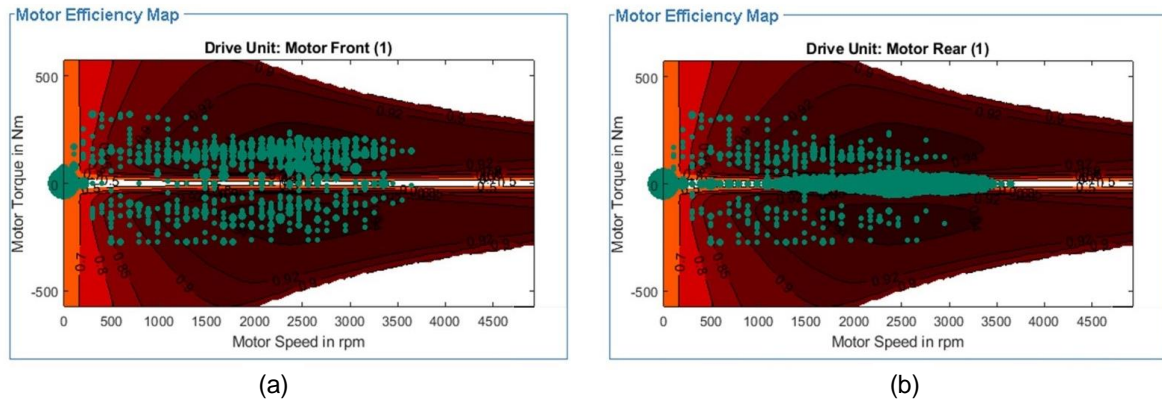
Figure 8-7   Load points on motor maps (a) Front axle (b) Rear axle

Figure G-7 in Appendix H shows the GUI of the cost estimation results. Apart from the overall cost of the concept, the tool provides a detailed split-up of component costs of all the subsystem. The user can analyse the cost of individual components further modify the selection if needed. The tool also provides an interactive slider to vary the cost of the individual subsystem to evaluate their influence on the overall cost of the concept. The results of the cost assessment for different concepts are evaluated, validated and discussed in detail in the following section.

Following the vehicle properties, energy consumption simulation and cost estimation the generated concepts can be visualised in 3D using the CATIA interface. The visualisation follows a similar procedure as the manual mode explained in section 8.1.1. Figure G-9 in Appendix H shows the GUI of the concept visualisation of the automated mode. Different pictures of the vehicle concept are presented along with the overview of vehicle specifications. The generated concept can be documented as a pdf with all the vehicle specifications and pictures of the CAD models.

8.2 Evaluation of the Results

Section 8.1 explained the results of vehicle concept generation with the manual mode and the automated mode. However, it is important to analyse the holistic tool and evaluate if the results generated by the tool are valid. From the literature, we know that there no existing studies to directly validate the AEV concepts generated by the tool. Therefore, this section will evaluate the vehicle concepts developed with the AEV tool. Section 8.2.1 analyses the weight over different vehicle concepts and compares them with the benchmark vehicles. Section 8.2.2 analyses the cost estimation of the vehicle concept. Section 8.2.3 discusses the environmental impacts of AEVs through the life cycle assessment study.

8.2.1 **Weight Assessment**

The weight assessment of the vehicle concepts is performed by comparing the weight of vehicle concepts with benchmark vehicles. One criterion for the selection of benchmark vehicles is that the buses should be of different sizes since the AEV tool can develop concepts of 4 m-14 m. The benchmark vehicles should also be electrified buses for precise comparison. Therefore, the benchmark buses selected for the evaluation included both autonomous and non-autonomous electric buses. This is due to the fact that the autonomous buses currently in the market are micro-transit vehicles of lengths between 3 m - 6 m as described in Section 2.1.2. Furthermore, most of the autonomous electric buses are still in the prototype phase. Hence, the buses with reliable data are selected for this analysis. The electric buses compared are of different lengths ranging from 6 m to 12 m.

The specifications of the selected electric buses are majorly from the *ZeEUS eBus Report* [31] and from manufacturers specifications. In total, three autonomous electric buses and eleven non – autonomous electric buses from various bus manufacturers are chosen, ranging from 4 m to 12 m [31, 61, 62, 64, 197, 198]. Table 8-3 shows the list of the selected buses for evaluation. The table includes the vehicle model, the length, the battery capacity and the kerb weight (weight without passenger and baggage) of the buses. Weight of the batteries plays a significant role in the overall weight of electric vehicles. Hence, the battery capacity is mentioned in Table 8-3. The battery capacity of some vehicles was not specified. The capacity for those was assumed based on the other vehicles. In Table 8-3 the impact of the battery capacity on the overall weight of the vehicle can be clearly seen.

For the weight assessment analysis, the vehicle concepts are generated by the AEV- tool based on the benchmark buses. During the weight comparison, change in the vehicle parameters such as wheelbase, the wheel size, the battery capacity, the powertrain configurations and other components were manually changed for different lengths to suit the specifications of the benchmark buses. The resulting kerb weight of the thus generated vehicle concepts is shown in Table 8-3 in addition. Figure 8-8 illustrates with a plot, the weight comparison between the benchmark buses and the vehicle concepts generated by the AEV Tool. The plot shows the kerb weight against the length of the vehicles (4 m – 12 m).

Table 8-3   Benchmark Electric Buses

Vehicle Model	Vehicle Length [m]	Battery Capacity [kWh]	Kerb weight [kg]	Kerb Weight of Vehicle Concept [kg]
Easy mile EZ10	4.0	30	2750	2791
Navya	4.8	33	2400	2790
Rivium GRT	6.0	36.8	4500	4258
Karsan Jest Electric	5.9	44	3700	4138
Karsan Atak Electric	8.0	220	7940	7978
Modulo C68e	8.0	141	7200	7278
BYD midi	8.7	-	9490	9112
Otokar Electra	9.0	170	9925	9426
Temsa MD9 electriCITY	9.3	200	9775	9740
VDL Citea LLE-99	9.9	248	10775	10557

SOR EBN 11	11.1	-	11170		11400
Sileo S12	12.0	230	12865		12868
ADL Enviro200EV	12.0	330	12750		12868
BYD 12 m China	12.0	-	13125		12868

From Figure 8-8, it can be clearly seen that the difference between the kerb weight of the benchmark buses and the bus concepts developed by AEV tool is very minimal. The weight of almost all the concepts is in line to that of the buses compared. The 5 m bus, the Navya autonomous shuttle has a weight difference of around 35 %. This is because of the composite vehicle structure used for its construction. With the AEV tool, steel and aluminium structures are possible. The 6 m Karsan Jest electric vehicle have a deviation of around 12 %. Similar to the 5 m buses, the concepts developed by the AEV tool are heavier. This could be because of multiple reasons. The models developed by the tool are less detailed since the target is the early concept phase. In addition, the energy density properties of the batteries from the manufacturers are unknown. This could have a significant impact on the results. However, the weight difference for all the other concepts are less than 5 %
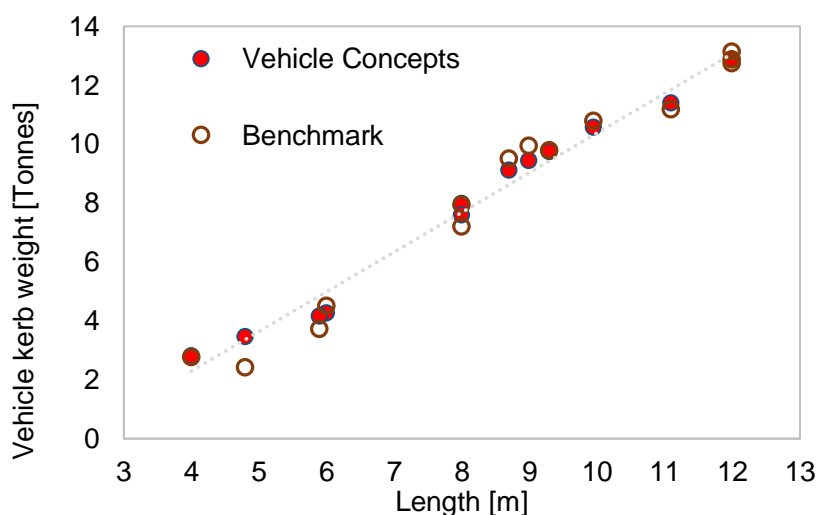
Figure 8-8   Vehicle Weight for Different Vehicle Lengths

Therefore, the results of the weight analysis from the AEV-tool can be considered reliable. However, the vehicle concepts comprise of various subsystems such as the powertrain, chassis, vehicle body, etc. So it is important to assess the influence of each of the subsystem to the overall weight of the concept. For instance, as described in the previous paragraph, the battery is one of the key components affecting the overall weight as shown in Table 8-3. In addition from Figure 8-8 it can be observed that there is an almost linear increase in the weight of the vehicle concepts with respect to the length. However, in this case, the linearity is impacted by the changing battery capacity and hence the battery weight. Therefore, it is interesting to see the influence of each component subsystems on the total weight of the vehicle and therefore is discussed in detail in the next section.

Influence of component systems on the total weight

As explained in the previous paragraph, the weight of the vehicle concept generated by the AEV tool is reliable. But it is important to discuss in detail, the influence of component subsystems that contribute to the total weight. However, for this assessment, unlike the

benchmark analysis, the vehicle concepts and its components should be varied uniformly to understand the impact of each subsystem. Hence, vehicle concepts between 4 m – 14 m are generated with a set of boundary conditions as shown in Table 8-4. The city bus is selected as the configuration, the interior layout is fixed to the urban layout -2 with a powertrain configuration and vehicle range of 300 km. Thereby, the battery capacity can be derived uniformly.

Table 8-4   Boundary Conditions for Weight Assessment

Vehicle Classification	City Bus
Vehicle Length	4 m - 14 m
Interior Layout	Urban layout 2
Maximum Range	300 Km
Powertrain Configuration	1 Motor at each axle

Table 8-5 shows the list of the generated vehicle concepts with weight breakdown of the weight of respective subsystems. Table 8-5 includes the length of the vehicle concepts with the passenger capacity of each concept, weight of individual subsystems and the kerb weight of the vehicle. The vehicle subsystems shown in Table 8-5 (as explained in chapter 6) are

- Body and structure (Vehicle body, interior, exterior, structure, etc.)
- Chassis (suspension, wheels, brakes and axles)
- Powertrain (motor, inverter, battery)
- Others (Air-conditioner, ramp, CAV components etc.)

Figure 8-9 shows the weight breakdown of all the subsystems for each vehicle concept. The plot clearly illustrates different subsystems. The linear characteristics of the increase in weight of subsystems can be clearly seen with the powertrain and chassis subsystem. The weight of the body and structure also increases almost linearly. Furthermore, based on the slope of different subsystems, it can be observed that the percentage weight distribution of the subsystems differs with different vehicle concepts.

Table 8-5   Weight Breakdown of Subsystems

Length [m]	Passenger capacity	Body and Structure [kg]	Chassis [kg]	Powertrain [kg]	Others [kg]	Vehicle Kerb weight [kg]
4	19	1838	696	1913	199	4646
5	27	2326	880	2180	252	5638
6	35	2722	1030	2446	294	6492
7	43	3066	1160	2777	331	7335
8	51	3646	1379	3044	394	8463
9	58	4114	1557	3310	445	9426
10	66	4696	1777	3577	508	10557
11	74	5084	1924	3843	550	11400
12	82	5862	2218	4155	634	12868
13	90	6513	2464	4421	704	14102
14	97	7092	2684	4688	767	15230
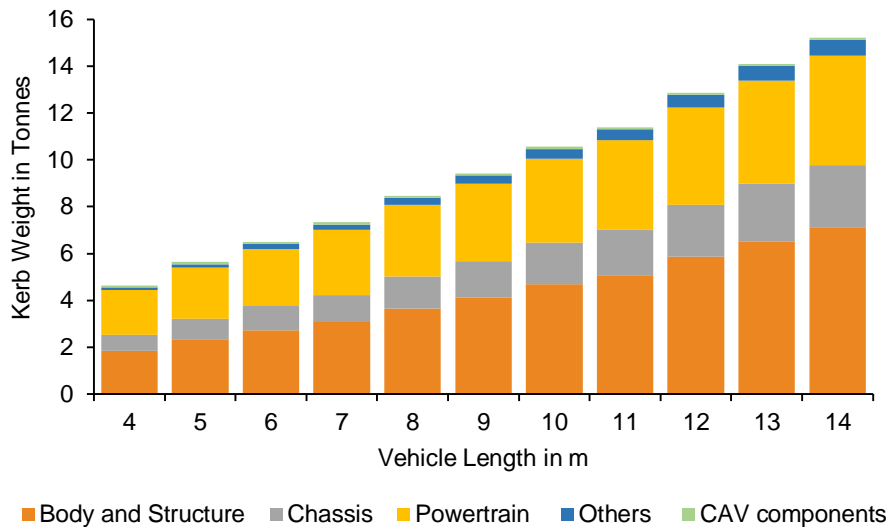
Figure 8-9   Weigh Breakdown of Different Vehicle Concepts

Figure 8-10 shows the weight breakdown of the subsystems for generated vehicle concepts in percentage. It can be seen that the weight percentage of the body and structure increases from 40 % of the total weight in the 4 m concept to 46 % in the 14 m concept. Similarly, the weight percentage of the chassis components also increase from 15 % of the total weight to 18 %. However, the powertrain weight has a decreasing trend. The weight percentage of the powertrain reduces from 40 % in 4 m to 32 % in 14 m. This can be justified by the boundary conditions and the battery capacity. Since the smaller concepts have less structural weight and a bigger battery pack to cover a 300 km range, the weight of the powertrain has a greater share in smaller vehicle concepts i.e. 4 m – 7 m. The influence of the weight of the battery pack reduces with increase in the vehicle length. With the increase in the length of the vehicles, the passenger capacity increases as seen in Table 8-5. Therefore, the weight of the body and structure and chassis components increase and this leads to a higher share of these subsystems in the total weight. From Figure 8-10, it can be seen that the change in the percentage share of other components is minimal and the percentage change of the CAV components is also insignificant due to their weight.
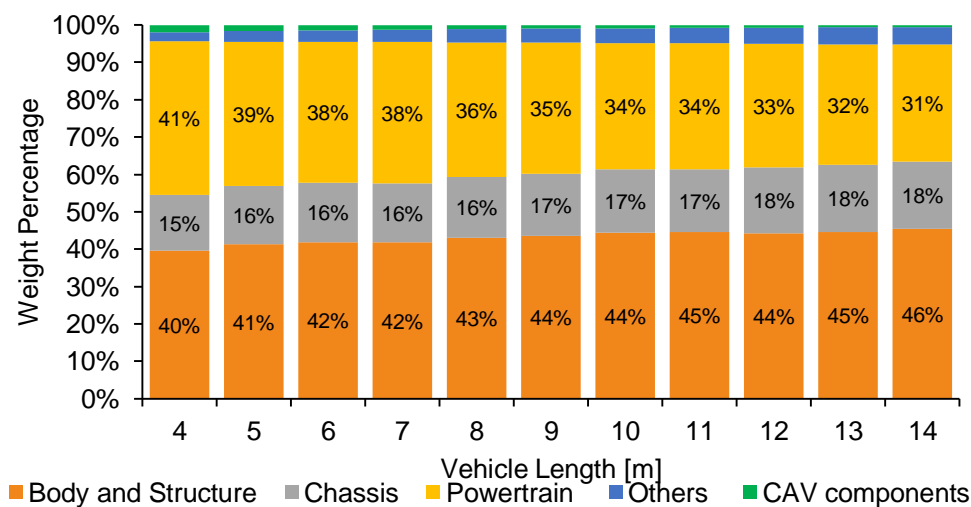
Figure 8-10   Subsystems Weight Distribution Over Vehicle Length

The results of the subsystem weight distribution analysis are evaluated by comparing with those results of existing studies. Since the AEV tool vehicle concepts are over a span of 4 m -14 m, the evaluation is compared with two different studies. The vehicle concepts with smaller lengths (4 m – 6 m) are comparable to passenger cars. A research conducted by the Argonne national lab on the studied the impacts of passenger cars electrification on the vehicle weight [199]. Hence, the results of this study are compared with the concepts developed by the tool. The weight breakdown results of the [199] showed that the weight of the powertrain and glider (chassis and body) of electric vehicles is around 35 % and 55 % respectively. This is very much comparable to the results produced by the tool as seen in Figure 8-10 where the glider weight share is around 55-60 % and weight share of the powertrain is around 38-40 %.

For evaluation of the bigger concepts (10 m – 12 m), research published by the American Public Transportation Association [200] is considered. The study analysed the weight of different transit buses in America. However, the evaluated buses are non-electric and hence, only the weight of glider is considered for our evaluation. The results of the study showed that the weight of the glider is around 65 % which is comparable to the result of concepts from the AEV tool, where the glider weight is 61 % - 63 % for vehicle length between 9 m-12 m. Therefore, the results from the tool can be considered acceptable for different vehicle concepts in the early concept phase and can be made better with further improvement of the component models.

8.2.2 Cost Assessment

The results of the cost estimation are shown in Figure G-8 in Appendix H. In addition to the cost of the components, the tool shows the percentage share of the cost of vehicle subsystems. Figure 8-11 shows the composition and its percentage of the total cost for the 30-passenger city bus concept. The components considered for the cost estimation are the powertrain, autonomous technology components, chassis with vehicle body and the HVAC system. It can be seen that the powertrain is the most expensive system with 44.5 % of the total share. The chassis components and the vehicle body contribute to 31 % of the cost. The high proportion of autonomous components is mainly due to the LIDAR sensors and the processor (computer), which is around 20 %.

Components	Percentage
Powertrain	44.43 %
Autonomous Technology	20.3 %
Chassis + Vehicle Body	31.14 %
HVAC	4.13 %
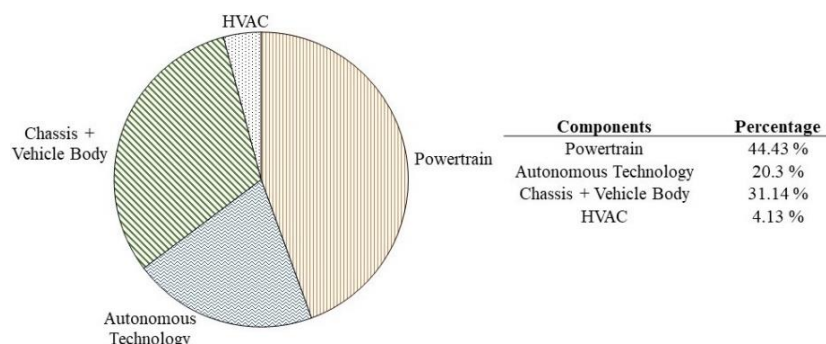
Figure 8-11   Percentage Share of Components

For the validation of the cost model, 66 different vehicle concepts of the coach, city bus and shuttle were considered. The number of passengers, the seating arrangements and the powertrain configuration was changed for each concept. The percentage range of the individual components is shown graphically with the box plot in Figure 8-12. In the figure, all the boxplots are narrow and have a low standard deviation. There are five boxplots listed, the first one illustrates the powertrain with a range of 39% to 52%. The powertrain includes all

drivetrain components with the battery. Hence, for vehicle concepts with a bigger battery pack, the influence on the cost is high. The autonomous technologies account for about 20% of the total costs. The third boxplot is the sum of the powertrain and the autonomous technology. This has a range of about 60% to 68% of the total cost. However, the deviation is very low. The chassis is just over 30% and the HVAC accounts for a very small proportion of the total cost.
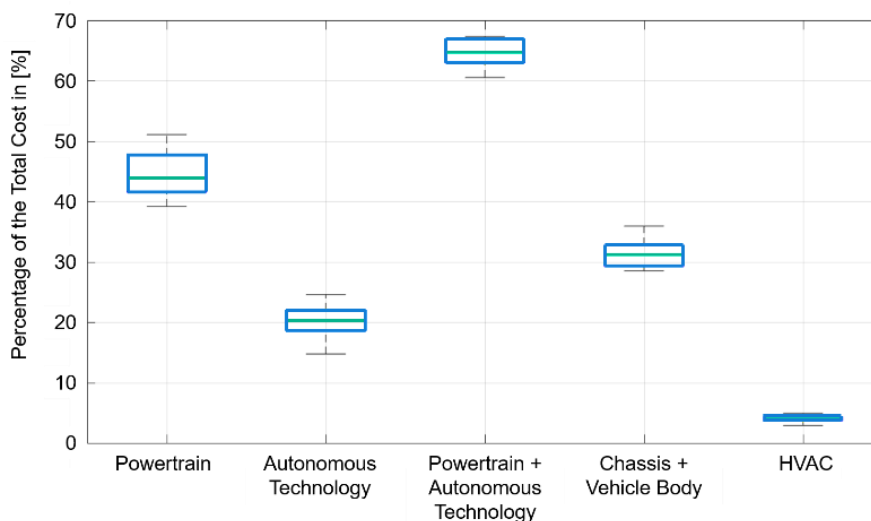
Figure 8-12   Boxplot – Subsystems share in Overall Cost.

Only a few studies have conducted a detailed cost assessment of electric vehicle and subsystems. In their research, [14] [115] [199] have derived identical results in the cost composition of an electric vehicle. [14] determined the cost of autonomous electric micro-transit vehicles and compared them with buses. In the cost breakdown, the study shows that the powertrain and autonomous technology component is 67 % and the chassis with vehicle body (including the HVAC components) is 33 %. [115] provided estimations of the costs of components and subsystems as a percentage of the total vehicle cost. The study estimates that the cost of the powertrain with battery ranges from 45 % to 70 % of the total cost and the cost of the glider can represent up to 28 % of the total cost. [199] discussed the impact of vehicle electrification and provided a cost breakdown in terms of the split between glider and powertrain. The study estimated the cost of the powertrain to be around 60 % and the cost of the glider to be around 40 % of the total vehicle cost. Table 8-6 shows the average results from the AEV tool and range based on the results from the literature. The table shows that the values from the AEV tool for the subsystems are within the range of the values from the existing studies.

Table 8-6   Test results compared to expected results

Components	AEV Tool Results	Results from [14] [115][199]
Powertrain & Autonomous Technology	64 %	60-70 %
Chassis & Vehicle Body	32 %	30-40 %
HVAC and Others	4 %	5-10 %

8.2.3 Lifecycle Assessment

The life cycle inventory analysis explained in section 7.4 is translated into a life cycle impact assessment. The impact categories used in this analysis are GHG and PM as explained in

section 7.4.1. The emissions from various phases of the life cycle inventories cumulatively result in the life cycle emissions. All the inputs required to calculate the emissions from the inventory in different phases of the AEVs are provided, AEV Tool. For example, the material mix of different subsystems required to calculate the production emissions of the AEVs is shown in Table I-1 in Appendix I.

As explained in the evaluation of the weight assessments in section 8.2.1, the weight distribution of each subsystem is obtained from the tool. Based on the weight of each subsystem and the material mix, the production emissions are calculated for various vehicle concepts. The regression function is generated and used for the calculation of emissions arising from each subsystem. Figure I-1 - Figure I-5 shows the production emissions of various subsystems of AEVs between 4 .m – 14 m in length expressed in Tonnes CO_2-eq emissions and kg PM_{10}-eq. Figure I-1 - Figure I-5 shows the production emissions arising from the vehicle body, chassis, battery cell, battery housing and drivetrain respectively. The emissions arising from the distribution, maintenance, the use phase and the EOL are calculated for 17 years and daily mileage based on the scope definition explained in section 7.4.1 and results from the tool.

8.2.3.1 Life Cycle Emissions comparison of 4 m to 14 m AEVs

The overall lifecycle GHG emissions (expressed in Tonnes CO2-eq.) of the AEVs between 4 m – 14 m are shown in Figure 8-13. The GHG emissions of the 12 m ICEV bus is also shown in the comparison. The figure shows emissions arising from all the different phases. It can be seen the overall GHG emission of all the AEV concepts are less than the emissions from ICEV. The production phase emissions of the AEVs are much higher compared to the ICEV due to the battery production emissions. However, the AEVs have '0' emission in the TTW phase where the ICEV`s contribution is around 85 % as seen in Figure 8-13. The recycling process in the EOL phase results in negative GHG emissions. In order to have a fair estimation, the 12 m AEV when compared to 12 m ICEV has a 42 % lesser overall GHG emission.
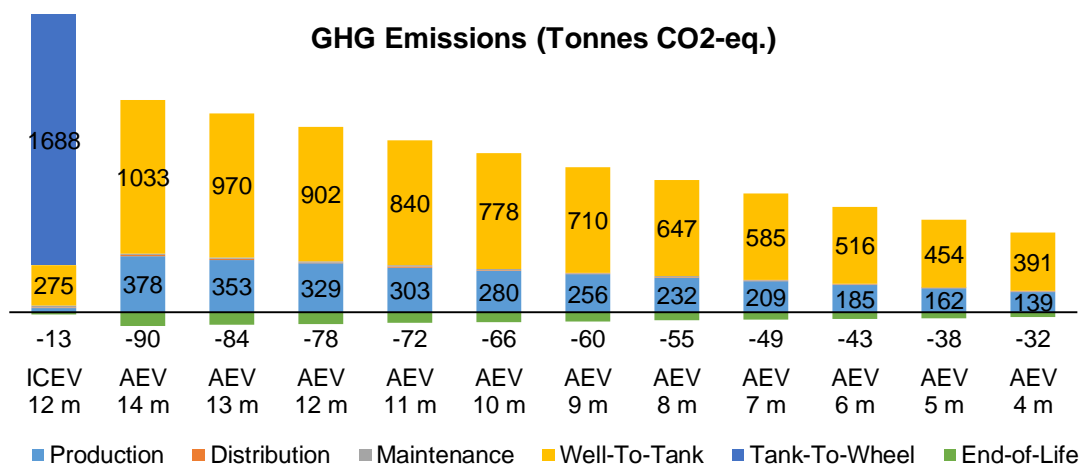
Figure 8-13   Overall GHG Emissions

Figure 8-14 shows the Overall PM emissions (expressed in kg PM10-eq.) of the AEVs between 4 m – 14 m and 12 m ICEV. The figure distinctly shows the emissions from different phases. Similar to the GHG emissions, the total PM emission from all the AEVs are lower than the emissions from the ICEV. In the AEVs, production phase has the highest emissions with

the battery production emissions contributing the most. As seen in Figure 8-14, compared to the 12 m ICEV, the 12 m AEV has 14 times more emissions in the production phase. However, the use of phase emissions (WTT and TTW) of the ICEV are higher than the 12 m AEV concept. The recycling of the batteries recompenses the production emissions caused by the battery and hence the EOL emissions are negative. It should be noted that the EOL phase reduces the total PM emissions of AEVs by around 40 %.

Particulate Matter (kg PM10-eq.)
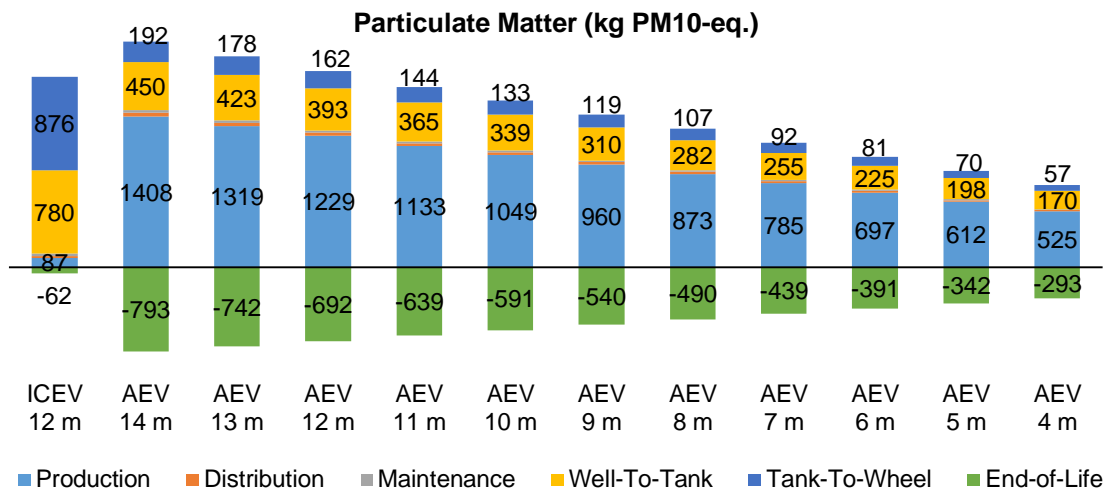
Figure 8-14   Overall PM Emissions

Based on the scope definition in section 7.4.1, the average passenger of the concepts are assumed to be 17 %. Figure 8-15 and Figure 8-16 shows the lifecycle GHG emissions (*g CO2- eq. per pkm*) and PM emissions (*mg PM10-eq. per pkm*) of the 12 m ICEV, AEVs between 4 m – 14 m respectively. It can be seen that the GHG emissions of the ICEV are and the emissions of 5-metre-long AEV are comparable. The GHG emissions per pkm of AEVs are reduced when vehicle length increases. The 4 m bus with the same occupancy emits 131 *g CO2- eq. per pkm,* while 14 m bus emits 68 *g CO2- eq. per pkm*. The PM emissions of AEVs have the same characteristics as GHG emissions. The emissions per pkm decrease with an increase in the bus size. Figure 8-16 shows that the ICEV has less *PM per pkm* emissions than all AEVs if the EOL recycling is ignored.

g CO2-eq. per passenger kilometre
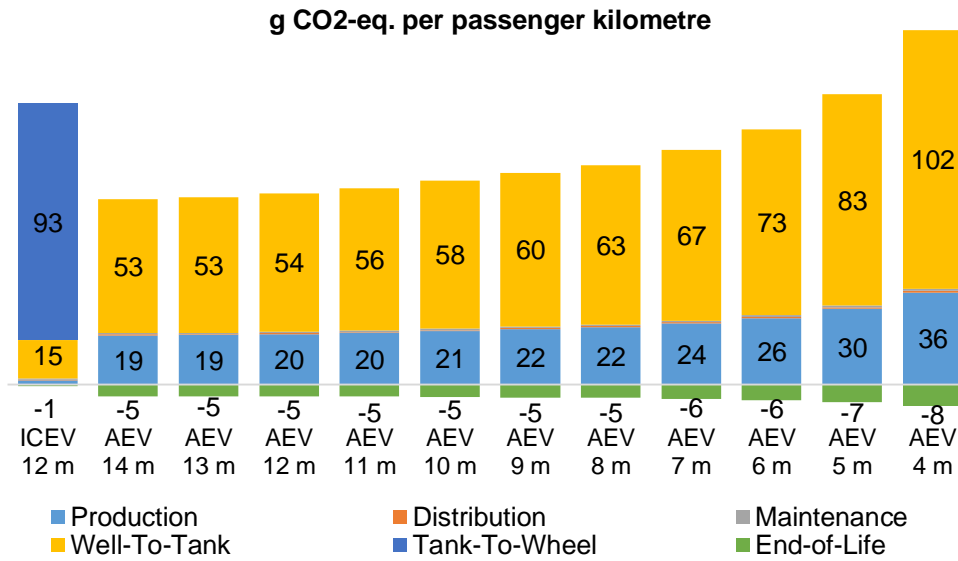
Figure 8-15   g CO2-eq. Emissions for Several AEV Sizes and Phases per pkm

mg PM10-eq. per passenger kilometre
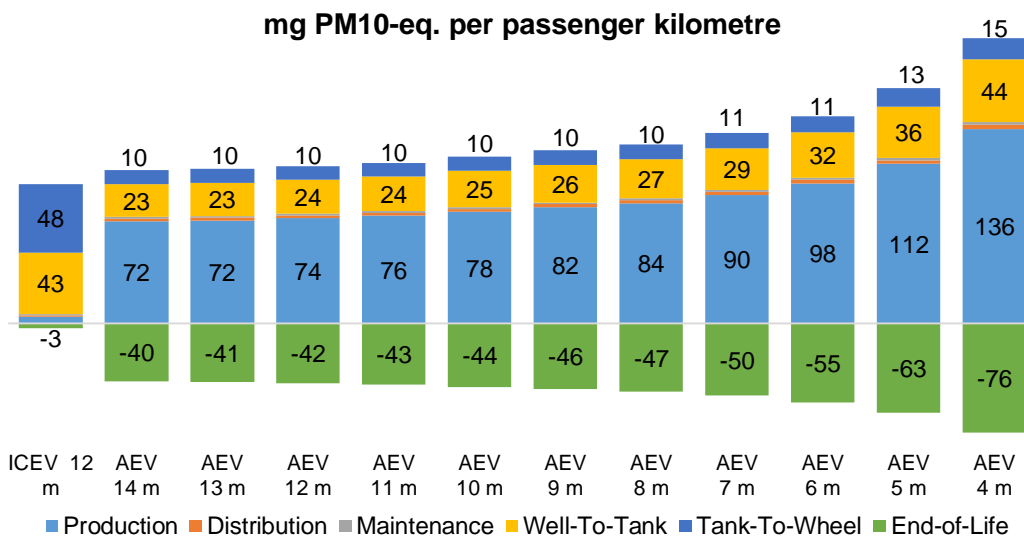
Figure 8-16   PM Emissions for Several AEV Sizes and Phases per pkm

From both the impact categories, it can be therefore seen that passenger occupancy plays an important role and in order to have lower emissions, the AEV concepts of size 4 m – 8 m should have high passenger occupancy compared to the AEVs of length 9 m – 14 m. Figure 8-17 shows the *g CO2- eq. per pkm* emission of a 12 m AEV with 17 % occupancy and 6 m AEV with passenger occupancy ranging between 17 % and 35 %. Figure 8-17 shows that the GHG emissions of 6 m AEV with passenger occupancy of 22.5 % are the same as the emissions from the 12 m AEV. The 6 m concept has lesser emissions when the passenger occupancy is increased to 25 % and by doubling its occupancy, the GHG emissions per pkm can be reduced by around 52 %.

The influence of passenger occupancy and its effects are discussed in detail in the next section with a case study scenario explained in Singapore.

g CO2-eq. per passenger kilometre
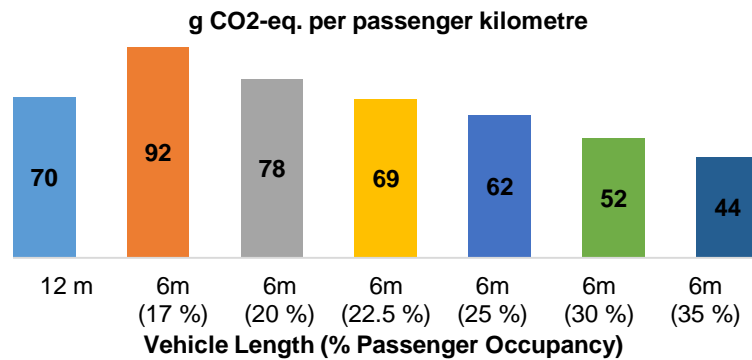
Figure 8-17   Variation of Occupancy for Smaller Buses

8.2.3.2 Scalable LCA model for 4 m to 14 m AEVs

The previous section discussed the life cycle emissions of AEV concepts of different size ranging between 4 m – 14 m. We could observe that the overall emissions of the AEVs increase with the length. Figure 8-18 shows the results of total emissions for various bus concepts. It can be seen that, for both impact categories, the emission has a linear increase with the size of the vehicle. The linear behaviour can be explained by the following supporting points.

Based on the scope definition in section 7.4.1, the average occupancy and the daily mileage of the vehicles are fixed. From the weight assessment results of the AEV tool in section 8.2.1, the weight increase is found to be linear. The material mix for the bus production for the different sizes is constant as seen in Table I-1 (Appendix I). In addition, the energy consumption of different AEVs has a nearly linear behaviour with an increase in weight. Therefore, the energy demand and use phase emissions also have linear behaviour with respect to the vehicle size. Hence, a scalable model LCA model could be easily developed for different vehicle classification if the scope of the LCA is defined. The equations to calculate the total GHG and PM emissions for different vehicle lengths is shown in Figure 8-18.

$y = 83.799x + 388.46$

$y = 83.612x + 417.65$
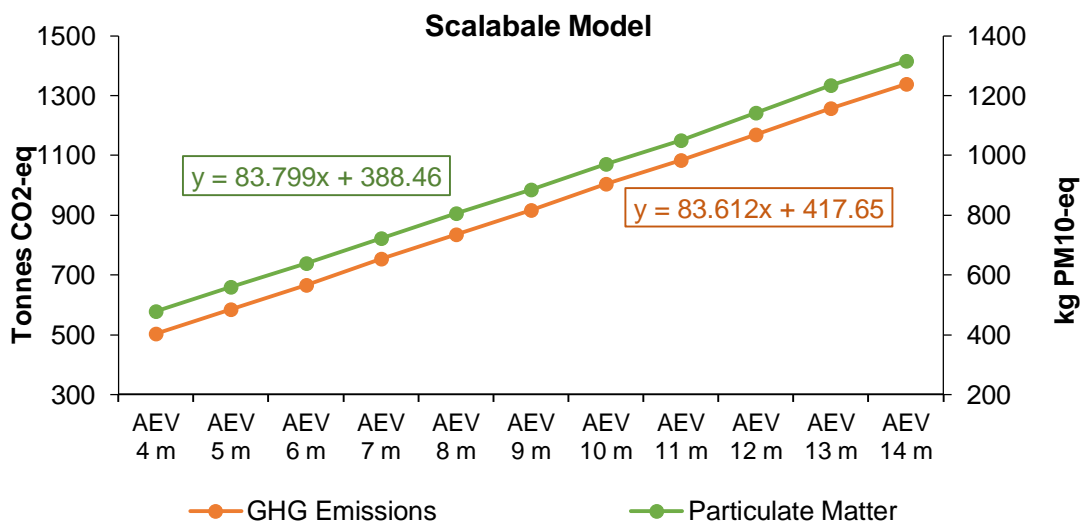
Figure 8-18   Scalable Emissions Model for AEVs

8.3 Comparison of Vehicle Concepts – A case study in Singapore

Section 8.1 explained the capability of the tool to generate numerous autonomous electric vehicle concepts. Following the concept generation, the section 8.2.1 and section 8.2.2 evaluated and validated the results of AEV tool in terms of the weight and cost estimation. Section 8.2.3 further evaluated the vehicle concepts for lifecycle emission and developed a scalable model for calculating the lifecycle emissions as seen in section 8.2.3.2. This section presents a case study in Singapore in order to provide a holistic overview of the benefits of the AEV tool by considering a real-time scenario. The case study presented here is based on the earlier research work of the author [201].

Singapore currently uses 12 m single deck buses and 13 m double deck buses in its public transportation system. The buses are powered by the internal combustion engines. However, by the year 2030, it is planned to integrate autonomous and electrified buses into the public transportation system of Singapore [202]. It is important to investigate the economic and environmental impacts of autonomous electric buses before the deployment. Therefore, this case study tries to demonstrate the effects of replacing the non-autonomous diesel buses operating in Singapore with autonomous electric buses on the life-cycle costs and global warming potential.

8.3.1 Overview of the Case Study

In order to assess the impacts of autonomous electric vehicles, seven existing bi-directional bus routes of Singapore were considered for the analysis. The methodology used in the study evaluates the variation in the operational strategy because of the variation in the vehicle concepts.

The methodology used for this evaluation is explained in the work presented by PATHAK ET AL. [201]. Figure 8-19 shows the methodology used in this case study. The method has four steps, namely the input, scheduling and timetabling, vehicle assignment and output as shown in Figure 8-19. The input includes the specification of the compared vehicles and passenger demand data and vehicle route data. The input data for the vehicle routes are obtained from the Land Transport Authority [203]. The data is further analysed to obtain the passenger demand, inter-stop travel times and origin-destination of passengers along the routes considered in the analysis.

Two vehicle concepts are compared in this study, the 12 m single deck ICEV and the 6 m AEV. The input parameters of the three different vehicle concepts compared in this study are shown in Table 8-7.The parameters of the conventional 12 m ICEV are taken from [181, 200] as seen in section 7.4.2. The parameters for the 6 m AEV concept including the longitudinal dynamics and energy consumption is obtained from the results of the AEV tool as seen in section 8.2.1. Since the vehicle operation, it is difficult to fix the battery capacity. Hence, the impacts of changing the battery capacity on the fleet size, emissions and the costs are analysed. However, the minimum capacity is assumed to be 120 kWh based on [14]. The three different battery capacities analysed in this study are 120 kWh, 160 kWh and 200 kWh as shown in Table 8-7.

The frequency and headway for each route are calculated based on the inputs and the timetable for each vehicle concept is obtained as shown in Figure 8-19. The scheduling and

timetabling approach are based on the method developed by [204, 205]. Based on the derived timetables, a vehicle assignment algorithm is then determined to acquire the blocks of the vehicles through the day and hence to calculate the total distance travelled by each bus and the fleet size of respective concept. Two integer linear programs are formulated based on the approaches developed by [206, 207] to determine the deployment for the two analysed vehicle concepts that complete all the scheduled trips with the least number of vehicles in the fleet and with least distance travelled.

Finally, the study is concluded by calculating the life cycle GHG emissions and lifecycle cost assessment. The GHG emissions are assessed based on the results of the LCA model discussed in section 8.2.3. However, the scope of the study is varied according to the boundary conditions of the case study The life cycle cost assessment is based on the approach developed by ONGEL ET AL. [14]. The Total Cost of Ownership (TCO) analysis carried out included the three major costs namely, the acquisition costs of the vehicle, the operating costs of the vehicle, and end-of-life costs. The two-vehicle concepts are finally evaluated based on the TCO and GHG emissions. It should be noted that the functional unit used in the case study for comparison is *per passenger-km* of vehicle operation.
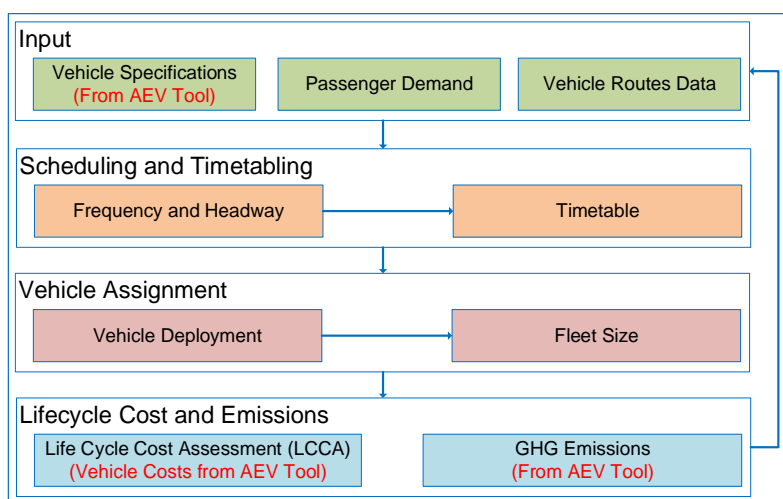
Figure 8-19   Overview of the Case Study [201]

Table 8-7   Parameters of the Vehicles Compared

Vehicle Parameters	12 m ICEV	6 m AEV
Kerb Weight in kg	10900	5280
Glider Weight in kg	9485	4014
Vehicle Length in m	12	6
Maximum Passenger Capacity	90	30
Battery Capacity in kWh	n/a	120-200

8.3.2 **Case Study Results**

Table 8-8 shows the comparison between the numbers of scheduled trips for the two-vehicle concepts, the 12 m ICEV and the 6 m AEV. The table shows the seven routes analysed, the length of each route and the resulting passenger occupancy for each of the seven routes. Since the functional unit of this study is per passenger-km, the passenger occupancy parameter is important. It can be seen that the total number scheduled trip for the 6 m AEV is 2487 whereas it is 1383 for the 12 m ICEV. The difference in the number of trips is due to the difference in passenger capacity between the vehicle concepts.

The passenger capacity 6 m AEV is three times lower than the 12 m ICEV. Therefore, the more number of trips are required to meet the demand. However, the mean passenger occupancy of the 6 m AEV is higher than the 12 m ICEV in each of the routes and overall the mean occupancy is 27.4 % for 6 m concept and 18.3 % for the 12 m concept as seen in Table 8-8. Higher number of departures is the main reason for the increase in the passenger occupancy. Due to the higher frequency, the headway between the vehicles is reduced leading to an increase in the mean passenger occupancy. This is clearly explained in the next paragraph.

Table 8-8   Trips and Mean Passenger Occupancy Comparison

Route	Length of the route in km	12 m ICEV		6 m AEV	
		No. of Trips	Mean occupancy in %	No. of Trips	Mean occupancy in %
1	25.2	211	24	567	26.7
2	19	206	17.2	440	24.3
3	24.8	206	22.8	460	30.7
4	12.6	238	19.6	495	28
5	23.6	180	15.9	382	22.3
6	18.1	171	15.3	235	33.3
7	16.2	171	13.7	268	26.2
Total	139.5	1383	18.3	2847	27.4

The frequency of the vehicles at every hour is calculated by the scheduling and timetabling model. In general, the frequency is high in the peak hours and lower in the off-peak hours. Figure 8-20 shows the cumulative plot of all the vehicle trips for the seven routes at each hour during the operation. We can clearly see the high peaks in the scheduled trips in the case of 6 m AEVs. This shows a significant difference in the vehicle frequencies during the peak and off-peak hours. On the other hand, the 12 m ICEVs have smaller peaks which means the change in the number of trips between the peak and the off-peak hours is not significant. This Figure 8-20 helps to clearly understand the reason for the higher number of trips for the 6 m AEVs and their distribution.
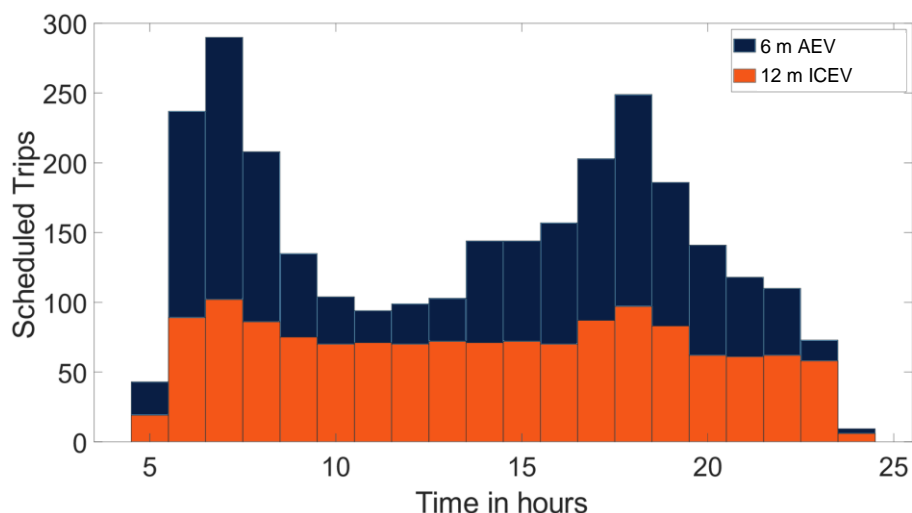
Figure 8-20   Total Hourly Vehicle Departures

Next to the scheduling and the timetabling, the fleet size for the two different concepts is calculated by optimally allocating the calculated vehicle trips in each route. Table 8-9 shows the comparison in the results of 12 m ICEV and 6 m AEV concepts. The results in the table show the required fleet size for the two compared concepts. The fleet size required to serve the trips in the seven routes with the 6 m AEV is 422 vehicles. Whereas the only 149 12 m buses are required to fulfil the trips for seven routes. The difference in the fleet size can be understood from the scheduling results.

Table 8-9 further shows the total distance covered by the whole fleet in a day. As seen, the total distance of 28146 km and 68368 km is covered by the 6 m and 12 m vehicle concepts respectively. As discussed in the previous section, the 6 m AEVs were evaluated for three different battery capacities: 120 kWh, 160 kWh and 200 kWh. The results showed no variation in the fleet size. However, the energy usage of the whole 6 m AEV fleet increased with the battery capacity. The increase in the energy demand with the battery capacity is due to the increase in the vehicle mass and hence, the energy consumption. Another interesting result as in Table 8-9 is the difference in the life of the battery. The battery life is the replacement time of the battery. This has a significant impact on the LCA and the TCO results. The concepts with battery capacities of 120, 160, 200, kWh resulted in the life of 4.38, 5.8 and 6.86 years respectively. However, considering the fleet size and lower energy usage, the 6 m AEV with 120 kWh is ideal and is being used in the TCO and LCA results.

Table 8-9   12 m ICEV and 6 m AEV Fleet size and operational comparison

Parameters	12 m ICEV	6 m AEV		
Battery capacity	-	120 kWh	160 kWh	200 kWh
Fleet Size	149	422	422	422
Daily distance	28146 km	68368 km	68368 km	68368 km
Daily mean distance	189 km	162 km	162 km	162 km
Daily Energy Usage	14355 Litres	38.9 MWh	39.5 MWh	40.1 MWh
Battery Life	-	4.38 years	5.80 years	6.86 years

Following the mean passenger occupancy, fleet size, vehicle distance and energy results, the TCO and GHG emissions can be calculated. Figure 8-21 shows the TCO comparison of the two-vehicle concepts. Figure 8-21 (a) shows the TCO comparison in the vehicle level and Figure 8-21 (b) shows the comparison at the fleet level. At the vehicle level, it can be clearly seen that the TCO of the 6 m AEV is around four times less compared to the 12 ICEV. This is mainly because of the personnel or the bus captain cost and the energy cost. Figure 8-22 shows the percentage share of the TCO of the 6 m AEV and 12 m ICEV. As shown, the share of the personnel cost is the highest contributing around 43 % for 12 m ICEV followed by the maintenance with 22 % and 17 % for acquisition. It should be noted that the AEVs have zero personnel cost. In the case of 6 m AEV, the share of the acquisition cost is the highest contributing around 54 % of the TCO followed by an almost equal contribution from the energy cost and the maintenance cost.

We know that the fleet size of 6 m AEVs is three times higher than the 12 m ICEV. However, as seen in Figure 8-21 (b), the TCO of the 6 m AEV fleet is still 1.5 times lower than the TCO of 12 m ICEV.
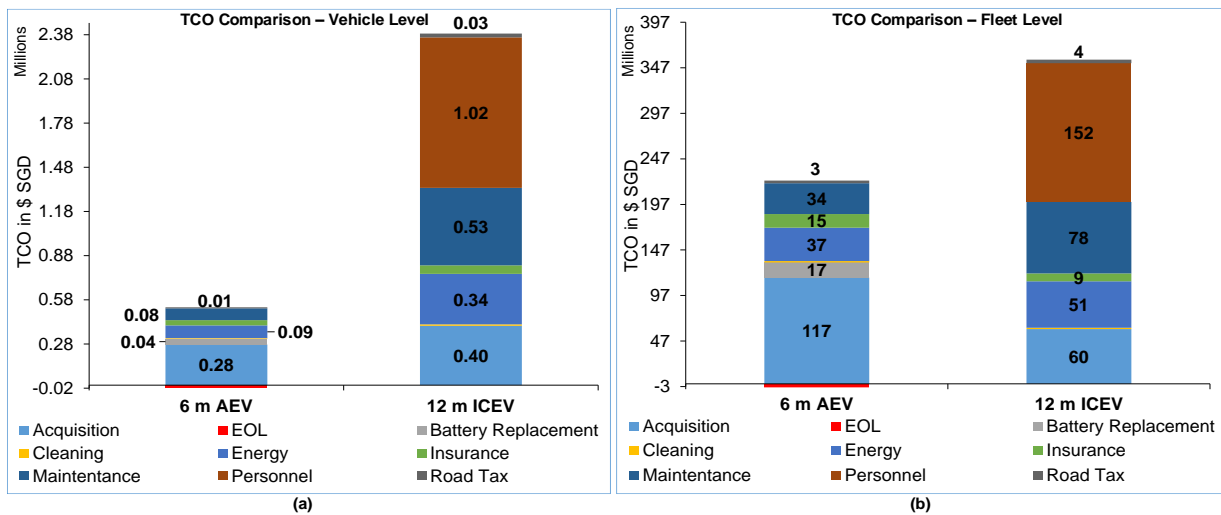
Figure 8-21   TCO Comparison (a) Vehicle Level   (b) Fleet Level
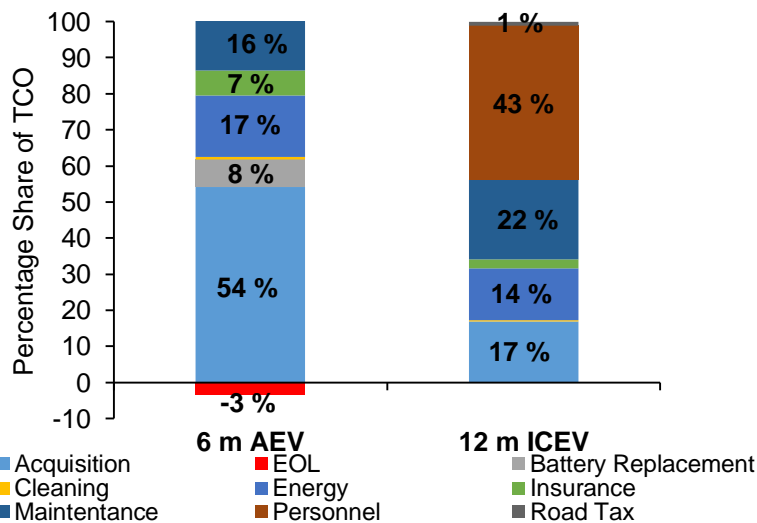
Figure 8-22   Percentage share of TCO

Since the functional unit of the study is *per passenger-km,* it is important to discuss the TCO per passenger-km. Figure 8-23 shows the fleet level TCO per passenger-km for the 12 m ICEV and the 6 m AEV. Similar to the overall TCO results, it can be seen that the 6 m AEV has a lower cost. The cost incurred by the 12 m ICEV is S$0.129/Passenger-km which is 76 % more than the cost incurred by 6 m AEV Thus, we can conclude that the 6 m AEVs with is significantly large fleet is economically advantageous than the existing single deck buses in Singapore. The Lifecycle emission is compared in the next paragraph.
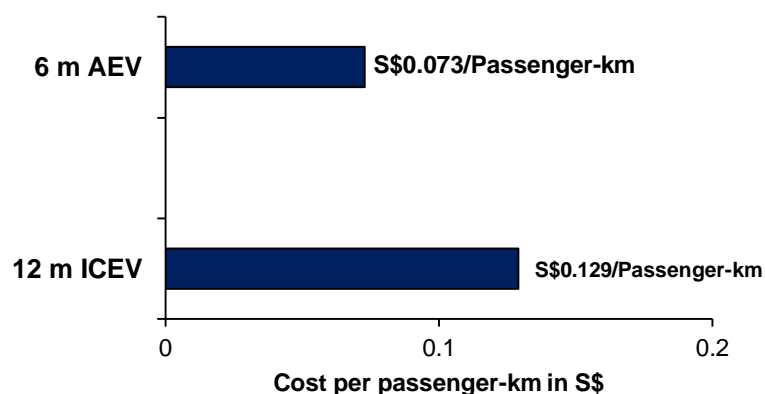
Figure 8-23   Comparison of fleet costs in per passenger-km

The vehicle level GHG emissions for the 12 m ICEV and the 6 m AEV is similar to the results presented in section 8.2.3.1. Figure 8-24 shows the GHG emissions comparison between the two vehicle concepts at Figure 8-24 (a) Vehicle level (in Tonnes CO_2-eq.) and Figure 8-24 (b) Fleet level (in million kg CO_2-eq.). From Figure 8-24 (a), it can be clearly seen that the at the vehicle level, the GHG emissions from the 6 m AEV is around 5 times less than that of the 12 m ICEV. As discussed in section 8.2.3.1, the TTW phase of the 12 m ICEV has the highest share of around 85 % of the total GHG emissions. But in the case of the 6 m AEV, the WTT phase has the highest share of around 77 % of the overall emissions and zero emissions in the TTW phase. Furthermore, the production phase of the 6 m AEV has a significant contribution compared to the ICEV.

From Figure 8-24 (b), it can be seen that the production phase emissions of the 6 m AEV fleet (42 million kg CO_2-eq.) is around 10 times higher than the 12 m ICEV fleet and the WTT phase emissions of the 6 m fleet is 3 times higher compared to the 12 m fleet. However, even with the large fleet size, the overall emissions of the 6 m AEV fleet has GHG emissions of around 144 million kg CO_2 – eq and is around 45 % lower compared to the 12 m ICEV (263 million kg CO_2 – eq).
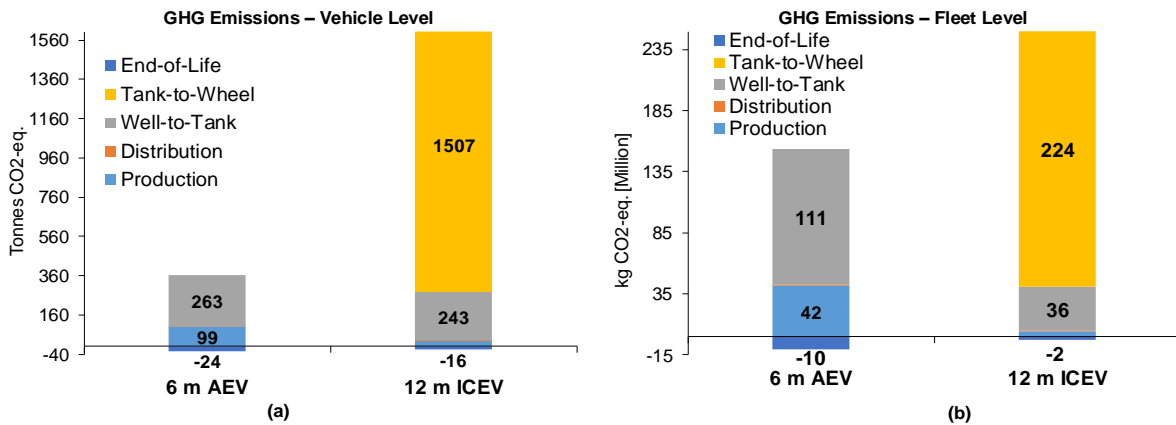
Figure 8-24   GHG Emissions Comparison (a) Vehicle level   (b) Fleet level

The GHG emissions are also evaluated in *per passenger-km* to analyse the influence of passenger occupancy. Figure 8-25 shows the fleet level GHG emissions per passenger-km for the 12 m ICEV and the 6 m AEV. It can be seen that the 6 m AEV resulted in lower emissions of 51.62 g CO_2/passenger-km compared to 94.62 g CO_2/passenger-km from the 12 m ICEV as shown in Figure 8-25 despite the increase in fleet size and daily distance travelled by the vehicle fleet.
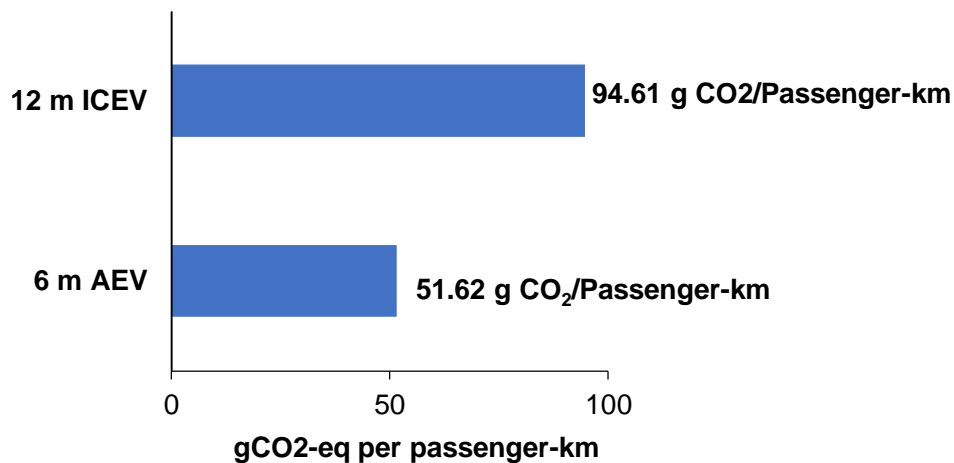
Figure 8-25   Fleet Level Comparison of GHG Emissions in pkm

Thus from the case study, comparing the currently used ICEV buses, the autonomous and electrified buses are proved to be advantageous economically and are more sustainable.

9 Discussion and Conclusion

9.1 Discussion

This work established a vehicle concept development tool for autonomous electric buses between 4 m - 14 m in the early concept phase. The main objective of the holistic tool is to reduce the overall concept development time in the early phase. To meet the primary objective, several target requirements of the tool were provided addressing some important factors. The expected requirements to meet the objective included different modes of operation, the scope of the components for a vehicle package, usability and performance of the tool, etc. All these requirements were considered in the presented method that allows the development of an AEV concept from the ground-up.

As explained in the results (Section 8.1), the AEV Tool was able to generate vehicle packages in two different modes. The manual mode was more detailed where the user input was the vehicle dimensions such as the exterior dimensions, wheelbase, ground clearance, interior configuration, geometry and material properties of all individual components and the output is the vehicle concept with the number of passengers, number of seats and mass of the vehicle. The manual mode was not incorporated with functions to automatically select and size the component subsystems. Therefore, the user was expected to have expert knowledge about different components and size them manually. While in the case of automated mode, the user input was basic such as the required type of vehicle and number of passengers and tool automatically selects the components and provides few topology options for user selection. The output of the automated mode was the vehicle concept generated with a detailed energy consumption simulation, cost estimation and life cycle emissions assessment.

One of the primary results of the AEV Tool and common to both the manual and automated was the visualisation of the vehicle concepts. Both modes were directly interfaced to the parametric CAD model developed with CATIA (Chapter 5). As explained in Section 6.2.6, for visualisation, all the parameters were stored in the parametric table in the form of a txt file which is later accessed by CATIA with the help of Macros (Section 6.2.6) to resize and visualise the CAD model. The CAD model included the geometry of all the components for vehicle packaging but also contained the material information of each component to calculate the weight and the centre-of-gravity of the vehicle. All the components of the parametric model were controlled by parameters and as explained in the definition of parameters in Section 5.1, the complexity of the model and hence the computational time would increase with the increase in the number of parameters. Therefore, the components of the CAD model were designed with basic shapes and structures. In addition, the tool develops vehicle concepts for early concept phase where the detailed component designs are not required.

As explained in Section 8.1.2, apart from the generation and visualisation of 3D vehicle package, the automated mode performed the selection and sizing of all the major subsystems and allowed user selection for powertrain and HVAC topologies, thus being able to generate

over 9600 unique vehicle concepts as seen in Section 8.1.2. Based on the requirements defined in Section 3.1, the automated mode increased the usability of the tool by allowing simultaneous development of vehicle concepts to result in reduced development time. In addition, as explained in Section 8.1.2, the developed concepts could be compared with the help of spider plots. The spider plots indicated the important vehicle properties such as the initial cost, energy consumption, vehicle range, number of passengers, vehicle dimensions, etc. This further helped in the reduction of overall concept development time. Furthermore, detailed models to estimate the cost and weight of the vehicle and its subsystems and life cycle emissions estimation of the concepts accomplished all the target requirements.

However, evaluation and validation of various important results from the tool are important to ensure the reliability of the results. Section 8.2.1 evaluated the weight estimations results for the tool by comparing with several electrified and autonomous shuttles and buses currently available in the market. The results showed that the weight of the vehicle concepts had a minimal deviation from its benchmark counterpart with an average difference of around 5 %-6 %. In order to ensure the reliability, the influence of each subsystem over different vehicle subsystem was studied. The results showed that the powertrain had higher influence in smaller buses of length between 4 m-7 m contributing around 39 %-41 % of the overall weight while the influence of body and structure increased for buses of length between 8 m-14 m contributing around 45 %-46 % of the overall weight. The results were compared with existing studies and found to be within the limits.

Section 8.2.2 evaluated the cost assessment results on the subsystem level. The difficulty with the cost estimation was the unavailability of the absolute initial cost data for bus type vehicle. In this work, for the evaluation, 66 different vehicle concepts were generated and the influence of each subsystem on the overall vehicle concept cost was analysed. The study showed that the powertrain has the highest influence on the vehicle cost contributing between 39 %-52 % followed by the chassis and body with 29 %-36 % and autonomous technology components with around 15 %-25 %. The results were compared with existing studies that showed an average deviation of 6 %-8 % for all the major subsystems confirming the validity of the cost model.

Section 8.2.3 presented the life cycle emissions of the emissions based on the LCA method developed in Section 7.4. The method used vehicle inputs such as the weight of the vehicle and components, associated materials of the components, the energy consumption of the AEV, etc. which were the outcomes of the AEV Tool. The overall emissions were assessed in two categories, GHG emissions in CO_2-eq and PM emissions in PM_{10}-eq. The results were compared to the lifecycle emissions of a 12 m ICEV. The evaluation showed that overall lifecycle emission of all the AEVs ranging between 4 m-14 m was less than that of the 12 m ICEV in both the impact categories. In addition, in the case of AEVs, the production phase emissions were very high in both the impact categories. This is due to the emissions caused by the production. The battery production was responsible for more than 60 % of the PM emissions. However, the impact of battery production emission reduced because of the EOL recycling process. The EOL phase contributed to around 30 % of emission reduction in the case of AEVs. Furthermore, the results showed that, for an identical scope of operation definition, the emissions results had an almost linear trend for AEVs of different sizes. The smaller vehicles had lower emissions which increased with the vehicle length. The generated scalable models were explained in Section 8.2.3.2.

The emission results were further evaluated in *per pkm* for all the AEVs in Section 8.2.3.1. The results showed that, in the case of AEVs of size 4 m-6 m, despite the lower overall

emissions, the emissions per pkm in both the impact categories we higher than the 12 m ICEV and other AEVs. Thus, it was clear that the passenger occupancy of has a higher influence in emissions and the smaller buses should have higher average occupancy than the bigger buses in order to the sustainable.

Finally, the overall applicability was the AEV Tool was explained with a case study in Singapore. The study evaluated the impacts of AEVs in public transport by comparing the TCO and emissions of a 6 m AEV with a conventional 12 ICEV in Singapore. For the analyses, seven existing bus routes in Singapore were selected and the method was implemented to simulate the two different bus concepts by changing the timetable and the deployment of vehicles. The resulting fleet size and average occupancy were used to find the lifecycle cost and emissions. The vehicle related inputs such as the size, passenger capacity, and energy consumption and emissions model were provided by the outcomes of the AEV Tool. The results of the study as explained in Section 8.3.2 showed that the required fleet size for 12 m ICEV and 6 m AEV were 149 and 422 respectively. However, the mean occupancy of 12 m ICEV and 6 m AEV was found to be around 18 % and 27 % respectively. Therefore, the lifecycle GHG emissions showed a reduction of CO_2-eq emissions and total lifecycle cost for the by 47 % and 43 % for the 6 m AEV in comparison to the 12 m ICEV despite the 6 m AEV requiring a larger number of vehicles.

Thus from the above discussions, it can be seen that the AEV Tool is able to develop, generate and visualize the vehicle concepts in few steps and in a very short time, thereby reducing the vehicle concept development time. In addition, the generated results from the tool are validated to ensure reliability. However, it should be noted that the tool focuses on the early concept development phase and the resulting vehicle concept will further need a manual package development. Furthermore, it is important to do a critical assessment of the limitation of the method employed in tool development.

Firstly, for visualisation of the vehicle concepts, currently the parametric CAD model is designed with simple geometry and shapes in order to reduce the computational effort involved in packaging and visualisation. The limitations in using the geometry of the simple component are the mass estimation of the final concept may not be precise. However, in order to overcome this limitation, regression models are used for subsystems such as the powertrain as explained in Section 4.1.3. The mass of subsystems vehicle body, the structure was derived from the material definition in the CAD model. Despite employing simple geometries, the interface between CATIA and MATLAB still requires high computational effort. Thus the time required to update the parametric model with updated parameters is high. The tool uses two different software programs and three different file types to complete the visualisation process. An optimisation of this process would make the tool operation more efficient and seamless. Another limitation that is caused by the CATIA-MATLAB interface that occurs during the initial tool set up is the incapability of the program to implement dynamic paths in the Macros scripts. The dynamic paths in MATLAB enable the user to set up the tool in different devices by just making a copy. However, the file paths have to be manually updated within the macros which as responsible for functions such as opening, updating, closing and measuring the CAD model

As seen from the results and discussions, the powertrain sizing has a significant impact in terms of performance, cost, and weight of the vehicle concept. As described in Section 4.1, the powertrain components namely the motor, inverter and the transmission are designed with efficiency maps and battery is designed with an equivalent circuit model. Hence the simulation is faster due to the low computational requirement. In this work, the powertrain components

are sized based on the longitudinal dynamics model. For the energy consumption simulation, the BRT cycle from Beijing is used as the input driving cycle for all the vehicle concepts as explained in Section 6.3.2. In addition, the passenger load for all the simulations were assumed at 100 % which results in high energy consumption. The buses used in public transit have a lower average occupancy. Lower passenger occupancy would result in lower energy consumption and hence a smaller battery pack. Another limitation with the powertrain selection is that only four predefined configurations are available for user selection and the minimum and maximum vehicle range requirement is set to 300 km and 400 km. Therefore, the tool is unable to create concepts with less than 300 km range in the automated mode. However, this can be overcome by expanding the powertrain database with more options in terms of the range or with a separate module to perform a new longitudinal simulation to assess different driving cycles, battery capacities and motor architectures.

The chassis sizing in the tool as uses database containing standard off-the-shelf components for the selection. Based on the weight of the glider and powertrain the sizing and selection algorithms are executed independently for suspension, braking and brakes sizing. However, implementation of dependant algorithms for sizing different subsystems might have provided more optimum solutions. Due to the symmetrical design of the AEVs in the parametric model with the battery pack being position centrally on the floor as explained in Section 3.4.3, the vehicle concepts have a 50-50 weight distribution and hence the tool sizes the same suspension and axle system for both the rear and front axles. The tool has not been integrated with an automatic third axle placement required for longer vehicle concepts such as 13 m and 14 m. However, considering the modularity and expandability of the parametric model third axle can be easily implemented.

The suspension database has yet another simulation while adding new components to the database. The chassis components are stored within SQL database as explained in Section 6.3.3. Therefore, a force struct has to be defined in order to interpolate the between pressure levels required for sizing the air suspension. Moreover, the MBS model used in the sizing of suspension and axles as explained in Section 4.2.4 requires around five to six minutes in order to complete the simulation. This is mainly due to the initialisation of the MBS software and the model. An alternate solution would find the standard axles and expand the database and further define an algorithm to select the axle according to the vehicle load. However, the parametric CAD model to define the axle would be a problem, since the detailed data of axle link design is not available.

The cost estimation of the AEV Tool is based on various existing cost models. The regression models for the powertrain components are validated scalable models and provide precise results for bus concepts. However, the cost model used for vehicle structure and body is derived based on the manufacturing data of passenger cars. Thus the absolute values of the cost might be inaccurate. Despite the assumption, the cost model validation proved to be closer to the values found in the literature.

Despite the limitations addressed in the above paragraphs, the method developed a holistic tool that enables the user to create autonomous electric bus concepts in few steps and short time. Therefore, the high complexity in developing the autonomous electric bus concepts have been overcome by addressing the research gap.

9.2 Conclusion and Outlook

Chapter 1 clearly explained the research motivation and explained the problem in the vehicle development process. The goal of this thesis was to develop a holistic tool to generate autonomous electric bus concepts while being able to size and select the components, create 3D vehicle package, provide an initial assessment of vehicle properties such as the cost, energy consumption and emissions.

The state of the art chapter explained the current vehicle development process and highlighted the importance of vehicle concept development at the early phase due to the packaging decisions and emphasized the requirement to speed-up the process. Furthermore, the chapter provided an insight into the characteristics of the vehicle packaging in the early phase, introduced and discussed several vehicle packaging strategies. Later, the significance of parametric modelling in vehicle concept development was explained. Furthermore, a literature review was conducted to evaluate existing parametric concept development and the review revealed that the majority of the existing methods are focused on the passenger cars of which powertrain design and optimization were significant. The review helped to clearly identify the gap in the literature for overall sizing and packaging tool for autonomous electric buses.

Consequently, Chapter 3 presented the method for the development of the holistic tool (AEV Tool) for generating autonomous electric bus concepts. Initially, the overview and the requirements of the tool was defined. The requirement addressed the functionality of the tool such as different methods of operation, the scope of the components, parametric CAD model, usability of the tool, etc. Based on the requirement the framework of the method was defined that included all the necessary models responsible for the vehicle concept development. The framework was divided into four phases namely the input, definition, design and evaluation. The primary step was initiated by the input phase that included the vehicle specification to define a vehicle concept derived by policies, requirement and benchmarking. Further, the vehicle and the package relevant components were defined by considering factors such as ergonomics, interior, exterior and interdependencies within the components.

Chapter 4 explained the components selection algorithms for the major subsystems namely the powertrain, chassis and HVAC. The powertrain components included motors, inverter, transmission and battery. The method presented a detailed longitudinal dynamics model that included control strategies for shifting gears and distributing power between motors. The chassis included the sizing of suspension, brakes, wheel, tire and axles. The chassis sizing used databases of standard off the shelf components and used an exclusion mechanism to select the component. In a similar way, the HVAC algorithm included the sizing of heat exchangers, compressors that achieved ideal cabin temperature and humidity.

Chapter 5 and Chapter 6 explained the design phase of the AEV Tool. The design of the parametric CAD model was described in Chapter 5. The parameter definition, boundaries and constraints of the model, parametric design of all the components in the vehicle package were clearly explained. The design of the architecture of the tool was explained the Chapter 6. The implementation of different modes of operation, the manual and automated mode were described in detail. The process flow of the concept development in both modes was kept identical. The interface between the component databases and the parametric 3D CAD model was explained. Finally, the design of the GUI as described.

The evaluation methods used in the tool was presented in Chapter 7. The evaluation methods included the energy consumption evaluation that was carried out with BRT Beijing driving

cycle. The simulation summarised the powertrain losses, battery performance and motor efficiency maps. The cost estimation model used several regression models available in the literature in order to provide an early cost estimate of the concept. A detailed LCA model was developed to summarise the cradle to grave emissions from the vehicle concept.

Chapter 8 presented a detailed explanation of the results that showed the vehicle concepts generation using the manual mode and the automated mode and the results were validated through comparison with benchmark vehicles and literature for vehicle weight and cost assessment. A detailed case study was also presented at the end of Chapter 8 to understand the overall applicability of the tool. Chapter 9 discussed in detail the implications of all the results and evaluation and also addressed the important limitations of the method. The discussion also provided suggestion and improvement to overcome some of the existing limitations of the method.

Bearing in mind the research gap explained in Chapter 2 and the requirements defined in Chapter 3, it could be seen that all the requirements have been fulfilled in the development of the AEV Tool. The AEV Tool can certainly reduce the vehicle concept development time with its simultaneous concept development and ensures a fast visualisation of the various bus concepts. The tool is able to size all the necessary subsystems and provide an initial estimation of the vehicle properties such as the cost, energy consumption, emission, passenger capacity, etc. The tool works with several databases which can be expanded to add more components and configurations. The usability and performance of the tool have been tested and despite using multiple software programs the tool has been consistently stable. Thus, the objectives of the thesis have been accomplished and the well-established parametric models and the databases create an essential foundation for further research on additional challenges in this research domain.

Considering the well-developed platform for creating new AEV concepts, there are still chances to improve the tool or extend the functionality of the tool. Figure 9-1 illustrates suggestions for future work that can be implemented. As discussed in Section 9.1, the powertrain has the highest impact in terms of performance, energy consumption, cost and emissions. Since AEV Tool considered a fixed driving cycle and powertrain configuration, it would be interesting to investigate further. Taking advantage of the modularity and expandability of the current AEV Tool, a powertrain design tool can be implemented that offers longitudinal simulation with multiple driving cycles, different motor size and type and architectures. The generated vehicle concept which is the outcome of the tool can be further as input for the simulation plug-in and the results of the energy consumption and powertrain cost can be instantly compared.

Since the AEV Tool focuses on buses that are majorly used for public transport, it is important to explore new bus concepts. A double-deck bus would be ideal to transport more passengers than compared to single-deck buses by having almost the same footprint. To have an initial assessment a parametric double-deck vehicle concept was developed as illustrated in Figure 9-1, that was not discussed in the thesis. A double-concept development includes several unique components that has to be addressed in the development. The components include an entire upper deck, stairs, additional doors, a third axle, different interior layouts, etc. The parametric model of the single deck needs to be expanded. In addition, in order to develop a double-deck concept, all the subsystems and components selection have to be modified or developed. For instance, the powertrain systems should be investigated for three axle architectures. The higher COG of the vehicle influences the chassis components mainly the suspension and braking system. The entire chassis components database has to be

expanded. The HVAC model should be extended considering the cabin volume of the upper deck and components packaging should be altered since HVAC might not be placed on the roof. The vehicle structure, body and frame have to be redesigned to meet the requirement of the double-deck buses. Furthermore, the weight estimation and cost estimation model have to be reworked.

Another important future work of the AEV Tool is the development of an algorithm to perform optimisation of the vehicle concept development. The algorithm can help to identify optimal concept parameters by evaluating the generated vehicle concepts. Currently, the AEV Tool develops concepts based on several user inputs and the ideal vehicle concept is manually chosen through iterative approach by comparing the vehicle properties. The optimisation algorithm as illustrated in Figure 9-1 is currently developed by PATHAK in TUMCREATE. For optimisation, vehicle parameters have to be grouped into the different property to groups such as comfort that includes seating and standing comfort, thermal comfort, riding comfort etc. Another example would be accessibility, which includes parameters such as door width, number of doors, entry height, step-free floor, etc. The property groups' parameters should be translated into quantifiable values. The available component modules of the AEV Tool can be made to calculate the properties of the vehicle being evaluated. Further, the property fulfilment of the vehicle properties can be compared against the TCO of the vehicle concept. Thus the main objectives can be the reduction of TCO and to maximise the fulfilment of properties. A genetic algorithm can be used for such optimisation. The package of optimised vehicle concept can be visualised in 3D with the help of developed parametric CAD model.
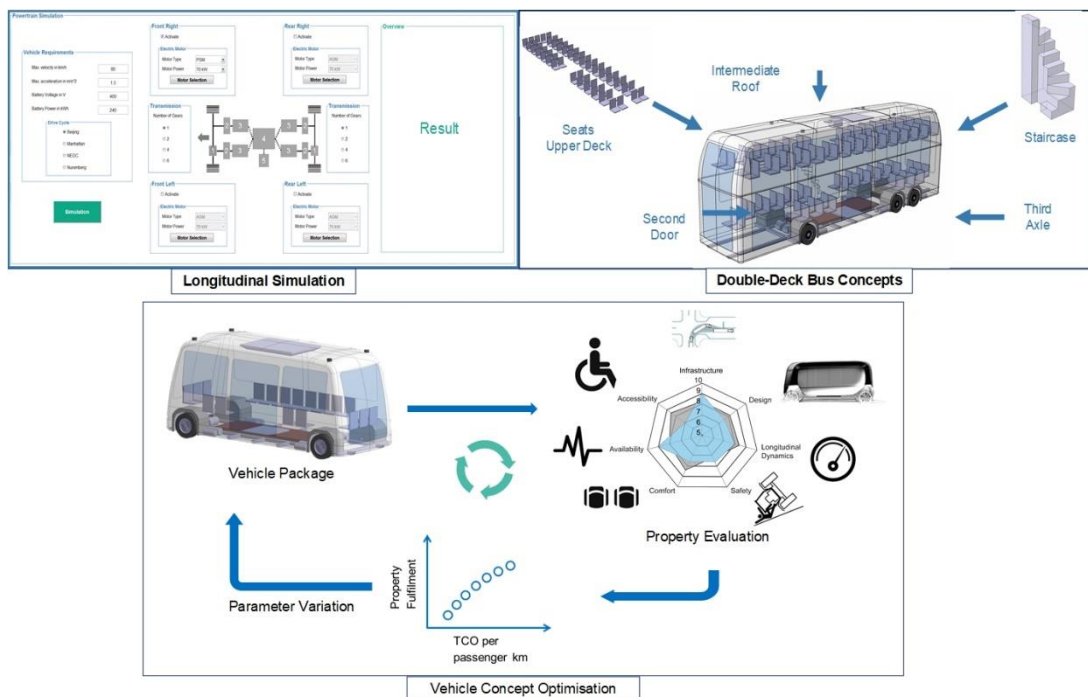
Figure 9-1   Future Work Topics

List of Figures

List of Tables

References

[1] United Nations, "World Urbanization Prospects," 2014. Accessed: Mar. 19 2018. [Online]. Available: http://esa.un.org/unpd/wup/CD-ROM/

[2] "Global Opportunity Report 2016," Accessed: Sep. 27 2019. [Online]. Available: https://www.unglobalcompact.org/docs/publications/Global_Opportunity_Report_2016.pdf

[3] UNECE, *Climate Change and Sustainable Transport - Transport - UNECE: United Nations Economic Commission for Europe (UNECE).* [Online]. Available: http://www.unece.org/?id=9890 (accessed: Sep. 27 2019).

[4] R. Sims *et al.,* "Transport Climate Change 2014: Mitigation of Climate Change. Contribution of Working Group III to the Fifth Assessment Report of the Intergovernmental Panel on Climate Change ed. Edenhofer et al," *Cambridge and New York: Cambridge University Press.*, 2014. [Online]. Available: http://www. ipcc. ch/pdf/assessment-report/ar5/wg3/ipcc_wg3_ar5_chapter8. pdf

[5] G. Meyer and S. Shaheen, "Disrupting Mobility: Impacts of Sharing Economy and Innovative Transportation on Cities," *Springer International Publishing*, 2017.

[6] F. Kuhnert and C. Stürmer, "Five Trends Transforming the Automotive Industry," *pwc*, 2018.

[7] M. Zackrisson, L. Avellán, and J. Orlenius, "Life cycle assessment of lithium-ion batteries for plug-in hybrid electric vehicles-Critical issues," *Journal of Cleaner Production*, vol. 18, no. 15, pp. 1519–1529, 2010.

[8] T. R. Hawkins, B. Singh, G. Majeau-Bettez, and A. H. Strømman, "Comparative environmental life cycle assessment of conventional and electric vehicles," *Journal of Industrial Ecology*, vol. 17, no. 1, pp. 53–64, 2013.

[9] Q. Wang and D. L. Santini, "Magnitude and value of electric vehicle emissions reductions for six driving cycles in four US cities with varying air quality problems," Argonne National Lab., IL (United States), 1992.

[10] J. Arbib and T. Seba, *Rethinking transportation 2020-2030: The disruption of transportation and the collapse of the internal-combustion vehicle and oil industries*: RethinkX, 2017.

[11] T. Litman, "Autonomous vehicle implementation predictions: Implications for transport planning," 2015.

[12] D. J. Fagnant and K. Kockelman, "Preparing a nation for autonomous vehicles: opportunities, barriers and policy recommendations," *Transportation Research Part A: Policy and Practice*, vol. 77, pp. 167–181, 2015, doi: 10.1016/j.tra.2015.04.003.

[13] K. M. Kockelman and T. Li, "Valuing the Safety Benefits of Connected and Automated Vehicle Technologies," in *Transportation Research Board 95th Annual MeetingTransportation Research Board*, 2016.

[14] A. Ongel, E. Loewer, F. Roemer, G. Sethuraman, F. Chang, and M. Lienkamp, "Economic Assessment of Autonomous Electric Microtransit Vehicles," *Sustainability*, vol. 11, no. 3, p. 648, 2019, doi: 10.3390/su11030648.

[15] International Transport Forum, *Urban Mobility System Upgrade: How shared self-driving cars could change city traffic*: OECD.

[16] J. Ainsalu *et al.,* "State of the art of automated buses," *Sustainability*, vol. 10, no. 9, p. 3118, 2018.

[17] W. Zhang, E. Jenelius, and H. Badia, "Efficiency of Semi-Autonomous and Fully Autonomous Bus Services in Trunk-and-Branches Networks," *Journal of Advanced Transportation*, vol. 2019, no. 5, pp. 1–17, 2019, doi: 10.1155/2019/7648735.

[18] J. Weber, *Automotive development processes: Processes for successful customer oriented vehicle development*. Berlin: Springer, 2009.

[19] V. D. Bhise, "Automotive Product Development - A Systems Engineering Implementation," *Taylor & Francis Group, LLC*, 2017.

[20] M. Lienkamp, "Vorlesung Fahrzeugkonzepte: Entwicklung und Simulation: Automobilentwicklungsprozess," Vorlesung, FTM, Technical University of Munich, Munich, 2018.

[21] Dassault Systems, *CATIA™ 3DEXPERIENCE® - Dassault Systèmes® 3D Software.* [Online]. Available: https://www.3ds.com/products-services/catia/?wockw= card_content_cta_1_url%3A%22https%3A%2F%2Fblogs.3ds.com%2Fcatia%2F%22 (accessed: Feb. 25 2020).

[22] *Vehicle and environment simulation software for virtual test driving.* [Online]. Available: https://www.tesis.de/en/products/?r=1 (accessed: Mar. 12 2020).

[23] *Simpack MBS Software | Dassault Systèmes.* [Online]. Available: https://www.3ds.com/ products-services/simulia/products/simpack/ (accessed: Mar. 12 2020).

[24] *Engineering Simulation & 3D Design Software | Ansys.* [Online]. Available: https:// www.ansys.com/ (accessed: Mar. 12 2020).

[25] *MATLAB.* [Online]. Available: https://de.mathworks.com/products.html?s_tid=gn_ps (accessed: Nov. 18 2018).

[26] G. Kukec, "Decreasing Engineering Time with Variable CAD Models: Parametric Approach to Process Optimization," *Computer-Aided Design and Applications*, vol. 12, no. 5, pp. 651–661, 2015, doi: 10.1080/16864360.2015.1014744.

[27] M. Brill, *Parametrische Konstruktion mit CATIA V5: Methoden und Strategien für den Fahrzeugbau*. München [u.a.]: Hanser, 2006.

[28] T. Richter, H. Mechler, and D. Schmitt, Eds., *Integrated parametric aircraft design,* 23rd ed. Toronto, 2002.

[29] LTA | Vehicle Population, "Motor Vehicle Population by Vehicle Type, LTA Singapore: Annual Vehicle Statistics 2018," 2018. [Online]. Available: https://www.lta.gov.sg/ content/dam/ltaweb/corp/PublicationsResearch/files/FactsandFigures/MVP01-1_MVP_ by_type.pdf

[30] NCCS | Transport, *National Climate Change Seceretariat (NCCS), Singapore.* [Online]. Available: https://www.nccs.gov.sg/climate-change-and-singapore/reducing-emissions/ transport (accessed: Jul. 8 2019).

[31] UITP, "ZeEUS eBus Report #2: An updated overview of electric buses in Europe," The International Association of Public Transport, 2018. Accessed: Mar. 1 2019. [Online]. Available: https://zeeus.eu/uploads/publications/documents/zeeus-ebus-report-2.pdf

[32] A. Kunith, "Elektrifizierung des urbanen öffentlichen Busverkehrs: Technologiebewertung für den kosteneffizienten Technologiebewertung für den kosteneffizienten Betrieb emissionsfreier Bussysteme," 2017.

[33] A. Lajunen, "Evaluation of Battery Requirements for Hybrid and Electric City Buses," *WEVJ*, vol. 5, no. 2, pp. 340–349, 2012, doi: 10.3390/wevj5020340.

[34] A. Lajunen, "Powertrain design alternatives for electric city bus," in *IEEE Vehicle Power and Propulsion Conference (VPPC), 2012: 9-12 Oct. 2012, Seoul, Korea*, Seoul, Korea (South), 2012, pp. 1112–1117.

[35] A. Lajunen, "Energy-optimal velocity profiles for electric city buses," in *2013 IEEE International Conference on Automation Science and Engineering (CASE 2013): Madison, Wisconsin, USA, 17-20 August 2013*, Madison, WI, USA, 2013, pp. 886–891.

[36] A. Lajunen, "Comparison of Different Powertrain Configurations for Electric City Bus," in *2014 IEEE Vehicle Power and Propulsion Conference (VPPC)*, Coimbra, Portugal, 2014, pp. 1–5.

[37] A. Lajunen, "Energy consumption and cost-benefit analysis of hybrid and electric city buses," *Transportation Research Part C: Emerging Technologies*, vol. 38, pp. 1–15, 2014.

[38] A. Lajunen, "Improving the Energy Efficiency and Operating Performance of Heavy Vehicles by Powertrain Electrification," Doctoral Dissertation, Department of Engineering Design and Production, Aalto University, Finland, 2014. [Online]. Available: https://aaltodoc.aalto.fi/bitstream/handle/123456789/13953/isbn9789526058252.pdf?sequence=1&isAllowed=y

[39] A. Lajunen and T. Lipman, "Lifecycle cost assessment and carbon dioxide emissions of diesel, natural gas, hybrid electric, fuel cell hybrid and electric transit buses," *Energy*, vol. 106, pp. 329–342, 2016.

[40] A. Lajunen, "Lifecycle costs and charging requirements of electric buses with different charging methods," *Journal of Cleaner Production*, vol. 172, pp. 56–67, 2018, doi: 10.1016/j.jclepro.2017.10.066.

[41] A. Lajunen and K. Tammi, *Evaluation of energy consumption and carbon dioxide emissions of electric city buses*. Finland: VTT Technical Research Centre of Finland, 2019.

[42] A. Pathak, G. Sethuraman, S. Krapf, A. Ongel, and M. Lienkamp, "Exploration of Optimal Powertrain Design Using Realistic Load Profiles," *World Electric Vehicle Journal*, vol. 10, no. 3, p. 56, 2019, doi: 10.3390/wevj10030056.

[43] G. Cooney, T. R. Hawkins, and J. Marriott, "Life cycle assessment of diesel and electric public transportation buses," *Journal of Industrial Ecology*, vol. 17, no. 5, pp. 689–699, 2013.

[44] X. Ou, X. Zhang, and S. Chang, "Alternative fuel buses currently in use in China: life-cycle fossil energy use, GHG emissions and policy recommendations," *Energy Policy*, vol. 38, no. 1, pp. 406–418, 2010.

[45] M. V. Chester, A. Horvath, and S. Madanat, "Comparison of life-cycle energy and emissions footprints of passenger transportation in metropolitan regions," *Atmospheric Environment*, vol. 44, no. 8, pp. 1071–1079, 2010.

[46] B. Zhou *et al.,* "Real-world performance of battery electric buses and their life-cycle benefits with respect to energy consumption and carbon dioxide emissions," *Energy*, vol. 96, pp. 603–613, 2016.

[47] Y. Xu, F. E. Gbologah, D.-Y. Lee, H. Liu, M. O. Rodgers, and R. L. Guensler, "Assessment of alternative fuel and powertrain transit bus options using real-world operations data: Life-cycle fuel and emissions modeling," *Applied Energy*, vol. 154, pp. 143–159, 2015.

[48] M. Mahmoud, R. Garnett, M. Ferguson, and P. Kanaroglou, "Electric buses: A review of alternative powertrains," *Renewable and Sustainable Energy Reviews*, vol. 62, pp. 673–684, 2016.

[49] U.-D. Choi, H.-K. Jeong, and S.-K. Jeong, "Commercial operation of ultra low floor electric bus for Seoul city route," in *IEEE Vehicle Power and Propulsion Conference (VPPC), 2012: 9-12 Oct. 2012, Seoul, Korea*, Seoul, Korea (South), 2012, pp. 1128–1133.

[50] M. Alexander-Kearns, M. Peterson, and A. Cassady, "The impact of vehicle automation on carbon emissions," *Center for American Progress. Retrieved from https://www. americanprogress. org/issues/green/reports/2016/11/18/292588/theimpact-of-vehicle-automation-on-carbon-emissions-where-uncertainty-lies*, 2016.

[51] "Reshaping Urban Mobility with Autonomous Vehicles - Lessons from the City of Boston," Boston Consulting Group. Accessed: Dec. 27 2019. [Online]. Available: http://www3.weforum.org/docs/WEF_Reshaping_Urban_Mobility_with_Autonomous_Vehicles_2018.pdf

[52] *Taxonomy and Definitions for Terms Related to On-Road Motor Vehicle Automated Driving Systems*, J3016, 2014.

[53] D. J. Fagnant, K. M. Kockelman, and P. Bansal, *Operations of Shared Autonomous Vehicle Fleet for Austin, Texas, Market*. transportation Research Record Journal of the Transportation Research Board, 2015.

[54] A. Brown, J. Gonder, and B. Repac, "An Analysis of Possible Energy Impacts of Automated Vehicles," in *Lecture Notes in Mobility, Road vehicle automation*, G. Meyer and S. Beiker, Eds., New York: Springer, 2014, pp. 137–153.

[55] T. Ringenson, M. Hoejer, A. Kramers, and A. Viggedal, "Digitalization and Environmental Aims in Municipalities," *Sustainability*, 10(4), 1278, 2018, doi: 10.3390/su10041278.

[56] Spieser, Kevin, Kyle Ballantyne, Treleaven, Rick Zhang, Emilio Frazzoli, Daniel Morton, Marco Pavone, "Toward a Systematic Approach to the Design and Evaluation of Automated Mobility-on-Demand systems - A Case Study in Singapore,"

[57] Antonio Loro Consulting Inc., *Planning for automated vehicles in Edmonton: Final report*. Autonomous Vehicles Study Update. [Online]. Available: https://www.edmonton.ca/city_government/documents/RoadsTraffic/2016_automated_vehicles_report.pdf (accessed: Nov. 16 2017).

[58] K. Bullis, *How Vehicle Automation Will Cut Fuel Consumption: Cars that park themselves and automatically convoy with other cars could reduce congestion and emissions.* [Online]. Available: https://www.technologyreview.com/s/425850/how-vehicle-automation-will-cut-fuel-consumption/#comments (accessed: Jan. 18 2018).

[59] A. Stocker and S. Shaheen, "Shared Automated Vehicles: Review of Business Models," *Transportation Sustainability Research Center, University of California, Berkeley, Berkeley, CA*, 2017.

[60] G. Sethuraman, S. S. Reddy Ragavareddy, A. Ongel, M. Lienkamp, and P. Raksincharoensak, "Impact Assessment of Autonomous Electric Vehicles in Public Transportation System," in *The 2019 IEEE Intelligent Transportation Systems Conference - ITSC: Auckland, New Zealand, 27-30 October 2019*, Auckland, New Zealand, 2019, pp. 213–219.

[61] Easy Mile, *Shared driverless transportation for the last mile.* [Online]. Available: http://easymile.com/ (accessed: Nov. 23 2017).

[62] Navya, *Autonom Shuttle, the Revolutionary First and Last Mile Travel Solution.* [Online]. Available: http://navya.tech/en/autonom-en/autonom-shuttle/ (accessed: Nov. 24 2017).

[63] Localmotors, *Autonomous for all of us - Meet Olli.* [Online]. Available: https://localmotors.com/meet-olli/ (accessed: Nov. 25 2017).

[64] 2getthere, *We Deliver Again: Technology GRT Vehicle Specification.* [Online]. Available: https://www.2getthere.eu/ (accessed: Jan. 15 2018).

[65] Next, *Next future transportation inc.* [Online]. Available: http://www.next-future-mobility.com/ (accessed: Jan. 5 2018).

[66] Matreshka, *Matreshka M2B8.* [Online]. Available: http://matreshka.ai/en (accessed: Nov. 29 2017).

[67] Daimler AG, *The Mercedes-Benz Future Bus. The future of mobility.* [Online]. Available: https://www.daimler.com/innovation/autonomous-driving/future-bus.html (accessed: Jan. 16 2018).

[68] E. Hoepke and S. Breuer, *Nutzfahrzeugtechnik: Grundlagen, Systeme, Komponenten,* 8th ed. Wiesbaden: Springer Vieweg, 2016.

[69] Navya, *Singapore opens an autonomous vehicle centre.* [Online]. Available: https://navya.tech/en/singapore-opens-an-autonomous-vehicles-centre/ (accessed: Nov. 1 2018).

[70] Y. Asiedu and P. Gu, "Product life cycle cost analysis: State of the art review," *International Journal of Production Research*, vol. 36, no. 4, pp. 883–908, 1998, doi: 10.1080/002075498193444.

[71] A. Frick, R. Müller, T. Blauß, and D. Schramm, "Quantification concept for vehicle packaging," in *Proceedings, Automobil- und Motorentechnik*, M. Bargende, H.-C. Reuss, and J. Wiedemann, Eds., Wiesbaden: Springer Vieweg, 2016, pp. 597–606.

[72] K. Kuchenbuch, *Methodik zur Identifikation und zum Entwurf eigenschaftsoptimierter Elektrofahrzeuge.* Berlin: Logos Berlin, 2012.

[73] J. Cagan, K. Shimada, and S. Yin, "A survey of computational approaches to three-dimensional layout problems," *Computer-aided design*, vol. 34, no. 8, pp. 597–611, 2002, doi: 10.1016/S0010-4485(01)00109-9.

[74] Y. Miao, *Packing optimization of engineering problems.* Ann Arbor, Michigon: ProQuest LLC, 2005.

[75] Y. Miao, G. M. Fadel, and V. B. Gantovnik, "Vehicle configuration design with a packing genetic algorithm," *IJHVS*, vol. 15, 2/3/4, p. 433, 2008, doi: 10.1504/IJHVS.2008.022252.

[76] B. van Oers, D. Stapersma, and H. Hopman, "A 3D Packing Approach for the Early Stage Configuration Design of Ships," 2010. [Online]. Available: https://www.researchgate.net/publication/265533476_A_3D_Packing_Approach_for_the_Early_Stage_Configuration_Design_of_Ships

[77] J. D. Foley, *Computer Graphics: Principles and practice,* 2nd ed. Boston, Mass., London: Addison-Wesley, 1995.

[78] S. M. Lock and D. P. M. Wills, "VoxColliDe: Voxel collision detection for virtual environments," *Virtual Reality*, vol. 5, no. 1, pp. 8–22, 2000, doi: 10.1007/BF01418972.

[79] M. P. Bendsøe and O. Sigmund, *Topology optimization: Theory, methods and applications / M.P. Bendsøe, O. Sigmund.* Berlin, London: Springer, 2003.

[80] R. Klette and A. Rosenfeld, *Digital Geometry: Geometric Methods for Digital Picture Analysis (Morgan Kaufmann series in computer graphics and geometric modeling)*: Morgan Kaufmann Publishers, 2004.

[81] G. Jacquenot, F. Bennis, J.-J. Maisonneuve, and P. Wenger, "2D Multi-Objective Placement Algorithm for Free-Form Components," in *Volume 5: 35th Design Automation Conference, Parts A and B*, San Diego, California, USA, 2009, pp. 239–248.

[82] B. Yao, H. Chen, C.-K. Cheng, and R. Graham, "Revisiting floorplan representations," in *Proceedings of the 2001 international symposium on Physical design - ISPD '01*, Sonoma, California, United States, 2001, pp. 138–143.

[83] T.-C. Chen and Y.-W. Chang, "Packing Floorplan Representations," in *Handbook of Algorithms for Physical Design Automation*, C. Alpert, D. P.Mehta, and S. Sapatnekar, Eds., Boca Raton: CRC Press, 2008.

[84] C. L. Valenzuela and P. Y. Wang, "A Genetic Algorithm for VLSI Floorplanning," in *Lecture Notes in Computer Science, Parallel Problem Solving from Nature PPSN VI*, G. Goos et al., Eds., Berlin, Heidelberg: Springer Berlin Heidelberg, 2000, pp. 671–680.

[85] X. Hong *et al.,* "Corner block list: An effective and efficient topological representation of non-slicing floorplan," in *IEEE/ACM International Conference on Computer Aided Design. ICCAD - 2000. IEEE/ACM Digest of Technical Papers (Cat. No.00CH37140)*, San Jose, CA, USA, 2000, pp. 8–12.

[86] H. Murata, K. Fujiyoshi, S. Nakatake, and Y. Kajitani, "Rectangle-packing-based module placement," in *Proceedings of IEEE International Conference on Computer Aided Design (ICCAD)*, San Jose, CA, USA, 1995, pp. 472–479.

[87] X. Tang and D. F. Wong, "FAST-SP: A fast algorithm for block placement based on sequence pair," in *Proceedings of the ASP-DAC 2001. Asia and South Pacific Design Automation Conference 2001 (Cat. No.01EX455)*, Yokohama, Japan, 2001, pp. 521–526.

[88] K. A. Doksum, "Mathematical Statistics: Basic and Selected Topics.," *Pearson Prentice-Hall*, 2007.

[89] D. Roller, "CAD Effiziente Anpassungs- und Variantenkonstruktion," *Springer Verlag*, pp. 12–14, 1995.

[90] M. Fries, M. Kruttschnitt, and M. Lienkamp, Eds., *Multi-objective optimization of a long-haul truck hybrid operational strategy and a predictive powertrain control system*: IEEE, 2017.

[91] S. Fuchs, "Verfahren zur parameterbasierten Gewichtsab-schätzung neuer Fahrzeugkonzepte," Universität München, 2014.

[92] E. Wiedemann, *Ableitung von Elektrofahrzeugkonzepten aus Eigenschaftszielen*: Cuvillier, 2014.

[93] S. Matz, *Nutzerorientierte Fahrzeugkonzeptoptimierung in einer multimodalen Verkehrsumgebung*: Verlag Dr. Hut, 2015.

[94] M. Ried, A. Kelnberger, A. Gumm, M. Jung, and I. D. Schramm, "Parametrische Geometriemodelle für die Konzeptgestaltung elektrifizierter Fahrzeuge," in *Schritte in die künftige Mobilität*: Springer, 2013, pp. 19–33.

[95] A. Förg, M. Kreimeyer, and M. Lienkamp, "Architecting new vehicle concepts: virtual design and performance based assessment," in *HVTT13: International Symposium on Heavy Vehicle Transport Technology, 13th, 2014, San Luis, Argentina*, 2014.

[96] *jReality: A java library for real-time interactive 3D graphics and audio*: ACM, 2009.

[97] G. Sethuraman, M. Schwarz, S. Maxl, A. Ongel, M. Lienkamp, and P. Raksincharoensak, "Development of an Overall Vehicle Sizing and Packaging Tool for Autonomous Electric Buses in the Early Concept Phase," *SAE Journal of commercial vehicles*, 2020, doi: 10.4271/02-13-01-0002.

[98] Á. Cabrera, W. C. Collins, and J. F. Salgado, "Determinants of individual engagement in knowledge sharing," *The International Journal of Human Resource Management*, vol. 17, no. 2, pp. 245–264, 2006, doi: 10.1080/09585190500404614.

[99] M. Patterson, P. Warr, and M. West, "Organizational climate and company productivity: The role of employee affect and employee level," *Journal of Occupational and Organizational Psychology*, vol. 77, no. 2, pp. 193–216, 2004, doi: 10.1348/096317904774202144.

[100] A. Preece, A. Flett, D. Sleeman, D. Curry, N. Meany, and P. Perry, "Better knowledge management through knowledge engineering," *IEEE Inteligent Systems*, 2001.

[101] Singapore Government, *Road Traffic (Motor Vehicles, Construction and Use) Rules: Road Traffic Act.* [Online]. Available: https://sso.agc.gov.sg/SL/RTA1961-R9?DocDate= 20120103&ValidDate=20151101&TransactionDate=20160101 (accessed: Mar. 28 2018).

[102] Land Transport Authority, *Bus Bay Dimensions.* [Online]. Available: https:// www.lta.gov.sg/content/dam/ltaweb/corp/Industry/files/SDRE(2014)/SDRE14- 11%20BUS%201-5-1DEC17.pdf (accessed: Mar. 23 2018).

[103] Land Transport Authority, *Street Hump Design Guidelines.* [Online]. Available: https:// www.lta.gov.sg/ (accessed: Mar. 28 2018).

[104] H. Dreyfuss and A. R. Tilley, *The measure of man and woman: Human factors in design / Henry Dreyfuss Associates.* New York: Wiley, 2002.

[105] J. Panero and M. Zelnik, *Human dimension & interior space: A source book of design reference standards.* New York: Whitney Library of Design, 1979.

[106] S. Openshaw and E. Taylor, *Ergonomics and design a reference guide.* [Online]. Available: http://www.allsteeloffice.com/SynergyDocuments/ ErgonomicsAndDesignReferenceGuideWhitePaper.pdf (accessed: Jan. 15 2018).

[107] G. Marinkovic, "SRT Vehicle Design: Progress update," TUMCREATE, Singapore, 2017.

[108] Land Transport Authority, *Standard Details of Road Elements.* [Online]. Available: https://www.lta.gov.sg/content/dam/ltaweb/corp/Industry/files/SDRE(2014)/ Content%20page.pdf (accessed: Mar. 12 2018).

[109] *Strength of seats and their anchorages (buses)*, ECE Regulation No. 80, 2011.

[110] *General construction of large buses and coaches*, ECE Regulation No. 36.

[111] J. A. Levis, "The seated bus passenger - a review," *Applied Ergonomics*, vol. 9, no. 3, pp. 143–150, 1978, doi: 10.1016/0003-6870(78)90004-2.

[112] S. Große, F. Vogt, and L. Hannawald, *Method for the estimation of the deformation frequency of passenger cars with the German In-Depth Accident Study (GIDAS).* [Online]. Available: http://bast.opus.hbz-nrw.de/volltexte/2012/560/pdf/Method_for_the_ estimation_of_the_deformation_frequency_of_passenger_cars.pdf (accessed: Dec. 15 2017).

[113] M. Lienkamp, "Auslegung von Elektrofahrzeugen," Technical University Munich. Munich, 2017.

[114] *Grundlagen der Nutzfahrzeugtechnik LKW und Bus: Lehrbuch der MAN Academy,* 4th ed. Bonn: Kirschbaum, 2016.

[115] A. Kampker, D. Vallée, and A. Schnettler, Eds., *Elektromobilität: Grundlagen einer Zukunftstechnologie.* Berlin, Heidelberg: Springer Vieweg, 2013.

[116] H.-H. Braess and U. Seiffert, *Vieweg Handbuch Kraftfahrzeugtechnik.* Wiesbaden: Springer Fachmedien Wiesbaden, 2013.

[117] J. M. Anderson, N. Kalra, K. D. Stanley, P. Sorensen, C. Samaras, and O. A. Oluwatola, *Autonomous vehicle technology: A guide for policymakers.* Santa Monica CA: Rand Corporation, 2014.

[118]   T. U. Pimmler and S. D. Eppinger, Eds., *Integration analysis of product decompositions*. Cambridge, Massachusetts, 1994.

[119]   U. Lindemann, M. Maurer, and T. Braun, *Structural complexity management: An approach for the field of product design / Udo Lindemann, Maik Maurer, Thomas Braun*. Berlin: Springer, 2009.

[120]   T. R. Browning, "Applying the design structure matrix to system decomposition and integration problems: a review and new directions," *IEEE Trans. Eng. Manage.*, vol. 48, no. 3, pp. 292–306, 2001, doi: 10.1109/17.946528.

[121]   S. Krapf, "Parametric Powertrain Design Exploration for Electric City Buses_Thesis," Institute of Automotive Technology (FTM), Technical University of Munich, 2017.

[122]   S. Mueller, S. Rohr, W. Schmid, and M. Lienkamp, "Analysing the Influence of Driver Behaviour and Tuning Measures on Battery Aging and Residual Value of Electric Vehicles," in *EVS30 International Battery, Hybrid and Fuel Cell Electric Vehicle Symposium*, 2017.

[123]   L. Horlbeck, "Auslegung elektrischer Maschinen für automobile Antriebsstränge unter Berücksichtigung des Überlastpotentials," Doctoral thesis, Institute of Automotive Technology, FTM, Technical University Munich, 2018.

[124]   F. Chang, O. Ilina, O. Hegazi, L. Voss, and M. Lienkamp, "Adopting MOSFET multilevel inverters to improve the partial load efficiency of electric vehicles," in *2017 19th European Conference on Power Electronics and Applications (EPE'17 ECCE Europe)*, Warsaw, 2017, P.1-P.13.

[125]   T. Lee, Y. Kim, and K. Nam, "Loss minimizing gear shifting algorithm based on optimal current sets for IPMSM," in *2017 IEEE Transportation Electrification Conference and Expo (ITEC)*, Chicago, IL, USA, 2017, pp. 135–140.

[126]   P. Spanoudakis, N. C. Tsourveloudis, G. Koumartzakis, A. Krahtoudis, T. Karpouzis, and I. Tsinaris, "Evaluation of a 2-speed transmission on electric vehicle's energy consumption," in *2014 IEEE International Electric Vehicle Conference (IEVC)*, Florence, Italy, 2014, pp. 1–6.

[127]   A. Schönknecht, A. Babik, and V. Rill, "Electric Powertrain System Design of BEV and HEV Applying a Multi Objective Optimization Methodology," *Transportation Research Procedia*, vol. 14, pp. 3611–3620, 2016.

[128]   G. Domingues, A. Reinap, and M. Alaküla, Eds., *Design and cost optimization of electrified automotive powertrain*: IEEE, 2016.

[129]   S. de Pinto, P. Camocardi, A. Sorniotti, G. Mantriota, P. Perlo, and F. Viotto, "A Four-Wheel-Drive Fully Electric Vehicle Layout with Two-Speed Transmissions," in *2014 IEEE Vehicle Power and Propulsion Conference (VPPC)*, Coimbra, Portugal, 2014, pp. 1–6.

[130]   M. Schwarz, "Development of a Parametric Model for Vehicle Packaging and Sizing of an Autonomous Electric Bus System," master's thesis, Institute of Automotive Technology (FTM), Technical University of Munich, 2018.

[131]   H. Naunheimer, *Automotive transmissions: Fundamentals, selection, design and application / by Harald Naunheimer … [et al.] ; translated by Aaron Kuchle,* 2nd ed. Heidleberg: Springer, 2011.

[132]   T. Pesce, *Ein Werkzeug zur Spezifikation von effizienten Antriebstopologien für Elektrofahrzeuge*: Verlag Dr. Hut, 2014.

[133]   F. Seeger, "Energetische Modellierung verschiedener Energetische Modellierung verschiedener Systeme zur Momentenverteilung für ein adaptives

Antriebsstrangmodell," Semester thesis, Institute of Automotive Technology, TUM, Munich, 2017.

[134]   D. V. Ngo, "Gear shift strategies for automotive transmissions," Doctoral Dissertation, Eindhoven University of Technology, Eindhoven, 2012.

[135]   I. Eroglu, "Fertigungstechnische Beurteilung, Kostenmodellierung und Analyse der Topologie elektrischer Antriebsstrangsysteme unter Berücksichtigung fahrdynamischer Eigenschaften," Master thesis, Institute of Automotive Technology FTM, Technical University Munich, 2017.

[136]   M. Fries, M. Kerler, S. Rohr, S. Schikram, M. Sinning, and M. Lienkamp, "An Overview of Costs for Vehicle Components, Fuels, Greenhouse Gas Emissions and Total Cost of Ownership Update 2017," 2017, doi: 10.13140/RG.2.2.19963.21285.

[137]   G. Domingues-Olavarria, P. Fyhr, A. Reinap, M. Andersson, and M. Alakula, "From Chip to Converter: A Complete Cost Model for Power Electronics Converters," *IEEE Trans. Power Electron.*, vol. 32, no. 11, pp. 8681–8692, 2017, doi: 10.1109/TPEL.2017.2651407.

[138]   S. Maxl, "Development of a Parametric Chassis Selection and Sizing Model for Autonomous Electric Buses," master's thesis, Institute of Automotive Technology (FTM), Technical University of Munich, 2018.

[139]   SQLite, *Distinctive Features Of SQLite.* [Online]. Available: https://sqlite.org/different.html (accessed: Nov. 21 2018).

[140]   DB Browser, *DB Browser for SQLite.* [Online]. Available: https://sqlitebrowser.org/ (accessed: Nov. 21 2018).

[141]   H. Pacejka, *Tire and vehicle dynamics: 3rd Edition*: Elsevier, 2012.

[142]   G. Genta and L. Morello, *The automotive chassis*. Dordrecht: Springer, 2009.

[143]   Ganesh Sethuraman, "Design Manual for Ride Map Data For Suspension Systems," Dec. 2000.

[144]   H. Wimmer and F. Alsdorf, "Modern Front Axle Systems for City Buses: Design Constraints, Concept and Tests," *ATZ*, 2006.

[145]   H. J. Pahl and L. F.T. Luftfedertechnik, "Luftfedern in Nutzfahrzeugen: Auslegung, Berechnung," *Praxis. Tönisvorst: LFT Luftfedertechnik*, 2002.

[146]   "Engineering Manual and Design Guide: Airmount Isolators and Airstroke Actuators," *Firestone Industrial Products Company*, vol. 2, 1996.

[147]   M. Mitschke, *Dynamik der kraftfahrzeuge.* [Place of publication not identified]: MORGAN KAUFMANN, 2015.

[148]   B. Breuer and K. H. Bill, *Bremsenhandbuch: Grundlagen, Komponenten, Systeme, Fahrdynamik*: Springer-Verlag, 2006.

[149]   T. Degenstein, "Kraftmessung in Scheibenbremsen," Dissertation, Technische Universität Darmstadt, 2007.

[150]   I. K. H. Bill and S. Dallmer, "Auslegung und Aufbau der Bremsanlagen für die 'Formula Student' -Rennfahrzeuge BRC08/BRC09,"

[151]   Bundesministerium der Justiz und für Verbraucherschutz, *Straßenverkehrs-Ordnung.* [Online]. Available: http://www.stvzo.de/stvzo/b4.htm (accessed: Mar. 13 2018).

[152]   *Bus Chassis - ZF.* [Online]. Available: https://www.zf.com/products/en/buses/productfinder/chassis.html?filter=ranges:Buses,groups:Chassis,categories:Axle%20Systems&filterLang=en (accessed: Jan. 26 2020).

[153]   MathWorks, *MATLAB and Simulink Racing Lounge: Vehicle Modeling with Simscape Multibody.* [Online]. Available: https://www.mathworks.com/matlabcentral/fileexchange/

64648-matlab-and-simulink-racing-lounge--vehicle-modeling-with-simscape-multibody?
s_tid=prof_contriblnk (accessed: Mar. 14 2018).

[154]   S. Miller, *Simscape Multibody Contact Forces Library*. [Online]. Available: https://
www.mathworks.com/matlabcentral/fileexchange/47417-simscape-multibody-contact-
forces-library (accessed: Mar. 21 2018).

[155]   M. Binder, "Parametric Development and Sizing of an Air Conditioning System for
Autonomous Electric Buses," Institute of Automotive Technology (FTM), Technical
University of Munich, 2018.

[156]   A. Pathak, M. Binder, A. Ongel, and H. W. Ng, "Investigation of a multi stage vapour-
injection cycle to improve air-conditioning system performance of electric buses," in
*2019 Fourteenth International Conference on Ecological Vehicles and Renewable
Energies (EVER)*, Monte-Carlo, Monaco, 2019, pp. 1–7.

[157]   American Society of Heating, Refrigerating and Air-Conditioning Engineers, Inc.,
Heating, Ventilating, and Air-Conditioning: Systems and Equipment. 2004 ASHRAE
HANDBOOK. Atlanta, Georgia, USA, 2004.

[158]   G. H. Lee and J. Y. Yoo, "Performance analysis and simulation of automobile air
conditioning system," *International Journal of Refrigeration*, vol. 23, no. 3, pp. 243–254,
2000, doi: 10.1016/S0140-7007(99)00047-X.

[159]   R. K. Shah and D. P. Sekulić, *Fundamentals of heat exchanger design*. New York,
Chichester: John Wiley & Sons, 2003.

[160]   GT-SUITE, *Flow Theory Manual: Version 2017*.

[161]   M. Rainer, "Functional Development of the Thermal Management and Air
Conditioning Control for an Electric Vehicle," Diploma Thesis, Chair of Automotive
Engineering, Technical University of Munich, Munich, Germany, 2013.

[162]   American Society of Heating, Refrigerating and Air-Conditioning Engineers, Inc.,
2011 ASHRAE handbook: Heating, Ventilating, and Air-Conditioning Applications.
Atlanta, Georgia, USA, 2011.

[163]   *ASHRAE Standard 55 - Thermal Environmental Conditions for Human Occupancy*,
1992.

[164]   J. Lai, L. Yu, G. Song, P. Guo, and X. Chen, "Development of City-Specific Driving
Cycles for Transit Buses Based on VSP Distributions: Case of Beijing," *J. Transp. Eng.*,
vol. 139, no. 7, pp. 749–757, 2013, doi: 10.1061/(ASCE)TE.1943-5436.0000547.

[165]   N. Yakah, "Heat Exchanger Design for a Solar Gas-Turbine Power Plant," Master's
Thesis, Division of Heat and Power, KTH School of Industrial Engineering and
Management, Stockholm, Sweden, 2014. [Online]. Available: http://kth.diva-portal.org/
smash/get/diva2:575441/FULLTEXT01.pdf

[166]   Oracle, *GT-SUITE Help Navigator*: GT-SUITE, 2018.

[167]   K. Dvorak, "Management of Parametric CAD Model by External Tools," *AMM*, vol.
390, pp. 616–620, 2013, doi: 10.4028/www.scientific.net/AMM.390.616.

[168]   J. Hansen, *Kochbuch CATIA V5 automatisieren: Vom Powercopy bis zur C♯-
Programmierung*. München: Hanser, 2009, ©2009.

[169]   D. R. Ziethen, *CATIA V5 - Makroprogrammierung mit Visual Basic Script*. [S.l.]: Carl
Hanser Verlag München, 2011.

[170]   S. Krapf, G. Sethuraman, A. Pathak, A. Ongel, and M. Lienkamp, Eds., *Improving
electric city bus powertrain efficiency and costs using design space exploration*, Oct.
2018.

[171]   B. Heißing and M. Ersoy, *Chassis handbook: fundamentals, driving dynamics,
components, mechatronics, perspectives*: Springer Science & Business Media, 2010.

[172]   MathWorks, *Create a Simple App Using GUIDE - MATLAB & Simulink.* [Online]. Available: https://www.mathworks.com/help/matlab/creating_guis/about-the-simple-guide-gui-example.html (accessed: Jan. 30 2020).

[173]   J. H. Gawron, G. A. Keoleian, R. D. de Kleine, T. J. Wallington, and H. C. Kim, "Life Cycle Assessment of Connected and Automated Vehicles: Sensing and Computing Subsystem and Vehicle Level Effects," *Environmental science & technology*, vol. 52, no. 5, pp. 3249–3256, 2018, doi: 10.1021/acs.est.7b04576.

[174]   S. Kalt, B. Danquah, and M. Lienkamp, Eds., *Electric machine design tool for permanent magnet synchronous machines*, 2019.

[175]   J. Fuchs, *Analyse der Wechselwirkungen und Entwicklungspotentiale in der Auslegung elektrifizierter Fahrzeugkonzepte,* 1st ed. Göttingen: Cuvillier Verlag, 2014. [Online]. Available: https://ebookcentral.proquest.com/lib/gbv/detail.action?docID=5021685

[176]   R. Kochhan, S. Fuchs, B. Reuter, P. Burda, S. Matz, and M. Lienkamp, "An overview of costs for vehicle components, fuels and greenhouse gas emissions," *researchgate.net*, 2014.

[177]   International Standard, "ISO 14040: First edition 1997-06-15," 1997.

[178]   Land Transport Authority (LTA), Personal Communication, 2017.

[179]   Umberto LCA+, *Umberto LCA+.* [Online]. Available: https://www.ifu.com/en/umberto/lca-software/ (accessed: Sep. 5 2019).

[180]   ecoinvent 3.5, *ecoinvent 3.5 – ecoinvent.* [Online]. Available: https://www.ecoinvent.org/database/older-versions/ecoinvent-35/ecoinvent-35.html (accessed: Jan. 10 2019).

[181]   GREET, *Argonne GREET Model.* [Online]. Available: https://greet.es.anl.gov/ (accessed: Jan. 7 2019).

[182]   M. Thomitzek, N. von Drachenfels, F. Cerdas, C. Herrmann, and S. Thiede, "Simulation-based assessment of the energy demand in battery cell manufacturing," *Procedia CIRP*, vol. 80, pp. 126–131, 2019, doi: 10.1016/j.procir.2019.01.097.

[183]   J.-H. Schünemann, *Modell zur Bewertung der Herstellkosten von Lithiumionenbatteriezellen: Zugl.: Braunschweig, Techn. Univ., Diss., 2015,* 1st ed. Göttingen: Sierke, 2015.

[184]   E. Erik and D. Lisbeth, "Lithium-Ion Vehicle Battery Production: Status 2019 on Energy Use, CO2 Emissions, Use of Metals, Products Environmental Footprint, and Recycling," 2019. [Online]. Available: https://www.ivl.se/download/18.14d7b12e16e3c5c36271070/1574923989017/C444.pdf

[185]   MAN SE, *MAN GRI Report: Corporate Responsibility at MAN* (accessed: Sep. 5 2019).

[186]   EMA Supply, *Energy Market Authority | Energy Supply.* [Online]. Available: https://www.ema.gov.sg/cmsmedia/Publications_and_Statistics/Publications/ses/2018/energy-supply/index.html (accessed: Oct. 5 2019).

[187]   Land Transport Authority, "Fuel Consumption of Single-deck Buses".

[188]   DEKRA, *Umwelt und CO2.* [Online]. Available: https://www.dekra.de/de/umwelt-und-co2/ (accessed: May 13 2019).

[189]   IINAS, *About IINAS - IINAS.* [Online]. Available: http://iinas.org/about.html (accessed: Jul. 15 2019).

[190]   COPERT, *COPERT | EMISIA SA.* [Online]. Available: https://www.emisia.com/utilities/copert/ (accessed: Jul. 15 2019).

[191] Umweltbundesamt, *Schwere Nutzfahrzeuge.* [Online]. Available: https://www.umweltbundesamt.de/themen/verkehr-laerm/emissionsstandards/schwere-nutzfahrzeuge (accessed: May 13 2019).

[192] LithoRec II, *Recycling of EV-Lithium-Ion-Batteries.* Accessed: Jan. 10 2019. [Online]. Available: http://www.lithorec2.de/index.php/en/

[193] S. Kelly and D. Apelian, "Final-Report-Automotive-Aluminum-Recycling-at-End-of-Life-A-Grave-to-Gate-Analysis," [Online]. Available: http://drivealuminum.wpengine.com/wp-content/uploads/2016/06/Final-Report-Automotive-Aluminum-Recycling-at-End-of-Life-A-Grave-to-Gate-Analysis.pdf

[194] S. McGlothlin, "Copper recycling process technology in End of Life Vehicle (ELV) shredder plants," 2012. [Online]. Available: https://www.metalbulletin.com/events/download.ashx/document/speaker/6539/a0ID000000X0jUWMAZ/Presentation

[195] Waste Statistics and Overall Recycling, *Waste Statistics and Overall Recycling.* [Online]. Available: https://www.nea.gov.sg/our-services/waste-management/waste-statistics-and-overall-recycling (accessed: Feb. 7 2019).

[196] Recycling, *Recycling | WorldAutoSteel.* [Online]. Available: https://www.worldautosteel.org/life-cycle-thinking/recycling/ (accessed: Feb. 7 2019).

[197] Karsan, *Atak - Electric Bus | Karsan.* [Online]. Available: https://www.karsan.com.tr/en/atak/atak-electric/atak-electric-highlights (accessed: Jul. 23 2019).

[198] Karsan, *Specs - Jest Electric | Karsan.* [Online]. Available: https://www.karsan.com/en/jest-electric-specs (accessed: Feb. 14 2020).

[199] V. Freyermuth and A. Rousseau, "Long Term Impact of Vehicle Electrification on Vehicle Weight and Cost Breakdown," in *SAE Technical Paper Series*, 2017.

[200] APTA, TCRP, and MORR Transportation Consulting, *An Analysis of Transit Axle Weight Issues.* [Online]. Available: http://onlinepubs.trb.org/onlinepubs/tcrp/docs/TCRPJ-11Task20-FR.pdf (accessed: Aug. 3 2019).

[201] A. Pathak, G. Sethuraman, A. Ongel, and M. Lienkamp, "Impacts of electrification & automation of public bus transportation on sustainability—A case study in Singapore," *Forsch Ingenieurwes*, 2020, doi: 10.1007/s10010-020-00408-z.

[202] A. Rau, L. Tian, M. Jain, M. Xie, T. Liu, and Y. Zhou, "Dynamic Autonomous Road Transit (DART) For Use-case Capacity More Than Bus," *Transportation Research Procedia*, vol. 41, pp. 812–823, 2019, doi: 10.1016/j.trpro.2019.09.131.

[203] Land Transport Authority (LTA), Singapore, *Land Transport DataMall.* [Online]. Available: https://www.mytransport.sg/content/mytransport/home/dataMall.html (accessed: Feb. 16 2020).

[204] A. Ceder, S. Hassold, and B. Dano, "Approaching even-load and even-headway transit timetables using different bus sizes," *Public Transp*, vol. 5, no. 3, pp. 193–217, 2013, doi: 10.1007/s12469-013-0062-z.

[205] Transitlink, *Bus Enquiry Electronic Guide.* [Online]. Available: https://www.transitlink.com.sg/eservice/eguide/service_idx.php (accessed: Jun. 1 2020).

[206] J.L. Saha, "An Algorithm for Bus Scheduling Problems," *Operational Research Quarterly*, vol. 21, no. 4, pp. 463–474, 1970.

[207] M. E. van Kooten Niekerk, J. M. van den Akker, and J. A. Hoogeveen, "Scheduling electric vehicles," *Public Transp*, vol. 9, 1-2, pp. 155–176, 2017, doi: 10.1007/s12469-017-0164-0.

Publication List

During the work on the dissertation topic, the author published and supervised the following papers and student thesis, which present the contents of this dissertation partially. The author is grateful for the contributions of the co-authors and the students.

Journal; peer-reviewed

[1]   G. Sethuraman, M. Schwarz, S. Maxl, A. Ongel, M. Lienkamp, and P. Raksincharoensak, "Development of an Overall Vehicle Sizing and Packaging Tool for Autonomous Electric Buses in the Early Concept Phase" SAE Int. J. Commer. Veh.13(1):2020, doi:10.4271/02-13-01-0002.

[2]   A. Pathak, G. Sethuraman, A. Ongel, and M. Lienkamp, "Impacts of electrification & automation of public bus transportation on sustainability—A case study in Singapore," Forsch Ingenieurwes, 2020, doi: 10.1007/s10010-020-00408-z.

[3]   A. Pathak, G. Sethuraman, S. Krapf, A. Ongel, and M. Lienkamp, "Exploration of Optimal Powertrain Design Using Realistic Load Profiles," World Electric Vehicle Journal, vol. 10, no. 3, p. 56, 2019, doi: 10.3390/wevj10030056.

[4]   A. Ongel, E. Loewer, F. Roemer, G. Sethuraman, F. Chang, and M. Lienkamp, "Economic Assessment of Autonomous Electric Microtransit Vehicles," *Sustainability*, vol. 11, no. 3, p. 648, Jan. 2019

Conference, Magazine, etc.; peer-reviewed

[1]   G. Sethuraman, S.S. Ragavareddy, A. Ongel, M. Lienkamp, and P. Raksincharoensak, "Impact Assessment of Autonomous Electric Vehicles in Public Transportation System," in Proceedings of the IEEE Intelligent Transportation Systems Conference - ITSC 2019, Auckland, New Zealand, Oct. 2019, pp. 1–7

[2]   G. Sethuraman, X. Liu, F. Bachmann, X. Meng, A. Ongel and F. Busch, "Effects of Bus Platooning in an Urban Environment," in Proceedings of the IEEE Intelligent Transportation Systems Conference - ITSC 2019, Auckland, New Zealand, Oct. 2019, pp. 1–7.

[3]   S. Krapf, G. Sethuraman, A. Pathak, A. Ongel, and M. Lienkamp, "Improving electric city bus powertrain efficiency and costs using design space exploration," in Proceedings of the 31st International Electric Vehicle Symposium & Exhibition (EVS31), Kobe, Japan, Oct. 2018, pp. 1–7

[4]   C. Angerer, N. Holjevac, G. Sethuraman, and M. Lienkamp, "AWD for electric vehicles – a revolution for vehicle efficiency?," in Proceedings of the 31st International Electric Vehicle Symposium & Exhibition (EVS31), Kobe, Japan, Oct. 2018.

Students Thesis Supervised

[1]   M. Schwarz, "Development of a Parametric Model for Vehicle Packaging and Sizing of an Autonomous Electric Bus System," master's thesis, Institute of Automotive

Technology (FTM), Technical University of Munich, 2018.

[2]   S. Maxl, "Development of a Parametric Chassis Selection and Sizing Model for Autonomous Electric Buses," master's thesis, Institute of Automotive Technology (FTM), Technical University of Munich, 2018.

[3]   P.Tran, "Development of a Parametric Packaging and Sizing Tool for Autonomous Electric Bus System," master's thesis, Institute of Automotive Technology (FTM), Technical University of Munich, 2019.

[4]   S. S. Ragavareddy, "Impact Assessment of Autonomous Electric Buses," master's thesis, Institute of Automotive Technology (FTM), Technical University of Munich, 2018.

[5]   E. Wesibrodt "Development of a Parametric Packaging and Sizing Tool for autonomous Electric Double Deck Bus Systems," master's thesis, Institute of Automotive Technology (FTM), Technical University of Munich, 2019.

[6]   A. Weerts, "Life Cycle Assessment (LCA) of Autonomous Electric Vehicles," master's thesis, Instituts für Werkzeugmaschinen und Fertigungstechnik, Technical University of Braunschweig, 2019.

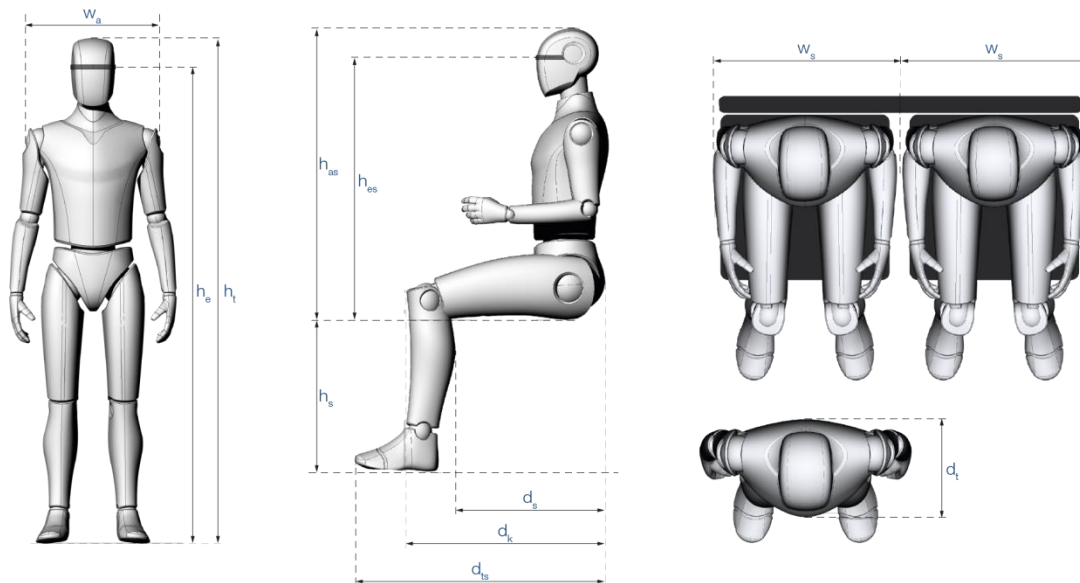# Appendix

Appendix A Anthropometric Data

Figure A-1   Anthropometric body size dimensions

Table A-1   Anthropometric Measures of Male and Female Passengers [105]

Symbol	Description	5% Female (minimum)	95% Male (maximum)
w_a	Shoulder width	330	529
w_h	Hip width	304	406
w_s	Seat width	610	610
h_t	Overall Height	1.454	1.847
h_e	Eye level height (standing)	1.354	1.752
h_{es}	Eye level height (sitting)	620	861
h_{ms}	Mid-shoulder height	483	696
h_{ss}	Sitting height	740	932
h_{as}	Popliteal height (as measured from seat surface)	319	932
d_{ts}	Back-toe length	495	940
d_k	Back-knee length	481	640
d_s	Back-popliteal length	390	546
d_t	Total body depth	257	330

Appendix B Components list and priority

Table B-1   List of Components and Priority

No.	Component	Assembly	Sub-assembly	Design Priority
1	Antennas	CAV Components	Electronics	2
2	LIDAR	CAV Components	Driving Sensors	2
3	Long Range Radar	CAV Components	Driving Sensors	2
4	Short Range Radar	CAV Components	Driving Sensors	2
5	Ultrasonic (Short Range)	CAV Components	Driving Sensors	2
6	Camera Vision Systems	CAV Components	Driving Sensors	2
7	Wi-Fi Router	CAV Components	Electronics	3
8	Wheels	Chassis	Wheel	1
9	Brake Discs	Chassis	Braking	1
10	Wheel Carrier	Chassis	Wheel	2
11	Spring/ Air Suspension	Chassis	Spring	2
12	Steering System	Chassis	Steering	1
13	Air Compressor	Chassis	Suspension	1
14	Air Tanks	Chassis	Suspension	1
15	Braking Actuators	Chassis	Braking	2
16	Brake Clippers/Pads	Chassis	Braking	1
17	Steering Actuator	Chassis	Steering	1
18	Compressor	HVAC	HVAC	2
19	Evaporator	HVAC	HVAC	2
20	Condenser and Fan	HVAC	HVAC	3
21	AC Ducts	HVAC	HVAC	3
22	Flaps Air Flow Control	HVAC	HVAC	3
23	Auxiliaries	Others	Miscellaneous	3
24	Simple Distance ranging	Others	Aux Sensor	2
25	Door Visual	Others	Aux Sensor	2
26	Door Infrared	Others	Aux Sensor	2
27	Temperature	Others	Aux Sensor	2
28	Infrared camera for thermal sensing	Others	Aux Sensor	2
29	Pyrometer Sensor	Others	Aux Sensor	2
30	Motor	Powertrain	Drivetrain	1
31	Transmission	Powertrain	Drivetrain	1
32	Differential	Powertrain	Drivetrain	2
33	Inverter	Powertrain	Power Electronics	1
34	Battery	Powertrain	Battery	1
35	Axles	Powertrain	Drivetrain	2
36	Cooling pump	Powertrain	Powertrain	2
37	Cooling Radiator	Powertrain	Powertrain	1
38	Cooling Fan	Powertrain	Powertrain	1
39	Cooling Hoses/ Pipes	Powertrain	Powertrain	2

40	Heat Exchanger for Battery	Powertrain	Powertrain	2
41	Frame	Vehicle Body and Structure	Structure	1
42	Floor	Vehicle Body and Structure	Structure	1
43	Crash Element Absorber	Vehicle Body and Structure	Structure	1
44	Wheelhouse	Vehicle Body and Structure	Structure	1
45	Body	Vehicle Body and Structure	Exterior	1
46	Doors	Vehicle Body and Structure	Exterior	1
47	Windows	Vehicle Body and Structure	Exterior	1
48	Lights	Vehicle Body and Structure	Exterior	3
49	Bumpers	Vehicle Body and Structure	Exterior	3
50	Display Screen	Vehicle Body and Structure	Exterior	3
51	Wiper Blades	Vehicle Body and Structure	Exterior	3
52	Charging Interface	Vehicle Body and Structure	Body	3
53	Seats	Vehicle Body and Structure	Interior	1
54	Handles	Vehicle Body and Structure	Interior	3
55	Poles	Vehicle Body and Structure	Interior	3
56	Screen	Vehicle Body and Structure	Information	3
57	Belts	Vehicle Body and Structure	Safety	3
58	Computer	Vehicle Body and Structure	Electronics	2
59	HMI System	Vehicle Body and Structure	Entertainment	3
60	Door Actuators	Vehicle Body and Structure	Body	2
61	Chargers (USB)	Vehicle Body and Structure	Entertainment	3
62	Box for Carriage/Bicycle	Vehicle Body and Structure	Body	3
63	Ramp	Vehicle Body and Structure	Body	1

Appendix C Parameter List

Table C- 1 Parameters list with default values

No.	Parameter Name	Description	Unit
1	l_overall	Overall Length	mm
2	w_overall	Overall Width	mm
3	h_overall	Overall Height	mm
4	wb	Wheelbase	mm
5	gc	Ground Clearance	mm
6	h_lift	Lifting Height	mm
7	lay_urban1	Activation Urban Layout 1	True/False
8	lay_urban2	Activation Urban Layout 2	True/False
9	lay_coach1	Activation Coach Layout 1	True/False
10	n_ul1_rear	Number of Seats Rear/Front UL1	
11	n_ul1_window	Number of Seats Window UL1	
12	n_ul1_door	Number of Seats Door UL1	
13	n_cl1_rear	Number of Seats Rear/Front CL1	
14	n_cl1_window	Number of Seats Window CL1	
15	n_cl1_door	Number of Seats Door CL1	
16	n_ul2_rear	Number of Seats Rear/Front UL2	
17	n_ul2_window	Number of Seats Window UL2	
18	n_ul2_door	Number of Seats Door UL2	
19	w_rest_gap_rear_cl1	Rest Gap Seat Rear/Front CL1	mm
20	w_rest_gap_window_cl1	Rest Gap Seat Window CL1	mm
21	w_rest_gap_door_cl1	Rest Gap Seat Door CL1	mm
22	w_rest_gap_window_ul1	Rest Gap Seat Window UL1	mm
23	w_rest_gap_rear_ul1	Rest Gap Seat Rear/Front UL1	mm
24	w_rest_gap_door_ul1	Rest Gap Seat Door UL1	mm
25	w_rest_gap_door_ul2	Rest Gap Seat Door UL2	mm
26	w_rest_gap_window_ul2	Rest Gap Seat Window UL2	mm
27	w_rest_gap_rear_ul2	Rest Gap Seat Rear/Front UL2	mm
28	seat_ul1_front	Activation Seat Front UL1	True/False
29	seat_ul1_rear	Activation Seat Rear UL1	True/False
30	seat_ul1_door_rear	Activation Seat Door Rear UL1	True/False
31	seat_ul1_door_front	Activation Seat Door Front UL1	True/False

32	seat_ul2_door_front	Activation Seat Door Front UL2	True/False
33	seat_ul2_front	Activation Seat Front UL2	True/False
34	seat_ul2_door_rear	Activation Seat Door Rear UL2	True/False
35	seat_ul2_rear	Activation Seat Rear UL2	True/False
36	seat_cl1_door	Activation Seat Door CL1	True/False
37	pattern_seat_ul1_front	Activation Pattern Seat Front UL1	True/False
38	pattern_seat_ul1_rear	Activation Pattern Seat Rear UL1	True/False
39	pattern_seat_ul1_door_rear	Activation Pattern Seat Door Rear UL1	True/False
40	pattern_seat_ul1_door_front	Activation Pattern Seat Door Front UL1	True/False
41	pattern_seat_ul2_door_front	Activation Pattern Seat Door Front UL2	True/False
42	pattern_seat_ul2_front	Activation Pattern Seat Front UL2	True/False
43	pattern_seat_ul2_door_rear	Activation Pattern Seat Door Rear UL2	True/False
44	pattern_seat_ul2_rear	Activation Pattern Seat Rear UL2	True/False
45	drivetrain_center_rear	Activation Drivetrain Center Rear	True/False
46	drivetrain_dual_all	Activation Drivetrain Dual Rear	True/False
47	cooler_all	Activation Cooler 4 Wheel	True/False
48	motor_all	Activation Motor 4 Wheel	True/False
49	trans_all	Activation Transmission 4 Wheel	True/False
50	inv_all	Activation Inverter 4 Wheel	True/False
51	ramp_in	Activation Ramp Pulled In	True/False
52	ramp_out	Activation Ramp Deployed	True/False
53	street	Activation Street	True/False
54	l_motor	Length Motor	mm
55	d_motor	Diameter Motor	mm
56	mat_motor	Material Motor	
57	l_cooler	Length Cooler	mm
58	h_cooler	Height Cooler	mm
59	t_cooler	Thickness Cooler	mm
60	mat_cooler	Material Cooler	
61	l_trans	Length Transmission	mm
62	w_trans	Width Transmission	mm
63	mat_trans	Material Transmission	
64	l_inv	Length Inverter	mm
65	w_inv	Width Inverter	mm
66	h_inv	Height Inverter	mm
67	mat_inv	Material Inverter	
68	V_bat	Volume Battery Cells	m^3

69	d_bat_cell	Diameter Battery Cell	mm
70	h_bat_cell	Height Battery Cell	mm
71	mat_bat_cell	Material Battery Cell	
72	t_bat_box	Thickness Battery Box	mm
73	h_bat_el	Height Battery Electronics	mm
74	mat_bat_box	Material Battery Box	
75	l_seat	Length Seat	mm
76	w_seat	Width Seat	mm
77	h_seat	Height Seat	mm
78	t_seat	Thickness Seat	mm
79	mat_seat	Material Seat	
80	h_backrest	Height Backrest	mm
81	l_leg_clearance	Length Leg Clearance	mm
82	w_seat_gap	Width Seat Gap	mm
83	w_passenger_shoulder	Width Shoulder Passenger	mm
84	bd_passenger	Depth Body Passenger	mm
85	w_tire	Width Tire	mm
86	d_tire	Diameter Tire	mm
87	t_tire	Thickness Tire	mm
88	t_rim	Thickness Rim	mm
89	mat_tire	Material Tire	
90	mat_rim	Material Rim	
91	da_bdisc	Outer Diameter Brake Disc	mm
92	di_bdisc	Inner Diameter Brake Disc	mm
93	t_bdisc	Thickness Brake Disc	mm
94	mat_bdisc	Material Brake Disc	
95	mat_bpad	Material Brake Pad	
96	mat_bcalliper	Material Brake Calliper	
97	l_wcarrier	Length Wheel Carrier	mm
98	w_wcarrier	Width Wheel Carrier	mm
99	mat_wcarrier	Material Wheel Carrier	
100	d_aarm	Diameter A-Arms	mm
101	t_aarm	Thickness A-Arms	mm
102	mat_aarm	Material A-Arms	
103	h_spring	Height Air Spring	mm
104	d_spring	Diameter Air Spring	mm
105	mat_spring	Material Air Spring	
106	d_air_tank	Diameter Air Tank	mm
107	l_air_tank	Length Air Tank	mm
108	t_air_tank	Thickness Air Tank	mm
109	mat_air_tank	Material Air Tank	
110	d_compressor	Diameter Compressor	mm
111	l_compressor	Length Compressor	mm
112	t_compressor	Thickness Compressor	mm
113	mat_compressor	Material Compressor	
114	a_front	Steering Angle Front	

115	a_rear	Steering Angle Rear	
116	t_axis	Thickness Axis	mm
117	d_axis	Diameter Axis	mm
118	mat_axis	Material Axis	
119	d_damper	Diameter Damper	mm
120	mat_damper	Material Damper	
121	h_r	Height Roof	mm
122	t_body	Thickness Body	mm
123	mat_body	Material Body	
124	mat_wh	Material Wheel House	
125	t_frame	Thickness Frame	mm
126	h_frame	Height Frame	mm
127	mat_frame	Material Frame	
128	t_window	Thickness Window	mm
129	h_window_shoulder	Height Window Shoulder	mm
130	h_window	Height Window	mm
131	mat_window	Material Window	
132	t_floor	Thickness Floor	mm
133	h_floor	Height Floor	mm
134	mat_floor	Material Floor	
135	h_door	Height Door	mm
136	w_door	Width Door	mm
137	t_door	Thickness Door	mm
138	mat_door	Material Door	
139	l_ramp	Length Ramp	mm
140	w_ramp	Width Ramp	mm
141	t_ramp	Thickness Ramp	mm
142	mat_ramp	Material Ramp	
143	h_curb	Height Curb	mm
144	h_lidar	Height LIDAR	mm
145	d_lidar	Diameter LIDAR	mm
146	mat_lidar	Material LIDAR	
147	l_ac	Length Air Condition	mm
148	w_ac	Width Air Condition	mm
149	h_ac	Height Air Condition	mm
150	mat_ac	Material Air Condition	

Appendix D Component Sizing

Appendix D1: Tire Selection Flowchart
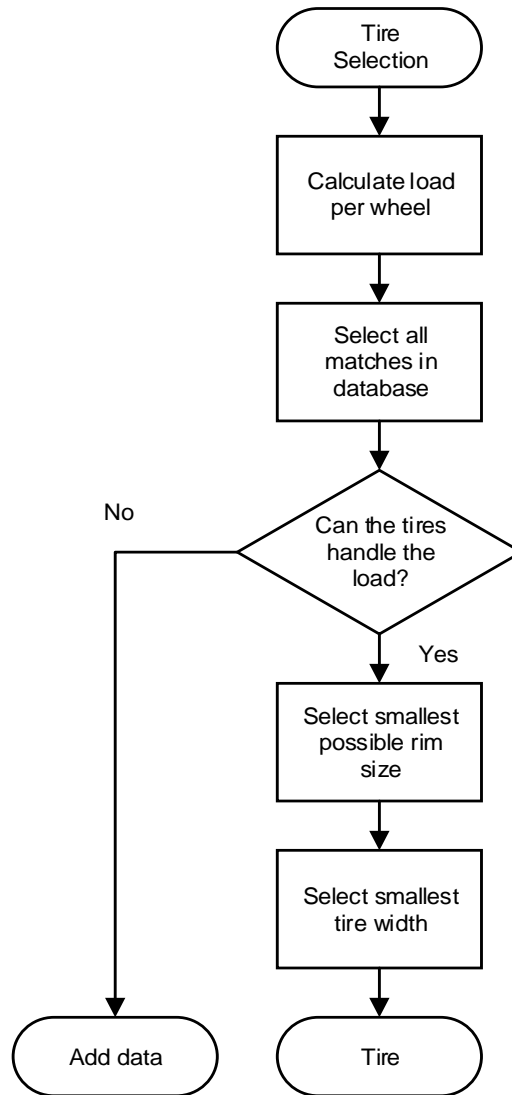
Figure D-1   Tire Selection Flowchart

Appendix D2: Air-Spring Selection Flowchart
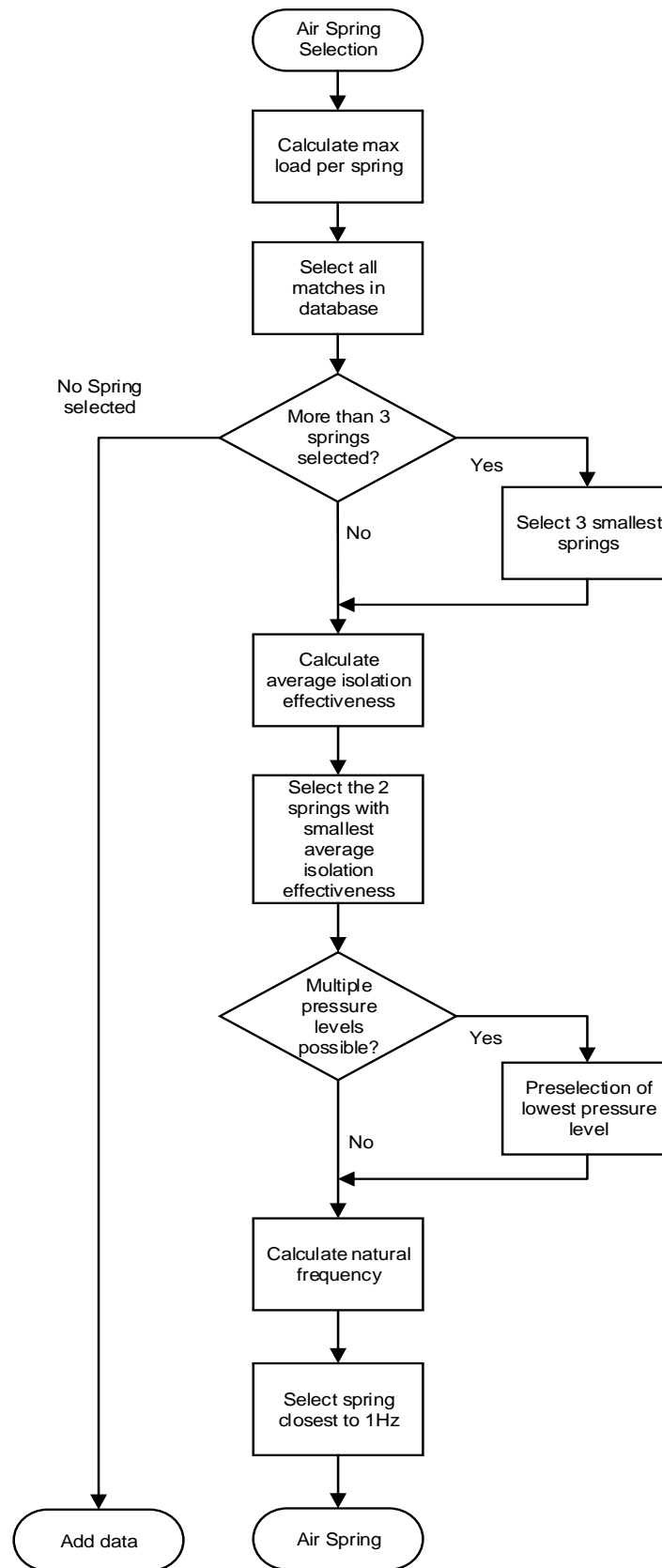
Figure D-2   Air Spring Selection Flowchart

Appendix D3: Brake Selection Flowchart
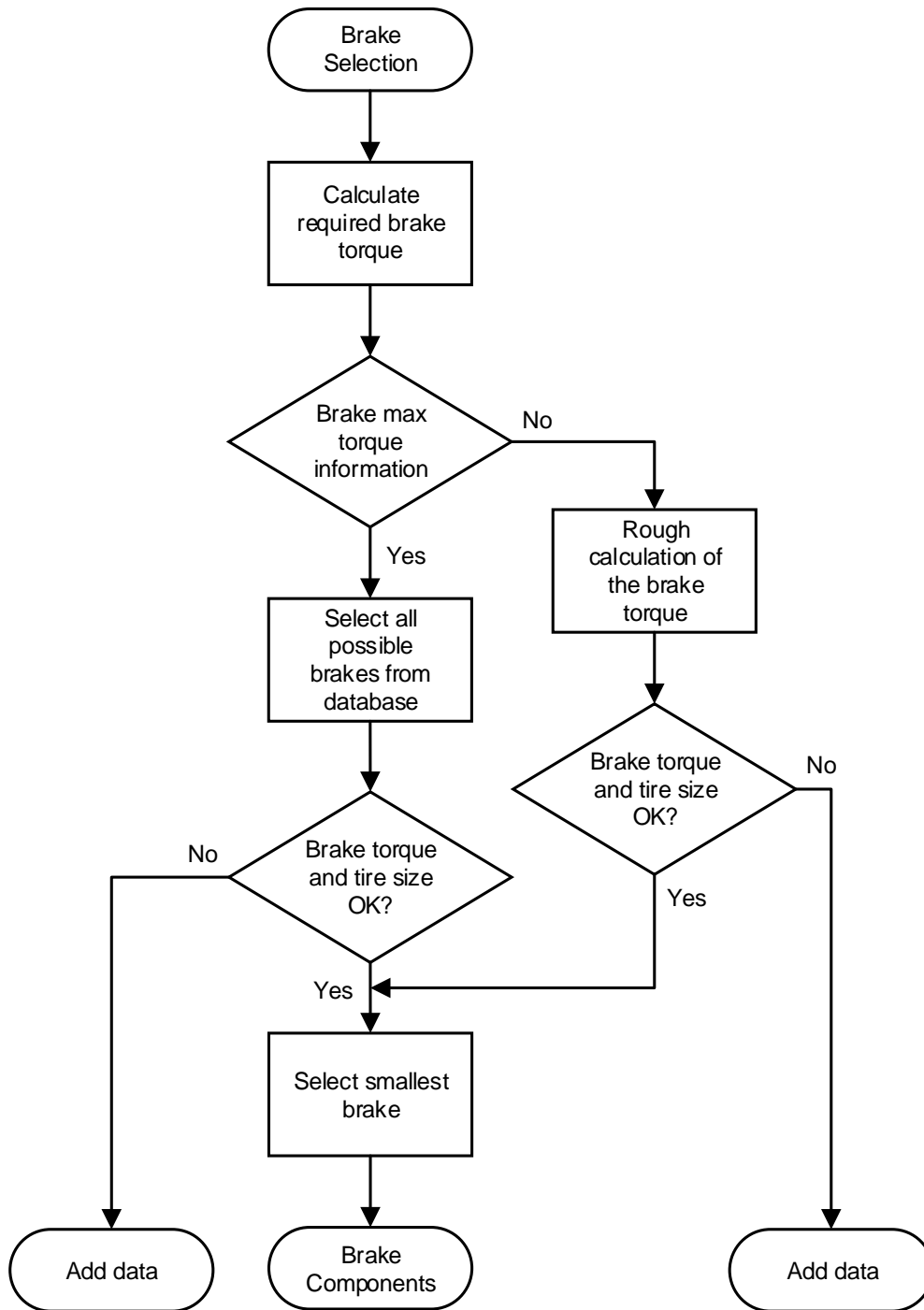
Figure D-3   Brake Selection Flowchart

d_t Total body depth   257   330

Appendix E Vehicle Specifications

Appendix E1: Determination of vehicle specification – Manual Mode

There are three different interior layouts available, the *Urban Layout I*, the *Urban Layout II* and the *Coach Layout I* as seen in Section 6.2.2. Based on the selected layout, the first step is to calculate the overall area for seating. Further, the seating and standing area are calculated. The number of seats are decided based on the seating area. Thereby, total number of passengers is calculated. Figure E-1 shows the illustration of Urban Layout 1. The following equations used in the explanation do not use parameter prefix *ul1* for a clear understanding. Please refer to the List of Symbols

Figure E-1   Urban 1 Layout Illustration

First, the distance between front and rear wheelhouse is calculated for placement of the seat along windows as shown in Equation (E.1).

$$l_{window} = l_{overall} - 2 \times \left(\text{wb} + \frac{2}{3} d_{tire} \right) \tag{E.1}$$

Secondly, in Equation (E.2), the distance between front and rear wheelhouse to the door is measured.

$$l_{door} = \frac{l_{overall} - w_{door} - 2 \times \text{wb} - \frac{4}{3} d_{tire}}{2} \tag{E.2}$$

Lastly, the distance between the left and the right wheelhouse is calculated. The 50 mm added in Equation (E.3) represents the distance between the tire and the air spring.

$$l_{rear} = w_{overall} - 2 \times \left(t_{body} + w_{tire} + d_{spring} + 50 \text{ mm} \right) \tag{E.3}$$

To calculate the number of seats fitting in the available distance, the integrated floor-command of MATLAB is used to round down the resulting value to an integer. Equation (E.4) displays the calculation of the number of seats in the window row for UL1.

$$n_{window} = floor \left(\frac{l_{window}}{w_{seat} + 2 \times w_{seat\_gap}} \right) \tag{E.4}$$

The calculations for the number of seats in the door section and the front and the rear section are equivalent to Equation (E.5). Equation (E.5) explains the calculation of the total number of seats in UL1. Rear and front seating sections are the same, that's why only the rear number is considered and doubled.

$$n_{seats} = n_{window} + 2 \times n_{door} + 2 \times n_{rear} \tag{E.5}$$

To provide that the CATIA model is able to position the seats always centred in the available seating space, the rest gap division is executed in the following Equation (E.6). This rest gap value is later divided by two in CATIA for centring the seats arrangement. For this calculation, the modulo-command is used to get a reminder after the division. For example, mod (11,3) = 2.

$$w_{rest\_gap\_window} = mod\left(l_{window}, \left(n_{window} \times \left(w_{seat} + 2 \times w_{seat\_gap}\right)\right)\right) \tag{E.6}$$

The calculations for the rest gaps of the door section and of the rear (front) section are equivalent to Equation (E.7).

As illustrated in the flow chart, a parallel calculation executed, is the calculation of passengers. For this calculation, the available space is needed where passengers can stand. All areas for this calculation are explained in the next paragraphs.

The total area of the bus is calculated in Equation (E.7). This equation includes the body thickness and 50 mm curvature distance of the body shape.

$$a_{bus} = \left(l_{overall} - t_{body} - 50 \text{ mm}\right) \times \left(w_{overall} - t_{body} - 50 \text{ mm}\right) \tag{E.7}$$

The wheelhouse area is calculated in Equation (E.8) in dependence of the air spring and the wheel.

$$a_{wheelhouse} = \left(wb + \frac{2}{3}d_{tire}\right) \times \left(t_{body} + w_{tire} + d_{spring} + 50 \text{ mm}\right) \tag{E.8}$$

The seat area is constructed in Equation (E.9)

$$a_{seat} = \left(l_{seat} + t_{seat} + l_{clearance}\right) \times \left(w_{seat} + 2 \times w_{seat\_gap}\right) \tag{E.9}$$

The area for a standing passenger is derived with Equation (E.10).

$$a_{passenger} = w_{passenger\_shoulder} \times bd_{body\_depth} \tag{E.10}$$

Due to the curvature of the body and the windows, a dead area exists behind the front and the rear seats, which is calculated in Equation (E.11).

$$a_{dead\_zone} = \left(w_{overall} - 2 \times \left(t_{body} + w_{tire} + d_{spring} + 50 \text{ mm}\right)\right) \times \left(\frac{l_{seat}}{2} + t_{seat}\right) \tag{E.11}$$

The centring of the seats in the available areas results in a development of dead zone areas where no passenger is able to stand. Thus, following Equation (E.12) needs to be considered.

$$a_{rest} = \left(l_{seat} + t_{seat}\right) \times \left(w_{rest\_gap\_window} + w_{rest\_gap\_door} + w_{rest\_gap\_rear}\right) \tag{E.12}$$

The standing area for passengers results of Equation (E.13).

$$a_{standing} = a_{bus} - \left(4 \times a_{wheelhouse} + n_{seats} \times a_{seat} + 2 \times a_{dead\_zone} + a_{rest}\right) \tag{E.13}$$

The number of standing people is calculated in Equation (E.14) by dividing the standing area by the area of a single passenger. Again, the floor-command is used to round the result.

$$n_{standing} = floor\left(\frac{a_{standing}}{a_{passenger}}\right)$$ (E.14)

The total number of passenger inside the bus results by adding the number of seats to the number of standing passengers. The number is considered as the maximum packing density of people and calculated in Equation (E.15).

$$n_{passenger} = n_{standing} + n_{seats}$$ (E.15)

Thus, the seating to standing ratio is derived from Equation (E.16).

$$ratio_{standing/sitting} = \frac{n_{standing} + n_{passenger}}{n_{seats} + n_{passenger}} \times 100$$ (E.16)

Appendix E2: Determination of vehicle specification – Automated mode

To determine the overall dimensions of the bus, the cabin area must be calculated. Cabin area is the sum of all the seating and standing areas inside the vehicle concept. The steps for calculating the seating areas is shown below. The seating arrangement of the Urban 2 layout is used as an example in the explanation, as illustrated in Figure E-2. As shown, the figure is divided into five different seating areas and one standing area to determine the length of the bus. All the areas added together determines the dimensions of the cabin and hence the dimensions of the vehicle concept.
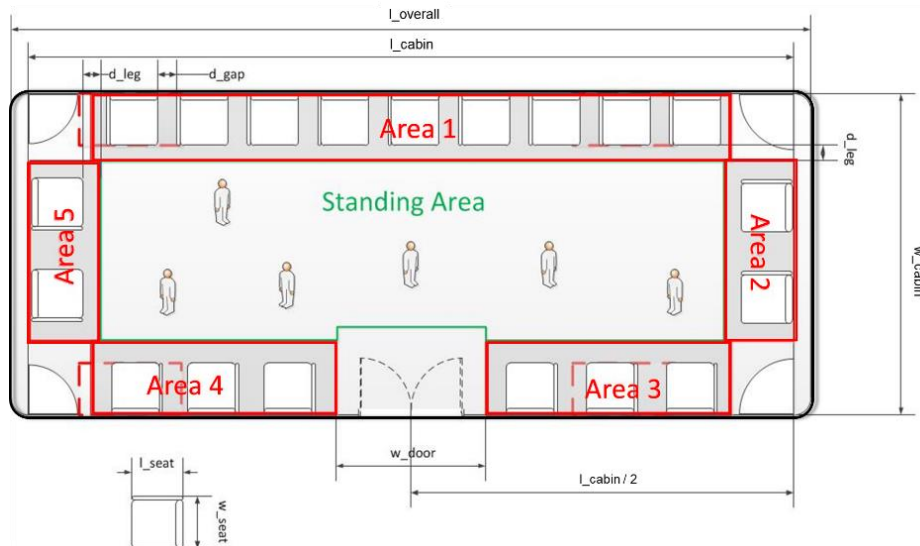
Figure E-2   Seating Layout illustration

Area 1:

$$A_{area,1} = \left(l_{cabin} - 2 \cdot \left(l_{seat} + d_{leg}\right)\right) \cdot \left(l_{seat} + d_{leg}\right)$$ (E.17)

$$n_{passenger,area_1} = \frac{l_{cabin} - 2 \cdot \left(l_{seat} + d_{leg}\right)}{w_{seat} + d_{gap}}$$ (E.18)

Area 2 = Area 5:

$$A_{area,2} = \left(w_{cabin} - 2 \cdot \left(l_{seat} + d_{leg}\right)\right) \cdot \left(l_{seat} + d_{leg}\right)$$ (E.19)

$$n_{passenger,area_2} = 2 = n_{passenger,area_5}$$ (E.20)

Area 3 = Area 4:

$$A_{area,3} = \left(\frac{l_{cabin}}{2} - \frac{w_{door}}{2} - (l_{seat} + d_{leg}) \right) \cdot (l_{seat} + d_{leg}) \tag{E.21}$$

$$n_{passenger,area_3} = \frac{\frac{l_{cabin}}{2} - \frac{w_{door}}{2} - (l_{seat} + d_{leg})}{w_{seat} + d_{gap}} = n_{passenger,area_4} \tag{E.22}$$

The number of seats is made up of the number of passengers in these five areas. Thereby, two seats are defined for the front and back area of the bus (Area 2 and 5):

$$n_{seats} = \sum_{i=1}^{5} n_{passenger,area_i} \tag{E.23}$$

$$A_{standing} = l_{cabin} \cdot w_{cabin} - A_{area,1} - 2 \cdot A_{area,2} - 2 \cdot A_{area,3} - w_{door} \cdot \frac{w_{door}}{2} - 4 \\ \cdot \left((l_{seat} + d_{leg})^2 \right) \tag{E.24}$$

$$n_{standing} = \frac{l_{cabin} \cdot w_{cabin} - A_{area,1} - 2 \cdot A_{area,3} - w_{door} \cdot \frac{w_{door}}{2} - 4 \cdot \left((l_{seat} + d_{leg})^2 \right)}{A_{1passenger}} \tag{E.25}$$

The total number of passengers is made up of the number of seats and standing.

$$n_{total} = n_{seats} + n_{standing} \tag{E.26}$$

The user specifies the desired number of passengers via the graphical user interface as explained in Section 6.3. Equations (E.24) and (E.25) are substituted into equation (E.26), resolved to find the length of the cabin. The determination of the length of the bus is implemented as a function in the overall script of the AEV Tool. In addition, a database for the vehicle specification with various vehicle classification, number of passengers and seat arrangements is created using a simulation in Matlab. This serves as input for the remaining databases.

Appendix F GUI Design

Appendix F1: List of Objects

Table F- 1   List of used objects for the GUI generation
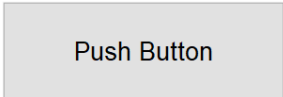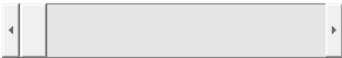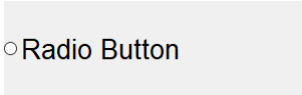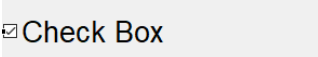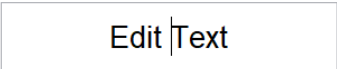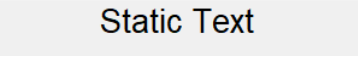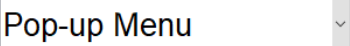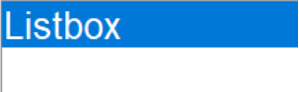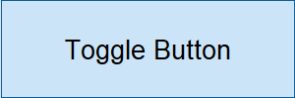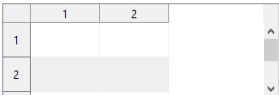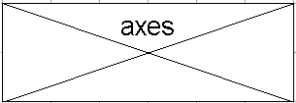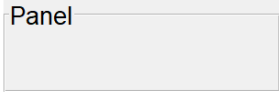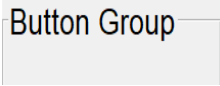
Image of the Object	Name of the Object	Description
Push Button	Push Button	Execution of an action by pushing
Slider	Slider	Moved horizontally or vertically to control a variable
Radio Button	Radio Button	Representing one of a set of options, only one of which can be selected at any time
Check Box	Check Box	By selection, shows that a particular feature has been enabled or a particular option chosen
Edit Text	Edit Text	Enable to input a value
Static Text	Static Text	Display text for different description
Pop-up Menu	Pop-up Menu	Offers different actions to choose for a specific context
Listbox	Listbox	Contains a list of options, one or more can be selected
Toggle Button	Toggle Button	Has an n and off state, allows to change a setting between two states
Table	Table	Set of facts or figures systematically displayed, especially in columns
axes	Axes	Allows to display graphs or images

Image of the Object	Name of the Object	Description
Panel	Panel	Provides a framework for related objects
Button Group	Button Group	Provides a framework for related buttons

Appendix F2: Visualisation Hierarchy

A hierarchy must be defined for the selection of a system. Therefore, the GUI is divided into different levels. The user is only shown Level 1 (L1) and can only edit this level. All the other levels are pushed into the background and are not visible to the user. Figure 5-5 illustrates the different levels as well as the main systems and their subsystems. Due to the clarity, the interactions are not shown there. The example uses three cases to show how a system can be brought into the front and made visible to the user. It starts with the case a) where system A is on the top level (L1), system B (L2) and C (L3) in the background. The user can only work on system A. To call system C, A will be pushed into the background to L3 and C is moved to the front at L1, this illustrates case b). In case c), B is brought to L1 and at the same time, C is pushed to L3. In summary, the desired system is always brought forward to L1 and simultaneously the current system is set back to L3.
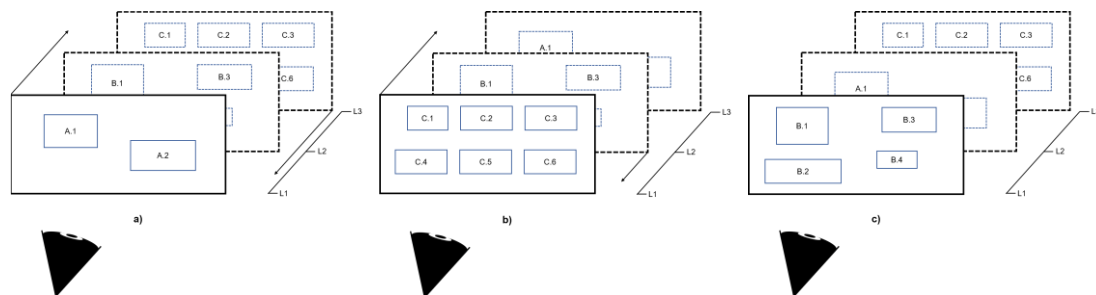
Figure F- 1   Hierarchy architecture of the AEV Tool

Appendix G GUI of the AEV Tool
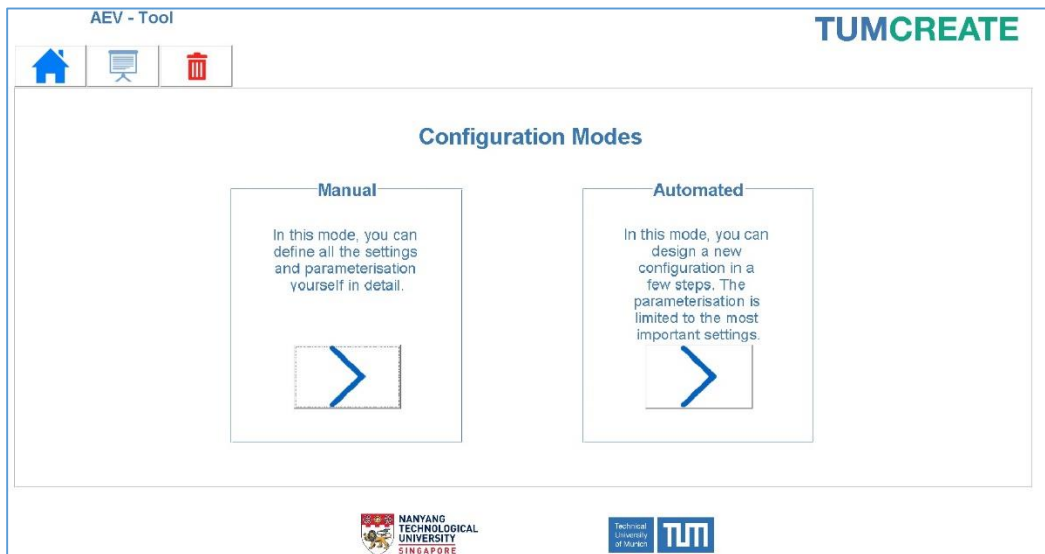
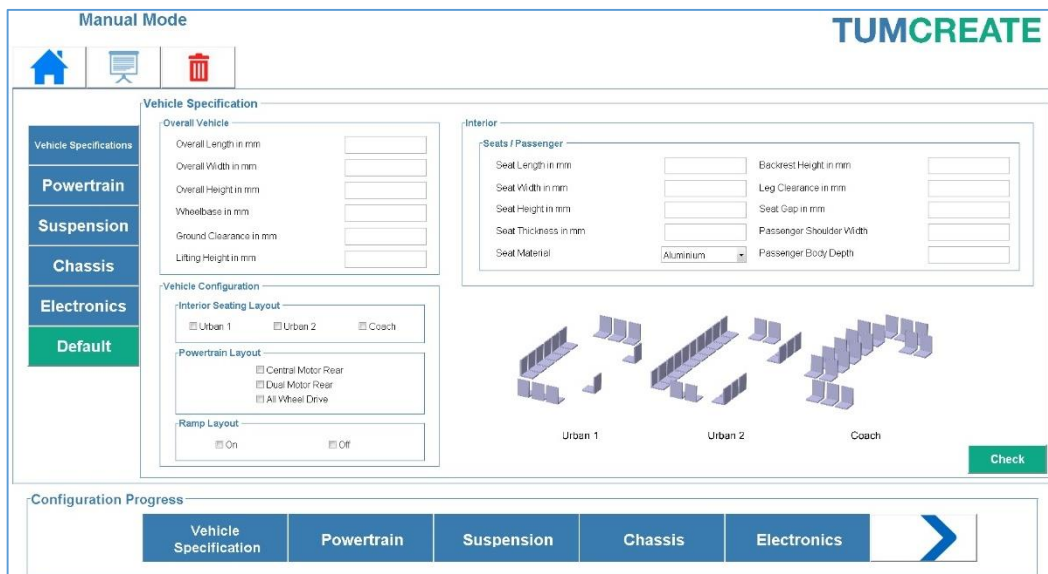Figure G-1   Main screen of the AEV tool

Figure G-2   GUI of Manual Mode
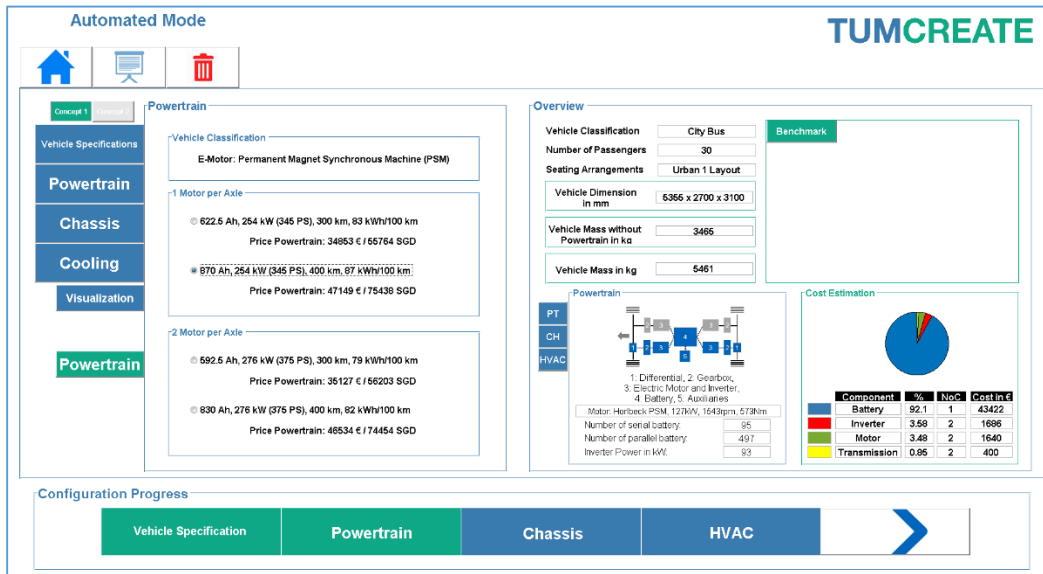
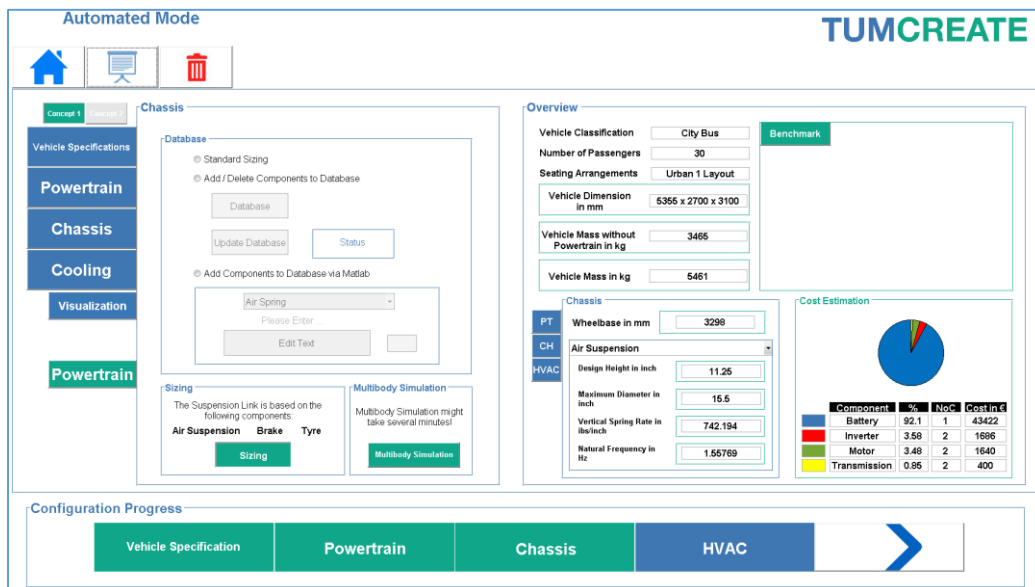Figure G-3   GUI of Powertrain Selection

Figure G-4   GUI of Chassis Selection
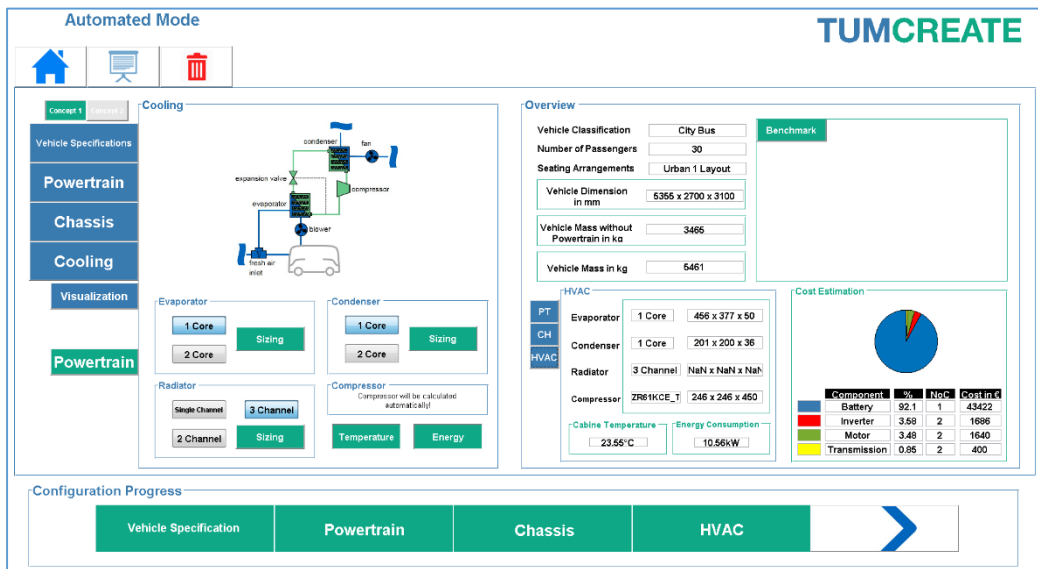
Figure G-5   GUI of HVAC Selection

Appendix H Results Visualisation

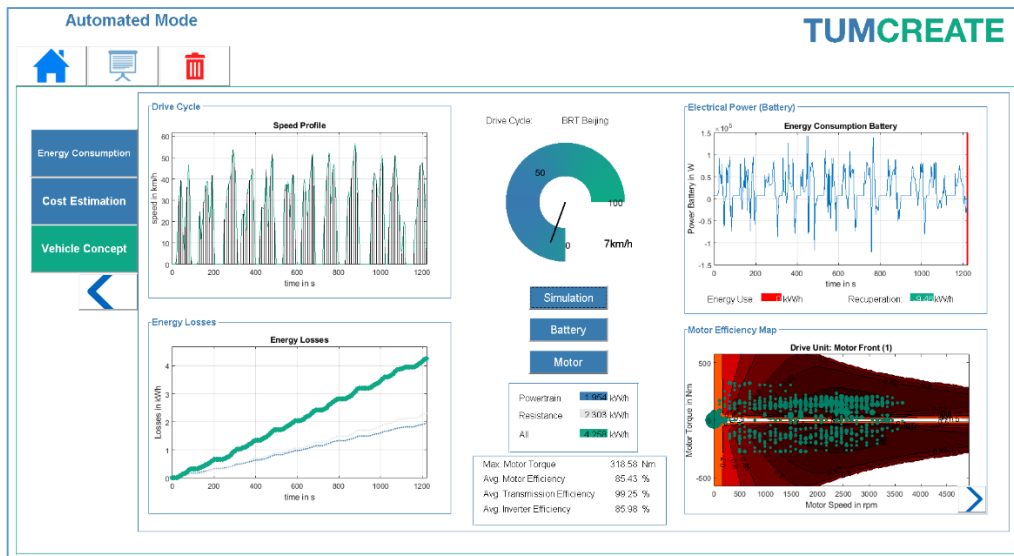Figure G-6   Manual Mode Concept Visualisation

Figure G-7   Results – Energy Consumption

Figure G-8   Results – Cost Estimation

Figure G-9   Automated Mode Concept Visualisation

Appendix I   Lifecycle Assessment

Table I-1   Material mix for different subsystems

Material/Component	Steel	Aluminium	Laminated Glass	Plastic	Rubber
Structure	100 %	-	-	-	-
Exterior	20 %	30 %	30 %	20 %	-
Interior	10 %	40 %	-	50 %	-
Chassis	80 %	16 %	-	-	4 %
Other	-	95 %	5 %	-	-
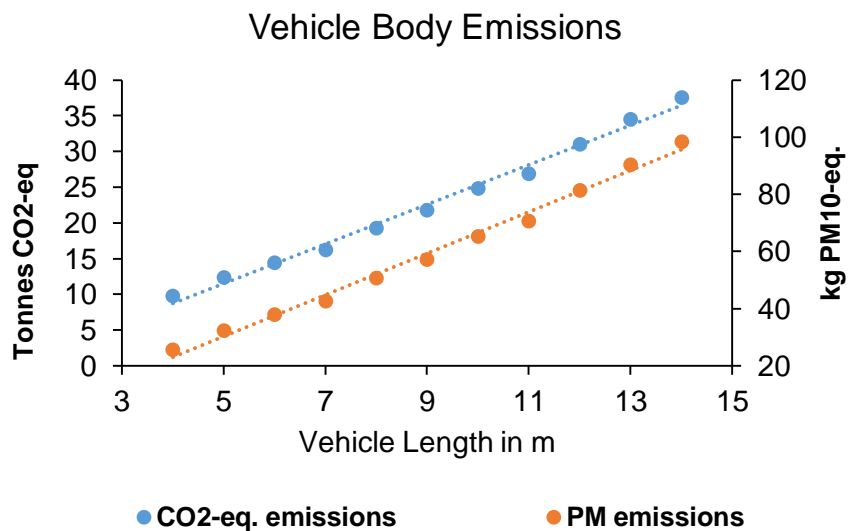
Figure I-1   Vehicle Body Production Emissions for Different Vehicle Length
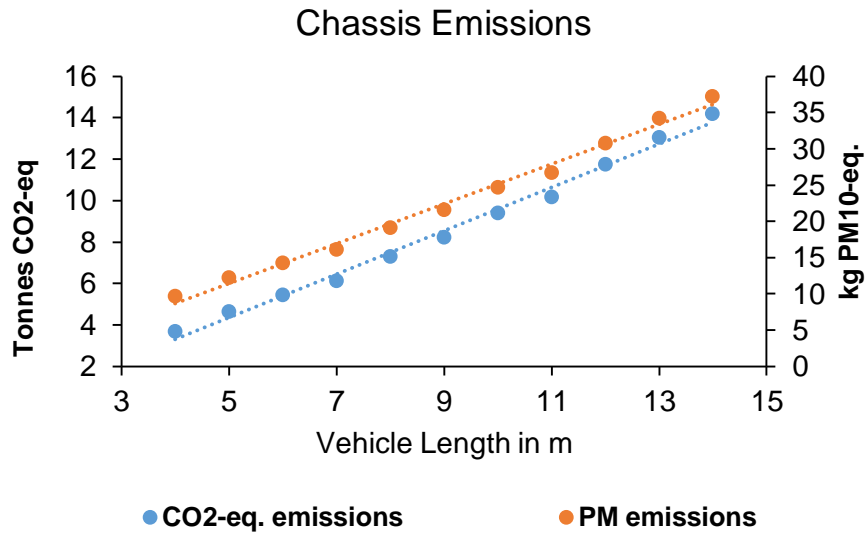
Chassis Emissions

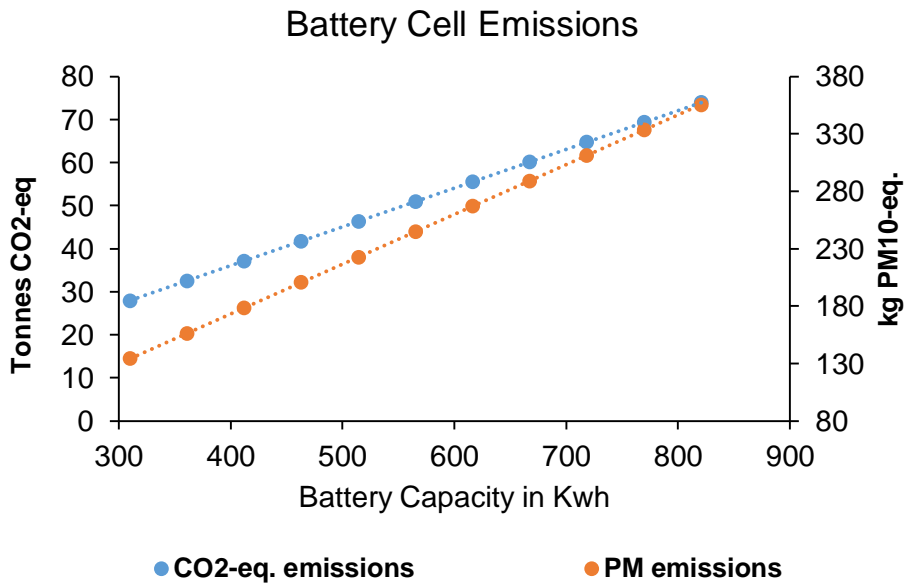Figure I-2   Chassis Components Production Emissions for Different Vehicle Length

Battery Cell Emissions

Figure I-3   Battery Cell Production Emissions for Different Capacities

Battery HousingEmissions

CO2-eq. emissions   **PM emissions**
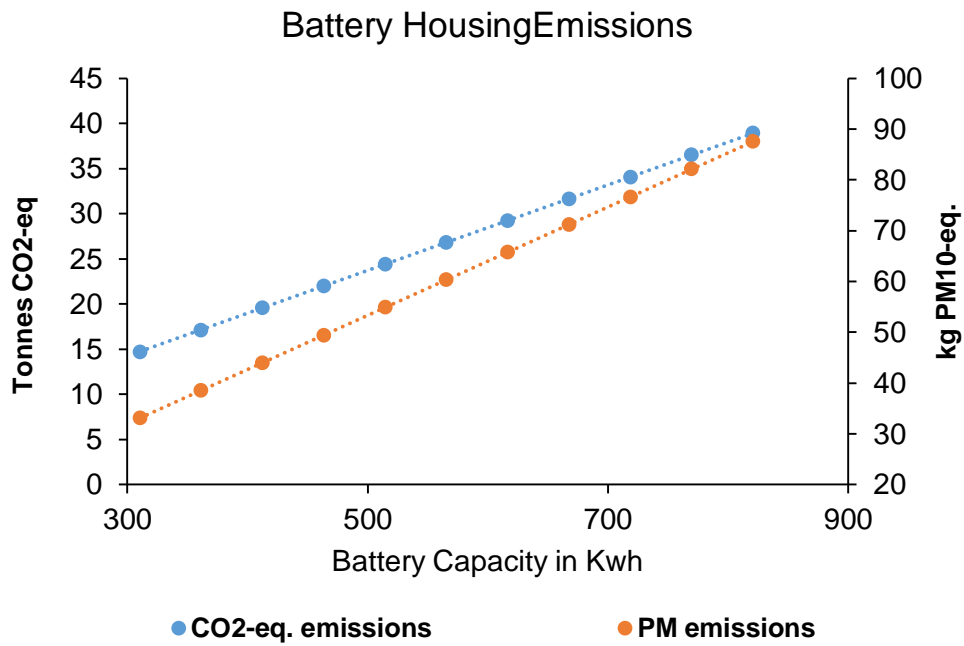
Figure I-4   Battery Housing Production Emissions for Different Battery Capacities

Drivetrain Emissions

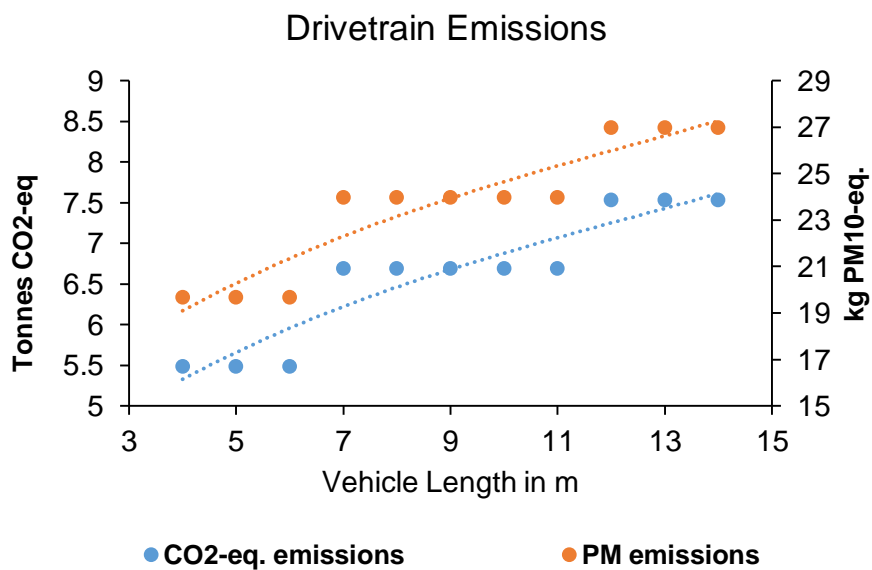**CO2-eq. emissions**   **PM emissions**

Figure I-5   Drivetrain Components Production Emissions for Different Vehicle Length